ZooKeys 835: 1–15 (2019)
doi: 10.3897/zookeys.835.27528
http://zookeys.pensoft.net

RESEARCH ARTICLE

A peer-reviewed open-access journal
ZooKeys
Launched to accelerate biodiversity research

Three new species of *Chromis* (Teleostei, Pomacentridae) from mesophotic coral ecosystems of the Philippines

B. Gabriela Arango[1], Hudson T. Pinheiro[1], Claudia Rocha[1], Brian D. Greene[2], Richard L. Pyle[2], Joshua M. Copus[3], Bart Shepherd[4], Luiz A. Rocha[1]

1 *Department of Ichthyology, California Academy of Sciences, 55 Music Concourse Dr., San Francisco, CA 94118, USA* **2** *Bernice P. Bishop Museum, Honolulu, HI 96817, USA* **3** *Department of Biology, University of Hawai'i at Mānoa, Hawai'i Institute of Marine Biology, Kāne'ohe, HI 96744, USA* **4** *Steinhart Aquarium, California Academy of Sciences, 55 Music Concourse Dr., San Francisco, CA 94118, USA*

Corresponding author: *B. Gabriela Arango* (Garango@calacademy.org)

Academic editor: *S. Kullander* | Received 15 June 2018 | Accepted 24 February 2019 | Published 4 April 2019

http://zoobank.org/CB272EFD-80D3-4C74-995C-69922D1BE401

Citation: Arango BG, Pinheiro HT, Rocha C, Greene BD, Pyle RL, Copus JM, Shepherd B, Rocha LA (2019) Three new species of *Chromis* (Teleostei, Pomacentridae) from mesophotic coral ecosystems of the Philippines. ZooKeys 835: 1–15. https://doi.org/10.3897/zookeys.835.27528

Abstract

Three new species of *Chromis* (Perciformes, Pomacentridae) from the Philippines, collected between 75–150 m depth, are described by a combination of morphological features and their coloration. *Chromis gunting* **sp. n.** was found in Batangas and Oriental Mindoro, and differs from its congeners in body depth (2.1–2.2 in SL), and color of adults, light brown, with a silver area on the anterior end and a bilateral black margin along the exterior side of the tail. It is most similar to *C. scotochiloptera*, with a 5.3% genetic divergence in COI. *Chromis hangganan* **sp. n.** was found around Lubang Island. Body depth (1.9–2.0 in SL) and adult coloration (yellowish with dark black outer margins on dorsal and anal fins) also separate this species from its congeners. It is most similar to *C. pembae*, with a 2.5% genetic divergence. *Chromis bowesi* **sp. n.** was found in Batangas, and also differs from its congeners by the combination of body depth (1.5–1.6 in SL), and color of adults (brownish grey in the dorsal side to whitish on the ventral side, with alternating dark and light stripes in the sides of body). It is most similar to *C. earina*, with a 3.6% genetic divergence in COI.

Keywords

Coral triangle, damselfish, deep reefs, planktivore, rebreather diving, reef fish, taxonomy

Introduction

Mesophotic coral ecosystems (MCEs; 30–150 m), also called the coral-reef "twilight zone", are uncommonly visited and relatively poorly-known deeper extensions of the coral-reef ecosystem (Rocha et al. 2018). Compared to shallow reefs, little is known about MCEs, mostly because they are beyond safe non-technical SCUBA diving depths (Pyle 2000). Submarines, remotely operated vehicles, or technical diving and special equipment (rebreathers and mixed gases) are needed to explore these depths (Pinheiro et al. 2016, Pyle et al. 2016, Baldwin et al. 2018). The rate of new species discovery within MCEs has been high (Pyle 2000), exceeding rates of discovery in any other marine habitat. As we are currently facing a decimation of coral reefs around the world due to anthropogenic impacts (Bellwood et al. 2004, Hughes et al. 2017), it is imperative that we study MCEs in an effort to understand their biodiversity and the threats they face.

The Pomacentridae (damselfishes and anemonefishes) is one of the largest families of reef fishes, with over 330 described species (Michael 2008) and varied morphological characters. The genus *Chromis* Cuvier, 1814, is composed of predominantly planktivorous species, and several studies have shown that the relative abundance of this group increases with depth (Thresher and Colin 1986, Bejarano et al. 2014, Pinheiro et al. 2016, Coleman et al. 2018). *Chromis* is the largest damselfish genus, with 103 described species, at least ten of which are found only on MCEs, below 60m (Allen and Erdmann 2012). The aim of this paper is to describe three new species of *Chromis* discovered during three expeditions conducted between 2013 and 2015 in the Philippines.

Materials and methods

Specimens were collected during expeditions to Batangas, Lubang, Puerto Galera, and Verde Island, Philippines, organized by the California Academy of Sciences, the Hawaii Institute of Marine Biology, and the Bishop Museum from 2013 to 2015. The research team used technical diving to access reefs and rocky structures at depths between 60–150 m. All species were collected using hand nets or a Hawaiian sling. The specimens were deposited in the fish collection of the Philippines National Museum of Natural History (**PNM**), the California Academy of Sciences (**CAS**), the Bernice Pauahi Bishop Museum (**BPBM**), and the United States National Museum (**USNM**). Comparative material was obtained from the California Academy of Sciences (CAS) ichthyology collection.

Counts were made using a stereo microscope, and morphological characters were measured with a digital caliper, to the nearest 0.01 mm and rounded to one decimal place, following Allen and Randall (2004) and Pyle et al. (2008). Rudimentary (spiniform) caudal fin-rays are those situated anteriorly to procurrent caudal-fin rays, only visible in X-radiographs. Vertebral counts include the first vertebra fused to the skull, and the last vertebra fused to the hypural plate. Measurements presented in the text are proportions of standard length (SL). Counts, measurements, and proportions inside

parenthesis represent ranges for paratypes, when different from the holotype. Values separated by a pipe character ("|") represent left|right sides of specimens. Molecular analysis and PCR amplification of the standard barcode fragment of the mitochondrial cytochrome c oxidase subunit I gene (COI) was performed following protocols established by the Center for Comparative Genomics laboratory (Sellas 2014) and compared with more than 60 other species of *Chromis* available from GenBank and the tissue collection at the California Academy of Sciences. Primers used were BOLFishF1/BOLFishR1 for every sample except for CAS 242278, which used FishF2/FishR2, following Weigt et al. (2012). Alignments of DNA sequences were done using the program Geneious 9.1.5 (Kearse et al. 2012). Genetic distances were calculated using Tamura-Nei model (Tamura and Nei 1993). New sequences were deposited in GenBank with the following accession numbers: *Chromis gunting* sp. n. (MH170474), *Chromis hangganan* sp. n. (MH170475 and MH170476), and *Chromis bowesi* sp. n. (MH170477, MH170478 and MH170479). Additional new sequences include: holotype of *Chromis earina* Pyle, Earl & Greene, 2008 (MH170472), *Chromis pembae* Smith, 1960 (MK049176), and *Chromis scotochiloptera* Fowler, 1918 (MK059781). We also used the following sequences from GenBank for comparisons: *Chromis analis* Cuvier, 1830 (JF493172.1), *Chromis cinerascens* Cuvier, 1830 (KU944441.1), *Chromis degruyi* Pyle, Earle & Greene, 2008 (EU358588.1), and *Chromis woodsi* Bruner & Arnam, 1979 (HM421816.1).

Results

***Chromis gunting* sp. n.**
http://zoobank.org/9BE50EAC-224B-4E20-B40A-19F6BD747EC9
Suggested English name: Scissors Chromis
Figure 1a–c, Table 1

Type material. Holotype: PNM 15357 (field code: LAR 1762). 67.7 mm SL, GenBank MH170474, Layaglayag point, Batangas, Philippines. 13°41'22.74"N, 120°50'12.46"E, 100 m, BD Greene and RL Pyle, 6 December 2013 (Figure 1a–c). **Paratype:** CAS 242328 (field code: HTP 509). 77.4 mm SL, Puerto Galera, Oriental Mindoro, Philippines. 13°31'17.68"N, 120°59'41.78"E, 100 m, LA Rocha, HT Pinheiro, B Shepherd, E Jessup and BD Greene, 9 April 2015.

Diagnosis. The following combination of characters distinguishes *Chromis gunting* sp. n. from all of its congeners: dorsal-fin rays XIII,11; anal-fin rays II,11–12; pectoral-fin rays 16–17; procurrent caudal-fin rays 3; tubed lateral-line scales 14–16; gill rakers 4–5+14–16 (total 19–20); body depth 2.1–2.2 in SL; color of adults when fresh is light brown, with a silver area on the anterior end and a bilateral black margin along the exterior side of the tail.

Description. Dorsal-fin rays XIII, 11 (XIII, 11); anal-fin rays II,11 (II,12); all dorsal and anal-fin rays branched, the last to base; pectoral-fin rays 16 (17), the up-

per and lowermost unbranched; pelvic-fin rays I,5; principal caudal-fin rays 7+6=13 (6+6=12); upper and lower procurrent caudal-fin rays 3; upper and lower rudimentary (spiniform) caudal-fin rays 2 and 2 respectively (3 and 3); tubed lateral-line scales 16|15 (14|damaged); posterior midlateral scales with a pore 7|7 (5|6); scales above dorsal fin to origin of dorsal fin 3|3; scales below lateral line to origin of anal fin 8|8 (7|7); circumpeduncular scales 12 (11); gill rakers 5+14=19 (4+16=20); vertebrae 25 (10 precaudal + 15 caudal).

Body depth 2.1 (2.2) in SL, and width 2.6 (2.4) in body depth; head length 3.2 (3.1) in SL; dorsal profile of head with slight convexity anterior to eye, straight dorsal to eye, and slight convexity on nape; snout length 8.0 (6.1) in head length; orbit diameter 2.6 (2.3) in head length; interorbital width 2.7 (2.4) in head length; caudal-peduncle depth 2.1 (2.4) in head length; caudal-peduncle length 2.4 (2.6) in head length.

Mouth terminal, oblique, upper jaw angle of about 35°; maxilla posterior edge vertical at anterior edge of pupil, upper jaw length 2.6 (3.1) in head length; teeth multi-serial, outer row of conical teeth in each jaw, largest anteriorly; narrow band of villiform teeth lingual to outer row, in 2–3 irregular rows anteriorly, narrowing to a single row on side of jaws; tongue triangular with rounded tip; gill rakers long and slender, longest on lower limb near angle almost two-thirds length of longest gill filaments; nostril without fleshy rim, located at level of middle of pupil.

Opercle ending posteriorly in flat spine, tip relatively obtuse and obscured by large scale; preopercle margin smooth, posterior margin extending dorsally to level of upper edge of pupil; suborbital with free lower margin extending nearly to a vertical at posterior edge of pupil. Scales finely ctenoid; anterior lateral line ending beneath rear portion of spinous dorsal fin (between 12th and 13th dorsal-fin spines); head scaled except lips; narrow scaly sheath at base of dorsal and anal fins, progressively wider on soft portion; column of scales on each membrane of dorsal fin, narrowing distally, those on spinous portion of dorsal progressively longer, reaching about half the distance to spine tips on posterior membranes; scales on anal-fin membrane in one column, progressively smaller distally; small scales on caudal fin extending slightly more than three-fourths distance to posterior margin; small scales on basal one-fifth of pectoral fins; median scaly process extending posteriorly from between base of pelvic fins, its length about half that of pelvic spine; axillary scale above base of pelvic spine slightly more or less than one-third length of spine.

Color. Fresh adult specimens (Figure 1a) brown dorsally, changing gradually to pinkish on center of body, to silver ventrally. Black margin along spinous dorsal fin, and on dorsal and ventral margins of caudal fin and peduncle. Soft dorsal fin translucent with dark rays. Anterior two-thirds of anal fin black, posterior with yellowish base and translucent bottom half with dark rays. Pectoral fin base gray, pectoral fin translucent with dark margins on rays. Pelvic fins light brown, almost translucent, with yellow membranes on basal half and gray rays. Color in alcohol similar to live specimen, but body overall browner, and shiny silver portions of anterior ventral portion replaced with whitish silver color.

Etymology. The name *Chromis gunting* sp. n. means scissors in Tagalog, in reference to the bilateral outermost black margins of fish's caudal fin that gives it the appearance of scissors. To be treated as a noun in apposition.

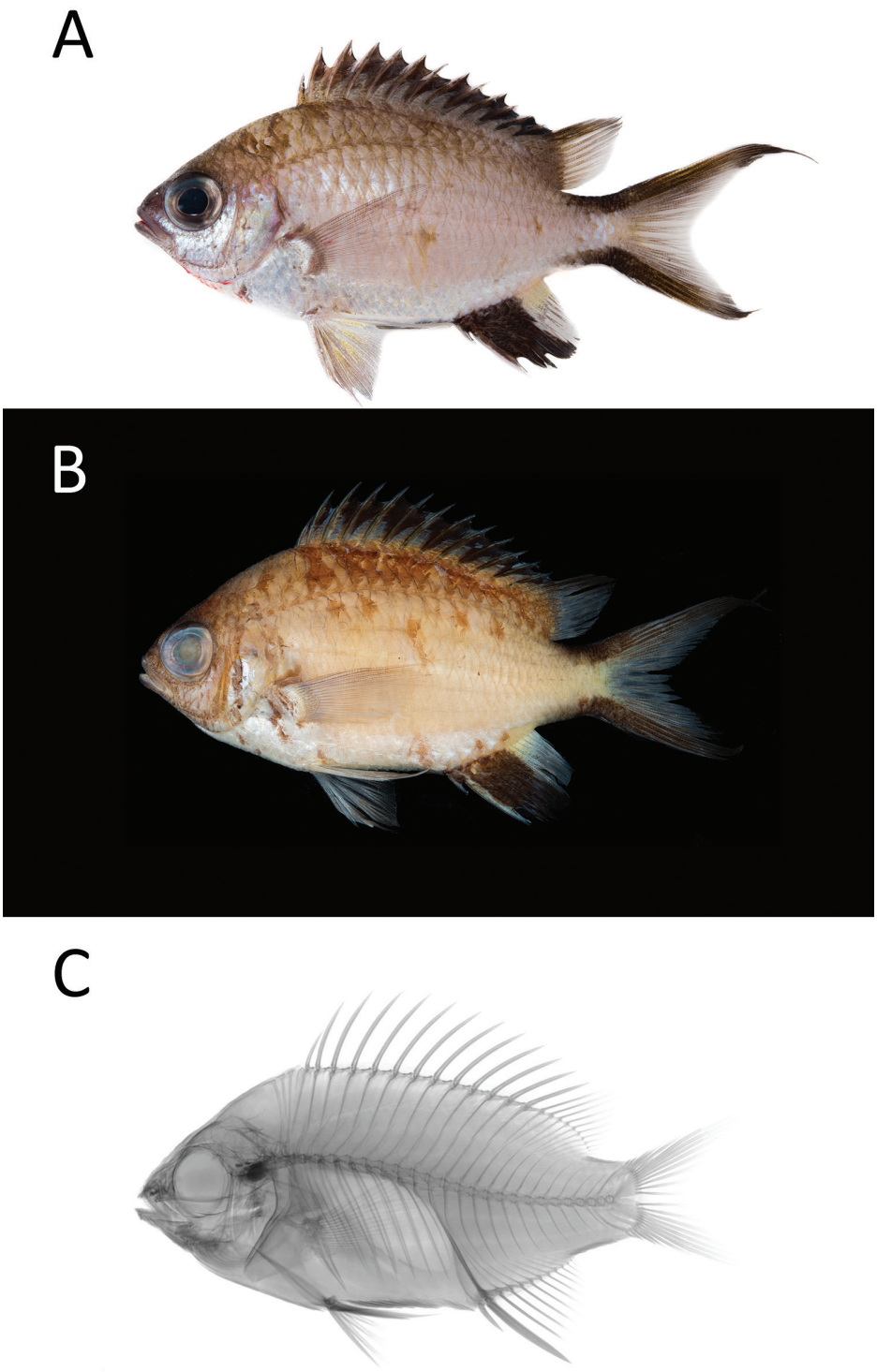

Figure 1. *Chromis gunting* sp. n. PNM 15357 **a** holotype shortly after death, 67.69 mm SL, photograph LA Rocha **b** preserved holotype, photograph JD Fong **c** radiograph of holotype by JD Fong.

Table 1. Percent measurements (%SL) of *Chromis gunting* sp. n., *C. hangganan* sp. n., and *C. bowesi* sp. n. Counts and measurements for the holotype are presented followed by ranges for paratypes (in parentheses). Values separated by a pipe "|" are left|right or upper|lower. Values that do not overlap between species of *Chromis* are in bold.

	Chromis gunting		*Chromis hangganan*		*Chromis bowesi*				
	Holotype PNM 15357	**Paratype CAS 242328**	**Holotype PNM 15358**	**Paratype CAS 243205**	**Holotype PNM 15359**	**Paratype CAS 242278**	**Paratype CAS 242324**	**Paratype BPBM 41350**	**Paratype USNM 440406**
Standard length (mm)	67.7	77.4	57.8	47.9	82.1	77.5	66.0	77.5	78.3
Body depth	**48.1**	**45.8**	52.5	50.0	**66.0**	**64.0**	**60.8**	**67.5**	**65.5**
Body width	**18.6**	**19.2**	17.7	16.3	**18.6**	**20.1**	**18.1**	**20.1**	**20.5**
Head length	31.7	32.4	33.1	31.6	30.4	36.7	33.2	30.7	33.2
Snout length	4.0	5.3	6.1	4.4	4.0	5.6	6.5	3.9	4.6
Orbit diameter	12.3	14.3	11.8	11.8	11.9	12.6	12.5	12.9	13.3
Interorbital width	11.8	13.6	11.4	9.7	12.6	12.0	12.0	13.0	13.2
Caudal-ped. depth	15.4	13.4	14.7	15.2	16.3	16.7	15.1	16.1	15.6
Caudal-ped. length	13.5	12.5	13.4	12.7	**10.6**	**9.6**	**8.6**	**10.6**	**8.6**
Upper jaw length	12.1	10.4	10.2	9.5	9.8	10.6	10.3	9.6	9.3
Predorsal length	43.4	45.5	47.4	46.2	44.5	46.0	43.4	46.0	47.1
Spinous dorsal-fin base	47.5	43.3	44.2	43.5	49.6	44.7	46.1	51.3	50.7
Soft dorsal-fin base	13.7	13.2	**16.0**	**16.0**	**18.4**	**20.2**	**17.4**	**18.0**	**17.5**
1st dorsal spine	8.7	9.1	6.9	7.8	8.2	8.4	9.4	7.8	6.6
2nd dorsal spine	14.5	14.0	12.8	14.1	14.8	13.7	13.0	14.6	13.0
3rd dorsal spine	17.3	16.4	15.7	16.0	18.4	17.4	16.4	17.8	15.9
4th dorsal spine	18.2	18.9	19.6	17.8	18.6	18.9	16.9	19.8	18.1
5th dorsal spine	22.3	20.2	17.0	18.3	18.8	20.6	19.4	20.3	17.7
6th dorsal spine	17.3	17.8	**17.0**	**17.1**	17.7	21.8	18.6	19.9	18.2
Last dorsal spine	14.8	11.7	13.1	11.7	12.7	17.5	14.0	13.9	14.6
Longest dorsal ray	23.4	21.7	**17.2**	**18.0**	23.7	27.6	25.7	24.3	24.6
Preanal length	71.5	71.0	77.3	78.7	71.0	76.1	77.4	71.2	73.5
1st anal spine	7.0	7.6	7.4	8.0	7.2	8.7	7.3	7.1	6.5
2nd anal spine	20.6	19.1	21.5	22.2	23.9	26.0	21.7	24.1	21.7
Longest anal ray	21.3	19.4	19.8	21.2	22.0	21.8	23.3	20.0	22.0
Anal-fin base	21.3	19.5	20.8	21.8	**26.6**	**25.9**	**26.04**	**28.0**	**26.1**
Caudal fin length	41.2	32.5	35.0	broken	38.7	44.1	38.3	38.2	38.6
Caudal concavity	21.4	14.3	16.4	broken	18.8	23.6	20.8	19.3	20.2
Longest pectoral ray	28.9	30.8	28.7	31.9	34.0	40.0	38.9	37.7	36.9
Prepelvic length	44.3	42.7	48.6	40.4	42.6	52.0	51.1	44.1	46.0
Pelvic-spine length	**18.5**	**17.9**	18.9	19.7	19.5	20.5	19.9	18.8	18.9
1st pelvic soft ray	26.8	29.3	25.9	21.5	26.9	34.6	34.1	23.7	28.3

Distribution and habitat. *Chromis gunting* sp. n. is only known from the Verde Island Passage, in Puerto Galera and Batangas. The species was recorded on MCEs at depths of 90–130 m.

Chromis hangganan sp. n.

http://zoobank.org/CCF56742-B8B7-410E-B15B-8CD7CBD5CAD0
Suggested English name: Dark-margin Chromis
Figure 2a, b, Table 1

Type material. Holotype: PNM 15358 (field code: HTP 352). 57.8 mm SL, GenBank MH170475, Lubang, Philippines. 13°45'44.71"N, 120°07'38.31"E, 130 m, RL

Pyle and BD Greene, 16 May 2014 (Figure 2a, b). **Paratype:** CAS 243205 (field code: HTP 355). 47.9 mm SL, GenBank MH170476, Lubang, Philippines. 13°45'44.71"N, 120°07'38.31"E, 130 m, RL Pyle and BD Greene, 16 May 2014.

Diagnosis. The following combination of characters distinguishes *Chromis hangganan* sp. n. from all of its congeners: dorsal-fin rays XIII, 10–12; anal-fin rays II,11–12; pectoral-fin rays 18; procurrent caudal-fin rays 3; tubed lateral-line scales 16; gill rakers 7+16–19 (total 23–26); body depth 1.9–2.0 in SL; color of adults when fresh yellowish with dark black margins on dorsal and anal fins.

Description. Dorsal-fin rays XIII, 10 (paratype XIII, 12); anal-fin rays II,11 (paratype II,12); all dorsal and anal-fin rays have branched tips; pectoral-fin rays 18, the upper and lowermost unbranched; pelvic-fin rays I,5; principal caudal-fin rays 8+7=15; upper and lower procurrent caudal-fin rays 3; upper and lower rudimentary (spiniform) caudal-fin rays 2 and 1 respectively (paratype 2 and 2); tubed lateral-line scales 16|16; posterior midlateral scales with a pore 9|10 (paratype 10|10); scales above dorsal fin to origin of dorsal fin 3|3 (paratype 2|3); scales below lateral line to origin of anal fin 8|8; circumpeduncular scales 11 (11); gill rakers 7+19=26 (paratype 7+16= 23); vertebrae 25 (11 precaudal + 14 caudal).

Body depth 1.9 (paratype 2.0) in SL, and width 3.0 (3.1) in body depth; head length 3.0 (3.2) in SL; snout very short, length 5.4 (7.1) in head length; orbit diameter 2.8 (2.7) in head length; interorbital width 2.9 (3.2) in head length; caudal-peduncle depth 2.3 (2.1) in head length; caudal-peduncle length 2.5 (2.5) in head length.

Mouth terminal, small, oblique, upper jaw angle of 35°; maxilla posterior edge beyond anterior edge of eye, upper jaw length 3.3 (3.3) in head length; gill rakers long and slender, longest on lower limb near angle about the length of longest gill filaments; nostril without fleshy rim, located above level of middle of pupil.

Opercle ending posteriorly in internal spine, obscured by scales; preopercle margin smooth, posterior margin extending on the top edge of pupil; suborbital with free lower margin extending nearly to a vertical at posterior edge of pupil. Scales finely ctenoid; anterior lateral line ending beneath the 13th dorsal-fin spine; head scaled except lips, tip of snout, and a narrow zone from orbit to edge of snout containing nostrils; scaly sheath at base of dorsal and anal fins; column of scales on membranes, spines and rays of dorsal and anal fins, progressively smaller distally; small scales on caudal fin extending slightly more than two-thirds distance to posterior margin; small scales on basal one-fifth of pectoral fins; median scaly process extending posteriorly from between base of pelvic fins, its length slightly more than half that of pelvic spine; axillary scale above base of pelvic spine slightly more than one-fifth length of spine.

Color. Images of fresh specimens not available. Our field notes characterize fresh specimens of *Chromis hangganan* sp. n. as having a yellowish body color, with light yellow caudal peduncle and caudal fin. Body overall brown, darker dorsally. Black outer margins of the spinous dorsal and anal fins, and yellowish dorsal rays. Ventral margin of body and anal fin spines also black. Anal-fin rays yellowish. Anterior (mouth and snout) and dorsal (nape) portions of the head and orbit dark brown. Ventral portion of head light brown. Black dot on dorsal 1/5 of pectoral fin base and axilla.

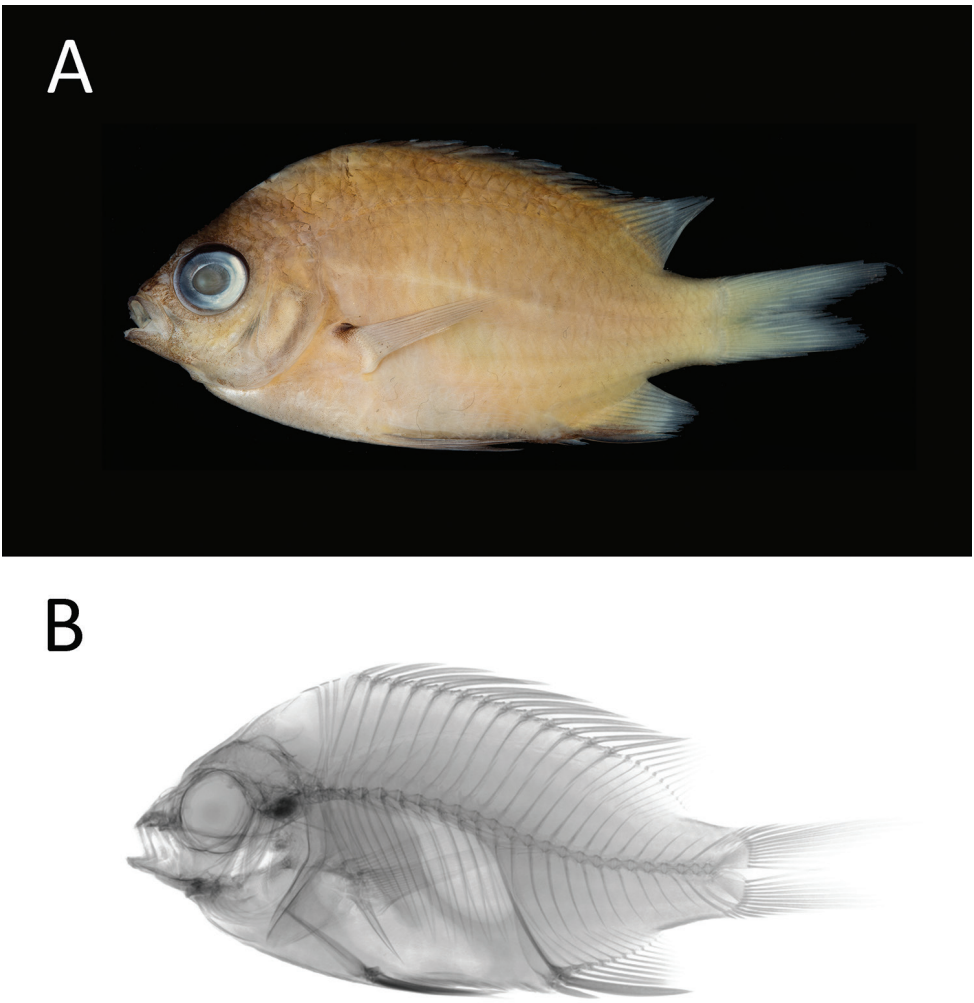

Figure 2. *Chromis hangganan* sp. n. PNM 15358 **a** holotype preserved in alcohol, 57.75 mm SL **b** radiograph (photographs JD Fong).

Etymology. The name *hangganan* means border in Tagalog, in reference to the black margins of the dorsal and anal fins. To be treated as a noun in apposition.

Distribution and habitat. Lubang Island, Philippines. Despite dives in several sites of the Verde Island Passage (VIP), Philippines, this species has not been collected outside of Lubang. The Lubang Island environment differs from the other survey sites in the Verde Island Passage by having more exposed and clearer oceanic waters, probably due to its proximity to the South China Sea. The species was recorded on MCEs at depths of 90–130 m.

***Chromis bowesi* sp. n.**
http://zoobank.org/25F8CF1E-1DF8-469A-B5A9-D2D9C20EA863
Suggested English name: Rhomboid Chromis
Figure 3a–c, Table 1

Type material. Holotype: PNM 15359 (field code: LAR 1851). 82.1 mm SL, GenBank MH170477, Dive and Trek, Batangas, Philippines. 13°48'3.52"N, 120°54'38.88"E, 120 m, RL Pyle and BD Greene, 12 December 2013 (Figure 3a–c). **Paratypes:** BPBM 41350 (field code: LAR 1852), 77.5 mm SL, GenBank MH170478, Dive and Trek, Batangas, Philippines. 13°48'3.52"N, 120°54'38.88"E, 120 m, RL Pyle and BD Greene, 12 December 2013. USNM 440406 (field code: LAR 1869), 78.3 mm SL, GenBank MH170479, Dive and Treck, Batangas, Philippines. 13°48'3.52"N, 120°54'38.88"E, 120 m, RL Pyle and BD Greene, 14 December 2013. CAS 242324 (field code: HTP 511), 66.0 mm SL, Puerto Galera Bay, Oriental Mindoro, Philippines. 13°31'339"N, 120°960'E, 105 m, LA Rocha, HT Pinheiro, B Shepherd, E Jessup, and BD Greene, 9 April 2015. CAS 242278 (field code: HTP 524), 77.5 mm SL, Verde Island, Batangas, Philippines. 13°31'941"N, 121°06'196"E, 110 m, LA Rocha, HT Pinheiro, E Jessup, and BD Greene, 12 April 2015.

Diagnosis. The following combination of characters distinguishes *Chromis bowesi* sp. n. from all of its congeners: dorsal-fin rays XIII,11–12; anal-fin rays II,11–13; pectoral-fin rays 17–19; procurrent caudal-fin rays 3; tubed lateral-line scales 13–15; gill rakers 6–9+18–19 (total 25–27); body depth 1.5–1.6 in SL; color of adults when fresh brownish grey in the dorsal side to whitish on the ventral side, with alternating dark and light stripes in the sides of body.

Description. Dorsal-fin rays XIII, 12 (two paratypes XIII, 11); anal-fin rays II,12 (one paratype II,11 and two paratypes II,13); all dorsal and anal-fin rays branched, the last to base in some specimens; pectoral-fin rays 18 (one paratype 17 and other 19), the upper and lowermost unbranched; pelvic-fin rays I,5; principal caudal-fin rays 8+7=15 (one paratype 7+6=13 and other 7+7=14); upper and lower procurrent caudal-fin rays 3; upper and lower rudimentary (spiniform) caudal-fin rays 2 and 3 respectively (three paratypes 2 and 2 and one 3 and 2); tubed lateral-line scales 14|14 (other paratypes 13|13, 13|14 and 14|15); posterior midlateral scales with a pore 8 |8 (three paratypes 7|7 and one 7|8); scales above dorsal fin to origin of dorsal fin 3|3 (one paratype 2|2); scales below lateral line to origin of anal fin 8|8; circumpeduncular scales 12 (12); gill rakers from two paratypes 9+18=27 and 6+19=25; vertebrae 26 (11 precaudal + 15 caudal).

Body depth 1.5 (paratypes 1.5–1.6) in SL, and width 3.5 (3.2–3.4) in body depth; head length 3.3 (2.7–3.3) in SL; dorsal profile of head with slight convexity anterior to eye, slight concavity dorsal to eye, and slight convexity on nape; snout very short, length 7.5 (5.1–7.9) in head length; orbit diameter 2.6 (2.4–2.9) in head length; interorbital width 2.4 (2.4–3.1) in head length; caudal-peduncle depth 1.9 (1.9–2.2) in head length; caudal-peduncle length 2.9 (2.9–3.9) in head length.

Mouth terminal, small, oblique, upper jaw forming an angle of 50°; maxilla posterior edge beyond anterior edge of orbit, upper jaw length 3.1 (3.2–3.6) in head length;

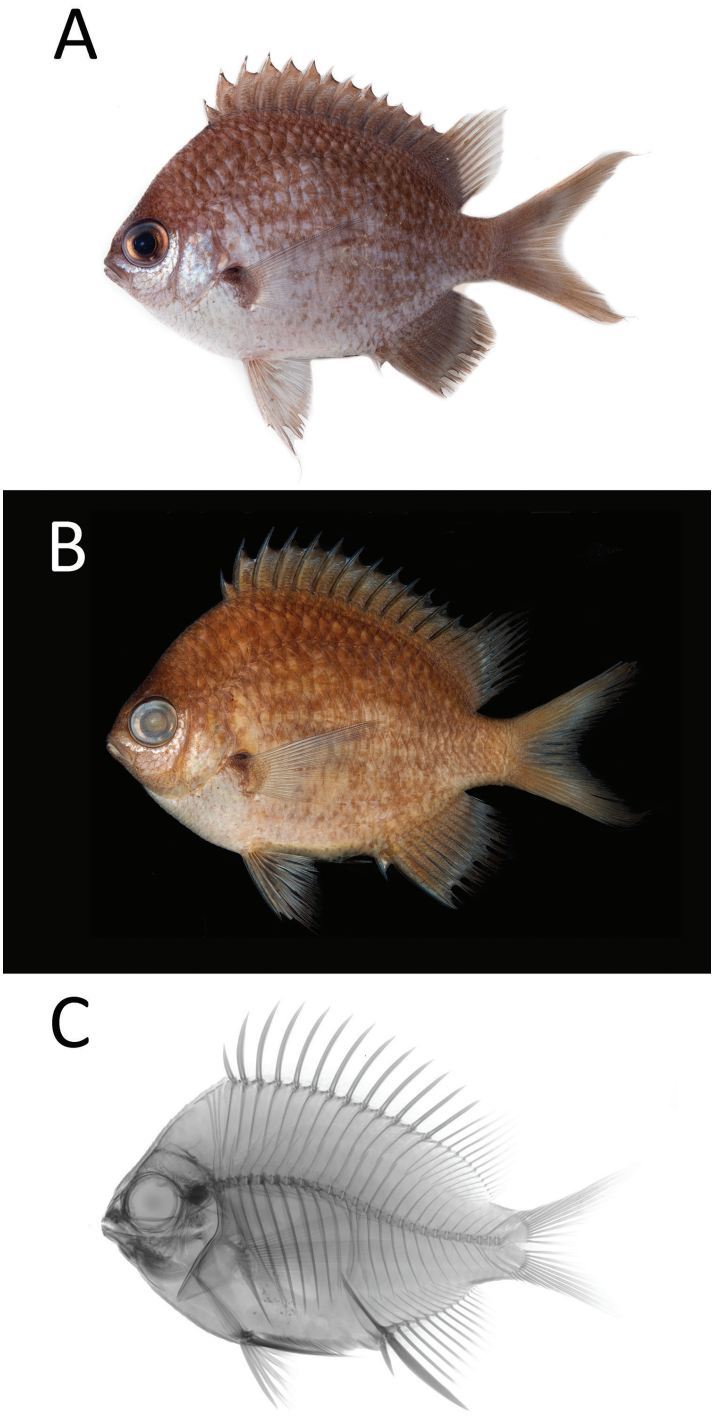

Figure 3. *Chromis bowesi* sp. n. PNM 15359 **a** holotype shortly after death, 82.07 mm SL, photograph LA Rocha **b** preserved specimen, photograph JD Fong **c** radiograph JD Fong.

teeth multi-serial, outer row of conical teeth in each jaw, largest anteriorly; narrow band of villiform teeth lingual to outer row, in two irregular rows anteriorly, narrowing to a single row on side of jaws; tongue oblong with rounded tip; gill rakers long and slender, longest on lower limb near angle about the same length of longest gill filaments; nostril with fleshy elevated rim, located above level of middle of pupil.

Opercle ending posteriorly in flat spine, tip relatively obtuse and obscured by large scale; preopercle margin smooth, posterior margin extending dorsally to level of upper edge of pupil; suborbital with free lower margin extending nearly to a vertical at posterior edge of pupil. Ctenoid scales; anterior lateral line ending beneath rear portion of spinous dorsal fin (between 10th and 11th dorsal-fin spines); head scaled except lips, tip of snout, and a narrow zone from orbit to edge of snout containing nostrils; narrow scaly sheath at base of dorsal and anal fins, about two-thirds pupil diameter at base of middle of spinous portion of dorsal fin, progressively narrower on soft portion; two columns of scales on each membrane of dorsal fin, narrowing distally, those on spinous portion of dorsal progressively longer, reaching about two-thirds distance to spine tips on posterior membranes; scales on anal-fin membrane in two columns, progressively smaller distally; small scales on caudal fin extending slightly more than one-third distance to posterior margin; small scales on basal one-fifth of pectoral fins; median scaly process extending posteriorly from between base of pelvic fins, its length about half that of pelvic-fin spine; axillary scale above base of pelvic-fin spine large, slightly more than two-thirds length of spine.

Color. Within its natural habitat, *Chromis bowesi* sp. n. has purplish blue body, with distinctive vertical faint light blue bar just behind pectoral fin. Spinous dorsal and pelvic fins light blue to white; soft dorsal translucent. Specimens photographed shortly after death (Figure 3a) are dark grayish brown dorsally, fading to light silvery white ventrally. Transition from dorsal to ventral sides marked by alternating indistinct light and dark stripes. Ventral portion of head below center of eye silvery white. Black blotch on upper base of pectoral fin. Spinous dorsal fin membranes brown with dark outer margin; proximal one-fourth of soft dorsal fin brown, distal three-fourths translucent with brown rays; anal fin dark brown with transverse lighter line located three-fourths to the edge of fin. Caudal fin same color and pattern as anal fin. Pelvic fin mostly whitish gray with light brown at base and distal end of fin. Color in alcohol similar to fresh color, except darker brown (Figure 3b).

Etymology. In honor of the late William K Bowes Jr, lead donor of the Hope for Reefs initiative from the California Academy of Sciences, we name *Chromis bowesi* sp. n. A pioneering venture capitalist and visionary Bay Area philanthropist, Bill Bowes was devoted to advancing science and generously supported groundbreaking research spanning across biotech, medical, and other scientific disciplines. The name is a noun in the genitive case.

Distribution and habitat. *Chromis bowesi* sp. n. was found in many localities of the Verde Island Passage, such as in Verde Island, Puerto Galera Bay, and Batangas Bay. The five specimens were recorded over low to moderate complexity habitats between 80 and 120 m depth. Specimens identified as *Chromis earina* were collected by Nishiy-

ama et al. (2012) in Iou-jima Island, Kagoshima Prefecture, Japan, between 70 and 80 m depth, but their mtDNA COI sequence and color description match *Chromis bowesi*, therefore this species is distributed at least to southern Japan. We also sequenced the holotype of *Chromis earina* and its sequence is clearly distinct from *C. bowesi*.

Discussion

The Verde Island Passage in the Philippines is known as the center of marine biodiversity (Carpenter and Springer 2005). However, little is known about its biodiversity at mesophotic depths (30–150 m) due to the previous lack of technical deep diving (Shepherd et al. 2018). The recent deep diving exploration of this region has led to the discovery of many new species (Anderson et al. 2016, Rocha et al. 2017), including the three species herein presented. Based on the rates of discovery, ongoing exploration should uncover many more species.

Species of *Chromis* are abundant on MCEs (Thresher and Colin 1986, Bejarano et al. 2014, Wagner et al. 2014, Pinheiro et al. 2016), and many of them have been recently discovered and described (e.g., Pyle et al. 2008). Ecological partitioning is known to drive diversification from highly diverse areas to peripheral habitats (Bowen et al. 2013). Thus, we believe that the intense competition on shallow coral reefs could be a factor leading to diversification and colonization of MCEs. The high relative abundance of *Chromis* in MCEs may be related to food (plankton) availability (Pinheiro et al. 2016). While other resources, such as corals and algae, are known to decrease with depth due to a decrease on sunlight, plankton is still abundant on MCEs, sustained mainly by currents, upwelling events and vertical migrations (Thresher and Colin 1986).

Among the new species, coloration and body depth are the most distinctive characters, information commonly used to distinguish *Chromis* species from each other (Allen and Erdmann 2009). Moreover, we compared the COI gene sequence of the new species with more than 60 other *Chromis* species available from GenBank and California Academy of Sciences. The closer relative of *C. gunting* seems to be *C. scotochiloptera*, a shallow water species endemic to the Coral Triangle. The closer relative of *C. hangganan* seems to be *C. pembae*, from shallow waters of the western Indian Ocean, and for *C. bowesi* seems to be *C. earina*, a conspicuous damselfish found in MCEs of the Western and Central Pacific, including the same reefs where we found *C. bowesi*. Although some *Chromis* species are missing for a complete phylogeny and understanding of the evolutionary history of the genus, these results indicate complex speciation processes, which can involve both sympatric and allopatric drivers.

Most of the species described here are only known from MCEs in the Philippines. However, they are not necessarily endemic species, as our knowledge of MCE biodiversity in the Indian and Pacific Oceans is very limited, and deep diving exploration is revealing new records of fishes in many different locations (Wagner et al. 2014, Pinheiro et al. 2015, Simon et al. 2016). For example, *C. earina* and *C. degruyi*, species exclusive to MCEs originally described from central and south Pacific islands (Pyle et al. 2008),

Table 2. COI genetic Tamura-Nei divergence between *C. gunting* sp. n., *C. hangganan* sp. n., *C. bowesi* sp. n., and their closest relatives available from GenBank. Closest divergences are in bold.

	C. earina	*C. analis*	*C. gunting*	*C. cinerascens*	*C. degruyi*	*C. hangganan*	*C. pembae*	*C. bowesi*	*C. scotochiloptera*
Chromis analis	12.05								
Chromis gunting sp. n.	10.67	8.90							
Chromis cinerascens	12.74	11.41	5.98						
Chromis degruyi	5.59	10.83	10.28	12.32					
Chromis hangganan sp. n.	10.50	8.90	8.22	9.06	10.59				
Chromis pembae	10.50	9.05	9.13	9.06	10.44	**2.55**			
Chromis bowesi sp. n.	**3.61**	12.27	11.42	12.86	**4.52**	10.84	10.84		
Chromis scotochiloptera	12.22	10.43	**5.33**	**3.44**	11.22	8.74	8.81	11.90	
Chromis woodsi	9.98	**7.96**	7.02	9.42	9.64	7.96	**8.74**	**11.08**	**8.42**

are reported here for the first time from the Philippines (CAS 242296, CAS 243185). Moreover, genetic comparisons reveal that the prior report of *C. earina* from Iou-jima Island, Kagoshima Prefecture, Japan (Nishiyama et al. 2012), is actually *C. bowesi*, described in this study. The continued exploration of mesophotic coral ecosystems will likely reveal many more new species, and increase the known ranges of known species.

Acknowledgements

This work was funded by the generous support of donors who endorsed the California Academy of Sciences' Hope for Reefs Initiative, and through grants from the National Science Foundation to T Gosliner, R Mooi, G Williams, and LA Rocha (DEB 12576304) and Brian Bowen (OCE 1558852) and the Seaver Institute to B Bowen and RL Pyle. BG Arango received a REU DBI fellowship (REU 1358680). We are grateful to JD Fong for pictures and x-rays of the holotypes, to D Catania and D Dumale for providing museum collection numbers, and to J Hallas for providing training and help analyzing the sequences. We are also thankful to many colleagues who helped in the field and with discussions: M Bell, B Bowen, E Jessup, M Lane, N Nazarian, T Phelps, D Pence, R Whitton, and W Pulawski. Hollis, Poseidon, and Anilao Beach Club provided gear and logistical support. Philippines research and collecting permits (GP-0072-13, GP-0077-14, and GP-0085-15) were provided by the Bureau of Fisheries and Aquatic Resources. This is a collaborative research initiative with key Philippine partners including the former Secretary of Agriculture PJ Alcala; former Philippine Consul General M Paynor and the Consular staff in San Francisco; former BFAR Director AG Perez; BFAR colleagues, especially A Vitug and L Labe; and NFRDI colleagues, especially Acting Director D Bayate and N Romena.

References

Allen GR, Randall JE (2004) Two new species of damselfishes (Pomacentridae: *Chromis*) from Indonesian seas. Aqua, Journal of Ichthyology and Aquatic Biology 9: 17–24.

Allen GR, Erdmann MV (2009) Two new species of damselfishes (Pomacentridae: *Chromis*) from Indonesia. Aqua, International Journal of Ichthyology 15: 121–134.

Allen G, Erdmann M (2012) Reef Fish of the East Indies. Volumes I–III. Tropical Reef Research, Perth, Australia, 1292 pp.

Anderson WD, Greene BD, Rocha LA (2016) *Grammatonotus brianne*, a new callanthiid fish from Philippine waters, with short accounts of two other Grammatonotus from the Coral Triangle. Zootaxa 4173: 289–295. https://doi.org/10.11646/zootaxa.4173.3.7

Baldwin CC, Tornabene L, Robertson DR (2018) Below the mesophotic. Scientific Reports 8: 4920. https://doi.org/10.1038/s41598-018-23067-1

Bejarano I, Appeldoorn RS, Nemeth M (2014) Fishes associated with mesophotic coral ecosystems in La Parguera, Puerto Rico. Coral Reefs 33: 313–328. https://doi.org/10.1007/s00338-014-1125-6

Bellwood DR, Hughes TP, Folke C, Nyström M (2004) Confronting the coral reef crisis. Nature 429: 827–833. https://doi.org/10.1038/nature02691

Bowen BW, Rocha LA, Toonen RJ, Karl SA, ToBo L (2013) The origins of tropical marine biodiversity. Trends in Ecology and Evolution 28: 359–366. https://doi.org/10.1016/j.tree.2013.01.018

Carpenter KE, Springer VG (2005) The center of the center of marine shore fish biodiversity: The Philippine Islands. Environmental Biology of Fishes 72: 467–480. https://doi.org/10.1007/s10641-004-3154-4

Coleman RR, Copus JM, Coffey DM, Whitton RK, Bowen BW (2018) Shifting reef fish assemblages along a depth gradient in Pohnpei, Micronesia. PeerJ 6: e4650. https://doi.org/10.7717/peerj.4650

Hughes TP, Barnes ML, Bellwood DR, Cinner JE, Cumming GS, Jackson JBC, Kleypas J, Van De Leemput IA, Lough JM, Morrison TH, Palumbi SR, Van Nes EH, Scheffer M (2017) Coral reefs in the Anthropocene. Nature 546: 82–90. https://doi.org/10.1038/nature22901

Kearse M, Moir R, Wilson A, Stones-Havas S, Cheung M, Sturrock S, Buxton S, Cooper A, Markowitz S, Duran C, Thierer T, Ashton B, Meintjes P, Drummond A (2012) Geneious Basic: An integrated and extendable desktop software platform for the organization and analysis of sequence data. Bioinformatics 28: 1647–1649. https://doi.org/10.1093/bioinformatics/bts199

Nishiyama H, Dewa S, Chiba S, Motomura H (2012) First Japanese record of a damselfish, *Chromis earina* (Perciformes, Pomacentridae), from Iou-jima Island, Kagoshima Prefecture, Japan. Japanese Journal of Ichthyology 59: 61–67.

Pinheiro HT, Bernardi G, Rocha LA (2016) *Pempheris gasparinii*, a new species of sweeper fish from trindade island, southwestern atlantic (Teleostei, Pempheridae). ZooKeys 561: 105–115. https://doi.org/10.3897/zookeys.561.7263

Pinheiro HT, Goodbody-Gringley G, Jessup ME, Shepherd B, Chequer AD, Rocha LA (2016) Upper and lower mesophotic coral reef fish communities evaluated by underwater visual censuses in two Caribbean locations. Coral Reefs 35: 139–151. https://doi.org/10.1007/s00338-015-1381-0

Pinheiro HT, Mazzei E, Moura RL, Amado-Filho GM, Carvalho-Filho A, Braga AC, Costa PAS, Ferreira BP, Ferreira CEL, Floeter SR, Francini-Filho RB, Gasparini JL, Macieira RM, Martins AS, Olavo G, Pimentel CR, Rocha LA, Sazima I, Simon T, Teixeira JB, Xavier LB, Joyeux JC (2015) Fish biodiversity of the Vitoria-Trindade seamount chain, southwestern Atlantic: An updated database. PLoS ONE 10(3): e0118180. https://doi.org/10.1371/journal.pone.0118180

Pyle RL (2000) Assessing undiscovered fish biodiversity on deep coral reefs using advanced self-contained diving technology. MTS Journal 34: 82–91. https://doi.org/10.4031/MTSJ.34.4.11

Pyle RL, Boland R, Bolick H, Bowen BW, Bradley CJ, Kane C, Kosaki RK, Langston R, Longenecker K, Montgomery A, Parrish FA, Popp BN, Rooney J, Smith CM, Wagner D, Spalding HL (2016) A comprehensive investigation of mesophotic coral ecosystems in the Hawaiian Archipelago. PeerJ 4: e2475. https://doi.org/10.7717/peerj.2475

Pyle RL, Earle JL, Greene BD (2008) Five new species of the damselfish genus *Chromis* (Perciformes: Labroidei:Pomacentridae) from deep coral reefs in the tropical western Pacific. Zootaxa 1671: 3–31. http://www.mapress.com/zootaxa/2008/f/zt01671p031.pdf

Rocha LA, Pinheiro HT, Shepherd B, Papastamatiou YP, Luiz OJ, Pyle RL, Bongaerts P (2018) Mesophotic coral ecosystems are threatened and ecologically distinct from shallow water reefs. Science 361: 281–284. https://doi.org/10.1126/science.aaq1614

Rocha LA, Pinheiro HT, Wandell M, Rocha CR, Shepherd B (2017) *Roa rumsfeldi*, a new butterflyfish (Teleostei, Chaetodontidae) from mesophotic coral ecosystems of the Philippines. ZooKeys 709: 127–134. https://doi.org/10.3897/zookeys.709.20404

Ronquist F, Huelsenbeck JP (2003) MrBayes 3: Bayesian phylogenetic inference under mixed models. Bioinformatics 19: 1572–1574. https://doi.org/10.1093/bioinformatics/btg180

Shepherd B, Pinheiro HT, Rocha LA (2018) Ephemeral aggregation of the benthic ctenophore Lyrocteis imperatoris on a mesophotic coral ecosystem in the Philippines. Bulletin of Marine Science 94(1): 101–102.

Simon T, Pinheiro HT, Moura RL, Carvalho-Filho A, Rocha LA, Martins AS, Mazzei E, Francini-Filho RB, Amado-Filho GM, Joyeux JC (2016) Mesophotic fishes of the Abrolhos Shelf, the largest reef ecosystem in the South Atlantic. Journal of Fish Biology 89: 990–1001. https://doi.org/10.1111/jfb.12967

Tamura K, Nei M (1993) Estimation of the number of nucleotide substitutions in the control region of mitochondrial DNA in humans and chimpanzees. Molecular biology and evolution 10: 512–526. https://doi.org/10.1093/molbev/msl149

Thresher RE, Colin PL (1986) Trophic structure, diversity and abundance of fishes of the deep reef (30–300m) at Enewetak, Marshall Islands. Bulletin of Marine Science 38: 253–272.

Wagner D, Kosaki RK, Spalding HL, Whitton RK, Pyle RL, Sherwood AR, Tsuda RT, Calcinai B (2014) Mesophotic surveys of the flora and fauna at Johnston Atoll, Central Pacific Ocean. Marine Biodiversity Records 7: e68. https://doi.org/10.1017/S1755267214000785

Weigt LA, Baldwin CC, Driskell A, Smith DG, Ormos A, Reyier EA (2012) Using DNA barcoding to assess Caribbean reef fish biodiversity: Expanding taxonomic and geographic coverage. PLoS ONE 7(7): e41059. https://doi.org/10.1371/journal.pone.0041059

ZooKeys 835: 17–41 (2019)
doi: 10.3897/zookeys.835.33166
http://zookeys.pensoft.net

RESEARCH ARTICLE

A peer-reviewed open-access journal
ZooKeys
Launched to accelerate biodiversity research

New species of leaf-mining *Phyllonorycter* (Lepidoptera Gracillariidae) from Siberia feeding on *Caragana* (Fabaceae)

Natalia Kirichenko[1,2,3], Paolo Triberti[4], Carlos Lopez-Vaamonde[3,5]

1 *Sukachev Institute of Forest SB RAS, Akademgorodok 50/28, 660036, Krasnoyarsk, Russia* **2** *Siberian Federal University, 79 Svobodny pr., 660041, Krasnoyarsk, Russia* **3** *INRA, UR0633 Zoologie Forestière, F-45075 Orléans, France* **4** *Museo Civico di Storia Naturale, Lungadige Porta Vittoria 9, I37129, Verona, Italy* **5** *Institut de Recherche sur la Biologie de l'Insecte, CNRS UMR 7261, Université de Tours, UFR Sciences et Techniques, 37200 Tours, France*

Corresponding author: *Natalia Kirichenko* (nkirichenko@yahoo.com)

Academic editor: *E.J. van Nieukerken* | Received 17 January 2019 | Accepted 28 February 2019 | Published 4 April 2019

http://zoobank.org/513A51CC-3D0E-43CD-8260-FEE88EC0D706

Citation: Kirichenko N, Triberti P, Lopez-Vaamonde C (2019) New species of leaf-mining *Phyllonorycter* (Lepidoptera Gracillariidae) from Siberia feeding on *Caragana* (Fabaceae). ZooKeys 835: 17–41. https://doi.org/10.3897/zookeys.835.33166

Abstract

During a DNA barcoding campaign of leaf-mining Gracillariidae from the Asian part of Russia, a new species of *Phyllonorycter* Hübner, feeding on the Siberian pea shrub, *Caragana arborescens* Lam. (Fabaceae) was discovered in Siberia. Here, this taxon is described as *Phyllonorycter ivani* **sp. n.** Among Fabaceae-feeding *Phyllonorycter*, so far only *P. caraganella* (Ermolaev) has been known to develop on *Caragana*. *Phyllonorycter ivani* and *P. caraganella* show a large divergence in morphology (external and male genitalia) and barcode region of the mtDNA-COI gene (8.6%). They feed on different host plants species and have different ranges in Russia. We show that DNA barcode data weakly supports the Fabaceae-feeding species groups. In addition, we show that morphologically (strongly) and genetically (weakly), *P. ivani* has affinity to the *haasi* species group, a West Palearctic group with asymmetrical male genitalia.

Keywords
Leaf-mining micromoths, legume, DNA barcoding, male genitalia morphology, Siberian peashrub

Introduction

Siberia represents approximately 9% of Earth's land surface, and its vast boreal forests contain a diverse insect fauna with Lepidoptera being particularly well represented, accounting over 5000 species (Sinev 2008). Among Lepidoptera, micromoths show high species richness with some species being agricultural and forest pests and invaders (Kuznetzov 1999; Kirichenko et al. 2018a). Despite their ecological and economic importance, micromoths remain largely understudied (Sinev 2008; Lees et al. 2013; Lopez-Vaamonde et al. 2018).

In Siberia, leaf-mining micromoths and particularly the economically important family Gracillariidae have been the focus of recent studies, using DNA barcoding as a main tool to discover new species and host plant associations (Kirichenko et al. 2016, 2017, 2018b, 2018c, 2019; Akulov et al. 2018; Knyazev et al. 2018). Among Gracillariidae, the genus *Phyllonorycter* Hübner, 1822 is the most diverse, with more than 400 species described worldwide (De Prins and De Prins 2018) and over 200 species recorded from the Asian part of Russia (Baryshnikova 2008, 2016; Kirichenko et al. 2019), feeding on plants from various families (De Prins and De Prins 2018).

Legumes (Fabaceae) belonging to eight tribes (Desmodieae, Fabeae, Genisteae, Hedysareae, Loteae, Phaseoleae, Robinieae, and Trifolieae) (Roskov et al. 2019) have been known as hosts for 57 *Phyllonorycter* species that are mainly distributed in the Palearctic (51 species) and a few species found in the Nearctic (3), Afrotropics (2) and Indomalaya (1) (Suppl. material 1: Table S1). Of these 57 species, 39 (i.e., 68%) are known to be strictly monophagous, feeding on a single legume species (Suppl. material 1: Table S1).

The majority of the Palearctic Fabaceae-feeding *Phyllonorycter* (48 species, i.e., 84%) have asymmetrical male genitalia (Suppl. material 1: Table S1), with a large left valva showing a pronounced spine at apex and a narrow right valva, with almost parallel costal and ventral margins. A small group of five species has symmetrical genitalia with thin and parallel-sided valvae (Suppl. material 1: Table S1). All species with the asymmetric male genitalia, except *P. nigrescentella* (Logan, 1851), *P. insignitella* (Zeller, 1846), *P. tangerensis* (Stainton, 1872), and *P. viciae* (Kumata, 1963), and one species with symmetrical male genitalia, *P. cerasinella* (Reutti, 1853) develop on legumes belonging to the Genisteae (Laštůvka and Laštůvka, 2006). This is a highly diverse tribe of the subfamily Faboideae, largely distributed in western Palearctic (Ainouche et al. 2003). An extensive study of the *Phyllonorycter* species developing on Genistae defined three groups based on morphology of male genitalia: the *haasi*, *fraxinella*, and *ulicicolella* groups, all including species with asymmetrical male genitalia (Laštůvka

and Laštůvka 2006). Subsequent phylogenetic analysis reconsidered the placement of *P. phyllocytisi* (Hering, 1936), *P. eugregori* Laštůvka & Laštůvka, 2006, *P. telinella* Laštůvka & Laštůvka, 2006, and *P. nevadensis* (Walsingham, 1908) (Laštůvka et al. 2013) that do not fit in any of those species groups and thus occupy a relatively isolated position.

Among Fabaceae-feeding *Phyllonorycter*, *P. caraganella* (Ermolaev, 1986) is the only species known to feed on the legume genus *Caragana* (De Prins and De Prins 2018). This plant genus belongs to the tribe Hedysareae, a clade significantly divergent from Genisteae (LPWG et al. 2009). *Phyllonorycter caraganella*, of which the males have symmetrical genitalia, develops on *Caragana manshurica* Kom. and is found exclusively in the Russian Far East, in the southern part of Primorsky Krai, the region bordering with Northeast China (Ermolaev 1986; Baryshnikova 2016).

During fieldwork in Central and Eastern Siberia, we collected two *Phyllonorycter* larvae mining leaves of the Siberian pea shrub, *C. arborescens* Lam. Analysis of the DNA barcodes of those two larvae revealed a large molecular divergence with DNA barcodes of *P. caraganella*. Further sampling and rearing and detailed morphological examination of adults confirmed the existence of a new *Phyllonorycter* species feeding on *C. arborescens*. Here we provide the description of this new species, *Phyllonorycter ivani* Kirichenko, Triberti & Lopez-Vaamonde sp. n. and expand the morphological description of *P. caraganella* from the Russian Far East. We also investigate whether DNA barcodes support the different Fabaceae-feeding *Phyllonorycter* species groups that have been based on the morphology of male genitalia.

Materials and methods

Sampling

Leaves with mines of *P. ivani* were collected in Central Siberia in Krasnoyarsk Krai (in the suburb of the city Krasnoyarsk, along the Yenisei river bank) and in Eastern Siberia in Transbaikal Krai (in the city Chita, Victory park) on *C. arborescens* from July to August 2014–2016 (Fig. 1). These two locations are over 2000 km apart along Trans-Siberian railway (Fig. 1). In addition, leaf mines with *P. caraganella* were collected in the Russian Far East, in the southern part of Primorsky Krai in two neighbouring locations near by the villages Glukhovka and Rakovka on *Caragana manshurica* in July 2016 (Fig. 1).

In total, six larvae (two *P. ivani* and four *P. caraganella*) were preserved in 96% ethanol and 17 adult moths (nine *P. ivani* and eight *P. caraganella*) were reared from mines (Fig. 1, Suppl. material 2: Table S2). To obtain adults, leaves with mines containing mature larvae were kept in the plastic boxes (200ml) at constant conditions (22 °C, 55% RH, L:D 18:6 h photoperiod) following Ohshima's (2005) protocol. Additionally, 20 leaves with mines (some leaves with larvae in mines) were placed in the

Figure 1. The study region in Russia. Sampling locations are indicated by yellow circles: Krasnoyarsk and Chita for *Phyllonorycter ivani*, Rakovka and Glukhovka for *P. caraganella.* Number of specimens is given for each sampled location: A adults, L larva. Regions: **KK** Krasnoyarsk Krai, **TK** Transbaikal (Zabaikalsky) Krai, **PK** Primorsky Krai. The Trans-Siberian railway (the total distance of 9288.2 km between Moscow to Vladivostok) is shown by red line.

annotated herbarium collection in SIF SB RAS. In June-July 2015–2017, an extensive survey of *Caragana* growing in the botanical gardens, city plantations and forests was carried out in Siberia (Tyumen Oblast, Khanty-Mansy Autonomous Okrug, Tomsk Omsk, Novosibirsk, Kemerovo Oblasts, Altai Krai, the Republics of Tuva and Buryatia, Irkutsk Oblast) and in the Russian Far East (Amur Oblast, Sakhalin Island) to check for presence of *Phyllonorycter* mines on leaves.

Morphology and nomenclature

We examined the morphology of 17 dried and pinned specimens belonging to *P. ivani* (nine specimens) and *P. caraganella* (eight specimens). The adults of both species were photographed with Leica digital microscope DMS1000 and the incorporated digital camera and processed using the stacking system software Leica Application Suite LAS X. Genitalia were dissected from five *P. ivani* and four *P. caraganella* moths (Suppl. material 2: Table S2) and their photographs were taken with Sony Nex3 Camera from

Carl Zeiss Stemi DV4 Stereo Microscope. Leaf mines were photographed in the field and in the laboratory using a digital camera Sony Nex3. All images were edited in Adobe Photoshop CS5 Extended.

Genitalia dissection and slide mounting followed Robinson (1976). Terminology of the genitalia followed Klots (1970) and Kristensen (2003).

Specimen depositories

MSNV	Museo Civico di Storia Naturale, Verona, Italy.
SIF SB RAS	Sukachev Institute of Forest, Siberian Branch of the Russian Academy of Sciences, Krasnoyarsk, Russia.
INRA	Institut National de Recherche Agronomique, Orléans, France.

Molecular analyses

We DNA barcoded ten specimens of four Fabaceae-feeding *Phyllonorycter* species sampled in the Asian part of Russia: *P. ivani* (two larvae), *P. caraganella* (two adults and four larvae), *P. medicaginella* (Gerasimov, 1930) (one larva), and *P. viciae* (Kumata, 1963) (one larva) (Suppl. material 2: Table S2). In addition, 43 DNA barcodes, including 38 published sequences (De Prins et al. 2009; Laštůvka et al. 2013; Huemer and Hebert 2016; Mutanen et al. 2016), overall corresponding to 35 Fabaceae-feeding *Phyllonorycter* were added to the analysis (Suppl. material 2: Table S2).

DNA was extracted from larvae and adults using NucleoSpin® tissue XS kit, Macherey-Nagel, Germany according to the manufacturer's protocol. The COI barcode fragment (658 bp) was amplified via PCR using the primers LCO (5' GGT CAA CAA ATC ATA AAG ATA TTG G 3') and HCO (5' TAA ACT TCA GGG TGA CCA AAA AAT CA 3') following standard conditions for the reaction (Folmer et al. 1994). Purification of PCR products was done using the NucleoSpin® Gel and PCR Clean-up kit Macherey-Nagel, Germany. For sequencing the Sanger method with Abi Prism® Big Dye®Terminator 3.1cycle sequencing kit was applied (25 cycles of 10s at 96 °C, 5s at 50 °C, 4 min at 60 °C). Sequencing was carried out using a 3500 ABI genetic analyzer. Sequence were revised and aligned in CodonCode Aligner 3.7.1. (CodonCode Corporation). DNA sequences, voucher data, images, and trace files were deposited in the Barcode of Life Data Systems (BOLD) (Ratnasingham and Hebert 2007; www.barcodinglife.org) and are available via public dataset: dx.doi.org/10.5883/DS-FABPHYL. The consensus sequences were also deposited in GenBank.

Barcode Index Numbers (BINs) were assigned by BOLD (Ratnasingham and Hebert 2013). Intra – and interspecific genetic distances were estimated using the

Kimura 2-parameter and a multiparametric bootstrap test with 2000 iterations, with complete deletion (Kimura 1980). A Maximum Likelihood (ML) COI tree was built based on the Kimura 2-parameter model (Kimura 1980) and rooted using DNA barcode of the two *Sauterina hofmanniella* (Schleich, 1867) (Gracillariidae) specimens collected on *Lathyrus* sp. (Fabaceae) in Siberia. The outgroup was sequenced following the protocol described above. All computations were done in MEGA 7.0 (Kumar et al. 2016).

Results

Key to male genitalia and forewing pattern of the *haasi* species group and related species

1 At least a part of markings margined with dark scales **2**
– Markings not margined with dark scales **8**
2 White dorso-basal spot connected to basal streak **3**
– White dorso-basal spot not connected to basal streak or absent **4**
3 White dorso-basal spot elongate towards base ..... ***telinella****
– White dorso-basal spot not elongate towards base ..... ***purgantella***
4 First costal and dorsal strigulae connected at an obtuse angle ..... ***ivani****
– First costal and dorsal strigulae not connected and forming an acute angle **5**
5 First and second costal strigulae connected or separated by a few black scales; left valva about 2× as wide as right one ..... ***scopariella***
– First and second costal strigulae well separated; left valva about 6× as wide as right one **6**
6 Apex of first dorsal opposite first costal strigula **7**
– Apex of first dorsal opposite second costal strigula ..... ***tridentatae****
7 Four costal strigulae ..... ***haasi***
– Five costal strigulae ..... ***balansae***
8 Only two dorsal strigulae, the first forms a zig zag ..... ***deschkanus***
– More than two dorsal strigulae **9**
9 First costal and dorsal strigulae forming a slightly angled fascia, if interrupted, the two strigulae are only slightly inclined ..... ***estrela***
– First costal and dorsal strigulae always separated and inclined at an acute angle. **10**
10 Subapical area without dark scales; saccus little differentiated from vinculum ..... ***baldensis***
– Subapical area with suffusion of dark scales; saccus filiform, well distinct from the vinculum ..... ***floridae***

* species that have affinity to the *haasi* group but not belonging to it.

***Phyllonorycter ivani* sp. n.**
http://zoobank.org/842E3172-2931-445C-98A4-F9603A68B250
Figs 2A, B, 3–5

Diagnosis. Forewing yellow ochre and white markings, with a basal streak, an angulated fascia in the median third and three costal and dorsal strigulae, all margined, often indistinctly, with darkish colour. Male genitalia asymmetric with a wide left valva, long spines apically and a thin right valva. Female genitalia with sterigma membranous and a large ostium bursae, signum consisting of an oval plate with two opposite spines in the centre.

The forewing pattern of *P. ivani* is similar to *P. caraganella* and *P. viciae*. It differs by the reduced or absent dark margins of all markings, a much angulated median fascia, an often present third strigula, and an indistinct apical spot, clearly defined in the other two species. In male genitalia, *P. ivani* is significantly different from *P. caraganella* by the asymmetrical valvae. For this character, *P. ivani* is similar to *P. viciae* but it is distinguishable for the just outlined saccus, which is very evident in *P. viciae*, a different curvature of the right valva and the sternum VIII rounded and not rectangular (Kumata 1963). In female genitalia, *P. ivani* differs from *P. caraganella* for the lobate posterior margin of the segment VII in the latter and for the spines in the signum which are opposite, on a horizontal plane, while are not aligned in *P. caraganella*. In *P. viciae* signum is similar to *P. ivani* but there is a very different fan-shaped lamella antevaginalis (Kumata 1963).

Type material. Holotype ♂ (Fig. 2A): Russia, Krasnoyarsk Krai, Krasnoyarsk, Akademgorodok, the river Yenisei (left bank), "Krasiviy bereg", 55.99N, 92.76E, 256 m, ex. *Caragana arborescens*, 2.VII.2015 (larva), 8.VII.2015 em., N Kirichenko leg., NK-69-15-6, genitalia slide TRB4117♂ (SIF SB RAS).

Paratypes. 6♂, 2♀ (Fig. 2B). Same location, date and host plant, N Kirichenko leg., NK-69-15-3 (♀), genitalia slide TRB4290♀ (MSNV); NK-69-15-9 (♂), genitalia slide TRB4129♂ (MSNV); NK-69-15-8 (♂), genitalia slide TRB4128♂ (MSNV); NK-69-15-1 (♂), genitalia slide NK-69-15-1♂; NK-69-15-2 (♂), genitalia slide NK-69-15-2♂; NK-95-15-4 (♂), NK-95-15-5 (♂); NK-95-15-7 (♂) (SIF SB RAS).

Further material examined. 2 larvae. 1 larva, Russia, Transbaikal (Zabaikalsky) Krai, Chita, Viktory park, 52.03N, 113.50E, 75 m, 11.VIII.2015, *C. arborescens*, N Kirichenko leg., field ID: NK-261-15, sample ID NK510, process ID: MICRU065-15; 1 larva, Krasnoyarsk Krai, Krasnoyarsk, Akademgorodok, Yenisei river bank, "Krasiviy bereg", 55.99N, 92.76E, 256 m, 15.VIII.2014, N Kirichenko leg., *C. arborescens*, filed ID: Kr-22, sample ID NK333, process ID: ISSIK282-14 (INRA).

Etymology. The species name, *ivani* is derived from the first name of Natalia Kirichenko's father, Ivan, who has continuously supported her interest in entomology.

Description. Male and female. Alar expanse: 6.5–7 mm (Fig. 2A, B).

Head. Vertex rough, white, with mixture of ochreous piliform scales anteriorly; frons smooth, with broad, lustrous white scales. Antenna light ochre, length approximately 0.7× that of forewing, each flagellomere ringed with dark brown apically, scape and pedicel yellow white, the first sometimes spotted with dark brown above, pecten of a few piliform scales. Maxillary and labial palpi white, the first very reduced, about 1/5 of the labial palpi.

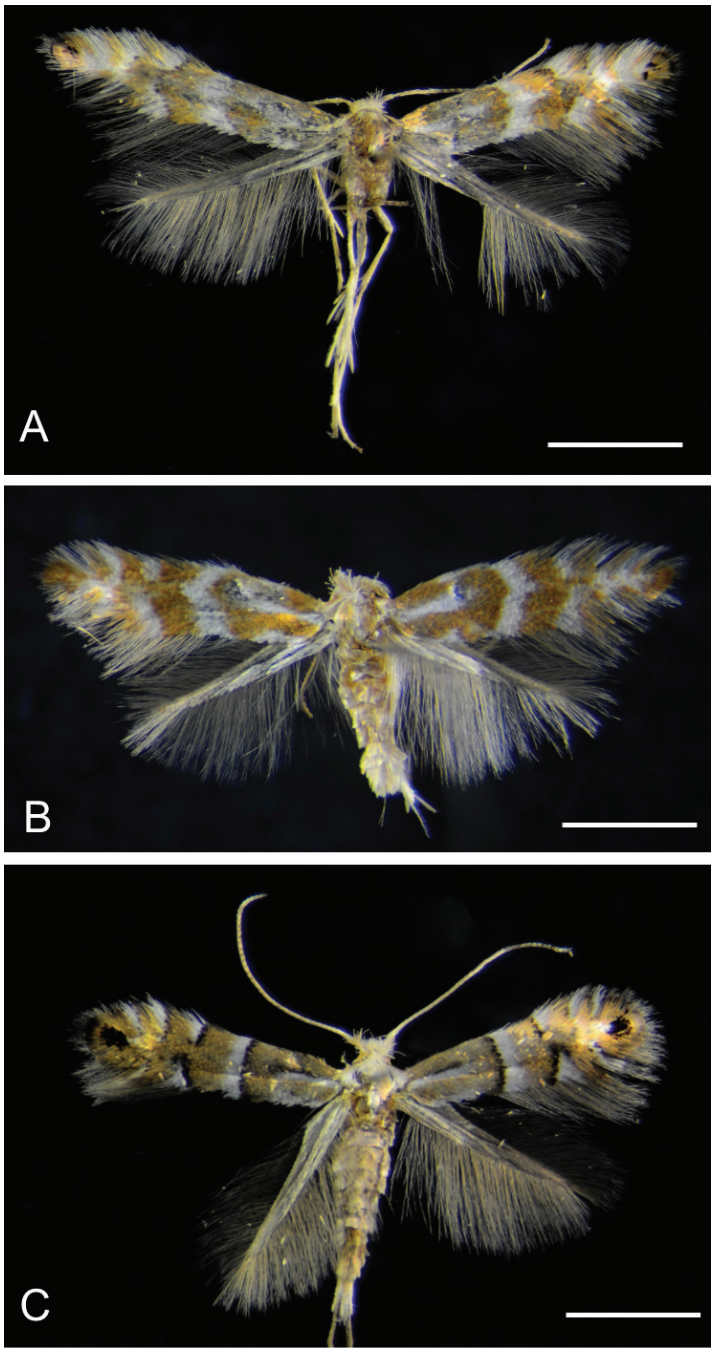

Figure 2. Adults of *Phyllonorycter ivani* sp. n. and *P. caraganella* **A, B** *P. ivani* (holotype, ♂), Russia, Krasnoyarsk, Akademgorodok, the river Yenisei, left bank, "Krasiviy bereg", ex. *Caragana arborescens,* 2.VII.2015, NK-69-15-6 (♂), genitalia slide TRB4117♂; same location, date and host, NK-69-15-3 (♀), genitalia slide TRB4290♀ **C** *P. caraganella*, Russia, Primorsky Krai, Rakovka, ex. *Caragana manshurica*, 27.VII.2016, NK-184-16-8A (♀), genitalia slide TRB4291♀. Scale bar: 1.2 mm.

Thorax (Fig. 2A–B). Yellow ochre with three longitudinal white lines, venter white. Forewing yellow ochre to orange, with a basal streak at basal one third, an angulated fascia in the median third and three costal and dorsal white strigulae, all the signs are slightly margined with dark colour, sometimes third dorsal strigula not perceptible; an indistinct apical dark spot, almost always represented by a few dark scales; cilia whitish. Hindwing pale grey, cilia pale ochreous grey. Legs mostly fuscous dorsally, white ventrally, fore and mid tarsi more or less annulated with brownish, hind tarsi white.

Abdomen. Sternum VIII of male shorter than right valve, with a round apex.

Male genitalia (Fig. 3A–B). Tegumen long, pointed, no apical microsetae. Valvae asymmetrical: left valva broad, variable in width, much broader near middle, about three times the width of right valva, and with a stout, sinuate spine arising near apex, length of spine about the width of valva; right valva slender, curved, with a big seta subapically. Vinculum short, saccus triangular but just outlined. Phallus slender, with a small subapical spine (Fig. 3A), length approximately equal to right valva.

Female genitalia (Fig. 4A–C). Papillae anales rather reduced, posterior apophyses almost twice the length of the anterior one (Fig. 4A, C). Sterigma membranous, ostium bursae rather large, antrum narrower, approximately half of the ostium, weakly sclerotized. Ductus bursae thin, membranous, extended to the segment II; bursa rounded with signum consisting of two opposite spines, arranged horizontally, in the centre of a small sclerotized plate (Fig. 4B, C). Ductus spermathecae with efferent canal forming 35–36 coils of equal diameter.

Biology. (Fig. 5). The mine is similar to other *Phyllonorycter* species. The early mine is a whitish flat blotch on the lower side of the leaflet (Fig. 5A). The long epidermal tunnel preceding the blotch mine, as often present in the mines of *Phyllonorycter caraganella,* has not been observed in *P. ivani* mines. The mine usually begins near the base of the leaflet, growing towards the leaflet tip or in the middle of the leaflet. Later it becomes a tentiform blotch with 2–4 folds on the lower epidermis covering the mine (Fig. 5B, C). Silken threads, which the larva attaches on the lower epidermis inside the mine, contract the epidermis, pulling the leaflet margins downward (Fig. 5D). The resulting narrowed leaflet may help to find the mine when examining leaves from the upper side. The mine may occupy the entire leaflet (Fig. 5D). Frass is in loose gains or in small batches, covered by silk. The larva primarily consumes spongy parenchyma and in the late stage it fragmentally gnaws the layer of palisade parenchyma. The latter results in the presence of small transparent dots that could be observed from the upper side of the leaf. Larva greenish white, before pupation greenish yellow (Fig. 5D, E). Pupation in the mine.

Phenology. In Siberia, in 2014–2015, mines with late instar larvae were found in early July and with young larvae in August suggesting that the insect develops in two generations. The first generation (egg laying) likely starts in late May – beginning of June and lasts till middle of July (adult appearance), the second starts in mid-July and lasts till the end of August – early September. The overwintering stage of this species is unknown.

Ecology and host plant range. The host plant is *Caragana arborescens* (Fabaceae). So far, *P. ivani* has been found in suburban areas. Indeed, the type locality is on the outskirts of Krasnoyarsk (Krasnoyarsk Krai, Russia) where the bushes of its host plant

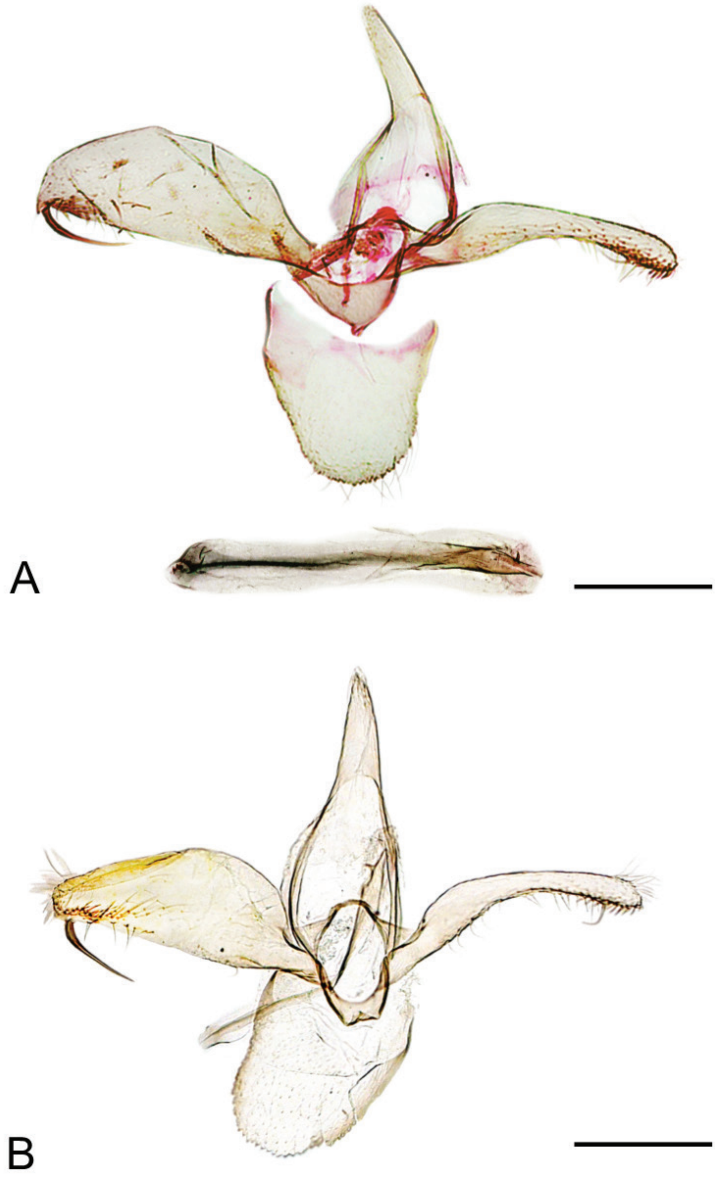

Figure 3. Male genitalia of *Phyllonorycter ivani* sp. n. Russia, Krasnoyarsk, Akademgorodok, the river Yenisei, left bank, "Krasiviy bereg", ex. *Caragana arborescens,* 2.VII.2015 **A** holotype, NK-69-15-6 (♂), genitalia slide TRB4117♂, phallus removed **B** paratype, NK-69-15-1 (♂), genitalia slide NK- 69- 15- 1♂. Scale bar: 200 μm.

are planted as an ornamental fence along the promenade on the left river bank of the river Yenisei. In Chita (Transbaikal Krai), the mines were found on bushes of *C. arborescens* in the city park.

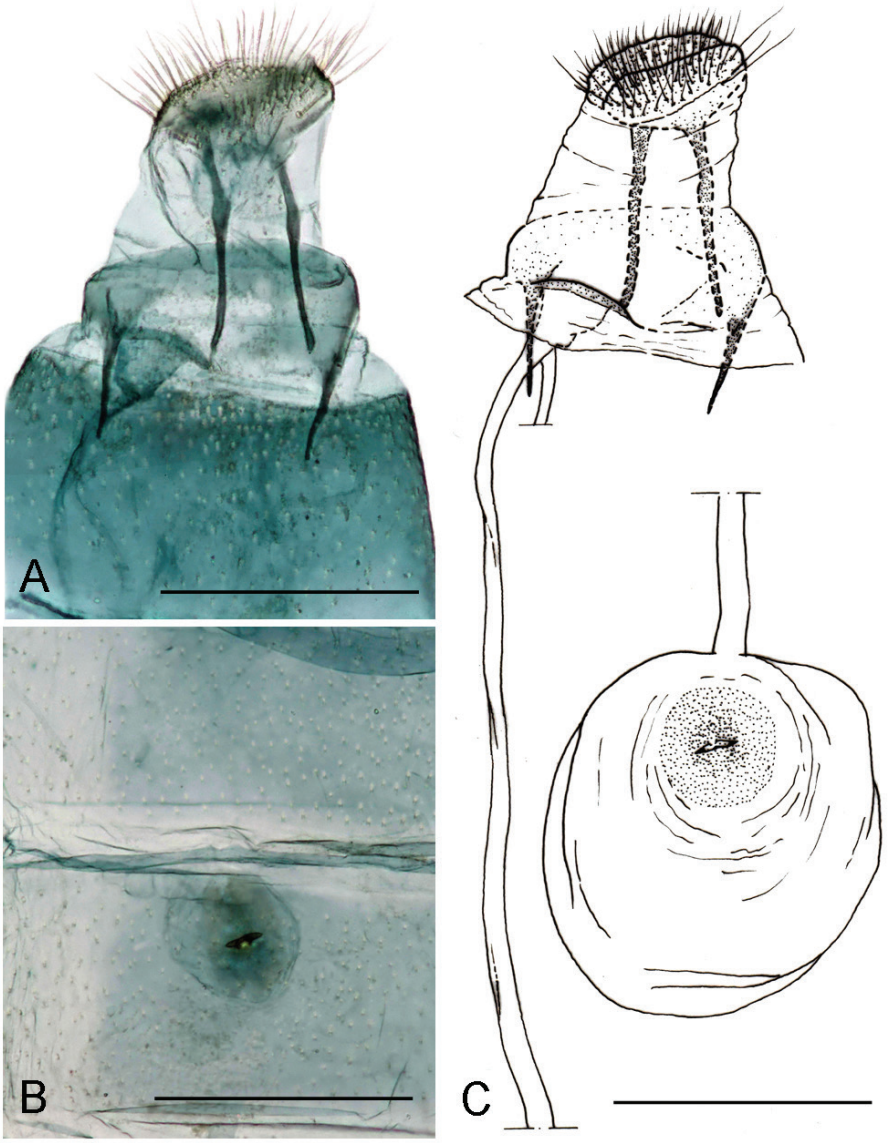

Figure 4. Female genitalia of *Phyllonorycter ivani* sp. n. Russia, Krasnoyarsk, Akademgorodok, the river Yenisei, left bank, "Krasiviy bereg", ex. *Caragana arborescens,* 2.VII.2015, NK-69-15-3, genitalia slide TRB4290♀ **A** last segments of abdomen **B** signum **C** drawing of female genitalia based on the genitalia slide TRB4290♀ . Scale bar: 300 μm.

Distribution. Russia: Central Siberia (Krasnoyarsk Krai, Krasnoyarsk), Eastern Siberia (Transbaikal Krai, Chita). In 2014–2017, no mines of *P. ivani* were found on *Caragana* spp. in other regions of Siberia: Tyumen, Omsk, Novosibirsk Oblasts, Khanty-Mansi Autonomous Okrug, Tomsk, Kemerovo, Irkutsk Oblasts, Altai Krai,

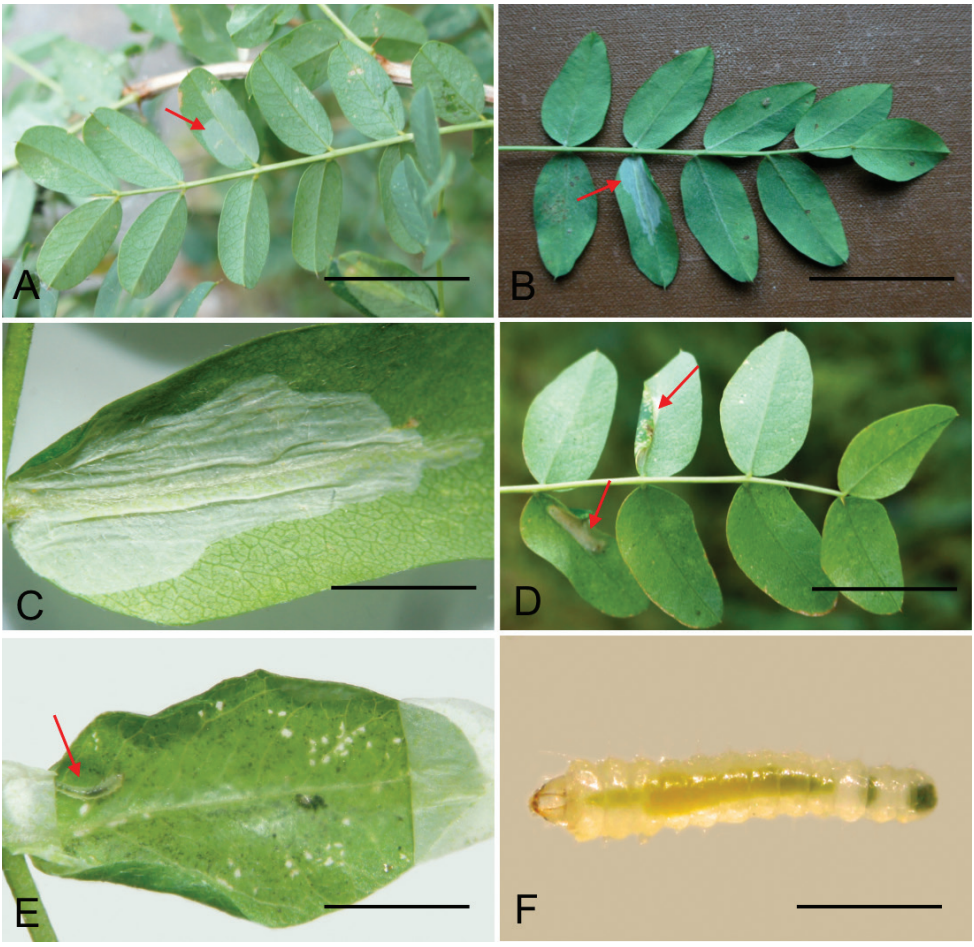

Figure 5. Biology of *Phyllonorycter ivani* sp. n., *Caragana arborescens*, Russia, Siberia **A** flat blotch mine (indicated by an arrow) on low side of the leaflet **B–C** tentiform mine with folded epidermis **D** the mine and leaf margin folded downward (an arrow) **E** opened mine with a larva (an arrow) inside **F** larva before pupation. **A** Transbaikal Krai, Chita, Viktory park, 11.VIII.2015 **B–F** Krasnoyarsk, the river Yenisei, left bank, "Krasiviy bereg", 15.VIII.2014. Scale bars: 20 mm (**A–B, D, F**); 10 mm (**C**); 15 mm (**E**).

the Republics of Tuva and Buryatia, neither in the Russian Far East (Amur Oblast, Sakhalin Island). However, it is highly likely that the species occurs in Eastern Siberia, on the territory between Krasnoyarsk and Transbaikal Krais.

Phyllonorycter caraganella (Ermolaev, 1986)

Figs 2C, 6–9

Diagnosis. Forewing bright yellow ochre, with a basal streak, a not angulated fascia in the median third and three costal and two dorsal strigulae, all markings clearly

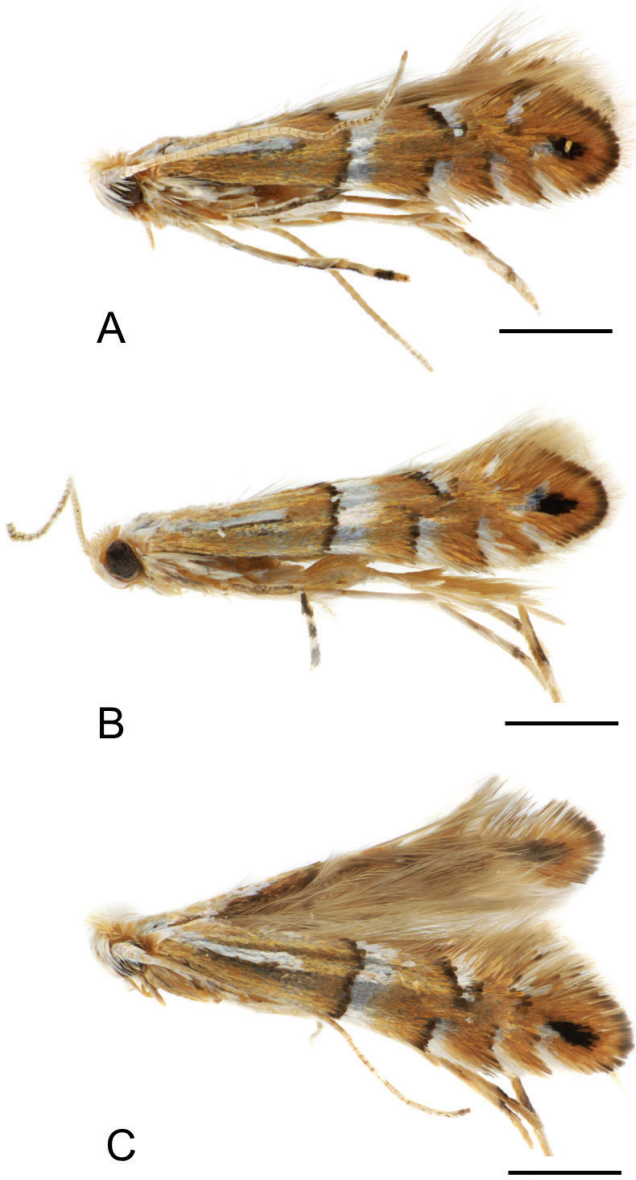

Figure 6. Male adults of *Phyllonorycter caraganella*. Russia, Primorsky Krai, 27.VII.2016, ex. *Caragana manshurica*, N. Kirichenko col. Sampling location, field ID **A** Glukhovka, NK-148-16-13A **B–C** Rakovka, NK-184-16-9A, NK-184-16-12A. Scale bar: 0.5 mm.

margined with dark colour. Male genitalia symmetrical with long thin valvae. Female genitalia with a rounded margin of sternum VII, signum consisting of an oval plate with two opposite spines not aligned horizontally.

Because of the symmetrical male genitalia, *P. caraganella* is close to *P. fabaceaella* (Kuznetzov, 1978) and *P. kuznetzovi* Ermolaev (Suppl. material 1: Table S1) but differs

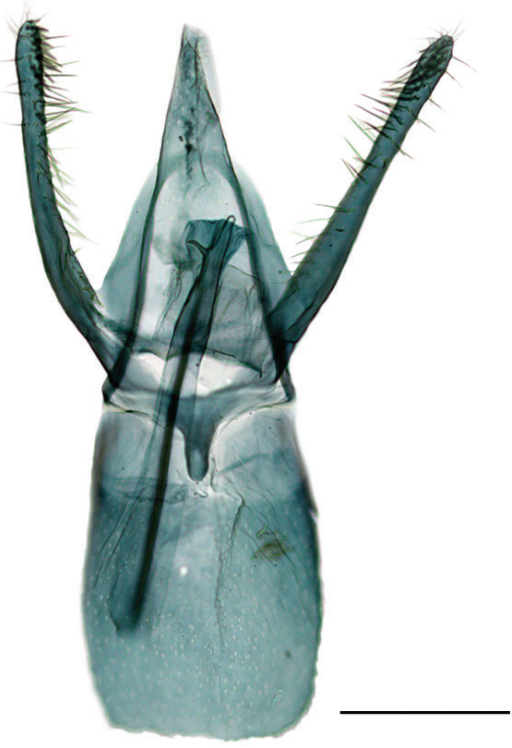

Figure 7. Male genitalia of *Phyllonorycter caraganella*. Russia, Primorsky Krai, Rakovka, ex. *Caragana manshurica*, N° 137, NK-184-16-11° (♂), genitalia slide TRB4292♂. Scale bar: 250 μm.

from the first by the presence of a large saccus (Kuznetzov 1981) and from the second by a very different shape of phallus and sternum VIII (Ermolaev 1982).

Material examined. 6♂, 2♀ 4 larvae (Figs 2C, 6). 1♂, Russia, Primorsky Krai, Glukhovka, vodorazdel, 43.74N, 132.13E, 68 m, ex. *Caragana manshurica*, 27.VII.2016, N Kirichenko leg., field ID NK-148-16-13A (♂) (SIF SB RAS); 2♂, 1♀, Primorsky Krai, Rakovka, forested area, 43.80N, 132.19E, 140 m, ex. *C. manshurica*, 27.VII.2016, N Kirichenko leg., NK-184-16-8A (♀) (MSNV), NK-184-16-9A (♂), NK-184-16-12A (♂), genitalia slide NK-184-16-12A♂ (SIF SB RAS); 1♂, 1♀, Primorskiy Krai, Rakovka, ex *Caragana manshurica*, 27.VII.2016, N Kirichenko leg., N° 137, NK-184-16-11° (♂), genitalia slide TRB4292♂, NK-184-16-3° (♀), genitalia slide TRB4295♀ (MSNV); 2♂, Primorsky Krai, Rakovka, forested area, 43.80N, 132.19E, 140 m, ex. *C. manshurica*, 27.VII.2016, N Kirichenko leg., NK-184-16-1A (♂) (sample ID NK526, process ID SIBLE015-17), NK-184-16-2A (♂) (NK527, SIBLE016-17); 2 larvae, same place, date and host plant, N Kirichenko leg., NK-184-16-1 (NK522, SIBLE011-17), NK-184-16-2 (NK523, SIBLE012-17); 2 larvae, Primorsky Krai, Glukhovka, vodorazdel, 43.74N, 132.13E, 68 m, *C. manshurica*, 27.VII.2016, N Kirichenko leg., NK-185-16-1 (NK524, SIBLE013-17), NK-185-16-2 (NK525, SIBLE014-17) (INRA).

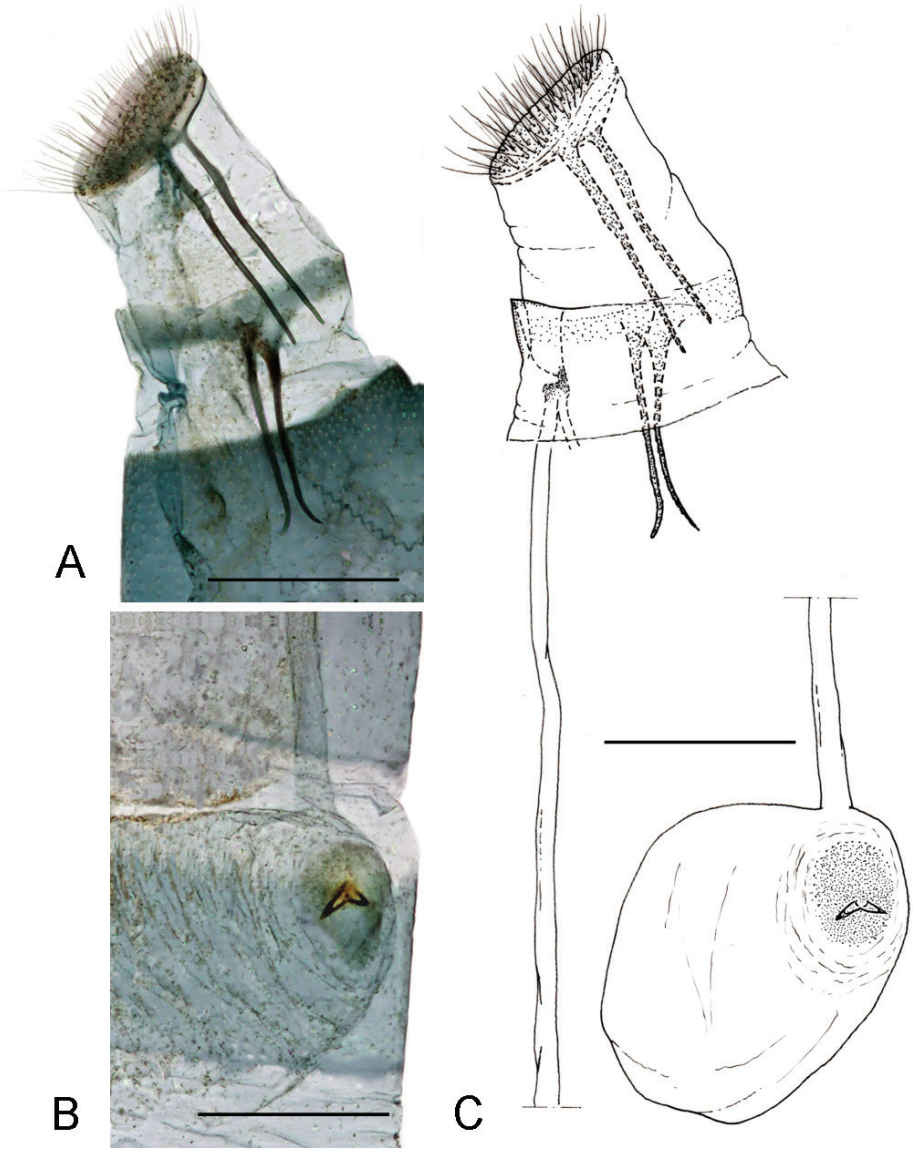

Figure 8. Female genitalia of *Phyllonorycter caraganella*. Russia, Primorsky Krai, Rakovka, ex *Caragana manshurica*, 27.VII.2016, N° 137, NK 184-16-3A, genitalia slide TRB4295♀ **A** last segments of abdomen **B** signum **C** drawing of female genitalia based on the genitalia slide TRB4295♀. Scale bar: 300 μm.

Description. Male and female. Alar expanse: 6.5–7.2 mm (Figs 2A, B, 7, 8).

Head. As in the previous species, dark scales on scape are not present.

Thorax (Fig. 2A–B). Yellow ochre with three longitudinal white lines, venter white. Forewing yellow ochre, with a basal streak at basal one third, a fascia in the median third (straight or weakly angled) and three costal and two dorsal white strigulae, all the

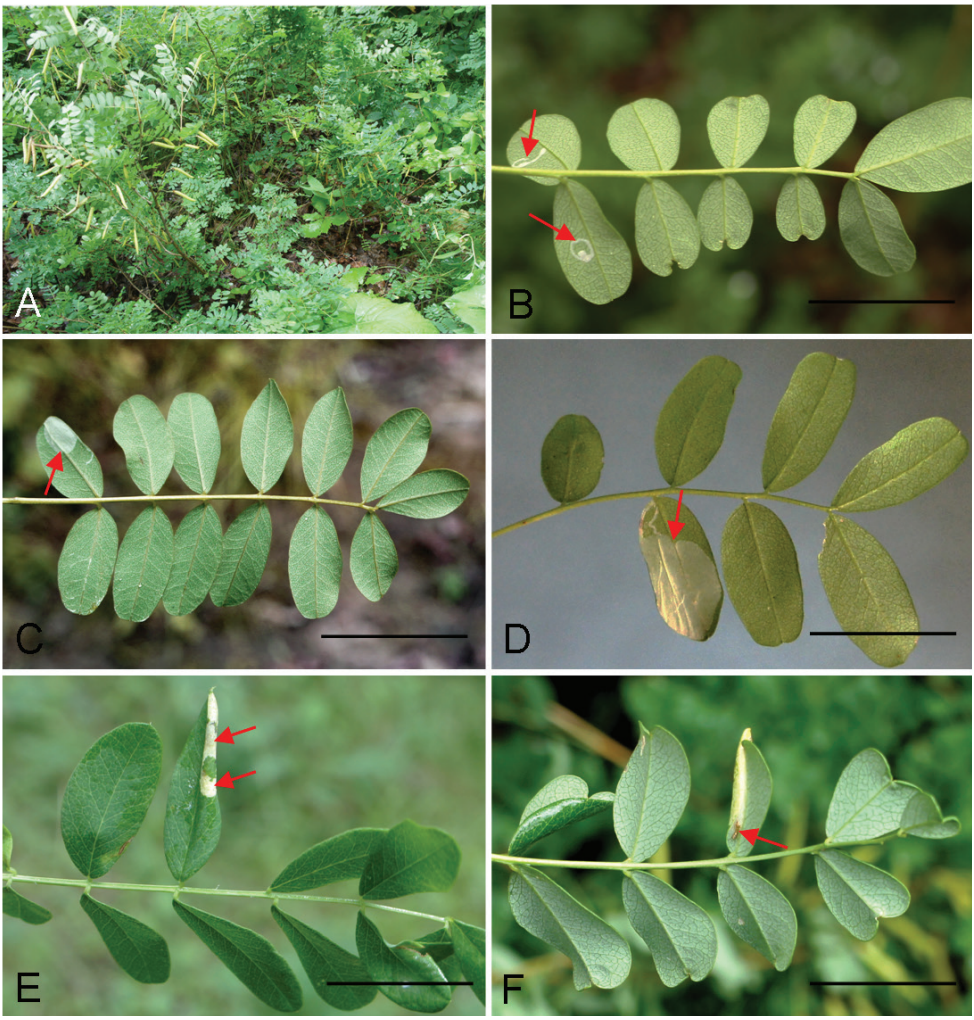

Figure 9. Biology of *Phyllonorycter caraganella* (Ermolaev, 1986) on *Caragana manshurica*, Russian Far East, Primorsky Krai, 27.VII.2016 **A** sampling plot **B** young epidermal tunnel mines on low side of the leaflet (indicated by the arrows) **C–D** flat blotch mine with the preceding epidermal tunnel (arrow) **E** tentiform mine with leaf margin folded downwards and with whitish "windows" – the regions of eaten out palisade parenchyma in the mine (arrows) **F** same mine (see **E**) from lower side of the leaflet, with pupal exuvium protruding the mine (arrow). Scale bar: 20 mm.

signs are clearly margined with dark brown; a subapical elliptical dark spot; cilia whitish. Hindwing pale grey, cilia pale ochreous grey. Legs mostly fuscous dorsally, white ventrally, fore and mid tarsi more or less annulated with brownish, hind tarsi white.

Abdomen. Sternum VIII rectangular, shorter than valva.

Male genitalia (Fig. 7). Tegumen long, pointed, no apical microsetae. Valvae symmetrical, thin, parallel-sided, slightly curved. Vinculum short, saccus pronounced, with a round apex. Phallus slender, with a small subapical spine, slightly longer than valva.

Female genitalia (Fig. 8A–C) Papillae anales rather reduced, posterior apophyses slightly longer than the anterior one (Fig. 8A, C). Sterigma membranous; with a rounded margin of sternum VII; a rather large ostium bursae, antrum membranous, strongly folded in the conjunction with ductus. Ductus bursae thin, membranous, extended to the segment II. Bursa rounded with signum consisting of two opposite spines, not aligned horizontally, in the centre of a small sclerotized plate (Fig. 8B, C). Ductus spermathecae with efferent canal forming 30 coils of equal diameter.

Biology. (Fig. 9). The mine is a whitish blotch on the leaflet underside. In contrast to *P. ivani*, the mine of *P. caraganella* often starts with a relatively long narrow, hardly widening, epidermal tunnel, that proceeds into a flat blotch mine (Fig. 9B–D). The later mine is tentiform, with leaf margins contracted downwards, reminding of the mine of *P. ivani* (Fig. 8E). Tentiform blotch with 2–5 folds, most often occupying the whole leaflet (Fig. 9D). The larva primarily consumes the spongy parenchyma and later feeds on palisade parenchyma, gnawing rather large "windows" visible from the upper side of the leaflet (Fig. 9E). Pupation occurs in the mine. After adult emergence, pupal exuviae can be found in the corner of the mine close to leaflet base (Fig. 9F).

Phenology. Two generations. In Russian Far East, vacated tentiform mines of the first generation and young mines (epidermial tunnels) of the second generation were found in the end of July 2016. It is unknown how the species hibernates.

Ecology and host plant range. (Fig. 9A). The host plant is *Caragana manshurica* (syn. *C. fruticosa* (Pallas) Besser) (Fabaceae). This species is very similar to *C. arborescens* (Koropachinsky and Vstovskaya 2012). The bushes of *C. manshurica* with *P. caraganella* mines were found in the canopy in the broadleaf forest in the southern part of Primorsky Krai.

Distribution. Russia, Russian Far East: Khasansky District (Barabash) (Ermolaev 1986), Ussurijsk District – Komarov Mountain-Taiga Station, village Gornotayezhnoe (SV Baryshnikova: personal communication), around the villages Glukhovka and Rakovka (present paper). In 2017, no mines of *P. caraganella* were found on *Caragana* spp. in the southern part of the Island Sakhalin (Russian Far East), nor could we find *P. caraganella* in Siberia during our extensive surveys in 2015–2017.

Remarks. The holotype (♂) and paratypes (4♂ and 7♀) that, according to Ermolaev (1986), are being stored in the Zoological Institute, Russian Academy of Science (Saint Petersburg, Russia), are not located there (SV Baryshnikova: personal communication). For a note about VP Ermolaev's research journey and the destiny of his gracillariid collections see Kirichenko et al. (2018b).

Molecular data

We obtained barcode data for 53 Fabaceae-feeding *Phyllonorycter* specimens belonging to 44 BINs and 39 species (Suppl. material 2: Table S2, Fig. 10). DNA barcodes of four

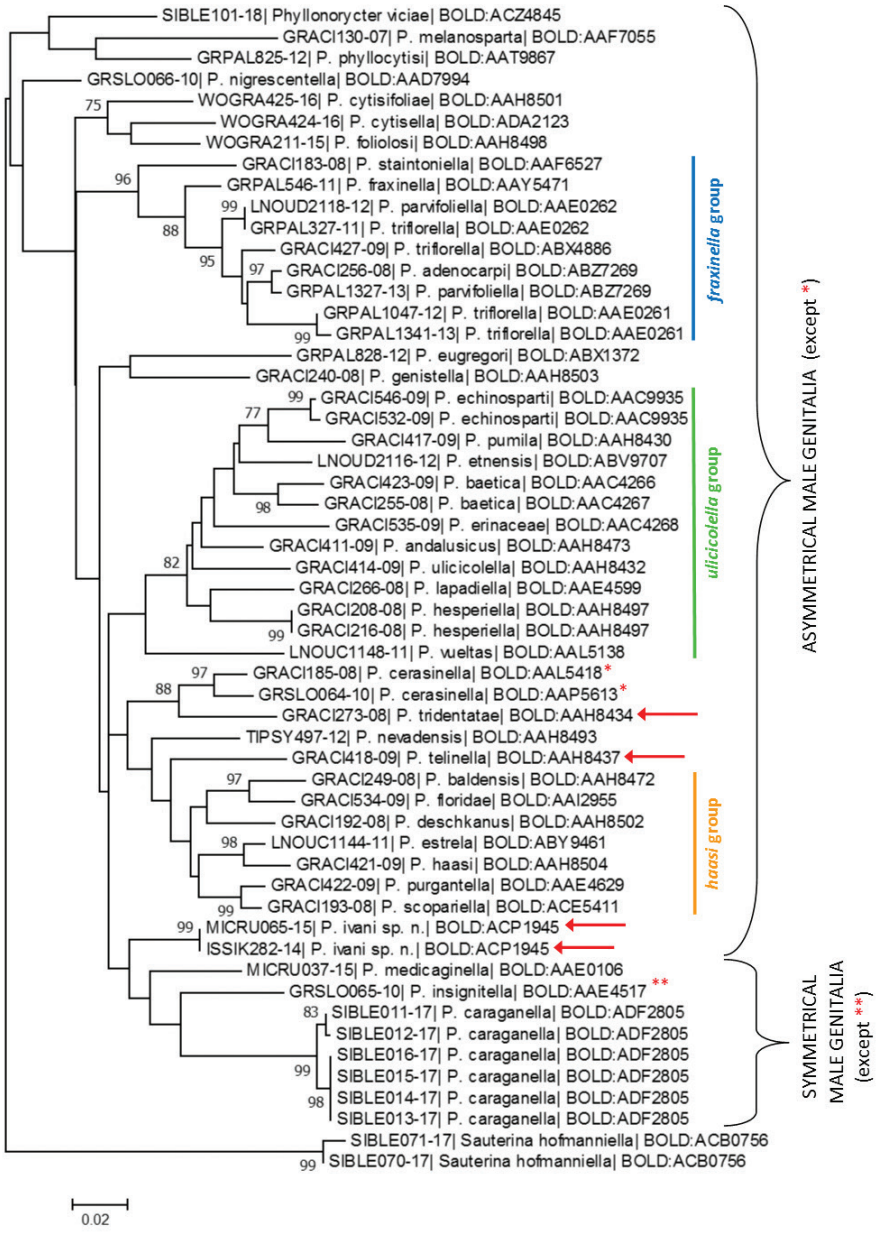

Figure 10. A Maximum Likelihood COI tree of the Fabaceae-feeding *Phyllonorycter* generated with the K2P nucleotide substitution model. Each specimen is identified by its Process ID code (see Table S2) and Barcode Index Number (BIN). Branch lengths are proportional to the number of substitutions per site. The percentage of trees in which the associated taxa clustered together is shown next to the branches, with the bootstrap values >70. Species indicated by red arrow highly similar to *haasi* group morphologically (male genitalia), but not genetically. **P. cerasinella* has symmetrical male genitalia, ***P. insignitella* asymmetrical (Laštůvka and Laštůvka 2006).

Table 1. Intra- and interspecific genetic divergences in DNA barcode fragments (COI mtDNA) between *Phyllonorycter ivani* sp. n. and the close neighbours – *Phyllonorycter* spp. with the asymmetrical male genitalia from haasi group (see Nr. 2, 3, 5, 7-12, 14) and *Phyllonorycter* spp. with the symmetrical male genitalia (4, 6, 13)*.

№	Species	*P. ivani* sp. n.	*P. purgantella*	*P. scopariella*	*P. medicaginella*	*P. nevadensis*	*P. insignitella*	*P. estrela*	*P. deschkanus*	*P. haasi*	*P. telinella*	*P. floridae*	*P. baldensis*	*P. caraganella*	*P. tridentatae*
		1	2	3	4	5	6	7	8	9	10	11	12	13	14
1	*P. ivani* sp. n.	**[0]**													
2	*P. purgantella* (Chrétien, 1910)	6.3	[–]												
3	*P. scopariella* (Zeller, 1846)	6.3	1.5	[–]											
4	*P. medicaginella* (Gerasimov, 1930)	6.4	7.4	7.4	[–]										
5	*P. nevadensis* (Walsingham, 1908)	6.5	6.0	5.9	7.4	[–]									
6	*P. insignitella* (Zeller, 1846)	7.1	8.9	8.8	7.7	9.3	[–]								
7	*P. estrela* Laštůvka & Laštůvka, 2006	7.2	4.3	4.4	8.7	6.5	9.6	**[3.1]**							
8	*P. deschkanus* Laštůvka & Laštůvka, 2006	7.7	5.2	4.7	8.0	7.2	8.6	4.7	[–]						
9	*P. haasi* (Rebel, 1901)	7.9	5.4	5.6	9.1	6.7	9.7	2.3	5.6	[–]					
10	*P. telinella* Laštůvka & Laštůvka, 2006	8.0	6.5	6.5	8.2	6.9	10.2	6.0	6.4	6.7	[–]				
11	*P. floridae* Laštůvka & Laštůvka, 2006	8.2	5.7	5.7	8.4	7.4	9.4	5.4	5.1	6.3	7.0	[–]			
12	*P. baldensis* Laštůvka & Laštůvka, 2006	8.2	5.2	5.6	8.7	7.7	10.0	6.1	5.6	7.0	7.7	3.5	[–]		
13	*P. caraganella* (Ermolaev, 1986)	8.6	8.6	8.5	8.7	9.1	8.8	10.2	8.7	10.4	9.2	8.5	9.5	**[0–1]**	
14	*P. tridentatae* Laštůvka & Laštůvka, 2006	8.7	7.9	8.1	8.9	8.9	10.0	8.6	8.1	10.0	8.4	8.2	9.3	10.1	[–]

*Kimura 2-parameter (K2P) distances (%); minimal pairwise distances are given for each species pair; values in square brackets represent maximal intraspecific distances.
[–] no data because a single specimen was DNA-barcoded.

Phyllonorycter species were assigned to more than one BIN in BOLD, i.e., *P. baetic*a Laštůvka & Laštůvka, 2006, *P. cerasinella* (Reutti, 1853) and *P. parvifoliella* (Ragonot, 1875) were assigned to two BINs each and *P. triflorella* (de Peyerimhoff, 1871) to three BINs (Fig. 10). DNA barcodes of *P. ivani* and *P. caraganella* were novel to BOLD and were assigned their own unique BINs, BOLD:ACP1945 and BOLD:ADF2805, respectively (Fig. 10). On the Maximum Likelihood COI tree, species with asymmetrical male genitalia grouped together in three main, weakly supported, species groups: the *fraxinella*, *ulicicolella* and *haasi* groups. Some species with asymmetrical male genitalia that did not fit any of the three groups based on their morphology (Laštůvka and Laštůvka 2006) occupied a relatively isolated position on the COI tree (Fig. 10). Species with symmetrical male genitalia (*P. medicaginella* and *P. caraganella*) clustered together, but including a species with asymmetrical male genitalia, *P. insignitella* (Zeller) (Fig. 10).

The nearest neighbours of the new species *P. ivani* were both *P. purgantella* (Chrétien, 1910) and *P. scopariella* (Zeller, 1846) from the *haasi* group (asymmetrical male genitalia) with 6.3% divergence, followed by *P. medicaginella* (symmetrical male genitalia clade) with 6.4% divergence (Table 1). The new species *P. ivani* did not fall

within the *haasi* species group but it clustered next to it (Fig. 10), which agrees with the features of its asymmetrical male genitalia (Fig. 3). *Phyllonorycter telinella* and *P. tridentatae* that, as *P. ivani*, are morphologically highly similar to the *haasi* group, did not enter the *haasi* clade on the COI tree (Fig. 10). The minimum interspecific genetic distance between the two *Caragana*-feeding species *P. ivani* and *P. caraganella* was 8.6% (Fig. 10; Table 1). No evidence for mitochondrial introgression between these two species was detected. The intraspecific distance in *P. caraganella* (based on DNA barcodes of six individuals), varied from 0 to 1.1%. No genetic divergence was found between the two specimens of *P. ivani* collected from the two distant localities in Siberia (Krasnoyarsk in Central Siberia vs. Chita in Eastern Siberia).

Discussion

The new species, *P. ivani* is the second *Phyllonorycter* species described from *Caragana* (Fabaceae). This species is clearly distinguishable from the other *Caragana*-feeding species, *P. caraganella* by external morphology (forewing pattern) and highly different male genitalia, i.e., asymmetric in *P. ivani* and symmetrical in *P. caraganella*. High genetic divergence found between these two gracillariid species, suggests that the plant genus *Caragana* has been colonized at least twice independently in the Eastern Palearctic.

Despite extensive field surveys in the Asian part of Russia, the new species has so far been detected only in two locations in Central and Eastern Siberia, whereas *P. caraganella* has been found exclusively in the southern territory of the Russian Far East. Both species are monophagous, feeding exclusively on *C. arborescens* (*P. ivani*) and *C. manshurica* (*P. caraganella*) respectively. The natural ranges of these plants do not overlap: *C. arborescens* occurs in the forest and forest-steppe zones in Siberia, China, Mongolia, and Kazakhstan, whereas *C. manshurica* grows in the Russian Far East, northeast China, and Korea (Liu et al. 2018). *Caragana arborescens* and *C. manshurica* are very similar morphologically (Koropachinsky and Vstovskaya 2012). *Caragana arborescens* was introduced to the European part of Russia, some European countries and North America for ornamental reasons and to protect landscapes (hedging, screening or wind-breaking). In North America, it became naturalized and weedy (Shortt and Vamosi 2012). However, no records of *Phyllonorycter* species on *Caragana* are known yet from the neocolonized range of *C. arborescens* (De Prins and De Prins, 2018).

The genus *Caragana* has 96 described species (The Plant List 2018). Bearing in mind the fact that *P. ivani* and *P. caraganella* feed on different host plants, it is likely that other new *Phyllonorycter* species will be found feeding on other *Caragana* species. More fieldwork and rearing efforts are needed to test this hypothesis.

DNA barcode data weakly support the different Fabaceae-feeding species groups, but data on more loci are needed to infer the phylogenetic interrelationships of those groups and the evolution of asymmetric genitalia (Doorenweerd 2016).

By its asymmetric male genitalia and specific valval structures, *P. ivani* is similar to the *haasi* group. According to their DNA barcodes, two species of the *haasi* group, *P.*

purgantella and *P. scopariella* are the nearest neighbours of *P. ivani* (Fig. 10). The identification of species within the *haasi* group is very difficult, due to the lack of diagnostic morphological characters. Indeed, species belonging to this group show a very uniform wing pattern and minor morphological characters in male genitalia, such as a subapical bristle or a small basal tuft of setae on the right valva (Laštůvka and Laštůvka 2006). Female genitalia in this species group are also poorly differentiated. A further source of confusion is that two other species groups of *Phyllonorycter* show a similar structure of the male genitalia. The first, the *hilarella* group, feeds on Salicaceae (Davis and Deschka 2001) and the second, the *acerifoliella* group, feeds on Sapindaceae (Gregor and Povolný 1950). Genitalia of both sexes and, very often, the forewing pattern of these two species groups are very similar to those of the Fabaceae groups. More DNA sequence data are needed to test the validity of those species groups and their phylogenetic relationships.

Acknowledgements

We thank Svetlana V Gorokhova (Russia) for organizing the field work in the Russian Far East, Svetlana V Baryshnikova (Russia) for checking the collection of the Zoological Institute, Russian Academy of Science for the presence of *P. caraganella* from its type location and for the fruitful discussions, Erik J van Nieukerken (The Netherlands), Aleš Laštůvka, Zdeněk Laštůvka (Czech Republic), Alain Cama (France), and Gerfried Deschka (Austria) for sharing specimens and/or DNA barcodes of some Fabaceae-feeding *Phyllonorycter* with us, Irina A Mikhailova (Russia) for the map construction, Vyacheslav I Zyryanov (Russia) for consultations on Photoshop, and Yuri N Baranchikov (Russia) for his support at different stages of the study. Special thanks to Erik J van Nieukerken, Camiel Doorenweerd (Hawaii, USA) and Zdeněk Laštůvka for insightful comments and revision of the manuscript. NK was supported by the Russian Foundation for Basic Research (project No. 15-29-02645), LE STUDIUM® fellowship program, Institute for advanced studies – Loire Valley (Orléans, France) and the French Embassy in Russia, Bourse Metchnikov (grant No. 908981L, Campus France), and the EU program COST Action FP1401 "Global Warning: A Global Network of Nurseries as Early Warning System against Alien Tree Pests".

References

Ainouche A, Bayer RJ, Cubas P, Misset MT (2003) Phylogenetic relationships within tribe Genisteae (Papilionoideae) with special reference to genus *Ulex*. In: Klitgaard BB, Bruneau A (Eds) Advances in legume systematics. Part 10, Higher Level Systematics, Royal Botanic Gardens, Kew, 239–252.

Akulov EN, Kirichenko NI, Ponomarenko MG (2018) Contribution to the Microlepidoptera fauna of the South of Krasnoyarsk Territory and the Republic of Khakassia. Entomological Review 98: 49–75. https://doi.org/10.1134/S0013873818010074

Baryshnikova SV (2008) Gracillariidae. In: Sinev SY (Ed.) Catalogue of the Lepidoptera of Russia. KMK Scientific Press, St. Petersburg – Moscow, 38–45. [In Russian]

Baryshnikova SV (2016) Gracillariidae. In: Leley AS (Ed.) Annotated catalogue of the insects of Russian Far east. Vol. II. Lepidoptera. Dal'nauka, Vladivostok, 50–59. [In Russian]

Davis DR, Deschka G (2001) Biology and systematics of the North American *Phyllonorycter* leafminers on Salicaceae, with a synoptic catalog of the Palearctic species (Lepidoptera: Gracillariidae). Smithsonian Contributions to Zoology 614: 1–89. https://doi.org/10.5479/si.00810282.614

De Prins J, De Prins W (2018) Global Taxonomic Database of Gracillariidae (Lepidoptera) http://www.gracillariidae.net/ [Accessed 15 December 2018]

De Prins J, Mozūraitis R, Lopez-Vaamonde C, Rougerie R (2009) Sex attractant, distribution and DNA barcodes for the Afrotropical leaf-mining moth *Phyllonorycter melanosparta* (Lepidoptera: Gracillariidae). Zootaxa 2281: 53–67.

Doorenweerd C (2016) Branching out: the role of host plants in the diversification of leaf-mining moths. PhD thesis. Universiteit van Amsterdam, The Netherlands. http://hdl.handle.net/11245/1.542646 [Accessed 7 February 2019]

Ermolaev VP (1982) A review of Gracillariidae (Lepidoptera) injurious to the legumens in the south of the Primorye Territory, with description of two new species. Entomologicheskoe Obozrenie 61: 572–581. [In Russian]

Ermolaev VP (1986) Two new species of leaf miners of the genus *Lithocolletis* Hbn. (Lepidoptera, Gracillariidae) damaging oak and pea shrub in southern Primorye. In: Ler PA (Ed.) Systematics and ecology of Lepidoptera from the Far East of the USSR, Vladivostok, 26–30. [In Russian]

Folmer O, Black M, Hoeh W, Lutz R, Vrijenhoek R (1994) DNA primers for amplification of mitochondrial cytochrome c oxidase subunit I from diverse metazoan invertebrates. Molecular Marine Biology and Biotechnology 3: 294–299.

Gregor F, Povolný D (1950) The members of *Lithocolletis* Hb. mining *Acer* and *Alnus*. Folia Entomologica, Brno 13: 129–151. [In Czech]

Huemer P, Hebert PDN (2016) DNA barcode library for Lepidoptera from South Tyrol and Tyrol (Italy, Austria) – Impetus for integrative species discrimination in the 21st Century. Gredleriana 16: 141–164.

Kimura M (1980) A simple method for estimating evolutionary rate of base substitutions through comparative studies of nucleotide sequences. Journal of Molecular Evolution 16: 111–120. https://doi.org/10.1007/BF01731581

Kirichenko N, Triberti P, Mutanen M, Magnoux E, Landry J-F, Lopez-Vaamonde C (2016) Systematics and biology of some species of *Micrurapteryx* Spuler (Lepidoptera, Gracillariidae) from the Holarctic Region, with re-description of *M. caraganella* (Hering) from Siberia. ZooKeys 579: 99–156. https://doi.org/10.3897/zookeys.579.7166

Kirichenko N, Petko VM, Magnoux E, Lopez-Vaamonde C (2017) Diversity and distribution of the leaf-mining insects on birch (*Betula* spp.) in Siberia. Entomological Review 97: 183–198. https://doi.org/10.1134/S0013873817020051

Kirichenko N, Augustin S, Kenis M (2018a) Invasive leafminers on woody plants: a global review of pathways, impact and management. Journal of Pest Science 92(1): 9–106. https://doi.org/10.1007/s10340-018-1009-6

Kirichenko N, Triberti P, Kobayashi S, Hirowatari T, Doorenweerd C, Ohshima I, Huang G-H, Wang M, Magnoux E, Lopez-Vaamonde C (2018b) Systematics of *Phyllocnistis* leafmining moths (Lepidoptera, Gracillariidae) feeding on dogwood (*Cornus* spp.) in Northeast Asia, with the description of three new species. ZooKeys 736: 79–118. https://doi.org/10.3897/zookeys.736.20739

Kirichenko NI, Skvortsova MV, Petko VM, Ponomarenko MG, Lopez-Vaamonde C (2018c) Leaf-mining insects on willow (*Salix* spp.) and poplars (*Populus* spp.) (Salicaceae) in Siberia: distribution, trophic specialization and pest status. Contemporary Problems of Ecology 11(6): 576–593. https://doi.org/10.1134/S1995425518060033

Kirichenko N, Triberti P, Akulov E, Ponomarenko M, Lopez-Vaamonde C (2019) Novel data on taxonomic diversity, distribution and host plants of leafmining moths Gracillariidae (Lepidoptera) in Siberia based on the DNA barcoding. Entomological Review. [Accepted]

Klots AB (1970) Lepidoptera. In: Tuxen SL (Ed.) Taxonomist's glossary of genitalia in insects. (Second revised and enlarged edition). Munksgaard, Copenhagen, 115–130.

Knyazev SA, Kirichenko NI, Baryshnikova SV, Triberti P (2018) The first records of the taxonomic diversity of leaf-mining micromoths, Gracillariidae (Insecta, Lepidoptera) in Omsk Province. Euroasian Entomological Journal 17: 261–272. https://doi.org/10.15298/euroasentj.17.4.04 [In Russian]

Koropachinsky IY, Vstovskaya TN (2012) Woody plants of the Asian part of Russia. GEO Publishing House of SB RAS, Novosibirsk, 707 pp. [In Russian]

Kristensen NP (2003) Skeleton and muscles: adults. In: Kristensen NP (Ed.) Lepidoptera, moths and butterflies. Vol. 2. Morphology, physiology, and development. Handbook of Zoology IV (36). Walter de Gruyter, Berlin, New York, 39–131. https://doi.org/10.1515/9783110893724.39

Kumar S, Stecher G, Tamura K (2016) MEGA7: Molecular Evolutionary Genetics Analysis version 7.0 for bigger datasets. Molecular Biology and Evolution 33: 1870–1874. https://doi.org/10.1093/molbev/msw054

Kumata T (1963) Taxonomic studies on the Lithocolletinae of Japan (Lepidoptera Gracillariidae). Part II. Insecta Matsumurana 26: 1–48.

Kuznetzov VI (1981) Fam. Gracillariidae (Lithocolletidae) – leaf blotch miners. In: Medvedev GS (Ed.) A guide to the insects of the European part of the USSR. Lepidoptera, vol. 4(2). Nauka, Leningrad, 149–311. [In Russian]

Kuznetzov VI (1999) The family Gracillariidae (Lithocolletidae). In: Kuznetsov VI (Ed.) Insects and mites – the pests of agricultural plants. III (2). Lepidoptera. Nauka, St. Petersburg, 9–46. [In Russian]

Laštůvka A, Laštůvka Z (2006) The European *Phyllonorycter* species feeding on the plants of the tribe Genisteae (Fabaceae), with descriptions of twelve new species (Lepidoptera: Gracillar-

iidae). Acta Universitatis Agriculturae et Silviculturae Mendelianae Brunensis 54: 65–83. https://doi.org/10.11118/actaun200654050065

Laštůvka Z, Laštůvka A, Lopez-Vaamonde C (2013) A revision of the *Phyllonorycter ulicicolella* species group with description of a new species (Lepidoptera: Gracillariidae). SHILAP Revista Lepidopterologia 41: 251–265.

Lees DC, Kawahara AY, Bouteleux O, Ohshima I, Kawakita A, Rougerie R, De Prins J, Lopez-Vaamonde C (2013) DNA barcoding reveals a largely unknown fauna of Gracillariidae leaf-mining moths in the Neotropics. Molecular Ecology Resources 14: 286–296. https://doi.org/10.1111/1755-0998.12178

Liu Y, Chang Z, Yakovlev GP (2018) *Caragana* Fabricius, Enum., ed. 2. 421. 1763. In: Flora of China, Vol. 10. http://www.efloras.org/florataxon.aspx?flora_id=2&taxon_id=105589 [Accessed 5 December 2018] [Accessed 15 February 2019]

Lopez-Vaamonde C, Sire L, Rasmussen B, Rougerie R, Wieser C, Ahamadi A, Minet J, deWaard JJR, Decaëns T, Lees D (2018) DNA barcodes reveal deeply neglected diversity and numerous invasions of micromoths in Madagascar. Genome. https://doi.org/10.1139/gen-2018-0065

LPWG [Legume Phylogeny Working Group], Bruneau A, Doyle JJ, Herendeen P, Hughes C, Kenicer G, Lewis G, Mackinder B, Pennington RT, Sanderson MJ, Wojciechowski MF, Koenen E (2013) Legume phylogeny and classification in the 21st century: progress, prospects and lessons for other species-rich clades. Taxon 62(2): 217–248. https://doi.org/10.5167/uzh-78167

Mutanen M, Kivelä SM, Vos RA, Doorenweerd C, Ratnasingham S, Hausmann A, Huemer P, Dincă V, van Nieukerken EJ, Lopez-Vaamonde C, Vila R, Aarvik L, Decaëns T, Efetov KA, Hebert PD, Johnsen A, Karsholt O, Pentinsaari M, Rougerie R, Segerer A, Tarmann G, Zahiri R, Godfray HC (2016) Species-level para – and polyphyly in DNA barcode gene trees: strong operational bias in European Lepidoptera. Systematic Biology 65(6): 1024–1040. https://doi.org/10.1093/sysbio/syw044

Ohshima I (2005) Techniques for continuous rearing and assessing host preference of a multivoltine leaf-mining moth, *Acrocercops transecta* (Lepidoptera: Gracillariidae). Entomological Science 8: 227–228. https://doi.org/10.1111/j.1479-8298.2005.00120.x

Ratnasingham S, Hebert PDN (2007) BOLD: The Barcode of Life Data System [http://www.barcodinglife.org]. Molecular Ecology Notes 7: 355–364. https://doi.org/10.1111/j.1471-8286.2007.01678.x

Ratnasingham S, Hebert PDN (2013) A DNA-Based Registry for All Animal Species: The Barcode Index Number (BIN) System. PLoS ONE 8: e66213. https://doi.org/10.1371/journal.pone.0066213

Robinson GS (1976) The preparation of slides of Lepidoptera genitalia with special reference to the Microlepidoptera. Entomologist´s Gazette 27: 127–132.

Roskov Y, Zarucchi J, Novoselova M, Bisby F (Eds) (2019) ILDIS World Database of Legumes (version 12, May 2014). In: Roskov Y, Ower G, Orrell T, Nicolson D, Bailly N, Kirk PM, Bourgoin T, DeWalt RE, Decock W, Nieukerken E van, Zarucchi J, Penev L (Eds) Species 2000 and ITIS Catalogue of Life, Species 2000: Naturalis, Leiden, the Netherlands. http://www.catalogueoflife.org/col/ [Accessed 12 February 2019]

Shortt KB, Vamosi SM (2012) A review of the biology of the weedy Siberian peashrub, *Caragana arborescens*, with an emphasis on its potential effects in North America. Botanical Studies 53: 1–8.

Sinev SY (2008) Catalogue of the Lepidoptera of Russia. KMK Press, St. Petersburg-Moscow, 425 pp. [In Russian]

The Plant List (2018) Version 1.1. *Caragana*. http://www.theplantlist.org/tpl1.1/search?q=Caragana [Accessed 15 December 2018]

Supplementary material 1

Table S1

Authors: Natalia Kirichenko, Paolo Triberti, Carlos Lopez-Vaamonde

Explanation note: Fabaceae-feeding *Phyllonorycter* of the world.

Link: https://doi.org/10.3897/zookeys.835.33166.suppl1

Supplementary material 2

Table S2

Authors: Natalia Kirichenko, Paolo Triberti, Carlos Lopez-Vaamonde

Explanation note: Fabaceae-feeding *Phyllonorycter* species involved in the study. Where relevent, genitalia preparation number is given in square brackets in the Life stage column. Both the Process ID and Sample ID codes link the record in the BOLD database and the voucher specimen from which the sequence is derived.

Link: https://doi.org/10.3897/zookeys.835.33166.suppl2

ZooKeys 835: 43–63 (2019)
doi: 10.3897/zookeys.835.32470
http://zookeys.pensoft.net

RESEARCH ARTICLE

A peer-reviewed open-access journal
ZooKeys
Launched to accelerate biodiversity research

Mitochondrial genomes of the stoneflies *Mesonemoura metafiligera* and *Mesonemoura tritaenia* (Plecoptera, Nemouridae), with a phylogenetic analysis of Nemouroidea

Jin-Jun Cao[1,2], Ying Wang[1,2], Yao-Rui Huang[1], Wei-Hai Li[1]

1 *Department of Plant Protection, Henan Institute of Science and Technology, Xinxiang, Henan 453003, China*
2 *Postdoctoral Research Base, Henan Institute of Science and Technology, Xinxiang, Henan 453003, China*

Corresponding author: *Wei–Hai Li* (lwh7969@163.com)

Academic editor: *M. Gottardo* | Received 17 December 2018 | Accepted 21 February 2019 | Published 4 April 2019

http://zoobank.org/6ED7560A-09BE-4340-8DF4-9121C4F80127

Citation: Cao J-J, Wang Y, Huang Y-R, Li W-H (2019) Mitochondrial genomes of the stoneflies *Mesonemoura metafiligera* and *Mesonemoura tritaenia* (Plecoptera, Nemouridae), with a phylogenetic analysis of Nemouroidea. ZooKeys 835: 43–63. https://doi.org/10.3897/zookeys.835.32470

Abstract

In this study, two new mitochondrial genomes (mitogenomes) of *Mesonemoura metafiligera* and *Mesonemoura tritaenia* from the family Nemouridae (Insecta: Plecoptera) were sequenced. The *Mesonemoura metafiligera* mitogenome was a 15,739 bp circular DNA molecule, which was smaller than that of *M. tritaenia* (15,778 bp) due to differences in the size of the A+T-rich region. Results show that gene content, gene arrangement, base composition, and codon usage were highly conserved in two species. Ka/Ks ratios analyses of protein-coding genes revealed that the highest and lowest rates were found in ND6 and COI and that all these genes were evolving under purifying selection. All tRNA genes in nemourid mitogenomes had a typical cloverleaf secondary structure, except for $tRNA^{Ser(AGN)}$ which appeared to lack the dihydrouridine arm. The multiple alignments of nemourid lrRNA and srRNA genes showed that sequences of three species were highly conserved. All the A+T-rich region included tandem repeats regions and stem-loop structures. The phylogenetic analyses using Bayesian inference (BI) and maximum likelihood methods (ML) generated identical results. Amphinemurinae and Nemourinae were sister-groups and the family Nemouridae was placed as sister to Capniidae and Taeniopterygidae.

Keywords

Amphinemurinae, comparative mitochondrial genomics, Nemouridae, phylogenetics, Plecoptera

Introduction

The mitochondrial genome (mitogenome) of insects is typically a small double-stranded circular molecule of 14–20 kb in size. It contains13 protein-encoding (PCGs), 22 transfer RNA (tRNAs), two ribosomal RNA (rRNAs) genes, and a putative control region (in arthropods, also known as A+T-rich region) where the necessary regulatory sequences for transcription and duplication of the DNA occur (Boore 1999). Because of their simple genomic organization, fast rate of nucleotide substitution, and low levels of sequence recombination, mitogenomes are used as good models in comparative and evolutionary genomics, population genetics, and phylogenetic studies at various taxonomic levels (Lin and Danforth 2004; Gissi et al. 2008; Cameron 2014; Song et al. 2016; Li et al. 2017).

The Plecoptera (stoneflies) comprises an ancient group of insects including about 3,900 described species worldwide (Dewalt et al. 2018). The family Nemouridae, belongs to the superfamily Nemouroidea within the family group Euholognatha in suborder Arctoperlaria (Dewalt et al. 2018). Nemouridae is one of the largest families of Plecoptera with approximately 400 species (Baumann 1975; Dewalt et al. 2018). Baumann (1975) divided the family Nemouridae into two subfamilies, the Amphinemurinae and the Nemourinae, and erected two oriental genera, *Mesonemoura* and *Indonemoura* in the latter subfamily, which also includes the genera *Amphinemura*, *Malenka,* and *Protonemura*. The Amphinemurinae are well distributed in the Palearctic, Nearctic, and Oriental regions. They occur in a wide variety of streams but are probably most diverse in smaller creeks and spring runs (Dewalt et al. 2018). Currently, the position of Nemouridae in Plecoptera has been resolved based on morphology (Illies 1965; Zwick 2000), but several different suggestions are proposed based on molecular data (Thomas et al. 2000; Terry and Whiting 2003; Chen and Du 2018; Wang et al. 2019), and the relationship within the Nemouroidea still lacks precise phylogeny. Up to now, only one nemourid mitogenome (*Nemoura nankinensis* Wu, 1926) has been sequenced (Chen and Du 2017a) and those conflicting opinions were mainly generated by the limited mitogenomic data. Therefore, more molecular data is required to reconstruct precise phylogeny (Misof et al. 2014; Wu et al. 2014).

To date, 27 mitogenomes of stoneflies have been sequenced (Wang et al. 2019), but those of the subfamily Amphinemurinae are still not reported, and the phylogeny of Nemouridae is still controversial due to lack of plenty molecular data. To facilitate the resolution of this problem, we report the complete mitogenomes of *M. tritaenia* Li & Yang, 2007 and *M. metafiligera* Aubert, 1967, analyze and compare their mitogenomic organizations, nucleotide compositions, codon usages, RNA secondary structures, Ka/Ks ratios of 13 PCGs, and novel features of the A+T-rich regions. Finally, we also reconstructed the phylogenetic tree of the superfamily Nemouroidea based on the concatenated nucleotide sequences of four datasets (PCGs, PCGR, PCG12 and PCG12R) by using Bayesian inference (BI) and Maximum likelihood (ML) methods, thus our result increases the understanding of stonefly phylogeny.

Materials and methods

Specimens and DNA extraction

Adult specimens of *M. tritaenia* and *M. metafiligera* were collected from Baiyun Mountain (Luoyang, Henan Province, China) in July 2015 and from Bolonggong (Tibet, China) in August 2015, respectively. We preserved specimens in 95% ethanol in the field and stored them at – 20 °C until tissues were used for DNA extraction. Voucher specimens of *M. tritaenia* (No. Vhem–0008) and *M. metafiligera* (No. Vhem–0061) were deposited in Entomological Museum of Henan institute of Science and Technology (HIST), Henan Province, China. Specimens were identified by Wei-Hai Li (HIST). We extracted total genomic DNA from thoracic muscle tissue using QIAamp DNA Blood Mini Kit (Qiagen, Duesseldorf, Germany) according to the manufacturer's protocols.

Genome sequencing, assembly, and annotation

The mitogenomes were amplified and sequenced as described in previous studies (Song et al. 2016; Li et al. 2017; Wang et al. 2017a, 2017b; Wang et al. 2018a, 2018b). From the genomic DNA, an Illumina TruSeq library with an insert size of 480 bp was generated. We sequenced our library on a single lane of Illumina Hiseq 2500 with 500 cycles of paired-end sequencing (250 bp reads). High-quality reads were generated using Trimmomatic v0.30 (Lohse et al. 2012). Then, IDBA-UD (Peng et al. 2012) was used for de novo assembling with these reads. A similarity threshold of 98% and minimum and maximum k values of 80 and 240 bp, respectively, were used to build assemblies. COI and srRNA fragments were amplified as bait sequences using PCR (Li et al. 2012; Wang et al. 2014) and previously designed primers (Simon et al. 2006) were used to determine the mt genome components. Raw sequences from the mitochondrial genome of each species were assembled into contigs with BioEdit 7.0.5.3 (Hall 1999). We identified protein-coding genes and two ribosomal RNA genes using BLAST searches in NCBI and by alignment with homologous genes from published stonefly species. tRNA genes were identified using the ARWEN online service and checked manually (Laslett and Canbäck 2008). Each protein-coding gene was aligned individually based on codon-based multiple alignments using the MAFFT algorithm within the TranslatorX online platform (Abascal et al. 2010). Before back-translating to nucleotides, poorly aligned sites were removed from the protein alignment using Gblocks in the TranslatorX with default settings. Nucleotide substitution rates, base composition, and codon usage were analyzed with MEGA 6.0 (Tamura et al. 2013). The GC and AT skews were calculated using the formulae: AT skew= (A–T)/ (A+T) and GC skew= (G–C)/ (G+C) (Perna and Kocher 1995).

We calculated the value of Ka (the rates of non-synonymous substitutions), Ks (the rates of synonymous substitutions) using DnaSP 5.1.0 (Librado and Rozas

2009). We also identified tandem repeats in the A+T-rich region using the Tandem Repeats Finder server (Benson 1999), and predicted the stem-loop structure using the mfold web server (Zuker 2003).

Phylogenetic analysis

The phylogenetic trees among three families of the superfamily Nemouroidea were reconstructed using DNA data from nine published and two newly sequenced mitogenomes. Two stonefly species, *Pteronarcys princeps* and *Styloperla spinicercia*, were used as outgroups (Table 1). We assembled the following datasets for phylogenetic analyses: 1) the "PCGs matrix" (total of 11,046 bp), inclusive of 13 PCGs; 2) the "PCG12 matrix" (total of 7,364 bp) which contains the first and second codon positions of protein-coding genes; 3) the "PCGR matrix" (total of 13,056 bp) which contains all three codon positions of protein-coding genes and two ribosomal RNA genes; 4) the "PCG12R matrix" (9374 bp) which contains the first and second codon of PCGs and two ribosomal RNA genes. The BI and ML analyses were carried out on the CIPRES Science Gateway (Miller et al. 2010). ML analyses were performed with RaxML-HPC2 on XSEDE 8.1.10 (Stamatakis 2006) using the GTRGAMMAI model, and node confidence was assessed with 1,000 bootstrap replicates. Bayesian analyses were carried out using MrBayes 3.2.6 on XSEDE (Ronquist et al. 2012). For BI analyses, GTR+I+G was the best-fit model for the nucleotide sequence alignments, using jModelTest 0.1.1 based on Akaike's information criterion (AIC) (Posada 2008). We conducted with two simultaneous runs for 10 million generations. Each set was sampled every 1,000 generations with a burn-in rate of 25%. Stationarity was examined by Tracer v.1.6 (http://tree.bio.ed.ac.uk/software/tracer/), and was considered to be reached when the ESS (estimated sample size) value was above 200.

Table 1. General information of the taxa used in this study.

Family	Species	Number (bp)	Accession number
Nemouridae	*Nemoura nankinensis*	16,602	KY940360
	Mesonemoura tritaenia	15,778	MH085451
	Mesonemoura metafiligera	15,739	MH085450
Capniidae	*Apteroperla tikumana*	15,564	NC_027698
	Capnia zijinshana	16,310	KX094942
	Mesocapnia arizonensis	14,921	KP642637†
	Mesocapnia daxingana	15,524	KY568983†
Taeniopterygidae	*Doddsia occidentalis*	16,020	MG589787
	Taeniopteryx ugola	15,353	MG589786
Styloperlidae (Outgroup)	*Styloperla spinicercia*	16,219	KX845569
Pteronarcyidae (Outgroup)	*Pteronarcys princeps*	16,004	NC_006133

† Incomplete genome sequence.

Results and discussion

Genome features

In the present study, two complete mitogenomes of *M. metafiligera* and *M. tritaenia* were sequenced and deposited in GenBank of NCBI under accession numbers MH085450–MH085451 (see Table 1 and Fig. 1). The *M. metafiligera* mitogenome was a 15,739 bp circular DNA molecule, which was smaller than *M. tritaenia* (15,778 bp) due to differences in the size of the A+T-rich region (Tables 1 and 2). The size of completely sequenced mitogenomes were medium-sized when compared with the mitogenomes of other stoneflies, which ranged from 16,602 bp (*N. nankinensis*) (Chen and Du 2017a) to 15,048 bp (*Isoperla bilineata*) (Chen et al. 2018). All genes identified in the two mitogenomes are typical animal mitochondrial genes with normal gene sizes. Mitochondrial gene order was the same as all previously published stonefly mitogenomes, as well as the ancestral gene order of insects, as exemplified by *Drosophila yakuba* (Clary and Wolstenholme 1985). When compared with the mitogenome of *N. nankinensis* (Chen and Du 2017a), the length variation was limited in the PCGs, tRNA, and rRNA genes, but very different in the A+T-rich region.

In the mitogenome of *M. metafiligera*, 50 overlapping nucleotides were located in 15 pairs of neighboring genes, while in the mitogenome of *M. tritaenia*, there were 51 overlapping nucleotides in 16 gene boundaries. These overlapping nucleotides varied in length from 1 to 8 bp (Table 2). When compared with the mitogenome of *N. nankinensis*, three conserved regions were found in overlapping regions of genes of each sequenced nemourid species and were also observed in some other stoneflies: AAGCCTTA (tRNA^{Trp}-tRNA^{Cys}), ATGATTA (ATP8–ATP6) and ATGTTAA (ND4–ND4L) (James and Andrew 2006; Qian et al. 2014; Wu et al. 2014; Elbrecht et al. 2015; Huang et al. 2015; Wang et al. 2017a, 2017b, 2018a). The ATP8/ATP6 and the ND4/ND4L gene pairs overlap are also found in many insect mitogenomes and thought to be translated as a bicistron (Stewart and Beckenbach 2005). The longest intergenic spacer we found located between tRNA$^{Ser(UCN)}$ and ND1 in two nemourid species, ranging from 35 bp in *M. metafiligera* to 38 bp in *M. tritaenia* (Table 2). In *Drosophila melanogaster*, two conserved non-coding intergenic regions (tRNA^{Glu}-tRNA^{Phe}, and tRNA$^{Ser(UCN)}$–ND1) have been shown to be binding sites for a bidirectional transcription termination factor (DmTTF) (Beckenbach 2012). For the first binding site of tRNA^{Glu}-tRNA^{Phe}, this region was absent in two nemourid mitogenomes (Table 2). Studies show that this region is absent or incomplete in other plecopteran species as well as in other insect orders (Beckenbach 2012). However, the second binding site of tRNA$^{Ser(UCN)}$–ND1 is found in two nemourid species. This region is more widely conserved and similar non-coding sequences are present at this site in other insect orders (Beckenbach 2012).

Similarly to what observed in other insects, the nucleotide composition of two nemourid mitogenomes was clearly biased towards a higher content of A/T nucleotides. The base composition bias of the *M. metafiligera* mitogenome is 69.1% A + T content,

Table 2. Mitochondrial genome structures of *Mesonemoura tritaenia* and *Mesonemoura metafiligera*.

Gene	Direction	*Mesonemoura tritaenia*				*Mesonemoura metafiligera*			
		Location (bp)	Size (bp)	Anti– or Start/Stop Codons	IGN	Location (bp)	Size (bp)	Anti– or Start/Stop Codons	IGN
$tRNA^{Ile}$	F	1–67	67	GAT		1–66	66	GAT	
$tRNA^{Gln}$	R	65–133	69	TTG	–3	64–132	69	TTG	–3
$tRNA^{Met}$	F	146–212	67	CAT	12	145–211	67	CAT	12
ND2	F	213–1247	1,035	ATG/TAG	0	212–1,246	1,035	ATG\TAG	0
$tRNA^{Trp}$	F	1,254–1,322	69	TCA	6	1,252–1,320	69	TCA	5
$tRNA^{Cys}$	R	1,315–1,377	63	GCA	–8	1,313–1,375	63	GCA	–8
$tRNA^{Tyr}$	R	1,385–1,450	66	GTA	7	1,382–1,448	67	GTA	6
COI	F	1,443–2,987	1,545	ATT/TAA	–8	1,441–2,985	1,545	ATT\TAA	–8
$tRNA^{Leu(UUR)}$	F	2,983–3,049	67	TAA	–5	2,981–3,047	67	TAA	–5
COII	F	3,052–3,739	688	ATG/T–	2	3,050–3,737	688	ATG\T–	2
$tRNA^{Lys}$	F	3740–3810	71	CTT	0	3,738–3,808	71	CTT	0
$tRNA^{Asp}$	F	3,810–3,877	68	GTC	–1	3,809–3,876	68	GTC	0
ATP8	F	3,878–4,036	159	ATT/TAA	0	3877–4035	159	ATT\TAA	0
ATP6	F	4,030–4,707	678	ATG/TAA	–7	4,029–4,706	678	ATG\TAA	–7
COIII	F	4,707–5,495	789	ATG/TAA	–1	4,706–5,494	789	ATG\TAA	–1
$tRNA^{Gly}$	F	5,495–5,560	66	TCC	–1	5,494–5,559	66	TCC	–1
ND3	F	5,561–5,914	354	ATT/TAG	0	5,560–5,913	354	ATT\TAG	0
$tRNA^{Ala}$	F	5,913–5,976	64	TGC	–2	5,912–5,975	64	TGC	–2
$tRNA^{Arg}$	F	5,977–6,041	65	TCG	0	5,976–6,040	65	TCG	0
$tRNA^{Asn}$	F	6,052–6,116	65	GTT	10	6,046–6,110	65	GTT	5
$tRNA^{Ser(AGN)}$	F	6,116–6,184	69	GCT	–1	6,110–6,178	69	GCT	–1
$tRNA^{Glu}$	F	6184–6249	66	TTC	–1	6,178–6,244	67	TTC	–1
$tRNA^{Phe}$	R	6,248–6,312	65	GAA	–2	6,243–6,307	66	GAA	–2
ND5	R	6,313–8,047	1,735	ATG/T–	0	6,308–8,042	1,735	GTG\T–	0
$tRNA^{His}$	R	8,048–8,113	66	GTG	0	8,043–8,109	67	GTG	0
ND4	R	8,115–9,455	1,341	ATG/TAA	1	8,111–9,451	1,341	ATG\TAA	1
ND4L	R	9,449–9,745	297	ATG/TAA	–7	9,445–9,741	297	ATG\TAA	–7
$tRNA^{Thr}$	F	9,748–9,813	66	TGT	2	9,744–9,809	66	TGT	2
$tRNA^{Pro}$	R	9,813–9,877	65	TGG	–1	9,809–9,873	64	TGG	–1
ND6	F	9,879–10,403	525	ATT/TAA	1	9875–10399	525	ATT\TAA	1
CytB	F	10,403–11,539	1,137	ATG/TAG	–1	10,399–11,535	1,137	ATG\TAG	–1
$tRNA^{Ser(UCN)}$	F	11,538–11,607	70	TGA	–2	11,534–11,603	70	TGA	–2
ND1	R	11,646–12,596	951	TTG/TAA	38	11,639–12,589	951	TTG\TAA	35
$tRNA^{Leu(CUN)}$	R	12,598–12,663	66	TAG	1	12,591–12,656	66	TAG	1
lrRNA	R	12,664–13,992	1,329		0	12,657–13,983	1,327		0
$tRNA^{Val}$	R	13,993–14,063	71	TAC	0	13,984–14,054	71	TAC	0
srRNA	R	14,064–14,857	794		0	14,055–14,846	792		0
A+T-rich region		14,858–15,778	921		0	14,847–15,739	893		0

IGN: Intergenic nucleotides.

made up of 66.9% in the PCGs, 71.3% in the tRNAs, 72.6% in the rRNAs and 84.1% in the A + T rich region. While the base composition bias of the *M. tritaenia* mitogenome is 68.6% A + T content, made up of 66.4% in the PCGs, 71.3% in the tRNAs, 72.0% in the rRNAs and 82.1% in the A + T rich region (Table 3). This is identical to the base composition biases reported in other stoneflies, which ranges from 62.5% (*Dinocras cephalotes* Curtis, 1827) to 71.5% (*Pteronarcys princeps* Banks,

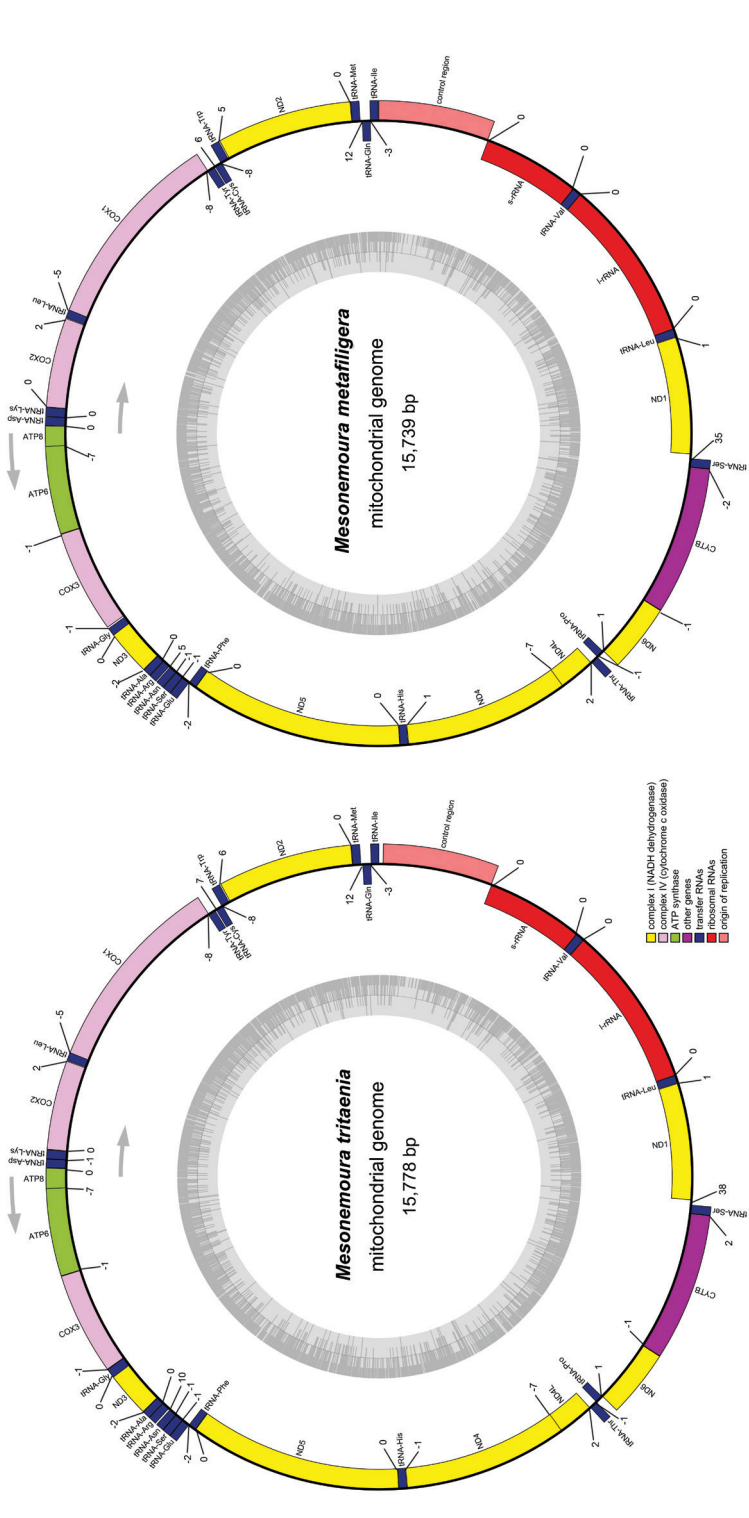

Figure 1. Map of the mitogenomes of *M. metafiligera* and *M. tritaenia*. Genes shown on the inside of the map are transcribed in a clockwise direction, whereas those on the outside of the map are transcribed counterclockwise. Different gene types are shown as filled boxes in different colors. Numbers show the sizes of intergenic spacers (positive values) and overlapping region between genes (negative values).

1907) (James and Andrew 2006; Elbrecht et al. 2015). After comparing the nucleotide compositions of four major partitions (PCGs, tRNAs, rRNAs, and the A+T-rich region), we found that all four partitions were consistently biased towards A and T. Among the four partitions, the lowest A + T content was found in PCGs, whereas the highest in the A+T-rich region of the two nemourid specimens. The strand bias also can be measured as AT– and GC-skews (Perna and Kocher 1995). Both two nemourid species had positive AT-skew and negative GC-skew values for the entire mitogenome (Table 3), showing a biased use for the A and C nucleotides, which was common in most other insects (Wei et al. 2010).

Protein-coding genes

The total length of all PCGs of both mitogenomes of *M. metafiligera and M. tritaenia* were 11,199 bp (Table 3). Most PCGs of the two mitogenomes initiated with the typical start codon ATN (Met/Ile), however TTG was proposed as the start codon for ND1 in two species (Table 2). Gene ND1 has been found to employ TTG as a start codon in some insects, thus minimizing intergenic spacing and avoiding overlap with adjacent genes (Bae et al. 2004; Sheffield et al. 2008; Wei et al. 2010). The ND5 gene of *M. metafiligera* has the unusual start codon GTG, as previously reported in other stoneflies (James and Andrew 2006; Elbrecht et al. 2015; Huang et al. 2015; Sproul et al. 2015; Chen et al. 2016; Elbrecht and Leese 2016; Chen and Du 2017b; Wang et al. 2017a, 2017b).

Similar to most other stoneflies, the most commonly used stop codon in two nemourid specimens was TAA, which was found in eight of the 13 PCGs (ATP6, ATP8, COI, COIII, ND1, ND4, ND4L and ND6) for both two nemourid mitogenomes. The stop codon TAG was used in ND2, ND3 and CytB. In *M. metafiligera and M. tritaenia*, both COII and ND5 terminate with incomplete stop codon T (Table 2). The phenomenon of incomplete stop codons is common in insect mitogenomes and it is likely that these truncated stop codons are completed by posttranscriptional polyadenylation (Ojala et al. 1981). Overall, the start and stop codons were similar in two nemourid specimens, and showed little differences between them in some PCGs (Table 2).

The genome-wide bias toward A+T content was also reflected in the codon usage by the PCGs. The relative synonymous codon usage (RSCU) showed high base compositional biases for AT in the mitogenomes of *M. tritaenia* and *M. metafiligera* (Suppl. material 1, Figure S1). The codons ending with A or U were preferred in both the four-fold and two-fold degenerate codons. However, in *M. metafiligera* mitogenomes, the RSCU value of GGG (Gly) was higher than GGT (Gly) (Suppl. material 1, Figure S1). This may be caused by the anticodon $tRNA^{Gly}$-TCC, which contain swinging nucleotides and can decode GGG (Mao and Dowton 2014).

In order to analyze the evolutionary patterns of PCGs in the three nemourid mitogenomes, we compared the ratio of Ka/Ks for each PCGs (Suppl. material 2, Figure S2). The observed average Ka/Ks ratios were consistently lower than 0.3, increasing

Table 3. The nucleotide composition of *Mesonemoura tritaenia* and *Mesonemoura metafiligera* mitogenome.

Genes or regions	Size	Nucleotides composition (%)				A+T (%)	AT Skew	GC Skew
		T	C	A	G			
Mesonemoura tritaenia								
Complete mitogenome	15,778	32.5	19.0	36.0	12.5	68.6	0.051	–0.208
PCGs	11,199	38.8	17.3	27.6	16.3	66.4	–0.169	–0.029
tRNA genes	1,471	35.9	12.6	35.4	16.1	71.3	–0.007	0.123
rRNA genes	2,123	39.6	9.8	32.4	18.2	72.0	–0.100	0.300
lrRNA	1,329	40.6	8.7	32.7	18.1	73.3	–0.109	0.352
srRNA	794	37.9	11.7	32.0	18.4	69.9	–0.085	0.222
A+T-rich region	921	39.5	11.8	42.6	6.1	82.1	0.037	–0.321
Mesonemoura metafiligera								
Complete mitogenome	15,739	33.0	18.6	36.2	12.3	69.1	0.046	–0.206
PCGs	11,199	39.9	16.5	27.0	16.6	66.9	–0.194	0.000
tRNA genes	1,473	36.0	12.8	35.3	16.0	71.3	–0.010	0.111
rRNA genes	2,119	39.5	9.5	33.1	17.8	72.6	–0.089	0.303
lrRNA	1,327	40.5	8.3	33.6	17.6	74.2	–0.093	0.359
srRNA	792	37.9	11.6	32.2	18.3	70.1	–0.081	0.224
A+T-rich region	893	39.6	10.4	44.5	5.5	84.1	0.057	–0.310

from 0.025 for ATP6 to 0.202 for ND6 (Suppl. material 2, Figure S2). The uniformly low values of Ka/Ks ratios for COI, COII, COIII and CytB indicate strong evolution constraints in cytochrome c oxidase (Schmidt et al. 2001; Zsurka et al. 2010). The Ka/Ks values for all PCGs were below 0.3, indicating that these genes are evolving under purifying selection. Therefore, all mitochondrial PCGs could be used to investigate phylogenetic relationships within nemourid.

Transfer and ribosomal RNAs

The sizes of 22 tRNA genes of *M. metafiligera* and *M. tritaenia* range from 63 bp to 71 bp, comprising 9.36% (1,473 bp) and 9.32% (1,471 bp) of the total mitogenomes, respectively (Table 2 and 3). By compared with *N. nankinensis* mitogenome, all 22 tRNA genes in the three nemourid species were identified and the secondary structures were shown in Fig. 2. Most tRNA genes could be folded into a classic cloverleaf secondary structure except for $tRNA^{Ser(AGN)}$ due to a lack of the dihydrouridine (DHU) arm (Fig. 2). The loss of the DHU arm in $tRNA^{Ser(AGN)}$ was a typical feature in metazoan mitogenomes (Negrisolo et al. 2011). However, we found that $tRNA^{Ser(AGN)}$ in the three nemourid mitogenomes possessed an unusual anticodon stem (9 pairs of nucleotides) with an extended nucleotide (Fig. 2). This is an unusual phenomenon, but has also been observed in the DHU arm in other stoneflies (Chen and Du 2017b; Wang et al. 2017a; Wang et al. 2018a, 2018b).

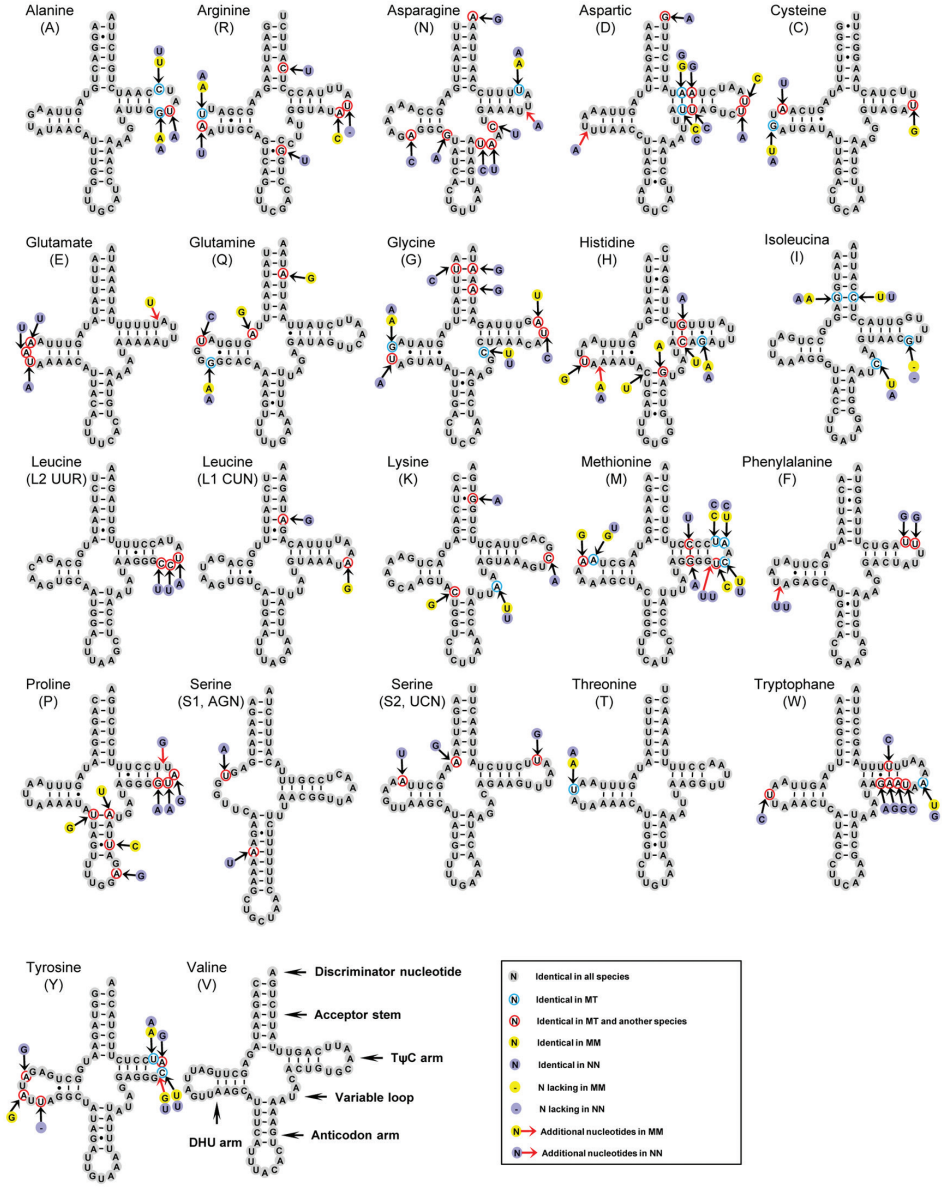

Figure 2. Secondary structure of tRNA families in nemourid mitogenomes. The nucleotide substitution pattern for each tRNA family is modeled using as reference the structure determined for *M. tritaenia*. Red arrows correspond to insertions. Inferred Watson-Crick bonds are illustrated by lines, whereas GU bonds are illustrated by dots.

According to the secondary structures and sequence alignment, the most conserved tRNAs in nemourid mitogenomes were $tRNA^{Val}$, $tRNA^{Thr}$, $tRNA^{Ser(AGN)}$ and $tRNA^{Leu(CUN)}$ with no more than two nucleotides substitution in each gene (Fig. 2).

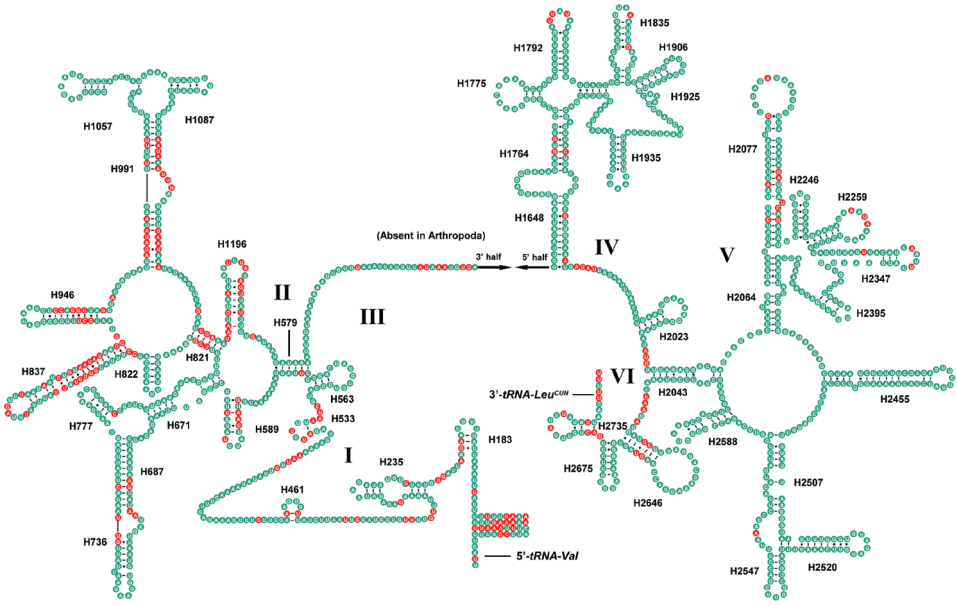

Figure 3. Predicted secondary structure of the *lrRNA* in *M. tritaenia*. Key: red circle, nucleotide conserved in three nemourid mitogenomes; green circle, nucleotide not conserved. Roman numerals represent the conserved domain structures. Dashes (–) indicate Watson-Crick base pairing, and dots (·) indicate G–U base pairing **I–VI** indicate six domains in the secondary structure of lrRNA.

Nucleotide insertion-deletion polymorphisms were mainly restricted to TΨC and DHU loops. As expected, tRNAs of *M. tritaenia* and *M. metafiligera* showed high level of sequence and structural identity, with five identical tRNAs (tRNA^{Val}, tRNA$^{Ser(UCN)}$, tRNA$^{Ser(AGN)}$, tRNA$^{Leu(UUR)}$ and tRNA^{Phe}) (Fig. 2). The eighteen remaining tRNAs only had four insertion-deletion positions in total (one insertion position in the DHU loop of tRNA^{His}, each with one insertion position in the TΨC loop of tRNA^{Glu} and tRNA^{Tyr}, and one deletion position in the TΨC loop of tRNA^{Ile}), and the nucleotide substitutions of individual gene were mostly restricted to 1–3 nucleotide sites, with the exception of tRNA^{His} and tRNA^{Met} with 5 and 6 sites respectively (Fig. 2).

The large subunit ribosome gene (lrRNA) was located between tRNA$^{Leu(CUN)}$ and tRNA^{Val}, while the small subunit ribosome gene (srRNA) was flanked by tRNA^{Val} and the A+T-rich region (Fig. 1). Two ribosome genes (srRNA and lrRNA) were identified at 794 and 1,329 bp in *M. tritaenia* and at 792 and 1,327 bp in *M. metafiligera* (Table 2). Our result shows that the size differences in both ribosomal subunits are not distinct among different species.

In this study, the secondary structures of the srRNA and lrRNA of *M. tritaenia* were constructed following the models proposed for other insects, with marked the conserved sites. The secondary structure of lrRNA contained five structural domains (I–II, IV–VI, domain III is absent in arthropods) and 44 helices (Fig. 3). The multiple alignments of

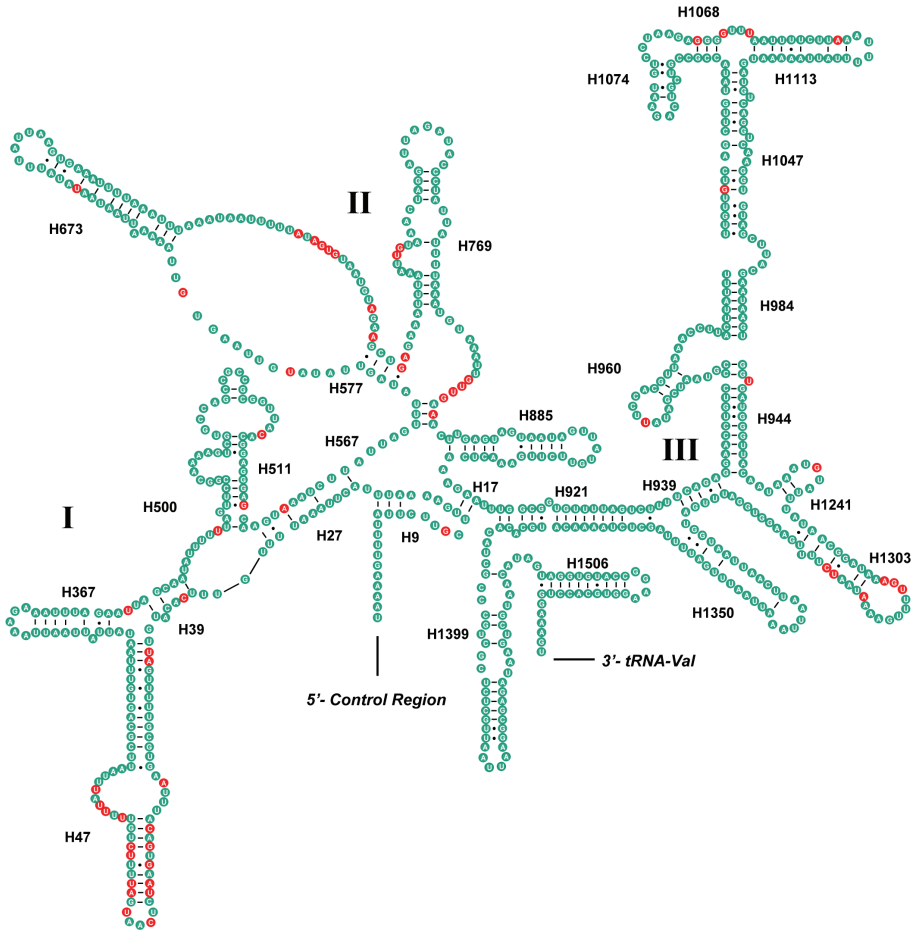

Figure 4. Predicted secondary structure of the *srRNA* in *M. tritaenia*. Key: red circle, nucleotide conserved in three nemourid mitogenomes; green circle, nucleotide not conserved. Roman numerals represent the conserved domain structures. Dashes (–) indicate Watson–Crick base pairing, and dots (·) indicate G–U base pairing **I–VI** indicate six domains in the secondary structure of srRNA.

nemourid lrRNA genes had 1,334 positions and contained 1,139 conserved positions (85.4%), 190 necleotide substitutions (14.2%) and 5 indels (0.4%), respectively. Nucleotide variability was unevenly distributed among domains and helices, mainly in domains I and II. Several helices (H821, H837, H946, H991, and H1196) in lrRNA, with high variability at the primary sequence level, showed conserved secondary structures. The secondary structure of srRNA contained three domains (I–IV) and 27 helices (Fig. 4). The multiple alignments of nemourid srRNA genes was inclusive of 795 positions and contained 737 conserved positions (92.7%), 56 necleotide substitutions (7.0%) and 2 indels (0.3%), respectively. Nucleotide variability was unevenly distributed among domains and helices, mainly in helices H47 of domain I.

A+T-rich region

The A+T-rich regions all locate between srRNA and $tRNA^{Ile}$ in *M. tritaenia* and *M. metafiligera* mitogenome with 921 bp and 893 bp in length, respectively (Table 2). This region is considered to be the control region as it contains both an origin of transcription and replication (Taanman 1999; Cameron 2014). The A+T-rich region is the most variable region in mitogenome due to insertion and deletion events, variation in numbers of tandem repeats, and differences in variable domain length (Zhang et al. 1995; Taanman 1999). In addition, some structural elements are founded in the A+T-rich region, such as poly-T stretch, stem-loop (SL) structures, tandem repeats (TRs) and G+A-rich region, etc. (Zhang and Hewitt 1997). A comparison of molecular features in A+T-rich region between the two newly sequenced mitogenomes was shown in Fig. 5. Some essential elements were observed: (1) a leading sequence adjacent to srRNA; (2) large tandem repeats present as two or more copies; (3) the remainder of the A+T-rich region (Fig. 5A).

Repeated sequences are common in the A+T-rich region for most insects, and length variations are decided to a large degree by the various numbers of repeats (Zhang and Hewitt 1997; Zhang et al. 1995). In the case of *M. tritaenia*, there is a large repeat region (positions: 15,243–15,483) which is 241 bp and contains two tandem repeat units plus a partial copy of the repeat. While in the A+T-rich region of *M. tritaenia* mitogenome, two tandem repeat regions (TR1 and TR2) were founded. TR1 region (positions: 15,265–15,428) is 164 bp and contains three tandem repeat units plus a partial copy of the repeat; In TR2 region (positions: 15,623–15,661), the two tandem repeats units were 21 and 18 bp (not strictly repeats). We also found some SL structures in two newly sequenced species. Two SL structures were predicted in the A+T-rich region of *M. metafiligera* mitogenome: SL–1 (positions: 15,122–15,146) and SL–2 (positions: 15,193–15,208) (Fig. 5B). In the A+T-rich region of *M. tritaenia* mitogenome, we found two long repeated sequences: 5'–TATATATATATATATAAATTAATAAATAATTTATTGTA–3'. Both of them can be folded into a stem-loop structure (SL–1 positions: 15,306–15,343; SL–2 positions: 15,352–15,389) (Fig. 5C). This special structure in the A+T-rich region of *M. tritaenia* mitogenome is quite different with that of other published stoneflies except for *Acroneuria hainana* Wu, 1938, and it may be able to adjust the replication speed of two replicate directions (Huang et al. 2015). The proposed "$G(A)_nT$" motif was detected in SL structures of *M. metafiligera* mitogenome, while it was modified as "GTA" in SL structures of *M. tritaenia* mitogenome. In the A+T-rich region of *N. nankinensis* mitogenome, five SL structures with three different motifs ("GTA", "$G(A)_nT$" and "TGA") were detected (Chen and Du 2017a). The stem-loop structure in the A+T-rich region is identified in many insects and it is thought to be the site of the initiation of minority strand (N-strand) synthesis in *Drosophila* (Clary and Wolstenholme 1987). By contrast, some tRNA-like structures also founded in *N. nankinensis* mitogenome, but these structures were not reported in our newly sequenced species.

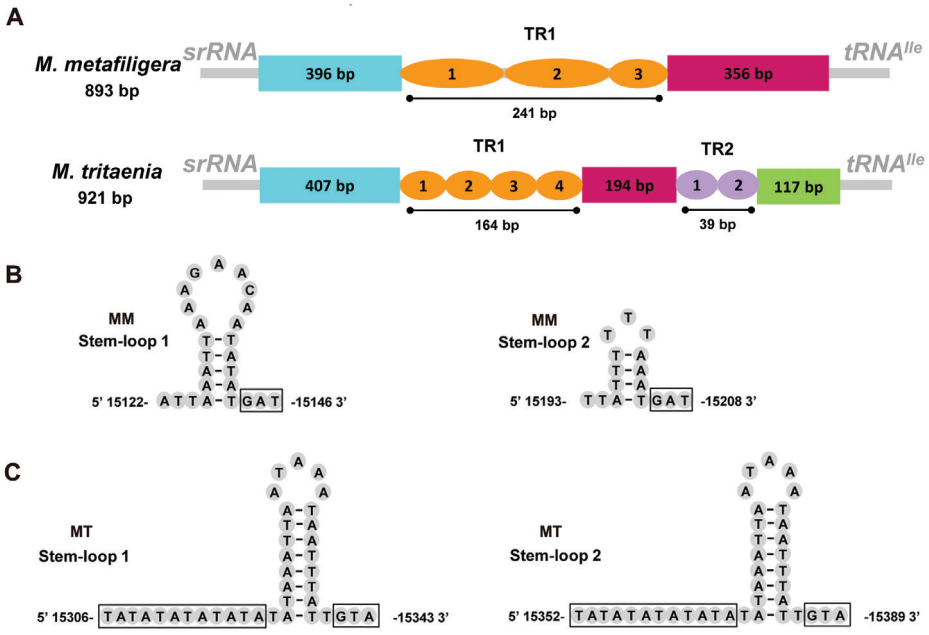

Figure 5. A+T-rich region of two nemourid mitogenomes **A** structure elements found in the A+T-rich region of two nemourid mitogenomes. TR is the abbreviation of tandem repeat units **B** putative stem-loop structures found in the A+T-rich region of *M. metafiligera* (MM indicate *M. metafiligera*) **C** putative stem-loop structures found in the A+T-rich region of *M. tritaenia* (MT indicate *M. tritaenia*).

Phylogenetic relationships

The phylogenetic trees based on Bayesian inference (BI) and maximum likelihood (ML) analyses of PCGs, PCGR, PCG12, and PCG12R datasets were given in Fig. 6. The two methods provided the same tree topology.

In Nemouridae, both ML and BI analyses of four datasets supported the sister-group relationship of Amphinemurinae and the Nemourinae species (Bayesian posterior probabilities (PP) = 1.00/1.00/1.00/1.00; Bootstrap values (BS) = 100/100/100/100), as previous analyses based on the morphological data had indicated (Baumann 1975). The family Capniidae had a closer relationship with Taeniopterygidae (PP = 0.81–1.00; BS = 89–100). However, high intermediate supports were present in both analyses indicating that the phylogenetic position of Capniidae and Taeniopterygidae might be unstable. Meanwhile, the family Nemouridae was placed as sister to Capniidae and Taeniopterygidae (PP = 1.00/1.00/1.00/1.00; BS = 100/100/100/100). Our results of the three families are congruent with our previous results generated by ML analysis of two datasets (PCGR and PCG12) and BI analysis of PCG12 (Wang et al. 2019), and this relationship is also well supported by some studies based on mitogenomes (Chen and Du 2017a) and transcriptome data (Davis 2013), but this placement disagrees somewhat with previous morphological hypotheses. Illies (1965) considered that the

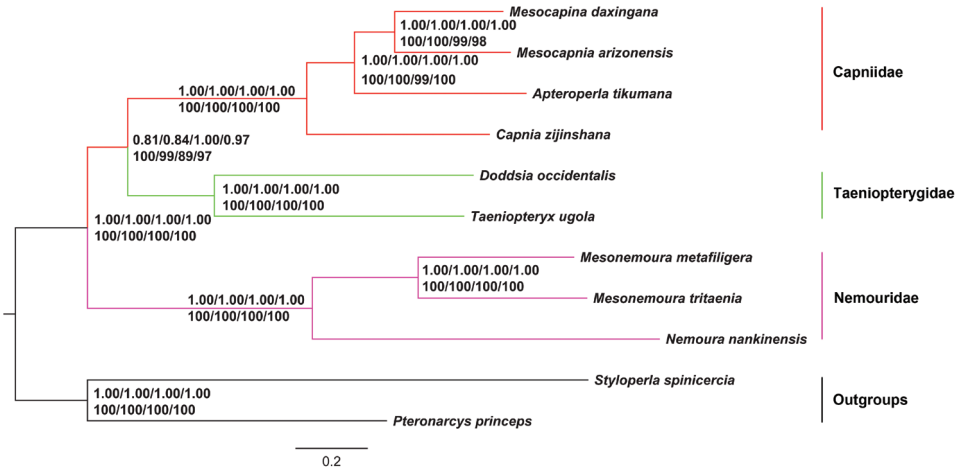

Figure 6. Phylogenetic tree of the eleven sequenced stoneflies. Bayesian inference and Maximum Likelihood analysis inferred from PCGs, PCGR, PCG12, and PCG12R supported the same topological structure. Values at nodes are Bayesian posterior probabilities (up) and ML bootstrap values (down) using the PCGs, PCGR, PCG12, and PCG12R datasets. The tree was rooted with two outgroups (*P. princeps* and *S. spinicercia*).

Taeniopterygidae was the sister-group to a clade Nemouridae + (Capniidae + Leuctridae). In Zwick's study, Taeniopterygidae was the sister-group to a clade (Capniidae + Leuctridae) + (Nemouridae + Notonemouridae) (Zwick 2000). In addition, our results are more incongruent with some molecular analysis. For example, Thomas et al. (2000) placed the Nemouridae and the rest of the Nemouroidea as a relatively derived clade, while Terry and Whiting (2003) supported Nemouridae as a sister taxon to Capniidae and then clustered with Taeniopterygidae. For this phenomenon, we believe that more comprehensive mitogenomes of Nemouroidea will solve this problem.

Conclusions

This study characterized two complete mitogenomes of the subfamily Amphinemurinae. The study provided the following conclusions: (1) Mitochondrial gene order of two Amphinemurinae species was the same as all previously published stonefly mitogenomes, as well as the ancestral pattern of insects, as exemplified by *D. yakuba*. (2) The evolutionary patterns of PCGs were observed in the three nemourid mitogenomes, which may indicate that these genes are evolving under purifying selection. (3) Novel structure characteristics were observed in the mitogenomes. In the two Amphinemurinae mitogenomes, stem-loop structures and tandem repeat sequences were detected. (4) Phylogenetic analysis supported that Amphinemurinae and Nemourinae were sister-group and the family Nemouridae was placed as sister to Capniidae and Taeniopterygidae. This study increases the understanding of stonefly phylogeny.

Acknowledgments

We thank Zachary Y Huang from Michigan State University, USA for improving the language. This research was supported by the Aid program for Science and Technology Innovative Research Team in higher Educational Institutions of Henan Province (17IRTSTHN18), the landmark Innovative Project of Henan Institute of Science and Technology (2015BZ04), the Key Scientific Research Project of Henan Province (16A210045), the National Natural Science Foundation of China (31372251; 31801999) and the initial Project of Henan Institute of Science and Technology (2014028).

References

Abascal F, Zardoya R, Telford MJ (2010) TranslatorX: multiple alignments of nucleotide sequences guided by amino acid translations. Nucleic Acids Research 38: W7–W13. https://doi.org/10.1093/nar/gkq291

Bae JS, Kim I, Sohn HD, Jin BR (2004) The mitochondrial genome of the firefly, *Pyrocoelia rufa*: complete DNA sequence, genome organization, and phylogenetic analysis with other insects. Molecular Phylogenetics and Evolution 32: 978–985. https://doi.org/10.1016/j.ympev.2004.03.009

Baumann RW (1975) Revision of the stonefly family Nemouridae (Plecoptera): a study of the world fauna at the generic level. Smithsonian Contributions to Zoology 40: 1–84. https://doi.org/10.5479/si.00810282.211

Beckenbach AT (2012) Mitochondrial genome sequences of Nematocera (Lower Diptera): evidence of rearrangement following a complete genome duplication in a winter crane fly genome. Genome Biology and Evolution 4: 89–101. https://doi.org/10.1093/gbe/evr131

Benson G (1999) Tandem repeats finder: a program to analyze DNA sequences. Nucleic Acids Research 27: 573–580. https://doi.org/10.1093/nar/27.2.573

Boore JL (1999) Animal mitochondrial genomes. Nucleic Acids Research 27: 1767–1780. https://doi.org/10.1093/nar/27.8.1767

Cameron SL (2014) Insect mitochondrial genomics: implications for evolution and phylogeny. Annual Review of Entomology 59: 95–117. https://doi.org/10.1146/annurev-ento-011613-162007

Chen ZT, Du YZ (2017a) First Mitochondrial genome from Nemouridae (Plecoptera) reveals novel features of the elongated control region and phylogenetic implications. International Journal of Molecular Sciences 18: 996. https://doi.org/10.3390/ijms18050996

Chen ZT, Du YZ (2017b) Complete mitochondrial genome of *Capnia zijinshana* (Plecoptera: Capniidae) and phylogenetic analysis among stoneflies. Journal of Asia-Pacific Entomology 20: 305–312. https://doi.org/10.1016/j.aspen.2017.01.013

Chen ZT, Du YZ (2018) The first two mitochondrial genomes from Taeniopterygidae (Insecta: Plecoptera): structural features and phylogenetic implications. International Journal of Biological Macromolecules 111: 70–76. https://doi.org/10.1016/j.ijbiomac.2017.12.150

Chen ZT, Wu HY, Du YZ (2016) The nearly complete mitochondrial genome of a stonefly species, *Styloperla* sp. (Plecoptera: Styloperlidae). Mitochondrial DNA Part A 27: 2728–2729.

Chen ZT, Zhao MY, Xu C, Du YZ (2018) Molecular phylogeny of Systellognatha (Plecoptera: Arctoperlaria) inferred from mitochondrial genome sequences. International Journal of Biological Macromolecules 111: 542–547. https://doi.org/10.1016/j.ijbiomac.2018.01.065

Clary DO, Wolstenholme DR (1985) The mitochondrial DNA molecule of *Drosophila yakuba*: Nucleotide sequence, gene organization, and genetic code. Journal of Molecular Evolution 22: 252–271. https://doi.org/10.1007/BF02099755

Clary DO, Wolstenholme DR (1987) Drosophila mitochondrial DNA: conserved sequences in the A+T rich region and supporting evidence for a secondary structure model of the small ribosomal RNA. Journal of Molecular Evolution 25: 116–125. https://doi.org/10.1007/BF02101753

Davis NG (2013) Application of next-generation transcriptomic tools for non-model organisms: gene discovery and marker development within Plecoptera (Insecta). All Theses and Dissertations 4265. https://scholarsarchive.byu.edu/etd/4265/

Dewalt RE, Maehr MD, Neu-Becker U, Stueber G (2018) Plecoptera species file online. Available at http://Plecoptera.SpeciesFile.org [accessed 28 Jun 2018]

Elbrecht V, Leese F (2016) The mitochondrial genome of the Arizona Snowfly *Mesocapnia arizonensis* (Plecoptera, Capniidae). Mitochondrial DNA Part A 27: 3365–3366. https://doi.org/10.3109/19401736.2015.1018223

Elbrecht V, Poettker L, John U, Leese F (2015) The complete mitochondrial genome of the stonefly *Dinocras cephalotes* (Plecoptera, Perlidae). Mitochondrial DNA 26: 469–470. https://doi.org/10.3109/19401736.2013.830301

Gissi C, Iannelli F, Pesole G (2008) Evolution of the mitochondrial genome of Metazoa as exemplified by comparison of congeneric species. Heredity 101: 301–320. https://doi.org/10.1038/hdy.2008.62

Hall TA (1999) BioEdit: A user-friendly biological sequence alignment editor and analysis program for Windows 95/98/NT. Nucleic Acids Symposium Series 41: 95–98.

Huang MC, Wang YY, Liu XY, Li W, Kang Z, Wang K, Li X, Yang D (2015) The complete mitochondrial genome and its remarkable secondary structure for a stonefly *Acroneuria hainana* Wu (Insecta: Plecoptera, Perlidae). Gene 557: 52–60. https://doi.org/10.1016/j.gene.2014.12.009

Illies J (1965) Phylogeny and zoogeography of the Plecoptera. Annual Review of Entomology 10: 117–140. https://doi.org/10.1146/annurev.en.10.010165.001001

James BS, Andrew TB (2006) Insect mitochondrial genomics 2: the complete mitochondrial genome sequence of a giant stonefly, *Pteronarcys princeps*, asymmetric directional mutation bias, and conserved plecopteran A + T-region elements. Genome 49: 815–824. https://doi.org/10.1139/g06-037

Laslett D, Canbäck B (2008) ARWEN, a program to detect tRNA genes in metazoan mitochondrial nucleotide sequences. Bioinformatics 24: 172–175. https://doi.org/10.1093/bioinformatics/btm573

Li H, Liu HY, Cao LM, Shi AM, Yang HL, Cai WZ (2012) The complete mitochondrial genome of the damsel bug *Alloeorhynchus bakeri* (Hemiptera: Nabidae). International Journal of Biological Sciences 8: 93–107. https://doi.org/10.7150/ijbs.8.93

Li H, Leavengood Jr JM, Chapman EG, Burkhardt D, Song F, Jiang P, Liu J, Zhou XG, Cai WZ (2017) Mitochondrial phylogenomics of Hemiptera reveals adaptive innovations driving the diversification of true bugs. Proceedings of the Royal Society B: Biological Sciences 284: 1862. https://doi.org/10.1098/rspb.2017.1223

Librado P, Rozas J (2009) DnaSP v5: A software for comprehensive analysis of DNA polymorphism data. Bioinformatics 25: 1451–1452. https://doi.org/10.1093/bioinformatics/btp187

Lin CP, Danforth BN (2004) How do insect nuclear and mitochondrial gene substitution patterns differ? Insights from Bayesian analyses of combined datasets. Molecular Phylogenetics and Evolution 30: 686–702. https://doi.org/10.1016/S1055-7903(03)00241-0

Lohse M, Bolger AM, Nagel A, Fernie AR, Lunn JE, Stitt M, Usadel B (2012) RobiNA: a user-friendly, integrated software solution for RNA-Seq based transcriptomics. Nucleic Acids Research 40: W622–W627. https://doi.org/10.1093/nar/gks540

Mao M, Dowton M (2014) Complete mitochondrial genomes of *Ceratobaeus* sp. and *Idris* sp. (Hymenoptera: Scelionidae): shared gene rearrangements as potential phylogenetic markers at the tribal level. Molecular Biology Reports 41: 6419–6427. https://doi.org/10.1007/s11033-014-3522-x

Miller MA, Pfeiffer W, Schwartz T (2010) Creating the CIPRES Science Gateway for inference of large phylogenetic trees. Gateway computing environments workshop (GCE): 1–8. https://doi.org/10.1109/GCE.2010.5676129

Misof B, Liu S, Meusemann K, Peters RS, Donath A, Mayer C, Frandsen PB, Ware J, Flouri T, Beutel RG et al. (2014) Phylogenomics resolves the timing and pattern of insect evolution. Science 346: 763–767. https://doi.org/10.1126/science.1257570

Negrisolo E, Babbucci M, Patarnello T (2011) The mitochondrial genome of the ascalaphid owlfly *Libelloides macaronius* and comparative evolutionary mitochondriomics of neuropterid insects. BMC Genomics 12: 221. https://doi.org/10.1186/1471-2164-12-221

Ojala D, Montoya J, Attardi G (1981) tRNA punctuation model of RNA processing in human mitochondria. Nature 290: 470–474. https://doi.org/10.1038/290470a0

Peng Y, Leung HCM, Yiu SM, Chin FYL (2012) IBDA-UD: a de novo assembler for single-cell and metagenomic sequencing data with highly uneven depth. Bioinformatics 28: 1420–1428. https://doi.org/10.1093/bioinformatics/bts174

Perna NT, Kocher TD (1995) Patterns of nucleotide composition at fourfold degenerate sites of animal mitochondrial genomes. Journal of Molecular Evolution 41: 353–358. https://doi.org/10.1007/BF01215182

Posada D (2008) jModelTest: phylogenetic model averaging. Molecular Biology and Evolution 25: 1253–1256. https://doi.org/10.1093/molbev/msn083

Qian YH, Wu HY, Ji XY, Yu WW, Du YZ (2014) Mitochondrial genome of the stonefly *Kamimuria wangi* (Plecoptera: Perlidae) and phylogenetic position of Plecoptera based on mitogenomes. PLoS ONE 9: e86328. https://doi.org/10.1371/journal.pone.0086328

Ronquist F, Teslenko M, van der Mark PVD, Ayres DL, Darling A, Höhna S, Larget B, Liu L, Suchard MA, Huelsenbeck JP (2012) MrBayes 3.2: efficient Bayesian phylogenetic inference and model choice across a large model space. Systematic Biology 61: 539–542. https://doi.org/10.1093/sysbio/sys029

Schmidt TR, Wu W, Goodman M, Grossman LI (2001) Evolution of nuclearand mitochondrial-encoded subunit interaction in cytochrome c oxidase. Molecular Biology and Evolution 18: 563–569. https://doi.org/10.1093/oxfordjournals.molbev.a003836

Sheffield NC, Song H, Cameron SL, Whiting MF (2008) A comparative analysis of mitochondrial genomes in Coleoptera (Arthropoda: Insecta) and genome descriptions of six new beetles. Molecular Biology and Evolution 25: 2499–2509. https://doi.org/10.1093/molbev/msn198

Song F, Li H, Jiang P, Zhou XG, Liu J, Sun C, Vogler AP, Cai WZ (2016) Capturing the phylogeny of Holometabola with mitochondrial genome data and bayesian site-heterogeneous mixture models. Genome Biology and Evolution 8: 1411. https://doi.org/10.1093/gbe/evw086

Sproul JS, Houston DD, Nelson CR, Evans PR, Crandall KA, Shiozawa DK (2015) Climate oscillations, glacial refugia, and dispersal ability: factors influencing the genetic structure of the least salmonfly, *Pteronarcella badia*, (Plecoptera), in Western North America. BMC Evolution Biolology 15, 1–18. https://doi.org/10.1186/s12862-015-0553-4

Stamatakis A (2006) RAxML-VI-HPC: Maximum likelihood-based phylogenetic analyses with thousands of taxa and mixed models. Bioinformatics 22: 2688–2690. https://doi.org/10.1093/bioinformatics/btl446

Stewart JB, Beckenbach AT (2005) Insect mitochondrial genomics: the complete mitochondrial genome sequence of the meadow spittlebug *Philaenus spumarius* (Hemiptera: Auchenorrhyncha: Cercopoidae). Genome 48: 46–54. https://doi.org/10.1139/g04-090

Taanman JW (1999) The mitochondrial genome: structure, transcription, translation and replication. Biochimica et Biophysica Acta 1410: 103–123. https://doi.org/10.1016/S0005-2728(98)00161-3

Tamura K, Stecher G, Peterson D, Filipski A, Kumar S (2013) MEGA6: molecular evolutionary genetics analysis version 6.0. Molecular Biology and Evolution 30: 2725–2729. https://doi.org/10.1093/molbev/mst197

Terry MD, Whiting MF (2003) Phylogeny of Plecoptera: molecular evidence and evolutionary trends. Entomologische Abhandlungen 61: 130–131.

Thomas MA, Walsh KA, Wolf MR, McPheron BA, Marden JH (2000) Molecular Phylogenetic analysis of evolutionary trends in stonefly wing structure and locomotor behavior. Proceedings of the National Academy of Sciences of the United States of America 97: 13178–13183. https://doi.org/10.1073/pnas.230296997

Uchida S, Isobe Y (1989) Styloperlidae, stat. nov. and Microperlinae, subfam. nov. with a revised system of the family group Systellognatha (Plecoptera). Spixana 12: 145–182.

Wang Y, Cao JJ, Li WH (2017a) The complete mitochondrial genome of the styloperlid stonefly species *Styloperla spinicercia* Wu (Insecta: Plecoptera) with family-level phylogenetic analyses of the Pteronarcyoidea. Zootaxa 4243: 125–138. https://doi.org/10.11646/zootaxa.4243.1.5

Wang Y, Cao JJ, Li WH (2018a) Complete Mitochondrial genome of *Suwallia teleckojensis* (Plecoptera: Chloroperlidae) and implications for the higher phylogeny of stoneflies. International Journal of Molecular Sciences 19: 680. https://doi.org/10.3390/ijms19030680

Wang Y, Cao JJ, Li WH, Chen XL (2017b) The mitochondrial genome of *Mesocapina daxingana* (Plecoptera: Capniidae). Conservation Genetics Resources 9: 639–642. https://doi.org/10.1007/s12686-017-0745-x

Wang Y, Cao JJ, Murányi D, Li WH (2018b) Comparison of two complete mitochondrial genomes from Perlodidae (Plecoptera: Perloidea) and the family-level phylogenetic implications of Perloidea. Gene 675: 254–264. https://doi.org/10.1016/j.gene.2018.06.093

Wang Y, Cao JJ, Li N, Ma GY, Li WH (2019) The first mitochondrial genome from Scopuridae (Insecta: Plecoptera) reveals structural features and phylogenetic implications. International Journal of Biological Macromolecules 122: 893–902. https://doi.org/10.1016/j.ijbiomac.2018.11.019

Wang Y, Li H, Wang P, Song F, Cai WZ (2014) Comparative mitogenomics of plant bugs (Hemiptera: Miridae): identifying the AGG codon reassignments between serine and lysine. PLoS ONE 9: e101375. https://doi.org/10.1371/journal.pone.0101375

Wei SJ, Tang P, Zheng LH, Shi M, Chen XX (2010) The complete mitochondrial genome of *Evania appendigaster* (Hymenoptera: Evaniidae) has low A+ T content and a long intergenic spacer between *atp8* and *atp6*. Molecular Biology Reports 37: 1931–1942. https://doi.org/10.1007/s11033-009-9640-1

Wu HY, Ji XY, Yu WW, Du YZ (2014) Complete mitochondrial genome of the stonefly *Cryptoperla stilifera* Sivec (Plecoptera: Peltoperlidae) and the phylogeny of Polyneopteran insects. Gene 537: 177–183. https://doi.org/10.1016/j.gene.2013.12.044

Zhang DX, Hewitt GM (1997) Insect mitochondrial control region: A review of its structure, evolution and usefulness in evolutionary studies. Biochemical Systematics and Ecology 25: 99–120. https://doi.org/10.1016/S0305-1978(96)00042-7

Zhang DX, Szymura JM, Hewitt GM (1995) Evolution and structural conservation of the control region of insect mitochondrial DNA. Journal of Molecular Evolution 40: 382–391. https://doi.org/10.1007/BF00164024

Zsurka G, Kudina T, Peeva V, Hallmann K, Elger CE, Khrapko K, Kunz WS (2010) Distinct patterns of mitochondrial genome diversity in bonobos (*Pan paniscus*) and humans. BMC Evolutionary Biology 10: 270. https://doi.org/10.1186/1471-2148-10-270

Zuker M (2003) Mfold web server for nucleic acid folding and hybridization prediction. Nucleic Acids Research 31: 3406–3415. https://doi.org/10.1093/nar/gkg595

Zwick P (2000) Phylogenetic system and zoogeography of the Plecoptera. Annual Review of Entomology 45: 709–746. https://doi.org/10.1146/annurev.ento.45.1.709

Supplementary material 1

Figure S1. Relative synonymous codon usage (RSCU) of each amino acid in the mitogenomes of *M. tritaenia* and *M. metafiligera*

Authors: Jin-Jun Cao, Ying Wang, Yao-Rui Huang, Wei-Hai Li

Data type: phylogenetic data

Explanation note: Codon families were provided on the x-axis. Stop codon is not given.

Link: https://doi.org/10.3897/zookeys.835.32470.suppl1

Supplementary material 2

Figure S2. Ka/Ks ratios of PCGs in the three nemourid mitogenomes

Authors: Jin-Jun Cao, Ying Wang, Yao-Rui Huang, Wei-Hai Li

Data type: molecular data

Explanation note: The blue columns indicate the average Ka/Ks for each gene.

Link: https://doi.org/10.3897/zookeys.835.32470.suppl2

ZooKeys 835: 65–86 (2019)
doi: 10.3897/zookeys.835.33231
http://zookeys.pensoft.net

RESEARCH ARTICLE

A peer-reviewed open-access journal
ZooKeys
Launched to accelerate biodiversity research

Re-evaluation of *Zospeum schaufussi* von Frauenfeld, 1862 and *Z. suarezi* Gittenberger, 1980, including the description of two new Iberian species using Computer Tomography (CT) (Eupulmonata, Ellobioidea, Carychiidae)

Adrienne Jochum[1], Carlos E. Prieto[2], Marian Kampschulte[3], Gunhild Martels[4], Bernhard Ruthensteiner[5], Marko Vrabec[6], Dorian D. Dörge[7], Anton J. de Winter[8]

1 *Naturhistorisches Museum der Burgergemeinde Bern (NMBE), CH-3005 Bern, Switzerland* **2** *Departamento de Zoología y Biología Cellular Animal, Universidad del País Vasco (UPV-EHU), 48080 Bilbao, Spain* **3** *Universitätsklinikum Giessen und Marburg GmbH-Standort Giessen, Center for Radiology, Dept. of Radiology, 35385 Giessen, Germany* **4** *Department of Experimental Radiology, Justus-Liebig University Giessen, Biomedical Research Center Seltersberg (BFS), 35392 Giessen, Germany* **5** *Section Evertebrata varia, Zoologische Staatssammlung München (ZSM), 81247 München, Germany* **6** *Department of Geology, Faculty of Natural Sciences and Engineering, University of Ljubljana,1000 Ljubljana, Slovenia* **7** *Institute for Ecology, Evolution and Diversity; Senckenberg Biodiversity and Climate Research Center (BiK-F); Senckenberg Gesellschaft für Naturforschung (SGN), Goethe-University (GU), 60438 Frankfurt/M., Germany* **8** *Naturalis Biodiversity Center, P.O. Box 9517, NL 2300 RA Leiden, The Netherlands*

Corresponding author: *Adrienne Jochum* (adrienne.jochum@gmail.com)

Academic editor: *Thierry Backeljau* | Received 21 January 2019 | Accepted 4 March 2019 | Published 4 April 2019

http://zoobank.org/1FAA0825-0D16-4017-8AC4-F6B96CCD294C

Citation: Jochum A, Prieto CE, Kampschulte M, Martels G, Ruthensteiner B, Vrabec M, Dörge DD, de Winter AJ (2019) Re-evaluation of *Zospeum schaufussi* von Frauenfeld, 1862 and *Z. suarezi* Gittenberger, 1980, including the description of two new Iberian species using Computer Tomography (CT) (Eupulmonata, Ellobioidea, Carychiidae). ZooKeys 835: 65–86. https://doi.org/10.3897/zookeys.835.33231

Abstract

The present study aims to clarify the confused taxonomy of *Z. schaufussi* von Frauenfeld, 1862 and *Zospeum suarezi* Gittenberger, 1980. Revision of Iberian *Zospeum* micro snails is severely hindered by uncertainties regarding the identity of the oldest Iberian *Zospeum* species, *Z. schaufussi* von Frauenfeld, 1862. In this paper, we clarify its taxonomic status by designating a lectotype from the original syntype series and by describing its internal and external shell morphology. Using SEM-EDX, we attempt to identify the area

of the type locality cave more precisely than "a cave in Spain". The shell described and illustrated by Gittenberger (1980) as *Z. schaufussi* appears not to be conspecific with the lectotype shell, and is considered a separate species, *Z. gittenbergeri* Jochum, Prieto & De Winter, **sp. n.**

Zospeum suarezi was described from various caves in NW Spain. Study of the type material reveals that these shells are not homogenous in shell morphology. The holotype shell of *Z. suarezi* is imaged here for the first time. The paratype shell, illustrated by Gittenberger (1980) from a distant, second cave, is described as *Zospeum praetermissum* Jochum, Prieto & De Winter, **sp. n.** The shell selected here as lectotype of *Z. schaufussi*, was also considered a paratype of *Z. suarezi* by Gittenberger (1980). Since this specimen is morphologically very similar to topotypic shells of *Z. suarezi*, the latter species is considered a junior synonym of *Z. schaufussi* (**syn. n.**). The internal shell morphology of all these taxa is described and illustrated using X-ray Micro Computer Tomography (Micro-CT).

Keywords

Cave-dwelling species, microgastropods, shell variability, subterranean land snail

Introduction

The Cantabrian-Pyrenean Region, encompassing 500 × 50 km of the northwestern part of the Iberian Peninsula, harbours a remarkable diversity of the cave-dwelling, land snail genus *Zospeum*. A number of species have been formally described. The oldest available name for a Spanish *Zospeum* species is *Z. schaufussi* von Frauenfeld, 1862. Since then, six more Spanish species have been described, viz., *Zospeum bellesi* Gittenberger, 1973; *Z. suarezi* Gittenberger, 1980; *Z. biscaiense* Gómez & Prieto, 1983; *Z. vasconicum* Prieto, De Winter, Weigand, Gómez & Jochum, 2015; *Z. zaldivarae* Prieto, De Winter, Weigand, Gómez & Jochum, 2015, and recently *Z. percostulatum* Alonso, Prieto, Quiñonero-Salgado & Rolán, 2018 (Fig. 1).

Insufficient knowledge, causing doubts about the identity of two of these species, *Z. schaufussi* and *Z. suarezi*, has blocked further descriptions of this potentially very speciose radiation in a region where many caves are inhabited by two or three different morphotypes (Alonso et al. 2018).

Zospeum schaufussi was the first *Zospeum* species reported from Spain. Detailed information about its provenance is lacking while its description is insufficient according to today's standards. When Gittenberger (1980) studied von Frauenfeld's original material, he could not accept the available shells as syntypes of *Z. schaufussi*, because the damaged shells possess distinct barriers within the body whorl, the absence of which was mentioned as a specific character by von Frauenfeld (1862). Instead, he described and illustrated a shell from Cueva [del Puente] de Inguanzo near Inguanzo (Asturias) as *Z. schaufussi*. However, he did not formalize his view by selection of a neotype. In this paper, we select the single, undamaged original syntype shell as lectotype of *Z. schaufussi* and provide a re-description of this previously unclear taxon.

When Gittenberger (1980) received *Zospeum* material from various northern Spanish caves, only two other Iberian species, *Z. bellesi* Gittenberger, 1973 and *Z. schaufussi*

were known. Since most of the shells appeared to be different from the latter two species, Gittenberger (1980) described this material as a new species, *Z. suarezi* Gittenberger, 1980, of which the holotype derived from the Cueva del Búho, Puente Viesgo (Cantabria). The new species, *Z. suarezi*, was illustrated by a drawing of a paratype shell from another cave, Cueva [del Puente] Inguanzo near Inguanzo (Asturias). These two caves are separated by a distance of 70 km. Illustrations of shells from the type cave have never been published.

Subsequent to its description, *Z. suarezi* was reported from Bizkaia, Burgos and Cantabria (e.g. Altonaga et al. 1994; Weigand et al. 2013). Weigand et al. (2013) attributed four populations (lineages Z13–Z16) to *Z. suarezi*. These populations showed significant variability in some genetic markers, but the provided images (BOLD database) of the now molecularly-processed voucher specimens, preclude study of their shell morphologies in sufficient detail. Later examination of additional material from these caves revealed ample variability in shell morphology, casting doubt as to the conspecificity of the populations used in this molecular study (unpublished results). Adding more confusion to the situation, a shell recently designated as *Z. suarezi* from Navarra, more than 200 km from the type cave, was illustrated in an authoritative guide to the land snails of the Iberian Peninsula (Cadevall and Orozco 2016). Whether these populations indeed belong to *Z. suarezi* is uncertain. Obviously, the identity of *Z. suarezi* needs clarifying.

Re-examination of the original material of *Z. suarezi* in RMNH Leiden, revealed that the holotype shell and the illustrated paratype shell exhibit subtle, but consistent differences in external morphology, which could be corroborated by study of the internal shell using x-ray Micro Computer Tomography (Micro-CT). In this paper, we re-describe and illustrate the shell morphology of *Z. suarezi* from the locus typicus. In addition, we describe the illustrated paratype shell as the holotype of a new species. Gittenberger (1980) also included the only undamaged syntype of *Z. schaufussi* from the von Frauenfeld collection in Vienna as paratype of *Z. suarezi*. This raises the question of their taxonomic relationship, which we address in this work.

Materials and methods

Material studied is housed in the following collections:

MHNG	Muséum d'Histoire Naturelle Genève, Geneva, Switzerland
NHMW	Naturhistorisches Museum Wien, Vienna, Austria
RMNH	Naturalis Biodiversity Center (formerly RijksMuseum van Natuurlijke Historie), Leiden, The Netherlands

Maps were produced with the freely available QGIS software (QGIS Development Team 2018). For shoreline vector data, we used the GSHHG database (Wessel and Smith 1996).

We emphasize that the RMNH catalog numbers, originally documented in Gittenberger (1980 fig. 2), partly differ from the ones nowadays employed in the RMNH collection. These were later changed because some numbers had been accidentally issued twice. For example, the *Z. suarezi* paratype lot, RMNH 55389, (Cueva del Búho, Puente Viesgo) was stated in Gittenberger (1980) as RMNH 55384 shells (see Table 1). We use the current catalog numbers here and list Gittenberger's (1980) notation in square brackets.

According to Emmanuel Tardy, curator at the MHNG, who imaged Gittenberger's (1980) designated paratype material before it got lost (in the mail) in January 2017, Gittenberger's data (1980) corresponded to two lots: MNHG 96219 (ex. 978.363), which consisted of one vial containing two gelatin capsules with 4 individuals out of the 5 specimens Gittenberger (1980) assessed, separated into two different capsules (Fig. 5G–R). A second lot, MHNG 96220 (ex. 978.364), contained one shell from Cueva de Los Quesos (Fig. 5A–F).

Additionally, as paratypes, Gittenberger (1980) included shells from still other caves, such as the Cueva de Ernialde (= Hernialde) (NHMW MOL75000-E48.815) (Fig. 6).

Table 1. Shell measurements in mm (for methodology, see Jochum et al. 2015, fig. 1) of *Zospeum schaufussi*, *Z. praetermissum* and *Z. gittenbergeri*. Most shells of *Z. schaufussi* are type material of *Z. suarezi* Gittenberger, 1980, from the Cueva del Búho. Collection numbers are those presently used in RMNH, some differ from those used in Gittenberger (1980). Abbreviations: SH, shell height; SD, shell diameter; HLW, height of last whorl; PH, peristome height; PD, peristome diameter; W, number of whorls (counted as in Kerney and Cameron 1979); CT, coiling tightness W:*ln*SH (Emberton 2001).

	collection	SH	SD	HLW	PH	PD	W	SH/SD	HLW/SH	PH/SH	PH/PD	CT
Z. schaufussi												
lectotype	NHMW 71837	1.30					6.00					2.34
Z. suarezi												
holotype	RMNH.MOL.55383	1.21	0.78	0.62	0.42	0.42	6.00	1.55	0.51	0.35	1.00	2.41
paratype	RMNH.MOL.55384	1.07	0.71	0.56	0.40	0.40	5.55	1.51	0.52	0.37	1.00	2.34
paratype	RMNH.MOL.55384	1.20	0.73	0.66	0.43	0.41	6.00	1.64	0.55	0.36	1.05	2.41
paratype	RMNH.MOL.55384	1.00	0.64	0.56	0.37	0.35	5.50	1.56	0.56	0.37	1.06	2.39
paratype	RMNH.MOL.55384	0.99	0.67	0.56	0.40	0.39	5.15	1.47	0.57	0.40	1.03	2.25
paratype	RMNH.MOL.55384	1.04	0.70	0.59	0.36	0.40	5.55	1.48	0.56	0.34	0.89	2.37
paratype	RMNH.MOL.55384	1.20	0.70	0.62	0.33	0.39	6.20	1.72	0.51	0.27	0.83	2.49
paratype	RMNH.MOL.55384	1.11	0.74	0.59	0.42	0.41	5.90	1.50	0.53	0.37	1.00	2.45
paratype	RMNH.MOL. 55390	0.99	0.62	0.53	0.35	0.35	5.4	1.60	0.54	0.35	1.00	2.36
paratype	RMNH.MOL. 55390	1.04	0.70	0.59	0.36	0.4	5.5	1.49	0.57	0.35	0.90	2.35
	mean/median	1.08	0.70	0.59	0.38	0.39	5.68	1.53	0.54	0.36	1.00	2.37
	min	0.99	0.62	0.53	0.33	0.35	5.15	1.47	0.51	0.34	0.83	2.25
	max	1.30	0.78	0.66	0.43	0.42	6.2	1.72	0.57	0.40	1.06	2.49
***Z. praetermissum* sp. n.**												
holotype	RMNH.MOL.55391	1.08	0.75	0.67	0.41	0.42	4.60	1.44	0.62	0.38	0.99	1.93
paratype	RMNH.MOL.339954	1.07	0.71	0.64	0.39	0.41	4.85	1.52	0.59	0.37	0.97	2.04
paratype	RMNH.MOL.339954	1.21	0.76	0.71	0.40	0.45	5.20	1.58	0.58	0.33	0.90	2.09
	mean/median	1.12	0.74	0.67	0.40	0.42	4.88	1.52	0.59	0.37	0.97	2.04
***Z. gittenbergeri* sp. n.**												
holotype	RMNH.MOL.234166	1.49	0.92	0.89	0.53	0.58	5.50	1.62	0.59	0.35	0.90	2.03

Image acquisition

Digital Images and measurements. Images were taken via a Leica DFC420 digital camera attached to a Leica M165C stereo microscope using Leica LAS V4.4 software.

Shell measurements were made on digital images as described in Jochum et al. (2015, fig. 1). The number of whorls of each shell was counted according to the method described in Kerney and Cameron (1979).

Micro-CT. Internal shell morphologies were accessed using different micro-CT systems. The lectotype shell of *Z. schaufussi* (NHMW 71837) was imaged and processed in animated video format at RJL Micro & Analytic GmbH, Karlsdorf-Neuthard, Germany using the system SkyScan 1172 (Bruker MikroCT, Kontich, Belgium). The scanner is equipped with a sealed micro focus X-ray source and an 11 Mpx CCD detector. The specimen was scanned with 4 µm pixel size in rotation steps of 0.6 ° at 59 kV tube voltage and 167 µA tube current during a 360 ° rotation. Reconstruction with cross sectional images was performed using a modified Feldkamp cone-beam reconstruction algorithm. The animated video was generated using a direct volume rendering method implemented in the software, CTvox.

Other *Zospeum* shells, except for the CT-imaged paratype of *Z. suarezi* (RMNH. MOL.55389 [55384] (Fig. 12) and the holotype of *Z. gittenbergeri* sp. n. (RMNH. MOL.234166) (Fig. 14), were imaged using a SkyScan 2011 (Bruker MicroCT, Kontich, Belgium) at the Department of Experimental Radiology, Justus-Liebig University Biomedical Research Center Seltersberg (BFS), Giessen, Germany. The shells were scanned 185 ° around their vertical axis in rotation steps of 0.23 ° at 80 kV tube voltage and 120 µA tube current. Reconstruction was performed using the Feldkamp cone beam reconstruction algorithm. Image resolution was 1.75 µm isotropic voxel side length with a grey scale resolution of 8 bit. Digital image post processing and visualization (maximum intensity projection – MIP, volume compositing and summed voxel projection) were displayed using the ANALYZE software package (ANALYZE 11.0, Mayo Clinic, Rochester, MN, USA).

Zospeum gittenbergeri sp. n. (RMNH.MOL.234166) was scanned at the Zoologische Staatssammlung München with a Phoenix Nanotom m (GE Measurement & Control, Wunstorf, Germany) cone beam CT scanner at a voltage of 80 kV and a current of 325 mA using a tungsten ("Standard") target. 1440 projection images were taken during a 360° rotation at a total duration of 120 minutes. The 16-bit data set generated by reconstruction (voxel size 0.769 µm) was cropped and converted to 8 bit using VGStudio MAX 2.2 software (Volume Graphics, Heidelberg, Germany). Further visualization procedures were carried out with Amira 6.4 software (Thermo Fischer Scientific, Electron Microscopy Solutions, Hillsboro, Oregon, USA) applying manual segmentation for discrimination of external and internal shell structures. Final visualization was conducted using the Volume Rendering module.

Scanning Electron Microscopy (SEM-EDX). SEM-EDX: Sections of the shell of the intact syntype *Z. schaufussi* (NHMW 71837) (SEM) and the elemental composition (EDX) of sediment encrusted on the shell were assessed using the FEI-ASPEX EXpress scanning electron microscope system (Pittsburgh, PA, USA), implementing

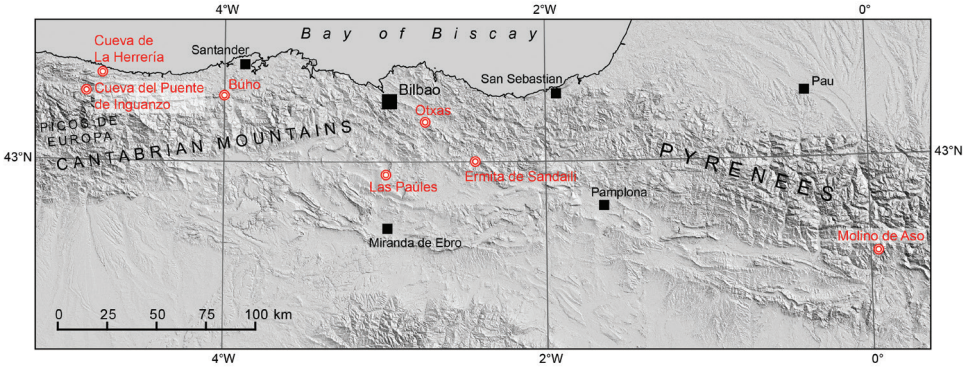

Figure 1. Map indicating geographic position of type locality caves of described species of *Zospeum* in northern Spain. From left to right: Cueva del Puente de Inguanzo (*Z. gittenbergeri* sp. n., *Z. praetermissum* sp. n.), Cueva de La Herrería (*Z. percostulatum*), Cueva de Búho (*Z. suarezi*, syn. n. of *Z. schaufussi*), Cueva de Las Paúles (*Z. zaldivarae*), Cueva de Otxas (*Z. biscaiense*), Cueva de la Ermita de Sandaili (*Z. vasconicum*) and Cueva Molino de Aso (*Z. bellesi*). Source of DEM data: ALOS Global Digital Surface Model (AW3D30), JAXA.

a BE-detector for image generation. The section of cardboard on which the shell was glued, was mounted on a computer-controlled stage for scanning. Elemental composition was detected (i.e. each element shows a multiple-peak pattern in the spectrum) by using an emission current of 35 µA, an electron beam acceleration voltage of 20 kV under sample pressure of 0.15 Torr and a working distance of 22.4 mm at RJL Micro & Analytic GmbH, Karlsdorf-Neuthard, Germany. Peak height represents the intensity of the element and this is proportional to the mass percentage present in the shell region tested.

Taxonomy

Family Carychiidae Jeffreys, 1830
Genus *Zospeum* Bourguignat, 1856

***Zospeum schaufussi* von Frauenfeld, 1862**
Figures 2–3, 4, 7–9

Zospeum schaufussi von Frauenfeld, 1862.
Zospeum suarezi Gittenberger, 1980: 204. **Syn. n.**

Material. Von Frauenfeld collection, a single undamaged syntype shell (NHMW 71837); 4 broken syntype shells (NHMW 71836). Terra typica: ".. einer neuen Art, welche ich von Hrn. Schaufuss in Dresden erhielt, die darum von Interesse ist, dass er sie in einer Höhle in Spanien auffand, daher die erste Art, welche das geographische

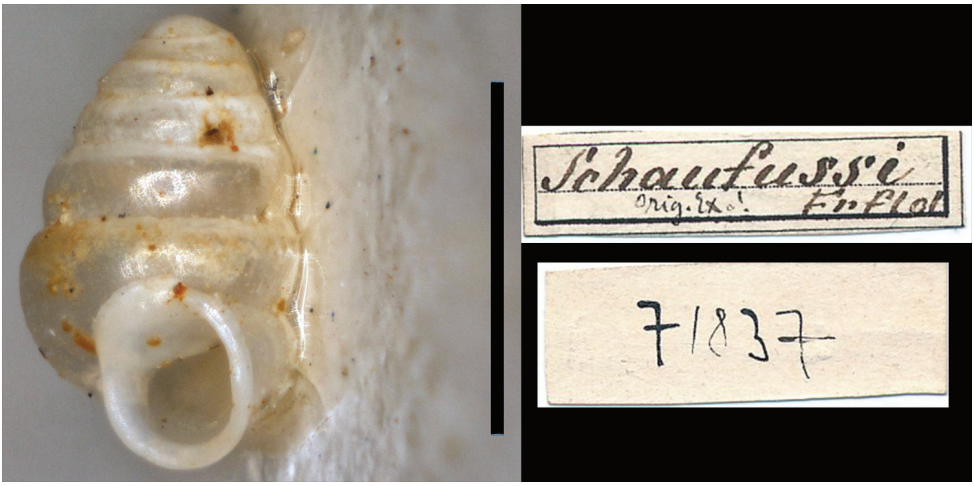

Figure 2. *Zospeum schaufussi* von Frauenfeld, 1862, lectotype and labels (NHMW 71837). Scale bar: 1 mm.

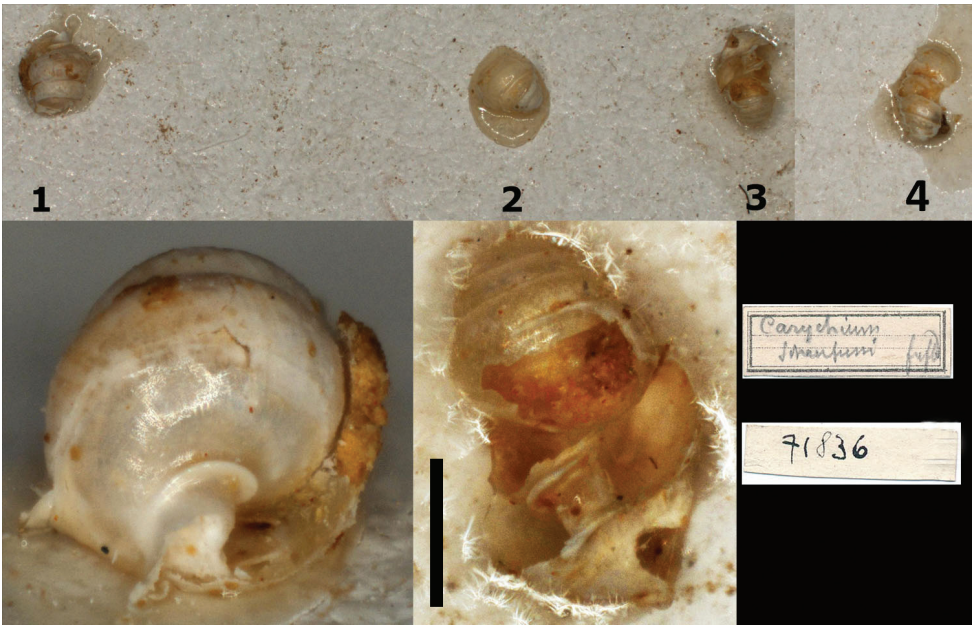

Figure 3. *Zospeum schaufussi* von Frauenfeld, 1862, damaged syntypes and labels (NHMW 71836). Scale bar: 500 μm.

Gebiet dieser Gattung mächtig erweitert." [.. a new species that I received from Mr. Schaufuss in Dresden, which is significant by the fact that he obtained it from a cave in Spain, ... which considerably expands the geographic range of this genus.]. Fischer (1887) narrowed the provenance of *Z. schaufussi* to the greater historical region of

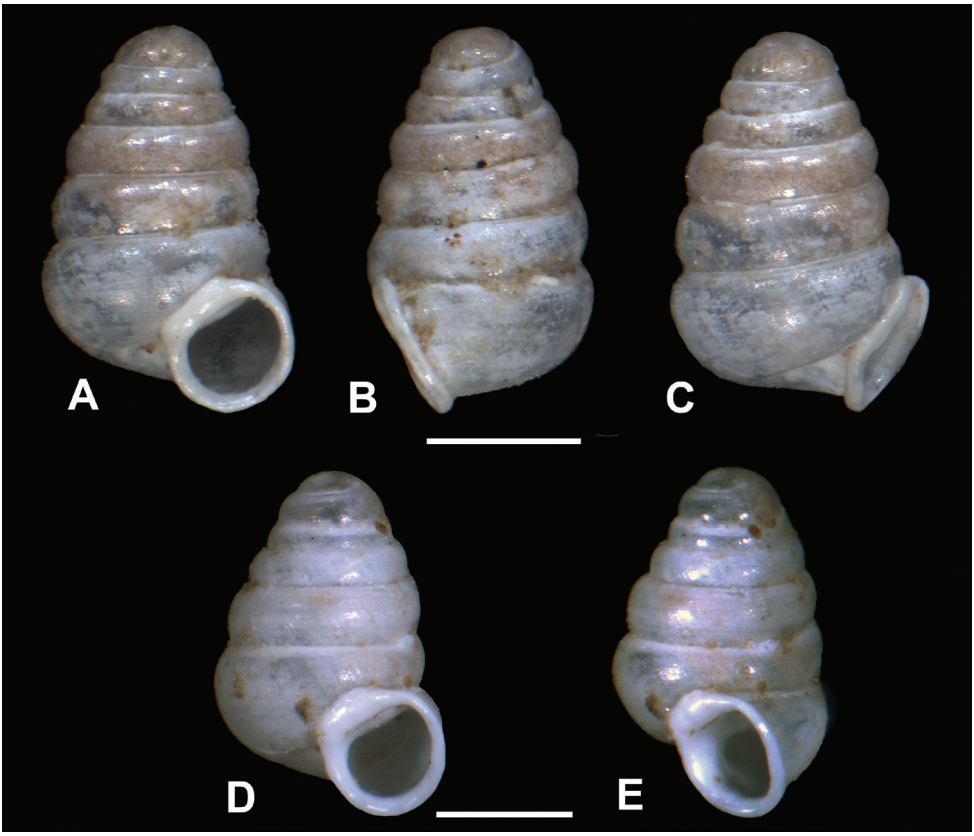

Figure 4. A–C *Zospeum schaufussi* von Frauenfeld, 1862, Cueva del Búho, Puente Viesgo, Santander, (holotype of *Z. suarezi*, RMNH.MOL.55383) **D–E** *Z. praetermissum* sp. n., Cueva del Puente de Inguanzo (RMNH.MOL55389). Scale bar: 500 μm.

Asturias and Cantabria (i.e. Asturia de Oviedo and Asturia de Santillana), but this was apparently overlooked by later authors.

Lectotype designation and rationale. Von Frauenfeld's (1862) original description [Z. minutissima, vix umbilicata, conica, hyalina, nitida, laeve, anfractibus 5, convexis, apertura rotundata, edentata, peristomate continuo, reflexo] was not detailed enough to recognize the species and lacks an illustration, which in his day, was perhaps deemed unnecessary as no other Iberian congeneric species were known. In Vienna, one of us (AJ) could study five original syntype shells of *Z. schaufussi* (NHMW 71836 – 71837), as was previously done by Gittenberger (1980). The syntypes are firmly glued on two pieces of cardboard (Figs 2–3). Von Frauenfeld mentions that he viewed "some damaged specimens .., without the slightest hint of dentition, such that I cannot doubt the consistent lack of teeth in this species" [translated from German]. All surviving shells, except one (NHMW 71837), are seriously damaged. Gittenberger (1980) concluded that the four damaged syntype shells could not be *Z. schaufussi* because internal barriers are clearly discernible and that the syntypes of the true, edentate,

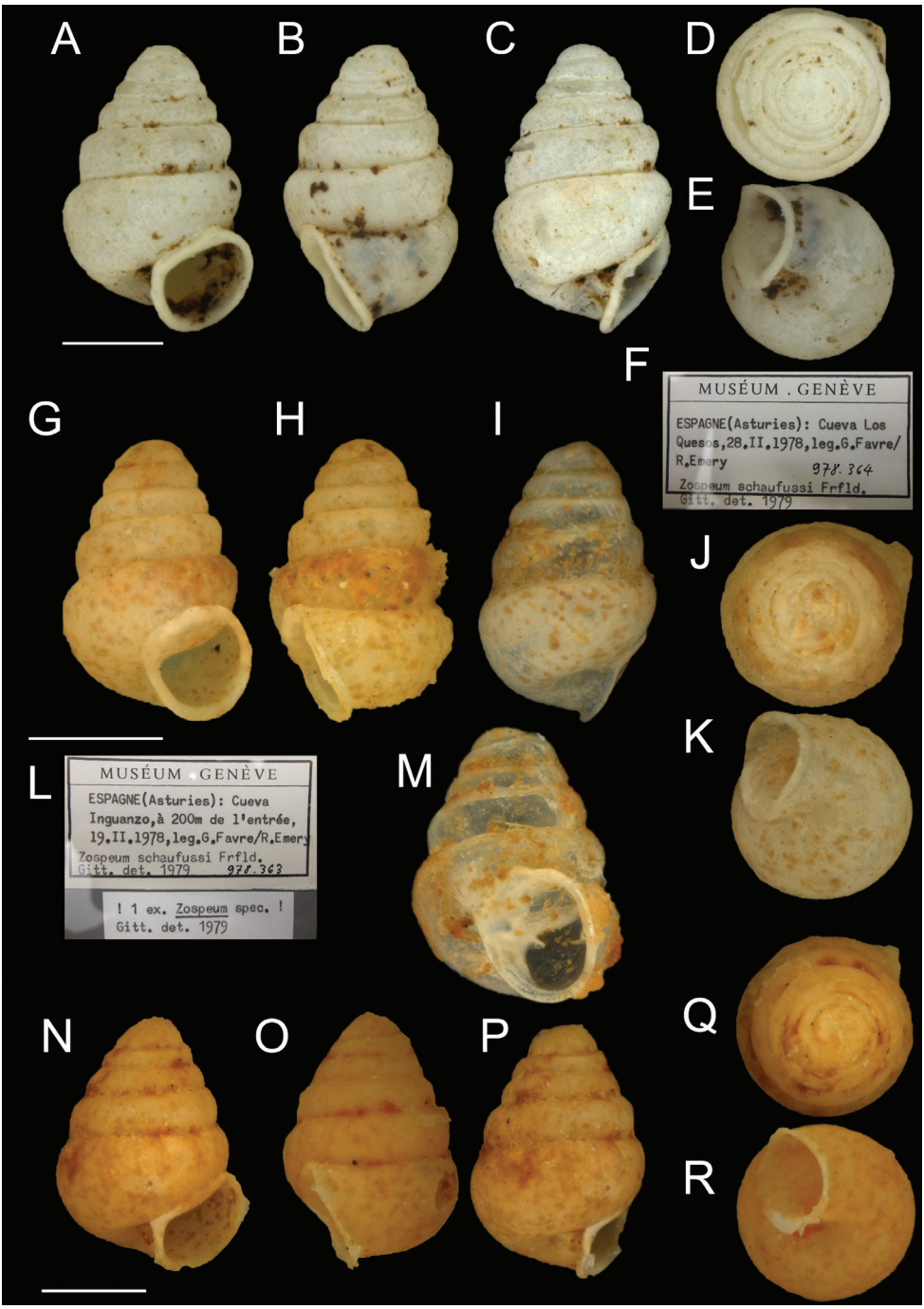

Figure 5. *Zospeum* material assessed in Gittenberger (1980). **A–F** *Zospeum praetermissum* sp. n. (paratype of *Z. suarezi*, MHNG-Mol 96220/1 shell, now lost), Cueva Los Quesos (showing ambivalent label, *Z. schaufussi* Frfld) **G–M** *Zospeum praetermissum* sp. n (figured paratype of *Z. suarezi*, MHNG-Moll 96219, now lost), Cueva del Puente de Inguanzo **L, N–R** *Zospeum gittenbergeri* sp. n. (figured shell of *Z. schaufussi* sensu Gittenberger (1980), MHNG 96219, now lost).

Figure 6. *Zospeum* cf. *vasconicum* Prieto, De Winter, Weigand, Gómez & Jochum, 2015. Ex. *Z. suarezi* paratype, NHMW-MO 75000-E-48815, Cueva Hernialde, Guipuzcoa, assessed in Gittenberger (1980) („NWW-Coll. Edlauer 48815, ex. Coll. Robić/1shell").

Z. schaufussi were missing or lost. We can confirm Gittenberger's observation of the damaged syntypes (see Fig. 3). Gittenberger (1980) attributed the single undamaged syntype shell to his new species, *Z. suarezi* (as a paratype), rather than to *Z. schaufussi*. We cannot concur with his view. Von Frauenfeld (1862) stressed the similarity with *Z. amoenum* von Frauenfeld, 1856, as the only other toothless *Zospeum* species; in fact, all other *Zospeum* species known by the end of the 19th Century have apertural teeth conspicuously present in frontal view, but the deeper, internal dentition, was often unknown or not specifically addressed in descriptions (see e.g. Kobelt 1899, pls 218–219). We therefore, assume that von Frauenfeld referred to the externally visible dentition in the "apertura"; "Mündung". The apertural dentition in the intact syntype shell is not, or barely, visible externally (Fig. 2). We conclude that this shell, bearing the label notation "Orig [inal] Ex [emplar]!" (Fig. 2), is the only remaining undamaged syntype of *Z. schaufussi* and thus, designate it here as the lectotype. The purpose of this

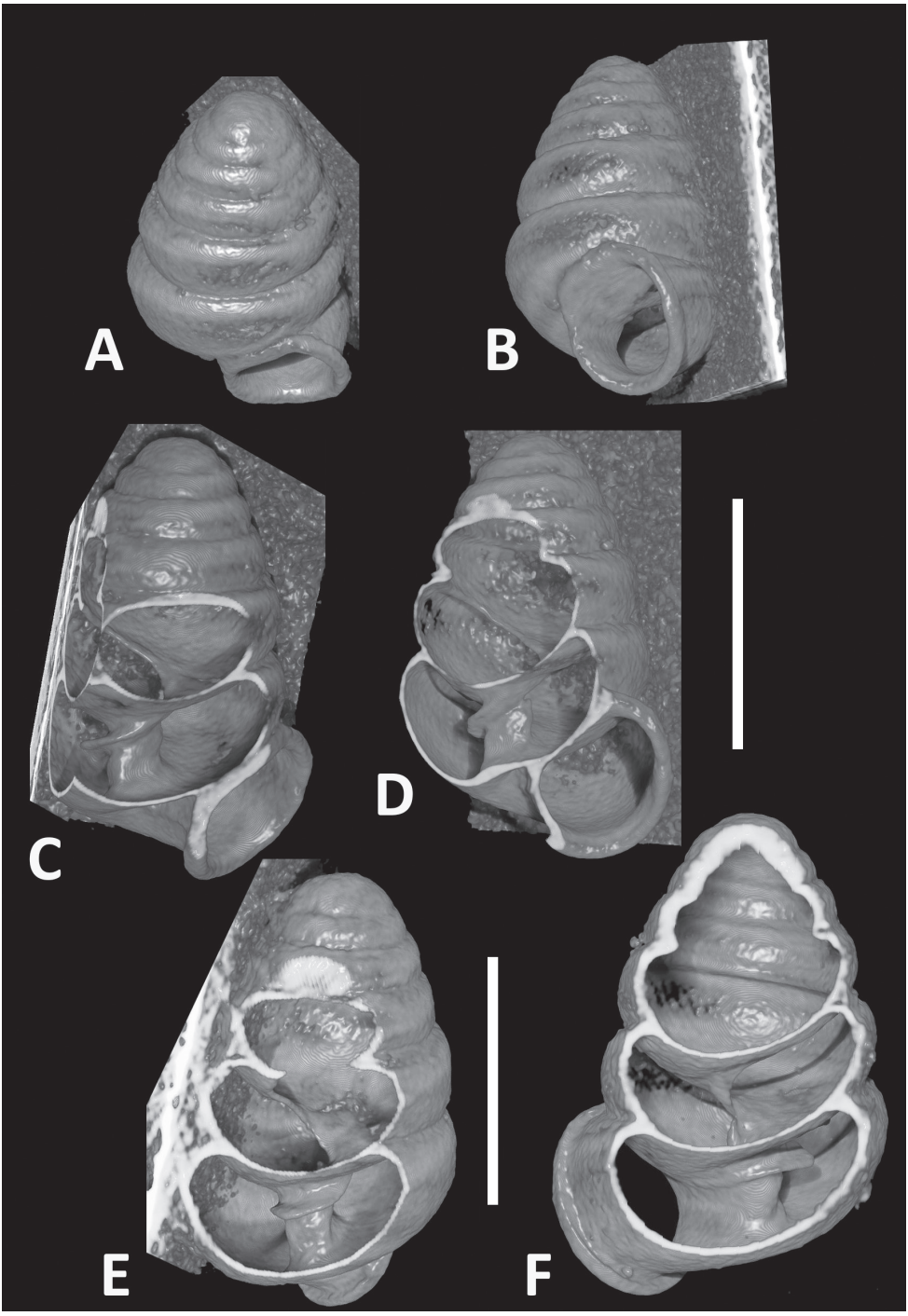

Figure 7. CT images showing columellar apparatus of *Zospeum schaufussi* von Frauenfeld, 1862, lectotype (NHMW 71837). Scale bar: 500 μm.

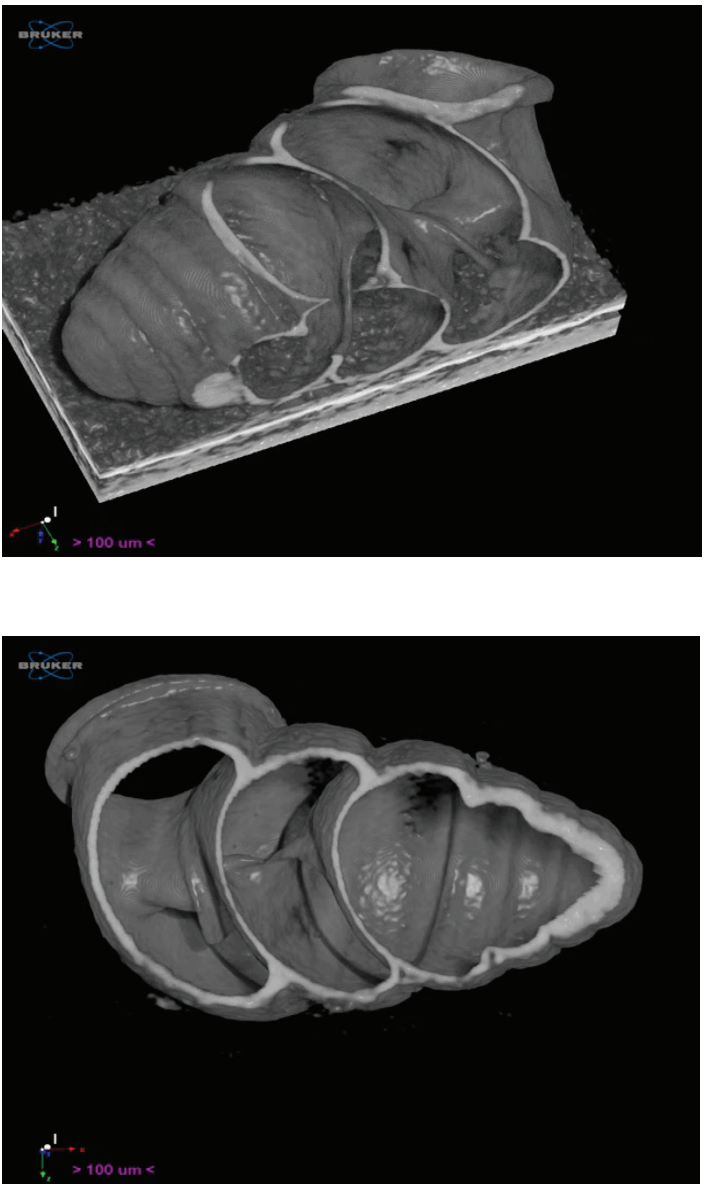

Figure 8. Animated video from CT scans of *Zospeum schaufussi* von Frauenfeld, 1862, lectotype (NHMW 71837). Scale bar: 500 μm.

lectotype designation is the fixation of a taxon name to a specific morphology and to stabilize nomenclature rather than reconstructing the historical course of events.

Lectotype description. Shell minute, ca. 1.3 mm, elongate-conical, with at least 5½ regularly coiled, convex whorls, suture deep; teleoconch smooth; aperture roundish-lunate; peristome thickened, elongate-roundish (not angular), closely adhering to spire; peristome height ca. 36% of shell height; umbilicus closed, umbilical depression

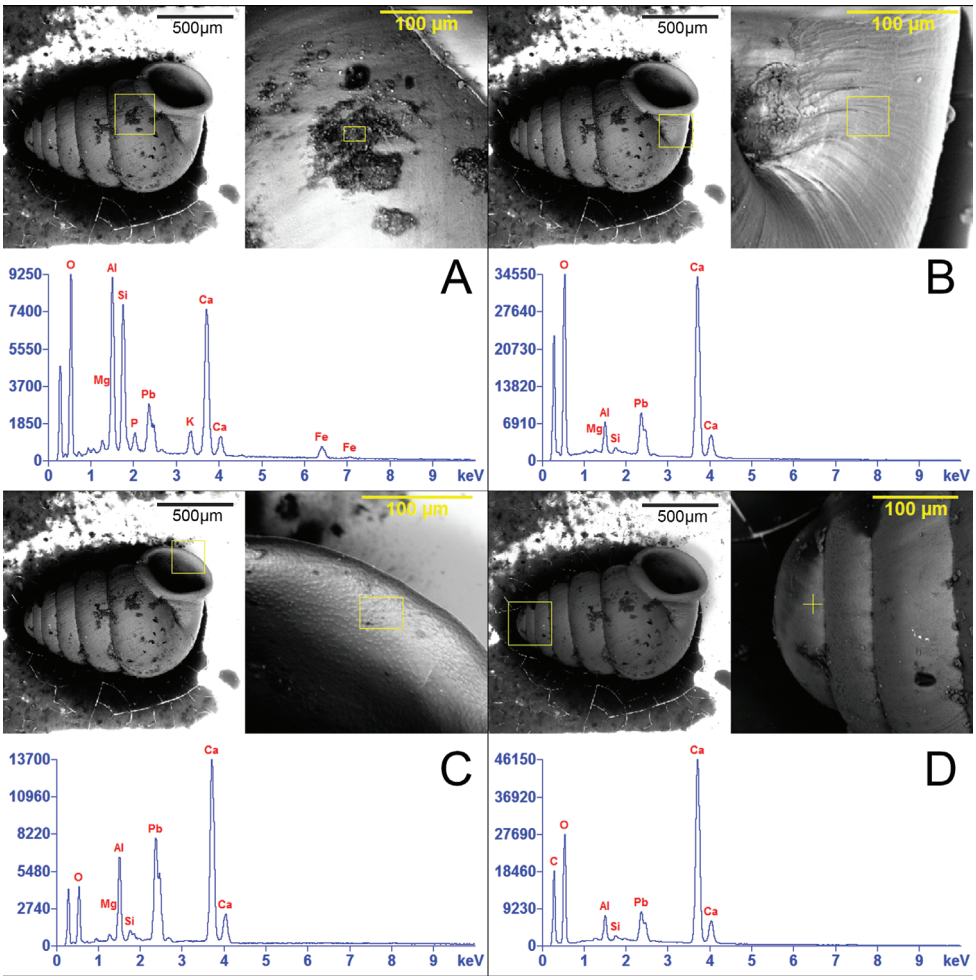

Figure 9. SEM-EDX spectroscopic images showing spectrum of elemental content in sediment encrusted on different regions of the lectotype of *Zospeum schaufussi* von Frauenfeld, 1862 (NHMW 71837). **A–D** Concentrations within yellow-framed zone of calcium (Ca), aluminum (Al), silicon (Si), magnesium (Mg), oxygen (O), carbon (C), iron (Fe), potassium (K), phosphor (P) and lead (Pb).

deep, wrinkles behind apertural lip leading to umbilicus (seen in SEM-EDX Fig. 9B). Externally, no apertural dentition is visible apart from a rather low lamella (appearing as a barely visible denticle) in the parietal-columellar corner, discernible only in a rather oblique apertural view. Internally, the columella appears as a short, slightly twisted stem, compressed-dilated at its base (Fig. 7C–F), circumscribed by a conspicuous, inclinate lamella that changes in extension along its course. In addition, there may be a hint of secondary lamellar growth at the base of the penultimate whorl (Fig. 7E).

Zospeum schaufussi is easily separable from *Z. biscaiense* and *Z. zaldivarae* in shell and peristome shape and apertural characters, whereas *Z. percostulatum* is distinctly ribbed.

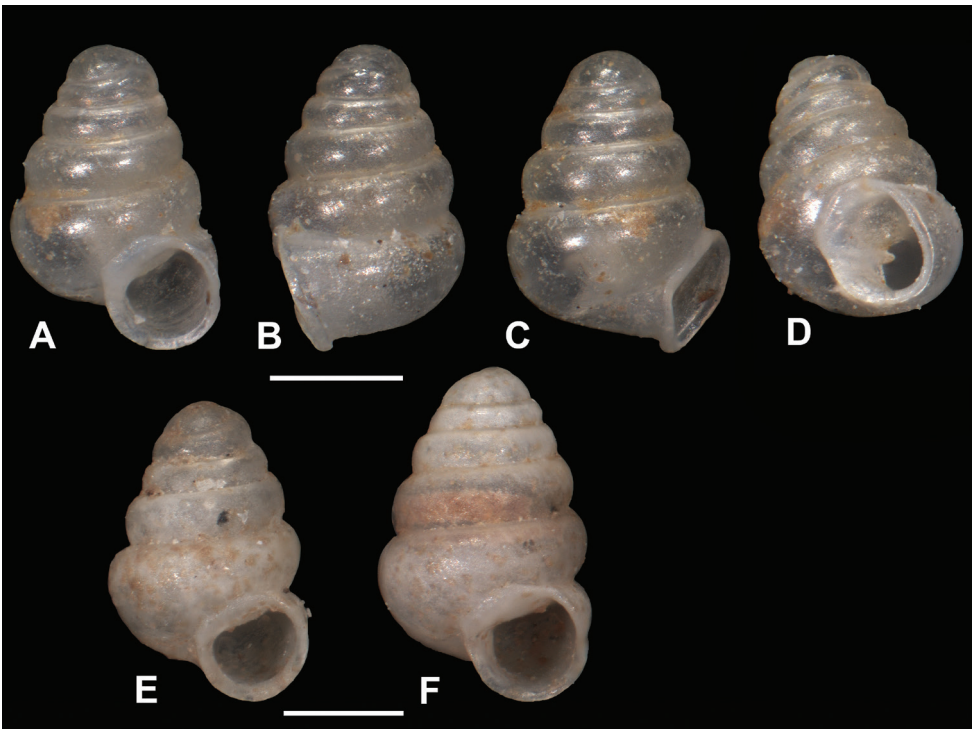

Figure 10. *Zospeum praetermissum* sp. n. **A–D** holotype (RMNH.MOL.55391), shell illustrated by Gittenberger (1980: fig. 2) **E–F** paratypes (RMNH.MOL.339954). Scale bar: 500 µm.

Zospeum vasconicum and *Z. bellesi* are more similar, but the latter has no apertural barriers or even a suggestion of any. The former has a much less prominent columellar lamella and is clearly less tightly coiled. The species described here as *Z. gittenbergeri*, differs by its angular rather than rounded peristome and slightly developed lamella on the columella.

Clearly, the lectotype of *Z. schaufussi* strongly resembles Gittenberger's topotypic *Z. suarezi*, to the extent that Gittenberger (1980) considered the lectotype shell a paratype of his species. The shell described below as *Z. praetermissum* sp. n., is distinct in its less elongate shell with less tightly coiled whorls and the presence of a second lamella on the base of the columella (Fig. 11G, I, K). Shells of *Z. suarezi* from the type cave agree with the *Z. schaufussi* lectotype in their elongate-conical shell and coiling tightness (see Table 1), rounded peristome, and barely visible dentition in the aperture. Internally, they have a similar columellar lamella configuration.

Remarks. Although our SEM-EDX analyses revealed no significant evidence linking the lectotype to a specific cave or potential cave region, this method, however, revealed some ecological information derivable from the sediment encrusting the shell. The sediment reflects a granitic context and minerogenetic processes (Onac and Forti 2011) acting in the cave environment. Detectable, are different concentrations of cal-

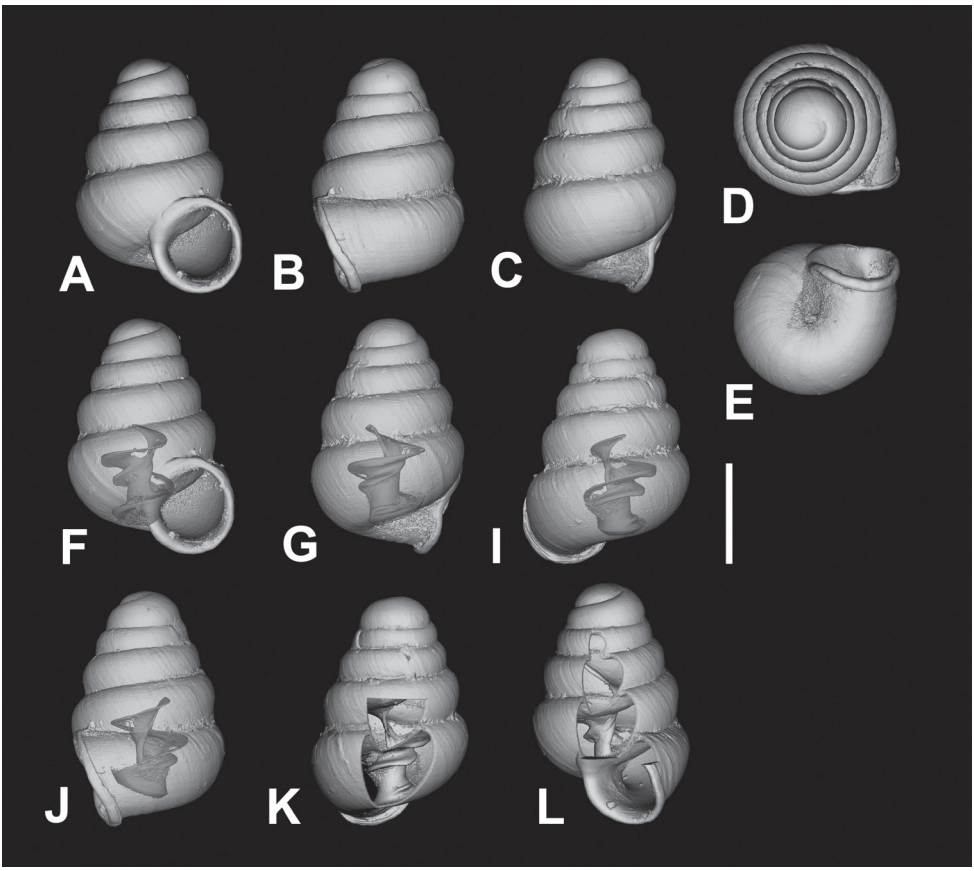

Figure 11. CT images of *Zospeum praetermissum* sp. n. holotype (RMNH.MOL.55391). **F** inclinate lamella **G, I, K** show upper lamellar bulge, central lamella, and columellar basal ridge. Scale bar: 500 μm.

cium (Ca), aluminum (Al), silicon (Si), magnesium (Mg), oxygen (O), carbon (C), iron (Fe), potassium (K), phosphor (P) and lead (Pb).

***Zospeum praetermissum* Jochum, Prieto & De Winter, sp. n.**
http://zoobank.org/3B97291A-8B05-41BA-96B1-8F6B50C22B69
Figures 5G–M, 10–11

Zospeum suarezi — Gittenberger 1980: 203, Fig. 2 (only shells from Cueva de Inguanzo).
Zospeum suarezi — Gómez and Prieto 1983: 8, Fig. 1 (only the named shell).

Type Material. Holotype. SPAIN Cueva del Puente de Inguanzo, Inguanzo, Concejo de Cabrales, Asturias, MGRS 30TUN4897097640; N43.315574, W4.860905;

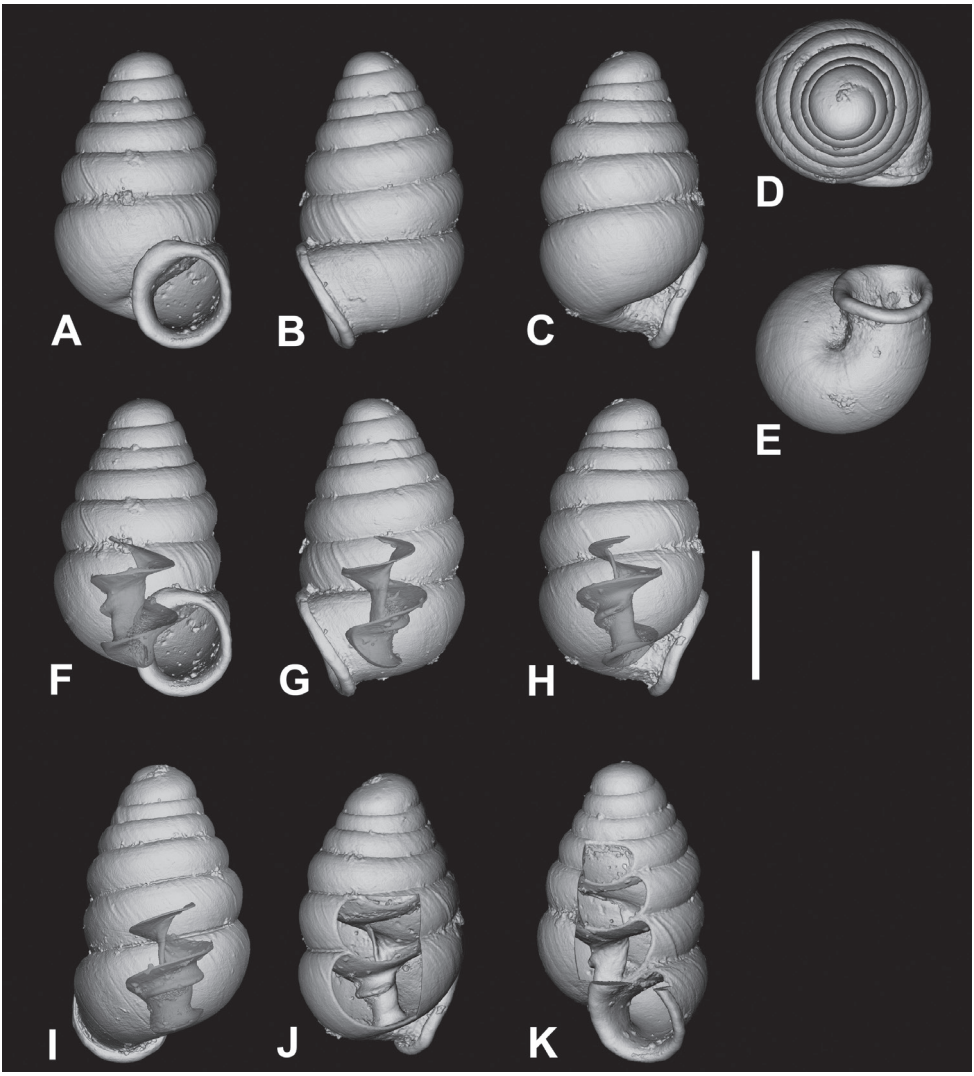

Figure 12. CT images of *Zospeum suarezi* syn. n. of *Z. schaufussi* von Frauenfeld, 1862, paratype *Z. suarezi* (Gittenberger 1980), RMNH.MOL.55389 from type locality. Scale bar: 500 µm.

230 m a.s.l.; 19 Feb 1979; G. Favre & R. Emery leg.; RMNH.MOL.55391 [55386]. **Paratypes.** SPAIN locus typicus: 2 shells; data as the holotype; RMNH.MOL.339954 [55386]. **Other material.** MHNG 96219/1 shell (now lost).

Diagnosis. Shell ca. 1.1–1.2 mm, conical with a roundish and moderately thick peristome, lacking apparent apertural barriers but with a small distinct lamella (denticle) in the parietal-columellar corner; internally, columella robust with a central lamella, a low upper columellar bulge and a basal umbilical ridge.

Description. Measurements of holotype and paratypes are presented in Table 1. Shell minute, fresh shells transparent, variable in shape (SH:SD ratio 1.41–1.57) with ca. 5 whorls, regularly coiled, suture deep, whorls convex, more or less strongly shoul-

dered; teleoconch sculpture consists of occasional blunt growth lines; robust columella with an inclinate, central lamella (Fig. 11F); an upper lamellar bulge swells from the base of the inner penultimate whorl above the central lamella (Fig. 11G, I, K); a distinct, short, ridge projects from the base of the columella above the umbilical indentation (Fig. 11G, I, K); aperture more or less circular; peristome adhering to spire, reflected, moderately thickened, roundish; umbilicus closed; apertural barriers absent apart from the low lamella that appears externally as a small, but distinct denticle on the parietal-columellar corner visible in oblique apertural view (Figs 5M, 10D).

Differential diagnosis. Differs from *Z. schaufussi* externally by its more conical shell with less tightly coiled whorls – adult shells having around 5 rather than 6 whorls of the same size – and a more pronounced lamella/denticle visible in the parietal-columellar corner in oblique view; internally by its robust columella and by its pronounced basal columellar ridge (above umbilical indentation). *Zospeum praetermissum* is easily distinguished from *Z. biscaiense* and *Z. zaldivarae* in shell and peristome shape and apertural characters, whereas *Z. percostulatum* is distinctly ribbed. *Zospeum gittenbergeri* differs by its broad, angular peristome and barely developed lamella on the columella. *Zospeum vasconicum* has a more rounded aperture with an almost uniformly-thickened peristome. *Z. bellesi* has no apertural barriers nor a columellar lamella.

Etymology. The name, *praetermissum*, refers to the situation that the holotype shell was originally not recognized as distinct from *Z. suarezi*.

Distribution. Only known from the type locality.

Ecology. According to the records of the speleologist Gérald Favre (pers. comm. 2017), the collection site was located ca. 200 m from the cave entrance (also noted on the data label NHMG-Moll 96219 (978.363)). His field notes document that the collection area consisted of sandy substrate, some chestnut fragments and that the humidity level was low. The total length of the cave is 1500 m.

Remarks. The label to the shell material Gittenberger (1980) assigned as *Z. suarezi* paratypes (NHMG-Moll.96219/1 shell), bore Gittenberger's apparent ambivalence "Zospeum schaufussi Frfld Gitt. det. 1979" (Fig. 5L). Although currently lost, this shell was most likely conspecific with *Z. praetermissum*. We consider the paratype *Z. suarezi* shell (NHMW-MO 75000-E-48815) from Cueva Hernialde, Guipuzcoa to be Z. cf. *vasconicum* (Fig. 6).

Zospeum gittenbergeri **Jochum, Prieto & De Winter, sp. n.**

http://zoobank.org/6506C1D6-746D-4ABE-B43E-6D51FCEAEF33
Figures 5L, N–R, 13–14

Zospeum schaufussi—Gittenberger 1980: 203, Fig. 1. [**non** *Zospeum schaufussi* von Frauenfeld, 1862]

Type material. Holotype (RMNH 234166/1 shell): Cueva del Puente de Inguanzo (Inguanzo, Concejo de Cabrales, Asturias, Spain), MGRS 30TUN4897097640 (N43.315574, W4.860905), 230 m a.s.l., 19.02.1979, leg. G Favre & R Emery. **Oth-**

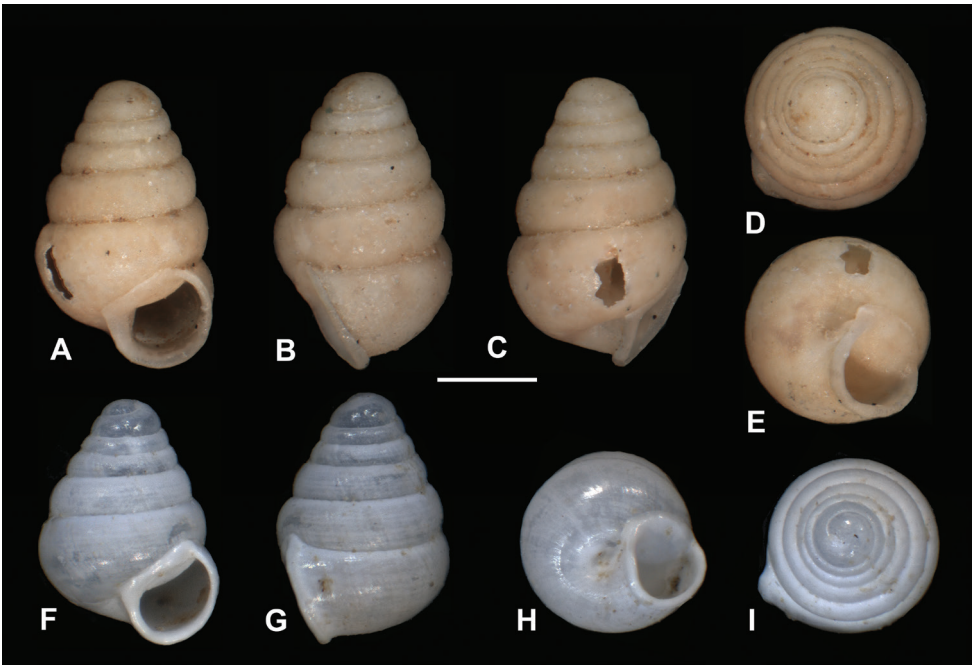

Figure 13. *Zospeum gittenbergeri* sp. n. **A–E** holotype (RMNH.MOL.234166) **F–I** *Z.* cf. *gittenbergeri* from Cueva del Búho (RMNH.MOL.234165). Scale bar: 500 µm.

er material: former *Z. suarezi* paratype shells mentioned in Gittenberger (1980): data as holotype: MHNG 96219/4 shells (now lost) (Fig. 5L, N–R).

Diagnosis. Holotype shell conical, larger than most Iberian *Zospeum*, SH nearly 1.5 mm with 5 1/2 moderately convex whorls. Parietal part of peristome straight and long, giving the peristome an angular rather than convex appearance. Internally, the lamella circumscribing the columella is very weak, but it is unclear if this is due to erosion or if it is covered by debris (Fig. 14G–J).

Description. Measurements of holotype provided in Table 1. Lost specimen of imaged MNHG 96219 shell (Fig. 5N–R) is smaller than holotype (SH 1.22 mm). Shell elongate-conical with approximately 5 ½ rounded whorls, regularly coiled, suture deep; teleoconch smooth with occasional blunt growth lines (Fig. 14A–D); aperture more or less circular; peristome closely adhering to spire, reflected, moderately thickened, with an angular, relatively long parietal callus; columella straight and aligned axially, single lamella small and non-extending, coiled tightly around the columella; columellar apertural edge (side view, aperture facing right) and the border of the parietal callus join at an angle of ca. 90 degrees (Fig. 13C); umbilicus closed, umbilical depression deep, moderately strong, wrinkly striae descend from last whorl behind apertural lip leading to umbilicus; apertural barriers lacking.

Differential diagnosis. Differs from *Z. biscaiense* by the larger, more elongate shell and the absence of major apertural barriers; from *Z. schaufussi* (lectotype) by its long and angular parietal callus, straight, axially aligned columella and its small,

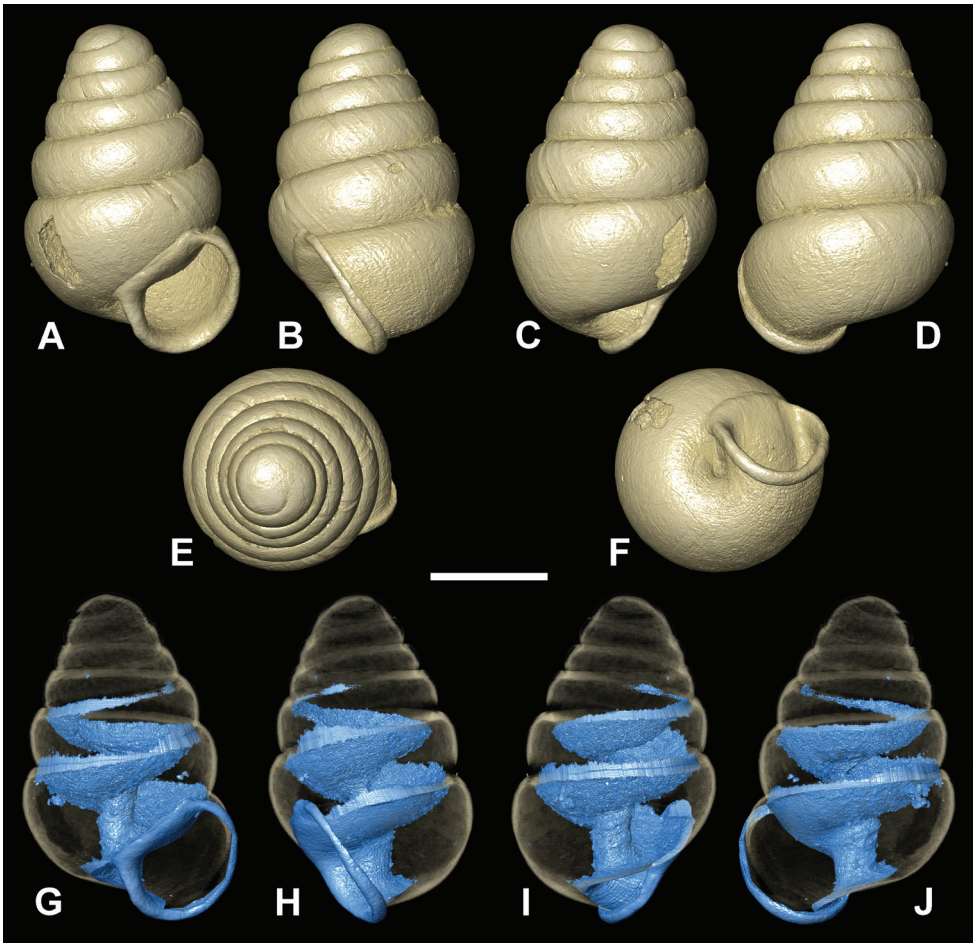

Figure 14. CT scans of *Zospeum gittenbergeri* sp. n. holotype (RMNH.MOL.234166). Scale bar: 500 μm.

non-extensive, tightly coiled lamella; in *Z. bellesi*, columellar elaboration is completely absent; from *Z. vasconicum* by its non-rounded aperture, more robust, axially aligned columella; from *Z. zaldivarae* by its more elongate shell, lack of apertural barriers; from *Z. percostulatum* by its non-costulate shell; from *Z. praetermissum* sp. n. by its long, parietal edge of the angular peristome and different columellar morphology.

Etymology. The new species is named in honour of Prof. Edmund Gittenberger, in recognition of his pioneering work on Iberian *Zospeum*.

Distribution. Only known from the type locality.

Ecology. According to the records of the collector, Gérald Favre (pers. comm. 2017), the collection site was located ca. 200 m from the cave entrance. His field notes document that the area consisted of sandy substrate, some chestnut fragments and that the humidity level was low.

Remarks. We formally describe the specimen illustrated by Gittenberger as a separate species. We confine the type material to the one shell known from the type

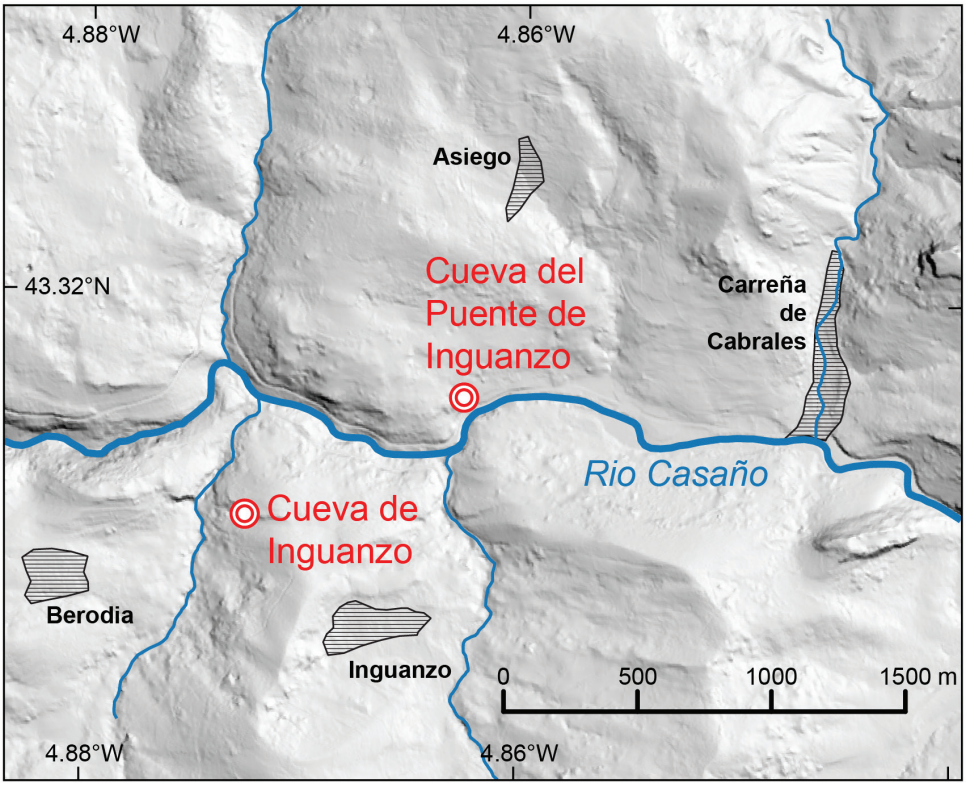

Figure 15. Map indicating geographic position of the two different Inguanzo-named caves on either side of the Rio Casaño: Cueva del Puente de Inguanzo (collection site of Gittenberger's (1980) shells) and Cueva de Inguanzo (site of Weigand et al. (2013) molecularly-assessed material). Source of DEM data: LiDAR-PNOA DGM 5 m owned by Instituto Geográfico Nacional (IGN) and provided under CC-BY 4.0 license.

cave. Although Gittenberger (1980) mentioned similar, but much less elongate shells from another cave (Cueva del Búho), we prefer to address these as *Z.* cf. *gittenbergeri* (Fig. 13 F–I). Shells with this shape and apertural morphology occur in various caves in sympatry with a *schaufussi*-like (in its present sense) species. This is seen for example in shells from Cueva del Linar (C. la Busta), where shells with angular peristomes, but much smaller than the holotype shell (SH 0.95 – 1.15; SD 0.64 – 0.74 mm) occur sympatrically with shells that are externally and internally indistinguishable from *Z. schaufussi*. Internal morphology of the Cueva de Linar shells so far shows a simple, tightly coiled singular lamella around the columella (unpubl. results, Jochum). Further study is needed to define *Z. gittenbergeri*, especially using molecular data.

A number of confusing discrepancies surfaced in addressing Gittenberger's (1980) material from Cueva del Puente de Inguanzo. Gittenberger (1980) cited only 1 shell (corresponding to the data of specimen MHNG 96219) for *Z. schaufussi* (= *Z. gittenbergeri* sp. n.), which he measured (1.45 mm) and illustrated (fig.1). For this shell, he cites "Cueva de Inguanzo near Inguanzo, 2 km SW of Cabrales, between Covadonga

and Panes, Oviedo; UTM U N 4 9; G. Favre & R. Emery leg., 19.ii.1979 (MHNG/i shell; RMNH/i shell)." However, our Figure 5 (L, N–R) is the shell imaged by the curator, Emmanuel Tardy, at the MHNG (2017) but it only measures 1.22 mm and does not correspond to the illustrated shell. On the other hand, the shell chosen as holotype (RMNH.234166), measures 1.49 mm and fits the one Gittenberger (1980) illustrated. It appears that Gittenberger (1980, fig. 1) erroneously indicated MHNG as the collection provenance of the shell, which is actually, the single shell at the RMNH.

An additional source of confusion is that there are two caves with similar, but not identical names referring to the town of Inguanzo, which are situated within one kilometer of each other (Fig. 15). The type cave, Cueva del Puente de Inguanzo, from where Gittenberger's (1980) material derives, is a different cave from where Weigand et al.'s (2013) material, from Cueva de Inguanzo (= Cueva de Bosque), derived. These two caves are separated by the Casaño River and it is not known if the two cave systems are contiguous. This important consideration became apparent when we contacted the collector of Gittenberger's (1980) material.

Acknowledgements

Special gratitude goes to Anita Eschner (NHMW) for helping AJ access the von Frauenfeld collection and for providing valuable insights and primary literature. We are grateful to Markus Heneka and Andreas Heneka (RJL Micro & Analytic GmbH, Karlsdorf-Neuthard) for their help and technical prowess with the CT and SEM-EDX scans. We thank Katharina Jaksch-Mason (NHMW) for LM imaging the *Z. schaufussi* syntype material. We also gratefully acknowledge Emmanuel Tardy's (MHNG) image contributions and notes of the Gittenberger (1980) material formerly housed in the MHNG collection. Appreciation also goes to Gérald Favre for sharing his excellent forty-year-old speleological field notes with us. We acknowledge Thomas Neubauer and Michael Duda for their kind help in transporting the lectotype back and forth from Vienna. We thank the editor, Thierry Backeljau, the ZooKeys editorial team and our reviewers, Benjamin Gómez, Edmund Gittenberger and Barna Páll-Gergely for their helpful suggestions towards improving the manuscript. Lastly, we are indebted to SYNTHESYS for providing generous support in the form of three grants to AJ from the SYNTHESYS Project http://www.synthesys.info/, which is financed by the European Community Research Infrastructure Action under the FP7 "Capacities" Program.

References

Alonso A, Prieto CE, Quiñonero-Salgado S, Rolán E (2018) A morphological gap for Iberian *Zospeum* filled: *Zospeum percostulatum* sp. n. (Gastropoda, Eupulmonata, Carychiidae) a new species from Asturias (Spain). Subterranean Biology 25: 35–48. https://doi.org/10.3897/subtbiol.25.23364

Altonaga K, Gómez BJ, Martin R, Prieto CE, Puente AI, Rallo A (1994) Estudio faunistico y biogeográfico de los Moluscos terrestres del norte de la Peninsula Ibérica. Ed. Eusko Legebiltzarra – Parlamento Vasco (Premio Xabier María de Munibe), Vitoria, 505 pp.

Bourguignat JR (1856) Aménités malacologiques. LI. Du genre *Zospeum*. Revue et Magasin de Zoologie pure et appliquée (2)8: 499–516.

Cadevall J, Orozco A (2016) Nuevas Guías de Campo Omega Caracoles y Babosas de la Península Iberica y Baleares. Ediciones Omega, Barcelona, 817 pp.

Emberton KC (2001) Dentate *Gulella* of Madagascar (Pulmonata: Streptaxidae). American Malacological Bulletin 16: 71–129.

Fischer P (1887) Manuel de conchyliologie et de paléontologie conchyliologique. Librairie F. Savy, Paris, 1567 pp.

Frauenfeld G von (1862) Ueber ein neues Höhlen-*Carychium* (*Zospeum* Brg.) und zwei neue fossile Paludinen. Verhandlungen der Zoologisch-Botanischen Gesellschaft in Wien 12: 969–972. http://www.biodiversitylibrary.org/item/95692#page/487/mode/1up

Gittenberger E (1973) Eine *Zospeum*-Art aus den Pyrenäen, *Zospeum bellesi* spec. nov. Basteria 37(5–6): 137–140.

Gittenberger E (1980) Three Notes on Iberian Terrestrial Gastropods. Zoologische Mededelingen 55(17): 201–213.

Gómez BJ, Prieto CE (1983) *Zospeum biscaiense* nov. sp. (Gastropoda, Ellobiidae) otro molusco troglobio para la Península Ibérica. Speleon 26–27: 7–10.

Jeffreys JG (1830) A synopsis on the testaceous pneumonobrancheous Mollusca of Great Britain. Transactions of the Linnean Society of London 16(2): 324, 362.

Jochum A, Winter AJ de, Weigand AM, Gómez BJ, Prieto CE (2015) Two new species of *Zospeum* Bourguignat, 1856 from the Basque-Cantabrian Mountains, Northern Spain (Eupulmonata, Ellobioidea, Carychiidae). ZooKeys 483: 81–96. https://doi.org/10.3897/zookeys.483.9167

Kerney MP, Cameron RAD (1979) A field guide to the Land Snails of Britain and north-west Europe. Collins Publishers, London, 102 pp.

Kobelt W (1899) Genus *Zospeum* Bourguignat. In: Rossmässler EA (Ed.) Iconographie der Land- & Süsswasser-Mollusken mit vorzüglicher Berücksichtigung der europäischen noch nicht abgebildeten Arten. Kreidel, Wiesbaden (2)9(1/2): 27–33. [pls 218–219]

Onac BP, Forti P (2011) Minerogenetic mechanisms occurring in the cave environment: an overview. International Journal of Speleology 40(2): 79–98. https://doi.org/10.5038/1827-806X.40.2.1

QGIS Development Team (2018) QGIS Geographic Information System. Open Source Geospatial Foundation. http://www.qgis.org

Weigand AM, Jochum A, Slapnik R, Schnitzler J, Zarza E, Klussmann-Kolb A (2013) Evolution of microgastropods (Ellobioidea, Carychiidae): Integrating taxonomic, phylogenetic and evolutionary hypotheses. BMC Evolutionary Biology 13(1): 18. https://doi.org/10.1186/1471-2148-13-18

Wessel P, Smith WHF (1996) A Global Self-consistent, Hierarchical, High-resolution Shoreline Database, Journal of Geophysical Research 101: 8741–8743. https://doi.org/10.1029/96JB00104

ZooKeys 835: 87–123 (2019)
doi: 10.3897/zookeys.835.33440
http://zookeys.pensoft.net

RESEARCH ARTICLE

A peer-reviewed open-access journal
ZooKeys
Launched to accelerate biodiversity research

A revision of *Dolichogenidea* (Hymenoptera, Braconidae, Microgastrinae) with the second mediotergite broadly rectangular from Area de Conservación Guanacaste, Costa Rica

Jose Fernandez-Triana[1], Caroline Boudreault[1], Tanya Dapkey[2], M. Alex Smith[3], Winnie Hallwachs[2], Daniel Janzen[2]

1 *Canadian National Collection of insects, Ottawa, Canada* **2** *Department of Biology, University of Pennsylvania, Philadelphia, PA 19194, USA* **3** *Department of Integrative Biology, University of Guelph, Guelph, Ontario, Canada*

Corresponding author: *Jose Fernandez-Triana* (jose.fernandez@canada.ca)

Academic editor: *C. van Achterberg* | Received 28 January 2019 | Accepted 16 March 2019 | Published 4 April 2019

http://zoobank.org/94548DD2-704E-459E-AD8C-48AE35D9EEA5

Citation: Fernandez-Triana J, Boudreault C, Dapkey T, Smith MA, Hallwachs W, Janzen D (2019) A revision of *Dolichogenidea* (Hymenoptera, Braconidae, Microgastrinae) with the second mediotergite broadly rectangular from Area de Conservación Guanacaste, Costa Rica. ZooKeys 835: 87–123. https://doi.org/10.3897/zookeys.835.33440

Abstract

The first species of *Dolichogenidea* (Hymenoptera: Braconidae, Microgastrinae) with the second mediotergite broadly quadrate to rectangular are revised, and eight new species from Area de Conservación Guanacaste (ACG), Costa Rica are described, all authored by Fernandez-Triana & Boudreault: *alejandromasisi*, *angelagonzalezae*, *carlosmanuelrodriguezi*, *genuarnunezi*, *josealfredohernandezi*, *melaniamunozae*, *rogerblanconi,* and *yeimycedenoae*. A new species group (*carlosmanuelrodriguezi*) within the genus is proposed to accommodate those species, as well as additional undescribed species from the Neotropical region found in collections. All new species are found in rainforests (120–900 m) and all are parasitoids of Depressariidae (except for one species parasitizing Choreutidae). The unique shape of the second mediotergite and long ovipositor are features shared with the *alejandromorai* species group in the genus *Apanteles*, an example of convergent evolution; both wasp groups also parasitize similar hosts in ACG.

Keywords

Area de Conservación Guanacaste, DNA barcoding, *Dolichogenidea*, Microgastrinae, parasitoid biology, taxonomic revision

Introduction

Dolichogenidea is a genus in the braconid subfamily Microgastrinae and contains almost 200 described species worldwide, with only four of them recorded from the Neotropics (Yu et al. 2016). However, there are hundreds of undescribed species in collections. For example, among the material from Costa Rica with DNA barcodes available (1,200+ species of Microgastrinae), there are more than 110 *Dolichogenidea* species, the great majority being undescribed (e.g., see DNA barcode data in Smith et al. 2013).

This study represents the first paper of a series dealing with *Dolichogenidea* from Area de Conservación Guanacaste (ACG) in northwestern Costa Rica. ACG contains 1,200 km^2 of terrestrial conserved wildland dry forest, cloud forest and rain forest, extending from 0 to 2,000 m elevation continuously from the Pacific coast to the Caribbean lowlands; its biodiversity is being intensively inventoried (e.g., Arias-Penna et al. 2013, Fernández-Triana et al. 2013, 2014a, 2014b, 2015, 2016, Fleming et al. 2018, Janzen and Hallwachs 2016, Hansson et al. 2015, Sharkey et al. 2011, 2018, Valerio et al. 2009, Whitfield et al. 2012).

Below we describe eight new species which represent a unique group among known *Dolichogenidea*. They are characterized by a broadly quadrate to rectangular second mediotergite, a feature never previously reported among the described species of the genus.

Materials and methods

The specimens studied for this paper are deposited in the: Canadian National Collection of Insects, Ottawa, Canada (**CNC**), with some paratypes and other specimens to be deposited in the National Museum of Natural History, Washington, USA (**NMNH**) and the Museo Nacional de Costa Rica, San José, Costa Rica (**MNCR**).

Morphological terms and measurements of structures follow those used by Mason (1981), Huber & Sharkey (1993), Whitfield (1997), Karlsson & Ronquist (2012), and Fernández-Triana et al. (2014a). The abbreviations F1, F2, F3, F14, F15, and F16 refer to antennal flagellomeres 1, 2, 3, 14, 15, and 16; T1, T2, and T3 refer to metasomal mediotergites 1, 2, and 3; and L and W refer to length and width respectively.

The descriptions of the new species contain a general but brief account of color, sculpture, and morphological features and commonly used ratios in taxonomic studies of Microgastrinae. Raw measurements of morphological structures (in mm) are also provided, which would allow for additional ratios to be explored in the future. When presenting raw measurements, the holotype value is given first, followed by the range of other specimens of the same species between parentheses.

In the species descriptions, the holotype labels are detailed verbatim, with / separating the different lines of each label. For paratypes, specimen information was generated using the CNC database (http://www.cnc-ottawa.ca/taxonomy/TaxonMain.php).

We DNA barcoded some specimens, using the standard animal locus of the 5' region of the cytochrome c oxidase I (COI) gene (Hebert et al. 2003). Briefly, DNA extracts were obtained from single legs using a glass fibre protocol (Ivanova et al. 2006), and total genomic DNA was re-suspended in 30 µl of dH2O. The barcode region (658 base pairs (bp) region near the 5' terminus of the COI gene) was amplified using standard primers following established protocols (see Smith et al. 2008). All information for the sequences associated with each individual specimen barcoded (including primers and trace files) is available on the Barcode of Life Data System (BOLD) (Ratnasingham & Hebert 2007) using the DOI dx.doi.org/10.5883/DS-ASDOLICH. We use the Barcode Index Number (BIN) System to discuss species limits, following the BIN concept detailed in Ratnasingham & Hebert (2013) but recognizing that within many higher taxa, several species, as distinguished by their barcodes combined with biology, may fall within a single BIN (e.g., Janzen et al. 2017). DNA barcodes from the specimens used in this paper were compared with 40,000+ barcodes of Microgastrinae available in BOLD as of January 2019, the great majority of which are from ACG.

Photographs were taken with a Keyence VHX–1000 Digital Microscope, using a lens with a range of 10–130 ×. Multiple images were taken of a structure through the focal plane and then combined to produce a single in-focus image using the software associated with the Keyence System. Images were corrected using Adobe Photoshop CS4, plates were prepared using Microsoft PowerPoint 2010 and saved as .tiff files.

Results

The genus *Dolichogenidea* was described by Viereck (1911), it is one of the closest to *Apanteles* sensu stricto, and is also the most controversial and difficult to separate from it (for extensive discussions on the topic see Mason 1981, Whitfield 1997, Fernández-Triana et al. 2014a). *Dolichogenidea* has a convex to almost straight vannal lobe, which is uniformly fringed by setae, whereas in *Apanteles* the vannal lobe is strongly concave to almost straight, and is lacking setae (partially or totally) at mid length; apart from morphology, DNA barcoding tends to clearly cluster the species of both genera separately (e.g., Fernández-Triana 2010; Smith et al. 2013). We follow here the generic concept of *Dolichogenidea* detailed in and adopted by Fernández-Triana et al. (2014a); that paper is also relevant because it includes a review of ACG *Apanteles* and establishes a foundation for future ACG studies on related genera such as *Dolichogenidea*.

The species described below are unique among all described *Dolichogenidea*. They can be easily distinguished from congeners by having the shape of T2 almost quadrate to broadly rectangular, and a relatively very long ovipositor and ovipositor sheaths. Because of their diagnostic value, both characters are described below with more details.

A perfectly quadrate T2 would have the same width at its posterior margin as its median length, i.e., the ratio between those two measurements would be 1.0 × (because anterior and posterior widths of T2 are usually different, the posterior width is

the commonly used trait). The species dealt with here (Figs 1E, 2D, 3B, 4F, 5B, 6E, 7E, 7F, 8E) have the T2 width at the posterior margin ranging from 1.3 × (i.e., almost quadrate) to 2.2 × its median length (i.e., broadly rectangular); very rarely the ratio is 2.3–2.4 ×. In contrast, all previously described *Dolichogenidea* species have a much more transverse T2, with posterior width of T2 being at least 3.0 × its median length (usually much more, and very rarely as low as 2.5 ×).

All eight species described here have ovipositor sheaths 1.8–2.5 × as long as their metatibia lengths (Figs 1A, 2A, 3A, 4E, 5A, 5E, 6A, 6D, 7A, 7D, 8A, 8D). Very few of the previously described *Dolichogenidea* have sheaths longer than 1.7 × its metatibia length (but see Fagan-Jeffries et al. 2018 for some examples in Australia); however, and unlike the ACG taxa, none of those Australian species have a broadly rectangular or quadrate T2. The caterpillar hosts of these wasps species all live inside a leaf roll, or have silked two leaves together. Although it could be speculated that comparatively long ovipositors are probably advantageous to penetrate the leaves, pierce the caterpillar skin, and lay the wasp eggs (inside the caterpillar), it must also be noted that many other leaf roller lepidopterans in ACG are parasitized by microgastrines with comparatively shorter ovipositors. Thus, based on what is known at present no generalizations are possible.

Because of its uniqueness, we propose here this group to be named as the *Dolichogenidea carlosmanuelrodriguezi* species group, consisting of eight new species; they have all been found in rainforests (120–900 m) in ACG, and all except one species are parasitoids of Depressariidae (with a single wasp species parasitizing Choreutidae), with both solitary and gregarious species (Figs 10–17). We have seen additional undescribed species from the Neotropical region in other collections.

Some of the new species described below are very similar morphologically. However, they are characterised by large interspecific molecular divergence within the DNA barcode region, with the interspecific distance ranging from 2.39 to 6.59 % (as compared with intraspecific distances between 0 and 0.61 %).

The species in the *D. carlosmanuelrodriguezi* group are surprisingly morphologically similar (regarding the shape of T2 and the comparatively long ovipositors) to the *alejandromorai* species group in the genus *Apanteles* (see Fernández-Triana et al. 2014a), and they even parasitize the same host families in ACG. Similarities in morphology and biology of these two species groups in two different genera of Microgastrinae are an extraordinary example of convergent evolution, and we speculate that it may be mostly related to their similar host relationships. Because the host records provided by Fernández-Triana et al. (2014a) for the *Apanteles alejandromorai* species group are now outdated, we present and update them here, altogether with the hosts of the *Dolichogenidea carlosmanuelrodriguezi* species group (Table 1). The species of the *Dolichogenidea carlosmanuelrodriguezi* group have been found to parasitize only one host species (at least based on ACG data), whereas only one quarter of the species in the *Apanteles alejandromorai* group parasitize one host in ACG, with the rest parasitizing between two and up to 16 different lepidopteran species, although always in the family Depressariidae. The two species groups are clearly distinct from a molecu-

Table 1. Updated information on the hosts of the *Apanteles alejandromorai* and *Dolichogenidea carlosmanuelrodriguezi* species groups in ACG, Costa Rica. For some host species only interim names are available at present. For an explanation on how those interim names are produced see Janzen & Hallwachs (2016) and also http://janzen.sas.upenn.edu/caterpillars/database.lasso.

Species	Host family (# of host species): host species names
Apanteles	
alejandromorai	Depressariidae (4): *Antaeotricha* Janzen 106; *Antaeotricha* Janzen 225; *Antaeotricha* Janzen 366; *Lethata trochalosticta*
deifiliadavilae	Depressariidae (12): *Antaeotricha marmorea*; *Antaeotricha radicalis*; *Antaeotricha* Janzen86; *Antaeotricha* Janzen204; *Antaeotricha* radicalisDHJ01; *Antaeotricha* radicalisEPR03; *Chlamydastis vitorbeckeri*; *Stenoma* Janzen19; *Stenoma* Janzen20; *Stenoma* Janzen210; two unidentified Stenomatinae species with interim names "elachJanzen01 Janzen204" and "elachJanzen01 Janzen211"
eulogiosequeirai	Depressariidae (1): *Stenoma* Janzen08
fernandochavarriai	Depressariidae (6): *Antaeotricha* BioLep46; *Antaeotricha* Janzen13; *Antaeotricha* Janzen31; *Antaeotricha* Janzen77; *Antaeotricha* Janzen290; *Antaeotricha* Janzen140DHJ01; *Antaeotricha* Phillips02
franciscoramirezi	Depressariidae (1): *Antaeotricha* Janzen727
freddysalazari	Depressariidae (2): *Antaeotricha* Janzen370; one unidentified Depressariinae species with interim name "elachJanzen01 Janzen227"
gabrielagutierrezae	Depressariidae (2): *Antaeotricha* Janzen301; *Antaeotricha* Phillips01
juancarrilloi	Depressariidae (16): *Antaeotricha renselariana*; *Antaeotricha* stigmatiasDHJ01; *Antaeotricha* Janzen07; *Antaeotricha* Janzen09; *Antaeotricha* Janzen10; *Antaeotricha* Janzen39; *Antaeotricha* Janzen110; *Antaeotricha* Janzen146; *Antaeotricha* Janzen366; *Lethata trochalosticta*; *Stenoma* Janzen58; *Stenoma* Janzen99; *Stenoma* Janzen244; three unidentified Depressariinae species with interim names "elachBioLep01 BioLep709"; "elachBioLep01 Janzen48"; and "elachJanzen01 Janzen725"
luisbrizuelai	Depressariidae (1): *Antaeotricha* Janzen128
luisgarciai	Depressariidae (1): unidentified Depressariinae species with interim name "elachJanzen01 Janzen301"
marvinmendozai	Depressariidae (4): *Antaeotricha* BioLep54; *Antaeotricha* Janzen84; *Antaeotricha* Janzen146; *Antaeotricha* Janzen222
minornavarroi	Depressariidae (4): *Antaeotricha renselariana*; *Antaeotricha* Janzen146; *Antaeotricha* Janzen146; one unidentified Depressariinae species with interim name "elachJanzen01 Janzen120"
tiboshartae	Depressariidae (16): *Anadasmus* Janzen16; *Anadasmus* Janzen25; *Antaeotricha renselariana*; *Antaeotricha* Janzen07; *Antaeotricha* Janzen09; *Antaeotricha* Janzen12; *Antaeotricha* Janzen86; *Antaeotricha* Janzen134; *Antaeotricha* Janzen146; *Antaeotricha* Janzen222; *Antaeotricha* Janzen228; *Antaeotricha* Janzen401; *Antaeotricha* radicalisDHJ01; *Stenoma* BioLep391; Stenoma Janzen144; one unidentified Depressariinae species with interim name "elachBioLep01 Janzen48"
Dolichogenidea	
alejandromasisi	Depressariidae (1): *Antaeotricha renselariana*
angelagonzalezae	Choreutidae (1): *Brenthia* Janzen12
carlosmanuelrodriguezi	Depressariidae (1): *Antaeotricha spurca*
genuarnunezi	Depressariidae (1): *Antaeotricha phaeoneura*
josealfredohernandezi	Depressariidae (1): *Stenoma* Janzen99
melaniamunozae	Depressariidae (1): *Cerconota recurvella*
rogerblancoi	Depressariidae (1): *Antaeotricha* radicalisDHJ01
yeimycedenoae	Depressariidae (1): *Antaeotricha* Janzen126

lar (DNA barcodes) perspective as well (Fig. 9), with interspecific divergences on average nearly 6% within the *Dolichogenidea* species and 13% between *Dolichogenidea* and *Apanteles* (in those two groups).

The patronyms for this group of *Dolichogenidea* are named in honor of the government team of Costa Rican biodiversity managers and administrators responsible for presenting the country to the 14th Conference of the Parties (COP 14) of the Convention for Biological Diversity, in October 2018.

Key to species of the *carlosmanuelrodriguezi* species group of *Dolichogenidea* in ACG

1 Larger size (body L 4.80–4.90 mm; fore wing L 4.70–4.80 mm; ovipositor sheaths L 3.00–3.40 mm); metatrochanter and metatrochantellus entirely black [Hosts: *Cerconota recurvella* (Walker, 1864) *Antaeotricha spurca* (Zeller, 1855) (Depressariidae)] ..... ***Dolichogenidea melaniamunozae* sp. n.**

– Smaller size (body L less than 4.00 mm; fore wing L less than 3.70 mm; ovipositor sheaths L less than 3.10 mm); metatrochanter and/or metatrochantellus at least partially yellow..... **2**

2 Mesofemur entirely yellow, metafemur almost entirely yellow (except for small, dark spot on anterior 0.1–0.2) **3**

– Mesofemur partially dark brown (rarely mostly yellow with small, dark spots), metafemur mostly to entirely dark brown to black..... **4**

3 Slightly smaller specimens (body L 3.70 mm; ovipositor sheaths 2.60 mm); T2 posterior W 2.0 × T2 L medially; F2 1.6 × as long as F14 [Host: *Antaeotricha spurca* (Zeller, 1855) (Depressariidae)] [A total of 21 DNA barcode diagnostic characters: 31T, 37A, 55G, 67A, 70A, 79A, 88A, 109A, 139A, 190C, 277A, 290G, 316G, 322G, 370T, 386T, 418T, 436T, 460A, 496G, 556A] ..... Dolichogenidea carlosmanuelrodriguezi **sp. n.**

– Slightly larger specimens (body L 3.90 mm; ovipositor sheaths 2.90 mm); T2 posterior W 1.8 × T2 L medially; F2 1.7–1.9 × as long as F14 [Host: *Stenoma* Janzen99] [A total of 21 DNA barcode diagnostic characters: 31A, 37G, 55A, 67T, 70G, 79T, 88T, 109G, 139T, 190A, 277T, 290A, 316A, 322T, 370A, 386A, 418A, 436A, 460G, 496A, 556GA]..... ..... ***Dolichogenidea josealfredohernandezi* sp. n.**

4 T1 comparatively broader, T1 L 1.5 × T1 anterior W, and T1 L 1.5 × T1 posterior W; T2 comparatively less quadrate (T2 posterior W 2.3 × T2 L medially); parasitizing caterpillars in the family Choreutidae [Host: *Brenthia* Janzen12]..... ***Dolichogenidea angelagonzalezae* sp. n.**

– T1 comparatively narrower, T1 L 1.9–2.4 × (very rarely 1.6 ×) T1 anterior W, and T1 L 1.9–3.0 × (very rarely 1.6–1.7 × in small specimens) T1 posterior W; T2 comparatively more quadrate, T2 posterior W 1.3–1.9 × (very rarely 2.0–2.1 × in small specimens) T2 L medially; parasitizing caterpillars in the family Depressariidae..... **5**

5 Mesofemur mostly yellow, at most with small, dark spots (***if*** mesofemur mostly brown, ***then*** specimens significantly smaller, with body L 2.50–3.00 mm) **6**

– Mesofemur mostly dark brown (body L at least 3.30 mm, usually more) **7**

6 F2 2.1–2.5 × (average: 2.3 ×) as long as F14; T2 posterior W 1.3–1.9 × (average: 1.6 ×) T2 L medially; pterostigma L 3.0–3.5 × (average 3.2 ×) pterostigma width [Host: *Antaeotricha renselariana* (Stoll, [1781])] ..... ***Dolichogenidea alejandromasisi* sp. n.**

– F2 1.8–2.1 × (average: 1.9 ×) as long as F14; T2 posterior W 1.6–2.1 × (average: 1.8 ×) T2 L medially; pterostigma L 2.7–3.0 × (average 2.8 ×) pterostigma width [Host: *Antaeotricha* radicalisDHJ01] ..... ***Dolichogenidea rogerblancoi* sp. n.**

7 Pterostigma L 3.0 × pterostigma width; posterior ocellar line 1.6 × lateral ocellus diameter; ocular ocellar line 1.2 × posterior ocellar line [Host: *Antaeotricha phaeoneura* (Meyrick, 1913)] ..... ***Dolichogenidea genuarnunezi* sp. n.**

– Pterostigma L 3.1–3.3 × (average 3.2 ×) pterostigma width; posterior ocellar line 1.8–2.0 × lateral ocellus diameter; ocular ocellar line 1.2–1.5 × posterior ocellar line [Host: *Antaeotricha* Janzen126] ..... ***Dolichogenidea yeimycedenoae* sp. n.**

Taxonomic treatment of species, in alphabetical order

***Dolichogenidea alejandromasisi* Fernandez-Triana & Boudreault, sp. n.**
http://zoobank.org/AC2F139B-53D9-451A-9B4F-1C9B7875398D
Figs 1A–E; 10A, B

Holotype. Female, Costa Rica, CNC.

Holotype voucher code. DHJPAR0035291.

Holotype locality. Rio Blanco Abajo, 500 m, 10.90037N, -85.37254W, Sector San Cristobal, ACG, Alajuela province, Costa Rica.

Holotype verbatim labels. COSTA RICA: Alajuela, ACG, / Sector San Cristobal, / Rio Blanco Abajo, 500 m, / 10.90037N, -85.37254W, / 03/22/2009 / DHJPAR0035291.

Paratypes. Ten female and five male specimens mounted on individual points (CNC). The pins where two of the female specimens are mounted also have a gel capsule each, with a few additional (unmounted) specimens. All paratypes either from the same holotype locality or the following three localities, all in ACG: 1) Leonel, 510m, 10.99637N, -85.40195W, Sector Pitilla, Guanacaste province; 2) Casa Roberto, 520m, 11.01095N, -85.42094W, Sector Pitilla, Guanacaste province; 3) Sendero Perdido, 620m, 10.8794N, -85.38607W, Sendero San Cristobal, Alajuela Province. Paratype voucher codes: DHJPAR0049092, DHJPAR0049097, DHJPAR0054587, 09–SRNP–72860, 12–SRNP–30564, 12–SRNP–30565.

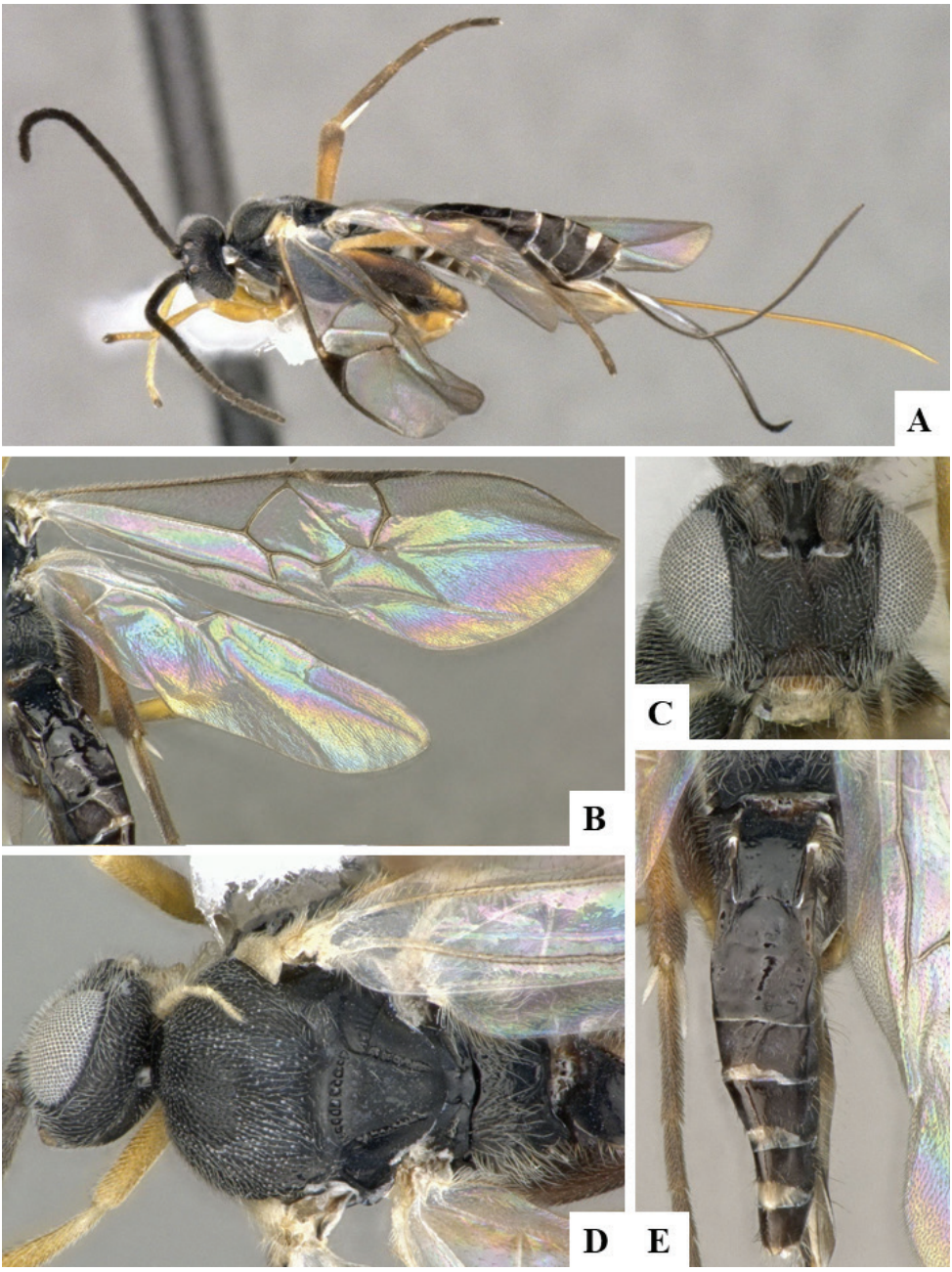

Figure 1. A–E *Dolichogenidea alejandromasisi* sp. n., holotype. **A** habitus, lateral **B** wings **C** head, frontal **D** head and mesosoma, dorsal **E** metasoma, dorsal.

Diagnosis. *Dolichogenidea alejandromasisi* can be recognized by its black to brown metafemur, comparatively narrower T1 (usually T1 L medially 2.0–3.0 × T1 posterior W), more quadrate T2 (T2 posterior W 1.30–1.90 × T2 L medially) and host being

Depressariidae. *D. rogerblancoi* shares those features and is very similar morphologically, but it differs from *alejandromasisi* by having shorter F1 L, relatively less quadrate T2 (T2 posterior W 1.6–2.1 × T2 L medially) and relatively broader pterostigma. The two species parasitize different hosts (although in the same genus *Antaeotricha*), but *alejandromasisi* tends to be found at higher altitudes.

Description. Body color: head and mesosoma black, metasoma black to dark brown; palpi, metatibial spines, tegula and most of humeral complex white-yellow; legs mostly orange-yellow, except for mesofemur (with small dark brown spots), metafemur (mostly brown), and apical 0.1–0.2 of metatibia and metatarsus brown; wing venation mostly white or transparent, except for fore wing veins R1, r, 2RS and 2M which are brown, pterostigma mostly brown but with small light spot at base. Anteromesoscutum mostly with setae and sculptured with punctures that do not fuse with each other; scutoscutellar sulcus relatively wide and with relatively deep crenulae; scutellar disc smooth and unsculptured, with isolated setae; propodeum mostly setose and with scattered punctures; propodeum areola partially defined on posterior half by longitudinal carinae, transverse carinae partially defined; T1 mostly smooth, with shallow and sparse punctures along lateral margins; T2+ smooth. Body Length: 3.66 (2.53–5.02). Fore wing L: 3.44 (2.55–3.80). Ovipositor sheaths L: 2.66 (1.98–2.90). F1 L: 0.26 (0.19–0.26). F2 L: 0.26 (0.19–0.27). F2 W: 0.07 (0.05–0.07). F3 L: 0.25 (0.19–0.27). F14 L: 0.11 (0.08–0.12). F14 W: 0.06 (0.04–0.06). F15 L: 0.10 (0.08–0.12). F16 L: 0.12 (0.10–0.14). Head height: 0.59 (0.48–0.60). Head width: 0.75 (0.62–0.80). Eye height: 0.39 (0.32–0.41). Malar distance: 0.11 (0.08–0.12). Mandible W: 0.12 (0.07–0.12). Ocular ocellar line: 0.13 (0.12–0.14). Posterior ocellar line: 0.13 (0.11–0.14). Lateral ocellar line: 0.08 (0.05–0.08). Scutellar disc L: 0.33 (0.26–0.35). Scutellar disc W at anterior margin: 0.32 (0.22–0.32). T1 L: 0.53 (0.38–0.58). T1 W at anterior margin: 0.33 (0.20–0.32). T1 W at posterior margin: 0.26 (0.20–0.28). T1 maximum width: 0.29 (0.22–0.33). T2 L: 0.20 (0.13–0.25). T2 W at anterior margin: 0.23 (0.18–0.25). T2 W at posterior margin: 0.28 (0.23–0.33). Metafemur L: 0.94 (0.68–0.94). Metafemur W: 0.28 (0.17–0.29). Metatibia L: 1.19 (0.84–1.30). Metatibial inner spur L: 0.32 (0.22–0.36). Metatibial outer spur L: 0.21 (0.12–0.23). Metatarsus first segment L: 0.67 (0.45–0.74). Pterostigma L: 0.70 (0.52–0.72). Pterostigma W: 0.21 (0.18–0.21). Fore wing vein R1 L: 0.83 (0.69–0.94). Fore wing vein r L: 0.26 (0.17–0.28). Fore wing vein 2RS L: 0.21 (0.14–0.21).

Biology. Reared from *Antaeotricha renselariana* (Stoll, [1781]) (Depressariidae). This is the only species of *Dolichogenidea* parasitizing that species of caterpillar in ACG, with 87 records out of 1,132 rearings.

Distribution. Costa Rica, ACG, Sectores San Cristobal & Pitilla, 500–620 m. Rain forest ecosystem.

Molecular data. This species is represented in BOLD by 78 sequences, which belong to BIN BOLD:ABX6174.

Etymology. *Dolichogenidea alejandromasisi* is dedicated to Alejandro Masis Cuevillas, Director of Area de Conservación Guanacaste, in recognition of his decades of protection and biodevelopment of the forests occupied by this wasp.

Dolichogenidea angelagonzalezae **Fernandez-Triana & Boudreault, sp. n.**
http://zoobank.org/915CF4E8-CA85-49EB-831B-7EEA50FED9A0
Figs 2A–E; 11A, B

Holotype. Female, Costa Rica, CNC.

Holotype voucher code. DHJPAR0020711.

Holotype locality. Vado Rio Francia, 400 m, 10.90093 -85.28915, Sector Rincon Rain Forest, ACG, Alajuela province, Costa Rica.

Holotype verbatim labels. COSTA RICA: Alajuela, ACG, / Sector Rincon Rain Forest, / Vado Rio Francia, 400 m, / 10.90093N, -85.28915W, / 08/22/2007 / DHJPAR0020711.

Paratype. One specimen of sex undetermined, from the same locality as holotype (CNC). The metasoma (except for T1) and tips of antennae are missing and thus is not possible to establish the sex of the specimen. Voucher code: DHJPAR0020708.

Diagnosis. *Dolichogenidea angelagonzalezae* can be recognized by its black to brown metafemur, comparatively broader T1 (T1 L medially 1.5 × T1 posterior W), less quadrate T2 (T2 posterior W 2.3 × T2 L medially) and host being Choreutidae.

Description. Body color: head and mesosoma black, metasoma black to dark brown; palpi, metatibial spines, tegula and most of humeral complex white-yellow; legs mostly orange-yellow, except for mesofemur (with small dark brown spots), metafemur (mostly brown), and apical 0.1–0.2 of metatibia and metatarsus brown; wing venation mostly white or transparent, except for fore wing veins R1, r, 2RS and 2M which are brown, pterostigma mostly brown but with small light spot at base. Anteromesoscutum mostly with setae and sculptured with punctures that do not fuse with each other; scutoscutellar sulcus relatively wide and with relatively deep crenulae; scutellar disc smooth and unsculptured, with isolated setae; propodeum mostly setose and with scattered punctures; propodeum areola partially defined on posterior half by longitudinal carinae, transverse carinae partially defined; T1 mostly smooth, with shallow and sparse punctures along lateral margins; T2+ smooth. Body Length: 3.72. Fore wing L: 3.88. Ovipositor sheaths L: 3.12. F1 L: 0.31. F2 L: 0.31. F2 W: 0.08. F3 L: 0.29. F14 L: 0.17. F14 W: 0.07. F15 L: 0.12. F16 L: 0.14. Head height: 0.61. Head width: 0.82. Eye height: 0.42. Malar distance: 0.11. Mandible W: 0.10. Ocular ocellar line: 0.14. Posterior ocellar line: 0.12. Lateral ocellar line: 0.08. Scutellar disc L: 0.39. Scutellar disc W at anterior margin: 0.32. T1 L: 0.50. T1 W at anterior margin: 0.33. T1 W at posterior margin: 0.32. T1 maximum width: 0.34. T2 L: 0.19. T2 W at anterior margin: 0.37. T2 W at posterior margin: 0.45. Metafemur L: 1.07. Metafemur W: 0.32. Metatibia L: 1.35. Metatibial inner spur L: 0.36. Metatibial outer spur L: 0.23. Metatarsus first segment L: 0.78. Pterostigma L: 0.74. Pterostigma W: 0.22. Fore wing vein R1 L: 0.91. Fore wing vein r L: 0.28. Fore wing vein 2RS L: 0.24.

Biology. Reared from *Brenthia* Janzen12 (Choreutidae). This is the only Microgastrinae known to parasitize that species of caterpillar in ACG, with three records out of four rearings, probably representing two sets of sibling caterpillars.

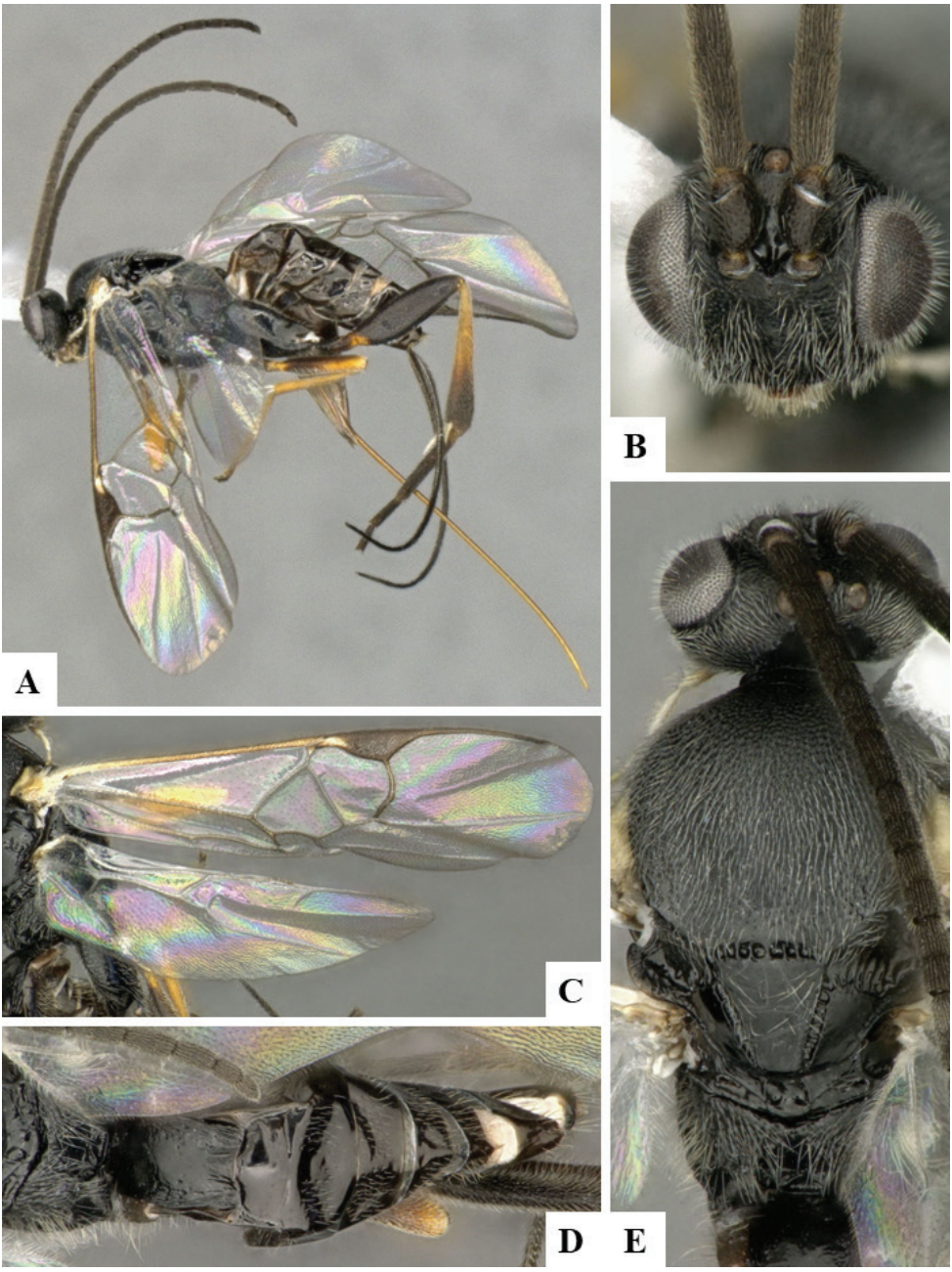

Figure 2. A–E *Dolichogenidea angelagonzalezae* sp. n., holotype. **A** habitus, lateral **B** head, frontal **C** wings **D** metasoma, dorsal **E** head and mesosoma, dorsal.

Distribution. Costa Rica, ACG, Sector Rincon Rain Forest, 400–460 m. Rain forest ecosystem.

Molecular data. This species is represented in BOLD by three sequences (two full barcodes and one sequence 421 bp), which belong to BIN BOLD:AAL2298.

Etymology. *Dolichogenidea angelagonzalezae* is dedicated to Angela Gonzalez Grau of Santo Domingo de Heredia, Costa Rica, in recognition of her dedication to supporting BioAlfa to render Costa Rica bioliterate, constructing CONAGEBIO (Comisión Nacional de Gestión de la Biodiversidad) as a biodiversity biodevelopment-friendly government agency, and for presenting Costa Rica's Biodiversity Clearing House to COP14 in October 2018.

Dolichogenidea carlosmanuelrodriguezi **Fernandez-Triana & Boudreault, sp. n.**
http://zoobank.org/F69A1114-3975-46E4-8E14-5EF2B515CEF6
Figs 3A–E; 12A, B

Holotype. Female, Costa Rica, CNC.

Holotype voucher code. DHJPAR0039047.

Holotype locality. Sendero Rally, 821 m, 10.75993 -85.28738, Sector Santa Maria, ACG, Guanacaste province, Costa Rica.

Holotype verbatim labels. COSTA RICA: Guanacaste, / ACG, Sector Santa Maria, / Sendero Rally, 821 m, / 10.75993N, -85.28738W, / 03/07/2010 / DHJPAR0039047.

Diagnosis. *Dolichogenidea carlosmanuelrodriguezi* can be recognized by its legs almost entirely orange-yellow (except for small, dark spot on posterior 0.1–0.2 of metafemur). It is very similar to *D. josealfredohernandezi,* but the later species is slightly larger and with a slightly more quadrate T2 (although the variation of those characters is very small, to the point that both species are almost indistinguishable morphologically). However, they parasitize different host species, in different genera, and they also differ in a total of 21 DNA barcode diagnostic characters. Additionally, the two species have been found at different altitudes.

Description. Body color: head and mesosoma black, metasoma black to dark brown; palpi, metatibial spines, tegula and most of humeral complex white-yellow; legs mostly orange-yellow, except for small, dark spot on posterior 0.1–0.2 of metafemur, and apical 0.1–0.2 of metatibia and metatarsus brown; wing venation mostly white or transparent, except for fore wing veins R1, r, 2RS and 2M which are brown, pterostigma mostly brown but with small light spot at base. Anteromesoscutum mostly with setae and sculptured with punctures that do not fuse with each other; scutoscutellar sulcus relatively wide and with relatively deep crenulae; scutellar disc smooth and unsculptured, with isolated setae; propodeum mostly setose and with scattered punctures; propodeum areola partially defined on posterior half by longitudinal carinae, transverse carinae partially defined; T1 mostly smooth, with shallow and sparse punctures along lateral margins; T2+ smooth. Body Length: 3.75. Fore wing L: 3.72. Ovipositor sheaths L: 2.62. F1 L: 0.29. F2 L: 0.28. F2 W: 0.09. F3 L: 0.28. F14 L: 0.17. F14 W: 0.07. F15 L: 0.12. F16 L: 0.15. Head height: 0.60. Head width: 0.84.

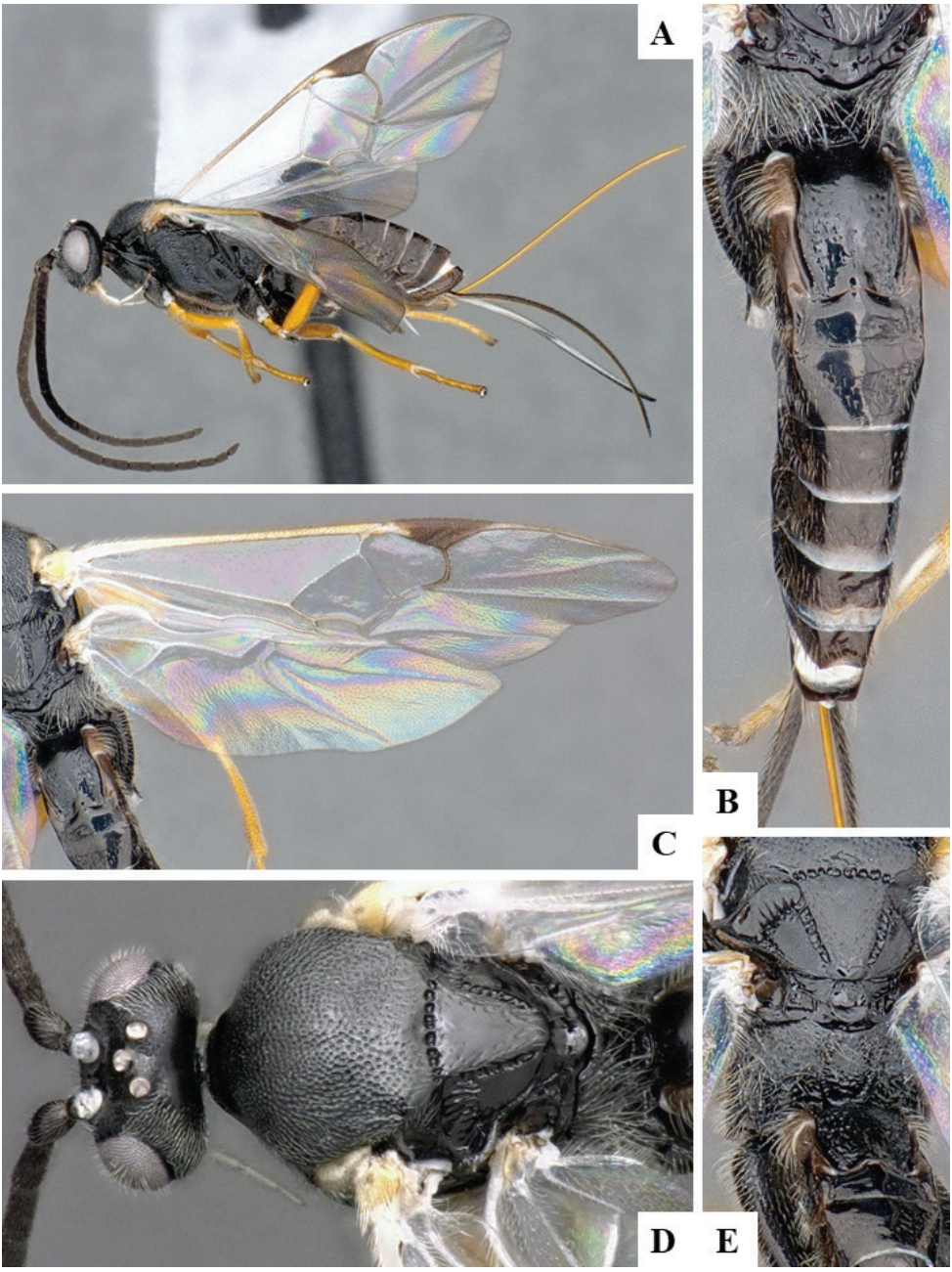

Figure 3. A–E *Dolichogenidea carlosmanuelrodriguezi* sp. n., holotype. **A** habitus, lateral **B** metasoma, dorsal **C** wings **D** head and mesosoma, dorsal **E** details of scutellar complex, propodeum and T1–T3.

Eye height: 0.42. Malar distance: 0.11. Mandible W: 0.11. Ocular ocellar line: 0.15. Posterior ocellar line: 0.12. Lateral ocellar line: 0.08. Scutellar disc L: 0.41. Scutellar disc W at anterior margin: 0.34. T1 L: 0.55. T1 W at anterior margin: 0.30. T1 W

at posterior margin: 0.30. T1 maximum width: 0.32. T2 L: 0.18. T2 W at anterior margin: 0.32. T2 W at posterior margin: 0.36. Pterostigma L: 0.69. Pterostigma W: 0.23. Fore wing vein R1 L: 0.88. Fore wing vein r L: 0.30. Fore wing vein 2RS L: 0.22.

Biology. Reared from *Antaeotricha spurca* (Zeller, 1855) (Depressariidae). This is the only species of *Dolichogenidea* known to parasitize that species of caterpillar in ACG, with four records out of 344 rearings.

Distribution. Costa Rica, ACG, Sector Santa Maria, 820 m. Rain forest ecosystem.

Molecular data. This species is represented in BOLD by four sequences which belong to BIN BOLD:ABZ4155. Interestingly, that BIN may contain more than *carlosmanuelrodriguezi*, as four other undescribed species (with interim names Janzen51, Janzen156, Janzen 251, and Janzen325) are also included within BOLD:ABZ4155. We have not been able to examine those specimens, and so while it is possible that they are all the same species, we doubt it owing to their different host records. Resolving this potential complex of cryptic species will require future examination of more specimens and is beyond the scope of the present paper.

Etymology. *Dolichogenidea carlosmanuelrodriguezi* is dedicated to Carlos Manuel Rodriguez of San Jose, Costa Rica, Minister of Environment & Energy (MINAE), in recognition of his life-long support of ACG and Costa Rican biodiversity conservation overall, as well as being today's Costa Rican representative for BioAlfa and other biodiversity conservation initiatives for the global Convention for Biological Diversity.

***Dolichogenidea genuarnunezi* Fernandez-Triana & Boudreault, sp. n.**
http://zoobank.org/6713B1B1-1337-4F01-A2EF-BC9F1FF5B1FC
Figs 4A–F; 13A

Holotype. Female, Costa Rica, CNC.

Holotype voucher code. DHJPAR0050092.

Holotype locality. Rio Blanco Abajo, 500 m, 10.90037N, -85.37254W, Sector San Cristobal, ACG, Alajuela province, Costa Rica.

Holotype verbatim labels. COSTA RICA: Alajuela, ACG, / Sector San Cristobal, / Rio Blanco Abajo, 500 m, / 10.90037N, -85.37254W, / 09/22/2012 / DHJPAR0050092.

Diagnosis. *Dolichogenidea genuarnunezi* can be recognized by its mesofemur mostly dark brown, comparatively narrower T1 (T1 L medially more than 2.0 × T1 posterior W), relatively more quadrate T2 (T2 posterior W 1.6 × T2 L medially) and host being Depressariidae. The mesofemur color would separate this species from *D. alejandromasisi* and *D. rogerblancoi*. However, *D. genuarnunezi* is very similar to *D. yeimycedenoae,* with only slight differences in pterostigma L/W ratio, as well as proportions of posterior ocellar line, lateral ocellus diameter and ocular ocellar line (see key above for details). The variation of those characters is very small, to the point that both species are very similar morphologically. However, they parasitize different host species, and also differ significantly molecularly (available DNA barcodes are 4.54% different). Additionally, the two species have been found at different altitudes.

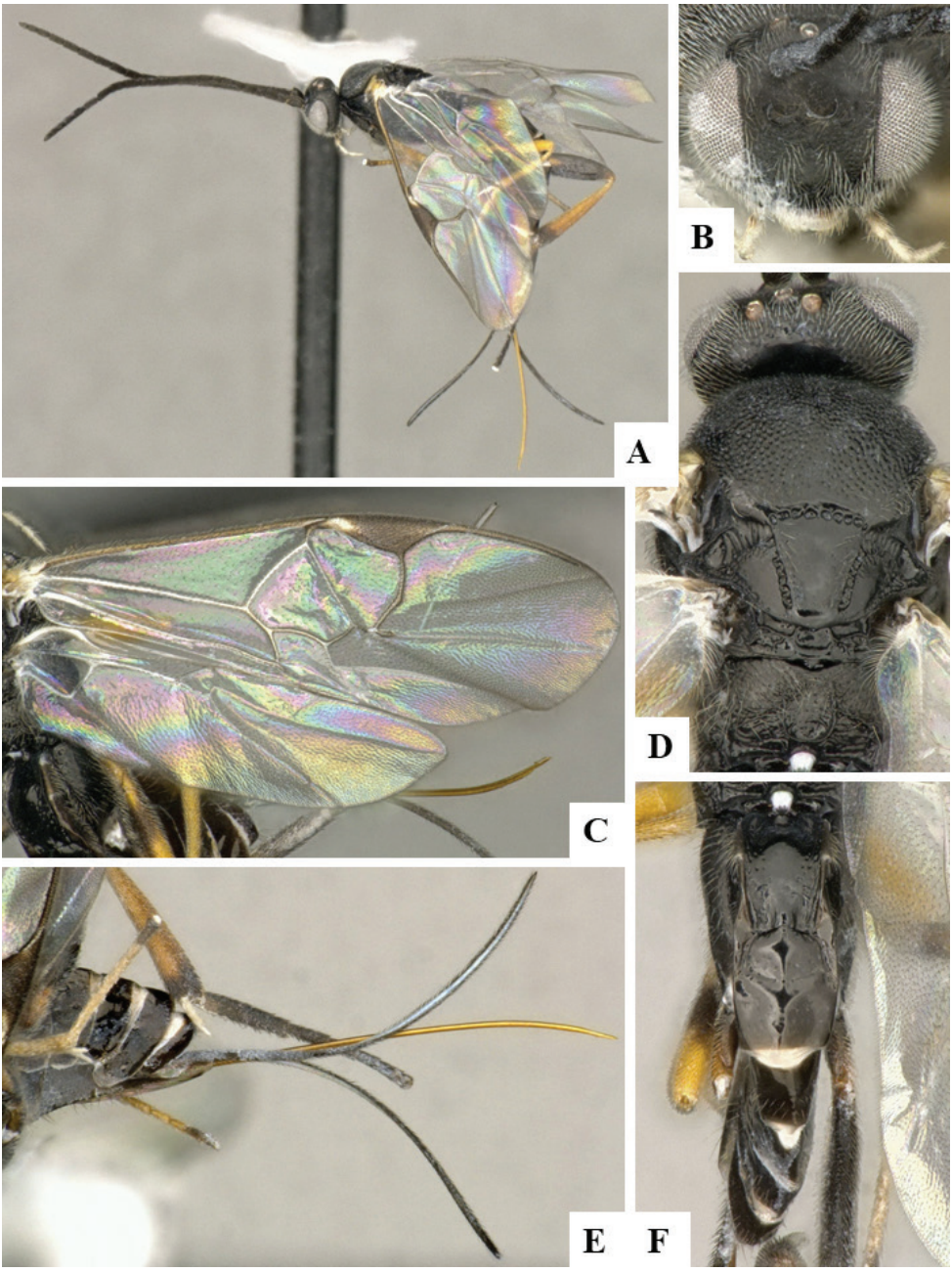

Figure 4.A–F *Dolichogenidea genuarnunezi* sp. n., holotype. **A** habitus, lateral **B** head, frontal **C** wings **D** head and mesosoma, dorsal **E** metasoma (partially), lateral **F** metasoma, dorsal.

Description. Body color: head and mesosoma black, metasoma black to dark brown; palpi, metatibial spines, tegula and most of humeral complex white-yellow; legs mostly orange-yellow, except for mesofemur and metafemur mostly brown, and

apical 0.1–0.2 of metatibia and metatarsus brown; wing venation mostly white or transparent, except for fore wing veins R1, r, 2RS and 2M which are brown, pterostigma mostly brown but with small light spot at base. Anteromesoscutum mostly with setae and sculptured with punctures that do not fuse with each other; scutoscutellar sulcus relatively wide and with relatively deep crenulae; scutellar disc smooth and unsculptured, with isolated setae; propodeum mostly setose and with scattered punctures; propodeum areola partially defined on posterior half by longitudinal carinae, transverse carinae partially defined; T1 mostly smooth, with shallow and sparse punctures along lateral margins; T2+ smooth. Body Length: 3.78. Fore wing L: 3.44. Ovipositor sheaths L: 2.74. F1 L: 0.27. F2 L: 0.28. F2 W: 0.09. F3 L: 0.28. F14 L: 0.13. F14 W: 0.07. F15 L: 0.12. F16 L: 0.15. Head height: 0.58. Head width: 0.77. Eye height: 0.39. Malar distance: 0.10. Mandible W: 0.10. Ocular ocellar line: 0.14. Posterior ocellar line: 0.12. Lateral ocellar line: 0.08. Scutellar disc L: 0.36. Scutellar disc W at anterior margin: 0.31. T1 L: 0.62. T1 W at anterior margin: 0.29. T1 W at posterior margin: 0.25. T1 maximum width: 0.32. T2 L: 0.21. T2 W at anterior margin: 0.22. T2 W at posterior margin: 0.33. Metafemur L: 0.96. Metafemur W: 0.26. Metatibia L: 1.22. Metatibial inner spur L: 0.32. Metatibial outer spur L: 0.20. Metatarsus first segment L: 0.64. Pterostigma L: 0.73. Pterostigma W: 0.24. Fore wing vein R1 L: 0.85. Fore wing vein r L: 0.27. Fore wing vein 2RS L: 0.22.

Biology. Reared from *Antaeotricha phaeoneura* (Meyrick, 1913) (Depressariidae). This is the only species of *Dolichogenidea* known to parasitize that species of caterpillar in ACG, with one record out of 25 rearings.

Distribution. Costa Rica, ACG, Sector San Cristobal, 500m. Rain forest ecosystem.

Molecular data. This species is represented in BOLD by one sequence belonging to BIN BOLD:ACC1300.

Etymology. *Dolichogenidea genuarnunezi* is dedicated to Genuar Roman Núñez Vega of Guadalupe, Costa Rica, in recognition of his dedication to supporting BioAlfa to render Costa Rica bioliterate, constructing CONAGEBIO as a biodiversity biodevelopment-friendly government agency, and constructing Costa Rica's Biodiversity Clearing House for COP14 of the Convention for Biological Diversity in October 2018.

Dolichogenidea josealfredohernandezi Fernandez-Triana & Boudreault, sp. n.

http://zoobank.org/6C5A5841-FC0E-4DC6-8793-D6F734F3D157
Figs 5A–F; 14A, B

Holotype. Female, Costa Rica, CNC.

Holotype voucher code. DHJPAR0049909.

Holotype locality. Sendero Anonas, 405 m, 10.90528N, -85.27882W, Sector Rincon Rain Forest, ACG, Alajuela province, Costa Rica.

Holotype verbatim labels. COSTA RICA: Alajuela, ACG, / Sector Rincon Rain Forest, / Sendero Anonas, 405 m, / 10.90528N, -85.27882W, / 08/04/2012 / DHJPAR0049909.

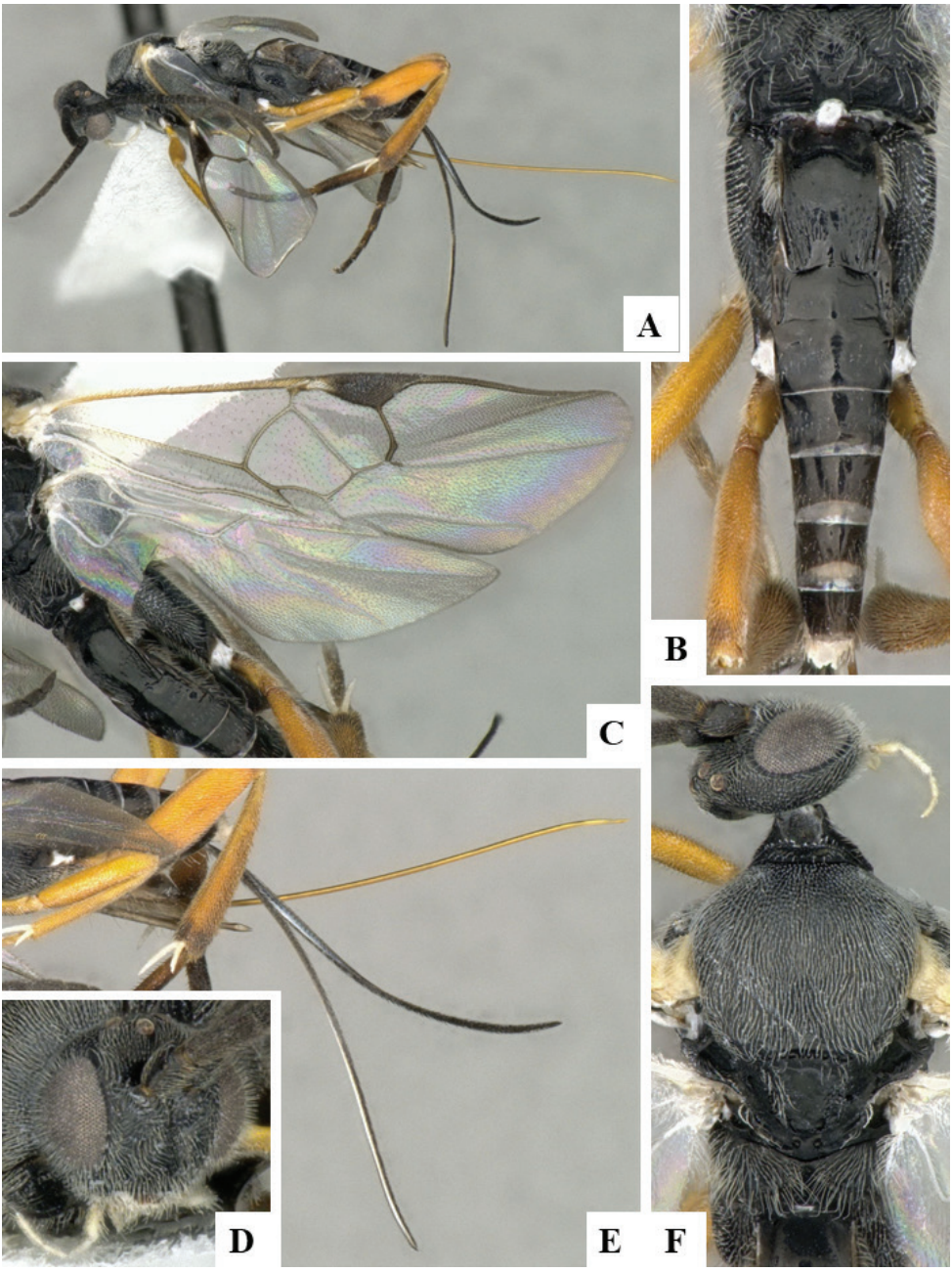

Figure 5. A–F *Dolichogenidea josealfredohernandezi* sp. n., holotype. **A** habitus, lateral **B** metasoma, dorsal **C** wings **D** head, dorsal **E** metasoma (partially), lateral **F** head and mesosoma, dorsal.

Paratype. One female (CNC). Vado Rio Francia, 400m, 10.90093 -85.28915, Sector Rincon Rain Forest, ACG, Alajuela province, Costa Rica Voucher code: DHJPAR0053856.

Diagnosis. *Dolichogenidea josealfredohernandezi* can be recognized by its legs almost entirely orange-yellow (except for small, dark spot on posterior 0.1–0.2 of metafemur). It is very similar to *D. carlosmanuelrodriguezi*, but the later species is slightly smaller and with a slightly less quadrate T2 (although the variation of those characters is very small, to the point that both species are almost indistinguishable morphologically). However, they parasitize different host species, in different genera, and they also differ in a total of 21 DNA barcode diagnostic characters. Additionally, the two species have been found at different altitudes.

Description. Body color: head and mesosoma black, metasoma black to dark brown; palpi, metatibial spines, tegula and most of humeral complex white-yellow; legs mostly orange-yellow, except for small, dark spot on posterior 0.1–0.2 of metafemur, and apical 0.1–0.2 of metatibia and metatarsus brown; wing venation mostly white or transparent, except for fore wing veins R1, r, 2RS and 2M which are brown, pterostigma mostly brown but with small light spot at base. Anteromesoscutum mostly with setae and sculptured with punctures that do not fuse with each other; scutoscutellar sulcus relatively wide and with relatively deep crenulae; scutellar disc smooth and unsculptured, with isolated setae; propodeum mostly setose and with scattered punctures; propodeum areola partially defined on posterior half by longitudinal carinae, transverse carinae partially defined; T1 mostly smooth, with shallow and sparse punctures along lateral margins; T2+ smooth. Body Length: 3.94 (3.92). Fore wing L: 3.72 (3.80). Ovipositor sheaths L: 2.88 (2.90). F1 L: 0.30 (0.32). F2 L: 0.30 (0.30). F2 W: 0.09 (0.10). F3 L: 0.29 (0.30). F14 L: 0.16 (0.18). F14 W: 0.07 (0.07). F15 L: 0.11 (0.13). F16 L: 0.13 (0.14). Head height: 0.60 (0.59). Head width: 0.80 (0.81). Eye height: 0.41 (0.41). Malar distance: 0.14 (0.11). Mandible W: 0.08 (0.11). Ocular ocellar line: 0.14 (0.15). Posterior ocellar line: 0.13 (0.13). Lateral ocellar line: 0.06 (0.08). Scutellar disc L: 0.36 (0.38). Scutellar disc W at anterior margin: 0.37 (0.39). T1 L: 0.62 (0.62). T1 W at anterior margin: 0.32 (0.31). T1 W at posterior margin: 0.32 (0.33). T1 maximum width: 0.37 (0.34). T2 L: 0.20 (0.22). T2 W at anterior margin: 0.29 (0.32). T2 W at posterior margin: 0.37 (0.40). Metafemur L: 1.04 (1.07). Metafemur W: 0.32 (0.33). Metatibia L: 1.32 (1.36). Metatibial inner spur L: 0.36 (0.36). Metatibial outer spur L: 0.22 (0.22). Metatarsus first segment L: 0.75 (0.81). Pterostigma L: 0.72 (0.72). Pterostigma W: 0.22 (0.23). Fore wing vein R1 L: 0.88 (0.93). Fore wing vein r L: 0.32 (0.23). Fore wing vein 2RS L: 0.18 (0.20).

Biology. Reared from *Stenoma* Janzen99 (Depressariidae). This is the only species of *Dolichogenidea* known to parasitize that species of caterpillar in ACG, with seven records out of 126 rearings.

Distribution. Costa Rica, ACG, Sector Rincon Rain Forest, 400m. Rain forest ecosystem.

Molecular data. This species is represented in BOLD by 5 sequences belonging to BIN BOLD:ABA9255.

Etymology. *Dolichogenidea josealfredohernandezi* is dedicated to José Alfredo Hernández of Alajuela, Costa Rica in recognition of his dedication to supporting Bio-Alfa to render Costa Rica bioliterate, representing CONAGEBIO and Costa Rican

membership in iBOL (=BioScan at http://ibol.org/site/), and supporting conservation biodevelopment of ACG.

Comments. *Dolichogenidea josealfredohernandezi* is very similar to *D. carlosmanuelrodriguezi* and we have not yet located a good morphological character to distinguish them. However, they parasitize quite different hosts on very different plants and their DNA barcodes are also very different (3.4% base pairs).

Dolichogenidea melaniamunozae **Fernandez-Triana & Boudreault, sp. n.**
http://zoobank.org/F26A45B1-A252-4D9D-AA3D-193EA513D9B9
Figs 6A–F; 15A, B

Holotype. Female, Costa Rica, CNC.

Holotype voucher code. DHJPAR0051857.

Holotype locality. Selva, 410 m, 10.92291N, -85.31877W, Sector Rincon Rain Forest, ACG, Alajuela province, Costa Rica.

Holotype verbatim labels. COSTA RICA: Alajuela, ACG, / Sector Rincon Rain Forest, / Selva, 410 m, 05/21/2012 / 10.92291N, -85.31877W, / DHJPAR0051857.

Paratypes. Six females (CNC), either from the same holotype locality or the following five localities, all in ACG, Sector Rincon Rain Forest, Alajuela province: 1) Finca Hugo, 540m, 10.88068N, -85.26968W; 2) Sendero Pila, 157 m, 10.93038N, -85.25682W; 3) Jacobo, 461 m, 10.94076N, -85.3177W; 4) Sendero Venado, 420m, 10.89678N, -85.27001W; 5) Estacion Llanura, 135 m, 10.93332N, -85.25331W. Voucher codes: DHJPAR0039738, DHJPAR0049295, DHJPAR0049431, DHJPAR0049474, DHJPAR0050153, DHJPAR0051842.

Diagnosis. This species can be recognized by its larger body size, fore wing L and ovipositor sheaths (as compared to all other described species in this group), and also because of its entirely black metatrochanter and metatrochantellus.

Description. Body color: head and mesosoma black, metasoma black to dark brown; palpi, metatibial spines, tegula and most of humeral complex white-yellow; legs mostly orange-yellow, except for mesofemur and metafemur mostly to entirely dark brown or black, and apical 0.3 of metatibia and metatarsus dark brown to black; wing venation mostly white or transparent, except for fore wing veins R1, r, 2RS and 2M which are brown, pterostigma mostly brown but with small light spot at base. Anteromesoscutum mostly with setae and sculptured with punctures that do not fuse with each other; scutoscutellar sulcus relatively wide and with relatively deep crenulae; scutellar disc smooth and unsculptured, with isolated setae; propodeum mostly setose and with scattered punctures; propodeum areola partially defined on posterior half by longitudinal carinae, transverse carinae partially defined; T1 mostly smooth, with shallow and sparse punctures along lateral margins; T2+ smooth. Body Length: 4.80 (4.48–4.90). Fore wing L: 4.80 (4.72–4.80). Ovipositor sheaths L: 3.44 (3.00–3.44). F1 L: 0.39 (0.37–0.40). F2 L: 0.37 (0.36–0.37). F2 W: 0.12 (0.10–0.12). F3 L: 0.36 (0.34–0.37). F14 L: 0.20 (0.18–0.20). F14 W: 0.08 (0.07).

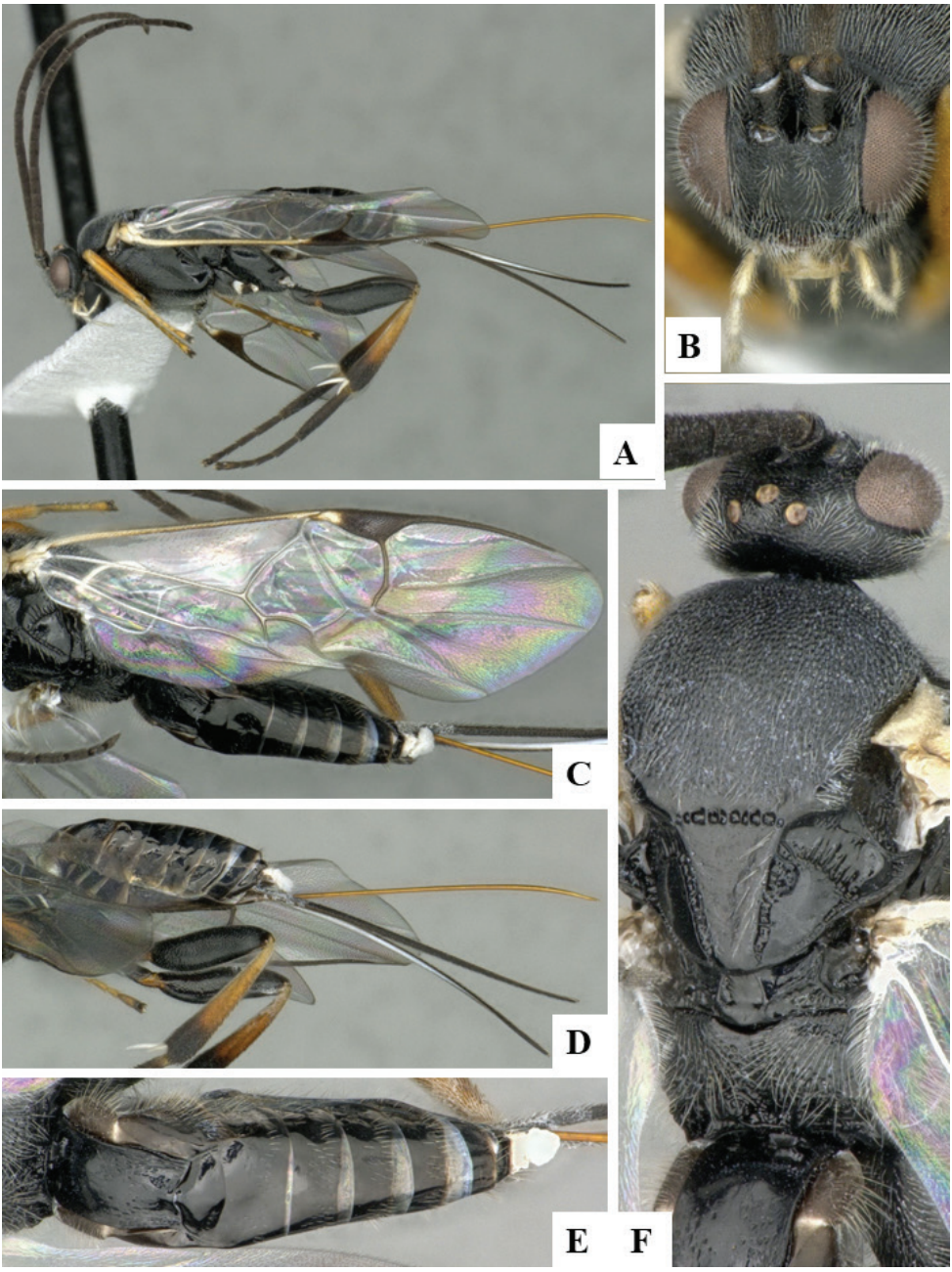

Figure 6. A–F *Dolichogenidea melaniamunozae* sp. n., holotype. **A** habitus, lateral **B** head, frontal; **C** wings **D** metasoma, lateral **E** metasoma, dorsal **F** head and mesosoma, dorsal.

F15 L: 0.13 (0.13–0.15). F16 L: 0.18 (0.15–0.17). Head height: 0.68 (0.67–0.69). Head width: 0.96 (0.92–0.96). Eye height: 0.48 (0.47–0.48). Malar distance: 0.10 (0.10–0.12). Mandible W: 0.12 (0.11–0.12). Ocular ocellar line: 0.17 (0.16–0.17).

Posterior ocellar line: 0.15 (0.15–0.17). Lateral ocellar line: 0.08 (0.08). Scutellar disc L: 0.53 (0.51–0.52). Scutellar disc W at anterior margin: 0.42 (0.42–0.43). T1 L: 0.69 (0.72–0.82). T1 W at anterior margin: 0.28 (0.37–0.45). T1 W at posterior margin: 0.41 (0.40–0.43). T1 maximum width: 0.46 (0.45–0.48). T2 L: 0.26 (0.21–0.26). T2 W at anterior margin: 0.43 (0.41–0.46). T2 W at posterior margin: 0.63 (0.43–0.61). Metafemur L: 1.25 (1.26–1.31). Metafemur W: 0.38 (0.37–0.40). Metatibia L: 1.60 (1.54–1.68). Metatibial inner spur L: 0.42 (0.40–0.45). Metatibial outer spur L: 0.25 (0.24–0.26). Metatarsus first segment L: 0.98 (0.93–0.98). Pterostigma L: 0.88 (0.86–0.89). Pterostigma W: 0.25 (0.26–0.28). Fore wing vein R1 L: 1.08 (0.99–1.05). Fore wing vein r L: 0.36 (0.33–0.39). Fore wing vein 2RS L: 0.22 (0.22–0.26).

Biology. Reared from *Cerconota recurvella* (Walker, 1864) (Depressariidae). This is the only species of *Dolichogenidea* known to parasitize that species of caterpillar in ACG, with 38 records out of 521 reared caterpillars of this species.

Distribution. Costa Rica, ACG, Sector Rincon Rain Forest, 135–540 m. Rain forest ecosystem.

Molecular data. This species is represented in BOLD by 35 sequences belonging to BIN BOLD:AAB5701.

Etymology. *Dolichogenidea melaniamunozae* is dedicated to Melania Muñoz García of San Jose, Costa Rica, in recognition of her dedication to the CONAGEBIO team of biodiversity administrators and her enthusiasm for understanding GDFCF (Guanacaste Dry Forest Conservation Fund) and ACG efforts to do conservation through biodiversity development.

Dolichogenidea rogerblancoi **Fernandez-Triana & Boudreault, sp. n.**
http://zoobank.org/D7E57262-3BAA-478F-B3CC-57B7F6E5E856
Figs 7A–F; 16A, B

Holotype. Female, Costa Rica, CNC.

Holotype voucher code. DHJPAR0049840.

Holotype locality. Finca Esmeralda, 123 m, 10.93548 -85.25314, Sector Rincon Rain Forest, ACG, Alajuela province, Costa Rica.

Holotype verbatim labels. COSTA RICA: Alajuela, / ACG, Sector Rincon Rain Forest, / Finca Esmeralda, 123 m, / 10.93548, -85.25314, / 06/24/2012 / DHJPAR0049840.

Paratypes. Twelve female and four male specimens (CNC), the pin where one of the male specimens is mounted also has a gel capsule with a few additional (unmounted) specimens. All paratypes either from the same holotype locality or from Sendero Carmona, 670m, 10.87621 -85.38632, Sector San Cristobal, Alajuela province. Voucher codes: DHJPAR0049206, DHJPAR0053702, DHJPAR0053756, 12–SRNP–75869, 12–SRNP–76060, 13–SRNP–4390.

Diagnosis. *Dolichogenidea rogerblancoi* can be recognized by its black to brown metafemur, comparatively narrower T1 (usually with T1 L medially 2.0–3.0 × T1 pos-

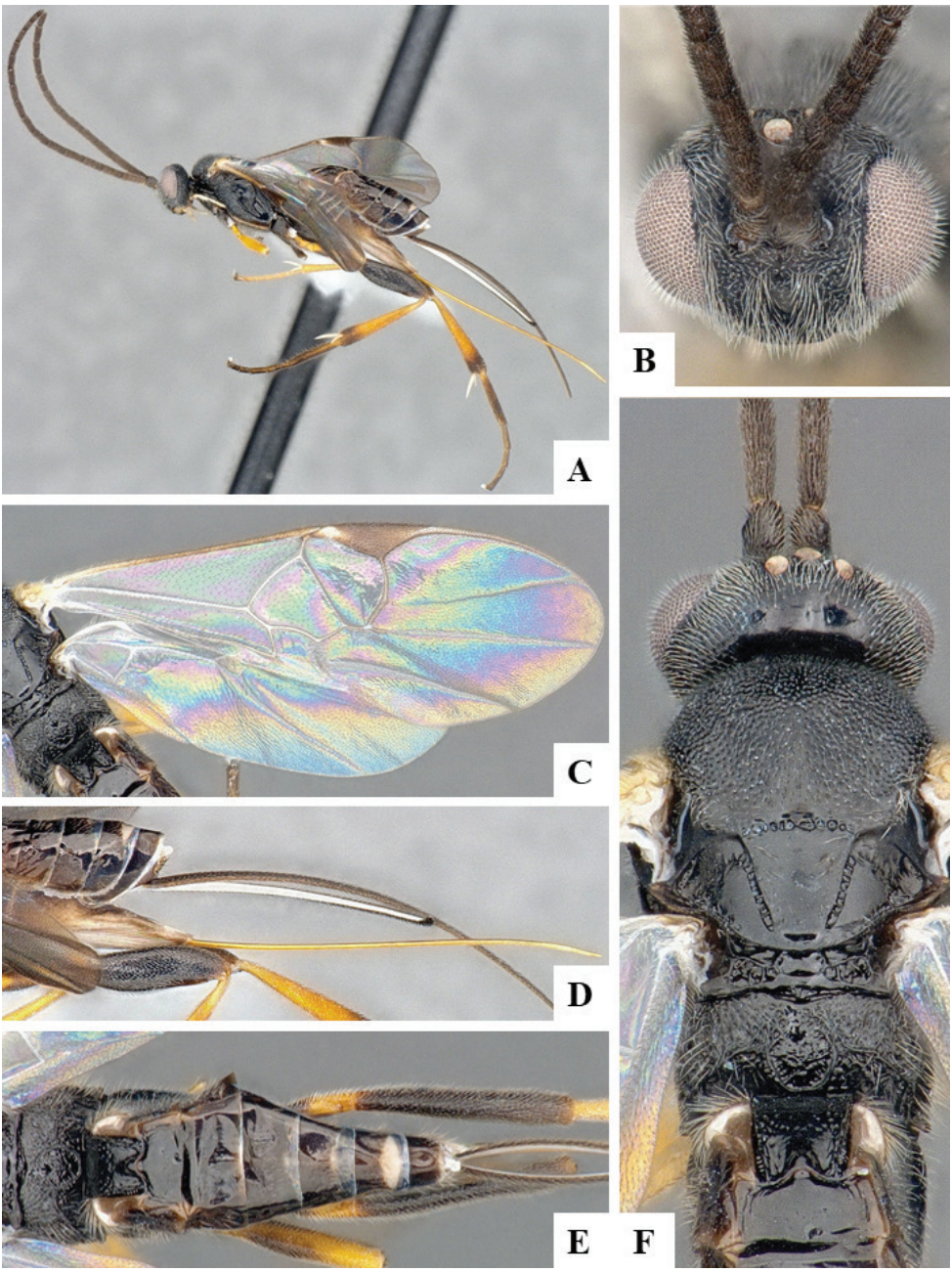

Figure 7. A–F *Dolichogenidea rogerblancoi* sp. n., holotype. **A** habitus, lateral **B** head, frontal **C** wings; **D** metasoma, lateral **E** metasoma, dorsal **F** head and mesosoma, dorsal.

terior W), more quadrate T2 (T2 posterior W 1.6–2.1 × T2 L medially) and host being Depressariidae. *D. alejandromasisi* shares those features and is very similar morphologically, but it differs from *rogerblancoi* by having longer F1 L, relatively more quadrate

T2 (T2 posterior W 1.3–1.9 × T2 L medially) and relatively narrower pterostigma. The two species parasitize different hosts (although in the same genus *Antaeotricha*), but *rogerblancoi* tends to be found at lower altitudes.

Description. Body color: head and mesosoma black, metasoma black to dark brown; palpi, metatibial spines, tegula and most of humeral complex white-yellow; legs mostly orange-yellow, except for mesofemur (with small dark brown spots), metafemur (mostly brown), and apical 0.1–0.2 of metatibia and metatarsus brown; wing venation mostly white or transparent, except for fore wing veins R1, r, 2RS and 2M which are light brown, pterostigma mostly brown but with small light spot at base. Anteromesoscutum mostly with setae and sculptured with punctures that do not fuse with each other; scutoscutellar sulcus relatively wide and with relatively deep crenulae; scutellar disc smooth and unsculptured, with isolated setae; propodeum mostly setose and with scattered punctures; propodeum areola partially defined on posterior half by longitudinal carinae, transverse carinae partially defined; T1 mostly smooth, with shallow and sparse punctures along lateral margins; T2+ smooth. Body L: 3.44 (2.73–3.84). Fore wing L: 3.41 (2.60–3.47). Ovipositor sheaths L: 2.94 (1.36–3.12). F1 L: 0.27 (0.18–0.29). F2 L: 0.26 (0.19–0.28). F2 W: 0.08 (0.06–0.08). F3 L: 0.26 (0.19–0.27). F14 L: 0.14 (0.10–0.14). F14 W: 0.06 (0.05–0.07). F15 L: 0.11 (0.08–0.12). F16 L: 0.14 (0.11–0.15). Head height: 0.58 (0.50–0.59). Head width: 0.77 (0.62–0.82). Eye height: 0.38 (0.32–0.40). Malar distance: 0.10 (0.09–0.12). Mandible W: 0.10 (0.08–0.11). Ocular ocellar line: 0.15 (0.13–0.15). Posterior ocellar line: 0.12 (0.10–0.12). Lateral ocellar line: 0.08 (0.05–0.08). Scutellar disc L: 0.34 (0.25–0.37). Scutellar disc W at anterior margin: 0.31 (0.20–0.29). T1 L: 0.65 (0.38–0.63). T1 W at anterior margin: 0.27 (0.22–0.32). T1 W at posterior margin: 0.26 (0.20–0.28). T1 maximum width: 0.28 (0.23–0.33). T2 L: 0.21 (0.14–0.22). T2 W at anterior margin: 0.27 (0.21–0.27). T2 W at posterior margin: 0.36 (0.29–0.38). Metafemur L: 0.98 (0.67–0.99). Metafemur W: 0.27 (0.17–0.27). Metatibia L: 1.22 (0.86–1.24). Metatibial inner spur L: 0.32 (0.22–0.34). Metatibial outer spur L: 0.18 (0.14–0.22). Metatarsus first segment L: 0.70 (0.48–0.73). Pterostigma L: 0.72 (0.54–0.71). Pterostigma W: 0.24 (0.19–0.25). Fore wing vein R1 L: 0.86 (0.68–0.88). Fore wing vein r L: 0.25 (0.17–0.26). Fore wing vein 2RS L: 0.20 (0.13–0.21).

Biology. Reared from *Antaeotricha* radicalisDHJ01 (Depressariidae). This is the only species of *Dolichogenidea* known to parasitize that species of caterpillar in ACG, with 24 records out of 243 reared caterpillars of this species. It does not parasitize any of the other ACG species of the "*Antaeotricha radicalis*" species complex.

Distribution. Costa Rica, ACG, Sectores San Cristobal & Rincon Rain Forest, 123–670 m. Rain forest ecosystem.

Molecular data. This species is represented in BOLD by 22 sequences belonging to BIN BOLD:AAL2325.

Etymology. *Dolichogenidea rogerblancoi* is dedicated to Roger Blanco Segura of Area de Conservación Guanacaste, co-coordinator of ACG Research & Subdirector of ACG Area Silvestre Protegido, in recognition of his many decades of protection and biodevelopment of the forests occupied by this wasp.

Dolichogenidea yeimycedenoae **Fernandez-Triana & Boudreault, sp. n.**
http://zoobank.org/4C86DA72-2C15-4B24-B266-D58D40548491
Figs 8A–F; 17A, B

Holotype. Female, Costa Rica, CNC.

Holotype voucher code. DHJPAR0054623.

Holotype locality. Sendero Orosilito, 900 m, 10.98332N, -85.43623W, Sector Pitilla, ACG, Guanacaste province, Costa Rica.

Holotype verbatim labels. COSTA RICA: Guanacaste, / ACG, Sector Pitilla, / Sendero Orosilito, 900 m, / 10.98332N, -85.43623W, / 11/06/2013 / 13–SRNP–31589.

Paratypes. Four females (CNC), the pin where one of the specimens is mounted also has a gel capsule with a few additional (unmounted) specimens. All paratypes either from the same holotype locality or from Jardin Estrada, 722 m, 10.86546N, -85.39694W, Sector San Cristobal, Alajuela province. Voucher codes: DHJPAR0054642, 13–SRNP–7638, 13–SRNP–31589.

Diagnosis. *Dolichogenidea yeimycedenoae* can be recognized by its mesofemur mostly dark brown, comparatively narrower T1 (T1 L medially more than 2.5 × T1 posterior W), relatively more quadrate T2 (T2 posterior W 1.5 × T2 L medially) and host being Depressariidae. The mesofemur color would separate this species from *D. alejandromasisi* and *D. rogerblancoi*. However, *D. yeimycedenoae* is very similar morphologically to *D. genuarnunezi,* with only slight differences in pterostigma L/W, as well as proportions of posterior ocellar line, lateral ocellus diameter and ocular ocellar line (see key above for details). The variation of those characters is very small, to the point that both species are very similar morphologically. However, they parasitize different host species, and also differ significantly molecularly (available DNA barcodes are 4.54% different). Additionally, the two species have been found at different altitudes.

Description. Body color: head and mesosoma black, metasoma black to dark brown; palpi, metatibial spines, tegula and most of humeral complex white-yellow; legs mostly orange-yellow, except for mesofemur and metafemur mostly brown, and apical 0.1–0.2 of metatibia and metatarsus brown; wing venation mostly white or transparent, except for fore wing veins R1, r, 2RS and 2M which are brown, pterostigma mostly brown but with small light spot at base. Anteromesoscutum mostly with setae and sculptured with punctures that do not fuse with each other; scutoscutellar sulcus relatively wide and with relatively deep crenulae; scutellar disc smooth and unsculptured, with isolated setae; propodeum mostly setose and with scattered punctures; propodeum areola partially defined on posterior half by longitudinal carinae, transverse carinae partially defined; T1 mostly smooth, with shallow and sparse punctures along lateral margins; T2+ smooth. Body Length: 3.96 (3.31–4.25). Fore wing L: 3.53 (3.44–3.75). Ovipositor sheaths L: 3.00 (2.28–3.19). F1 L: 0.28 (0.26–0.28). F2 L: 0.31 (0.28–.029). F2 W: 0.07 (0.07–0.08). F3 L: 0.27 (0.25–0.28). F14 L: 0.15 (0.12–0.17). F14 W: 0.06 (0.06–0.08). F15 L: 0.12 (0.10–0.12). F16 L: 0.16 (0.12–0.15). Head height: 0.58 (0.58–0.61). Head width: 0.77 (0.73–0.79). Eye height: 0.39 (0.36–0.39). Malar distance: 0.11 (0.09–0.11). Mandible W: 0.11 (0.08–0.12). Ocu-

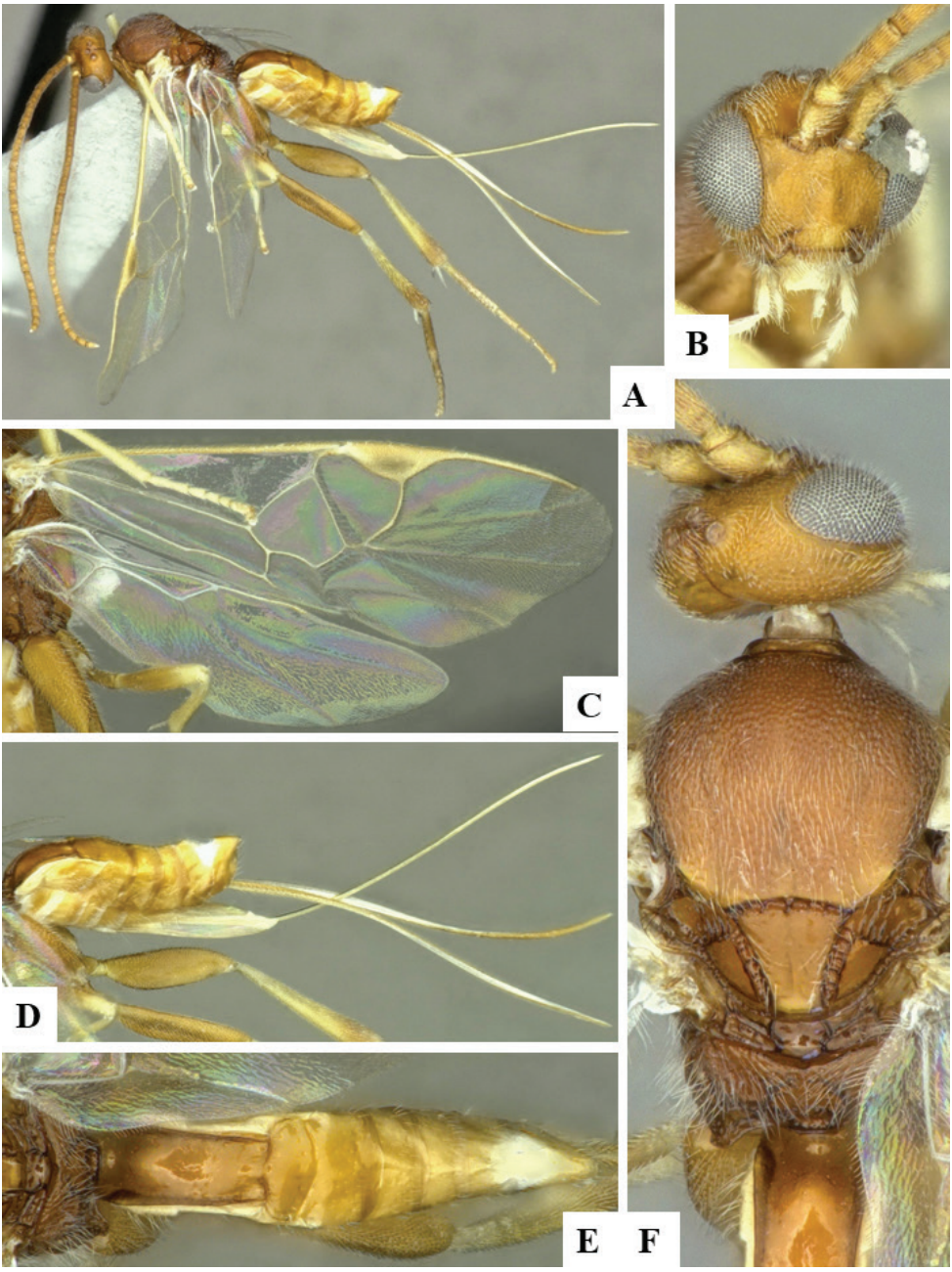

Figure 8.A–F *Dolichogenidea yeimycedenoae* sp. n., holotype. **A** habitus, lateral **B** head, frontal **C** wings **D** metasoma, lateral **E** metasoma, dorsal **F** head and mesosoma, dorsal.

lar ocellar line: 0.18 (0.17–0.18). Posterior ocellar line: 0.12 (0.13–0.14). Lateral ocellar line: 0.07 (0.07–0.08). Scutellar disc L: 0.35 (0.34–0.38). Scutellar disc W at anterior margin: 0.32 (0.28–0.32). T1 L: 0.60 (0.57–0.66). T1 W at anterior margin: 0.28

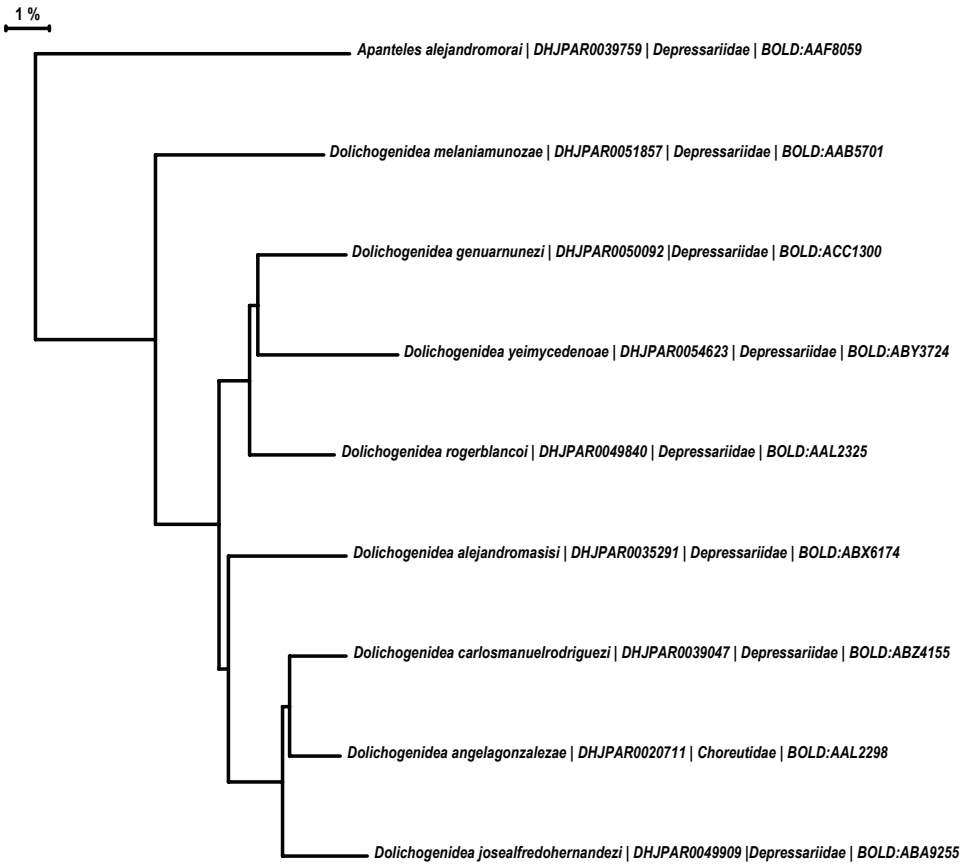

Figure 9. A neighbour-joining tree representing the interspecific variation in the DNA barcode region for the holotypes of the *Dolichogenidea* species described in this paper. The tree was built in MEGA X (Kumar et al. 2018) based on the K2P model (Kimura 1980). Tip labels are: Species name | Voucher code | Host family | BIN number in BOLD. The holotype of the morphologically similar, but genetically quite diverse, *Apanteles alejandromorai* Fernandez-Triana is included to demonstrate the large genetic divergence between the two genera (nearly 13%).

(0.29–0.30). T1 W at posterior margin: 0.22 (0.22–0.25). T1 maximum width: 0.27 (0.29–0.32). T2 L: 0.22 (0.18–0.21). T2 W at anterior margin: 0.31 (0.28–0.30). T2 W at posterior margin: 0.33 (0.34–0.38). Metafemur L: 1.05 (0.96–1.18). Metafemur W: 0.27 (0.25–0.31). Metatibia L: 1.25 (1.19–1.34). Metatibial inner spur L: 0.33 (0.31–0.32). Metatibial outer spur L: 0.17 (0.18–0.20). Metatarsus first segment L:

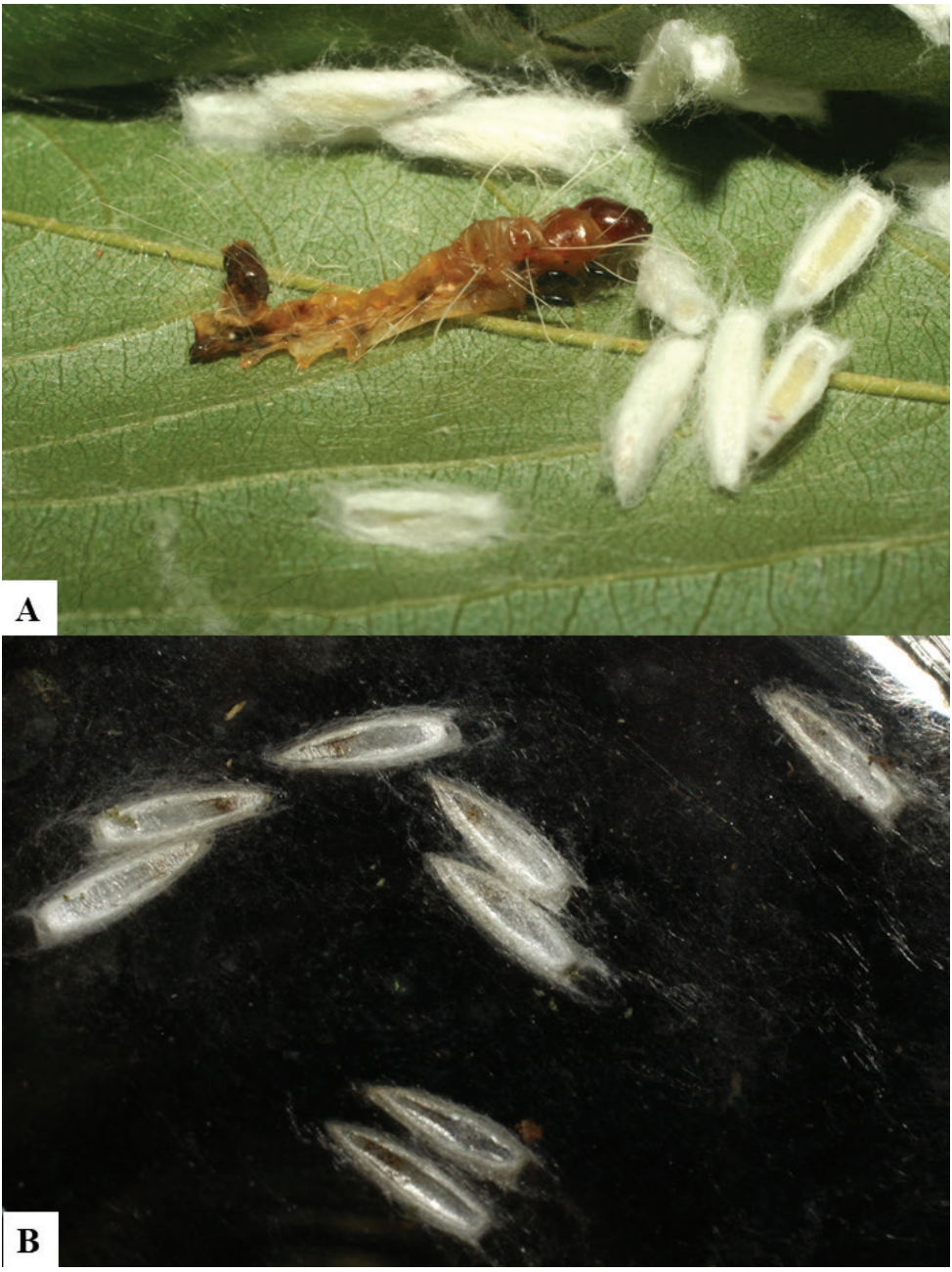

Figure 10. A, B Cocoons of *Dolichogenidea alejandromasisi* sp. n.

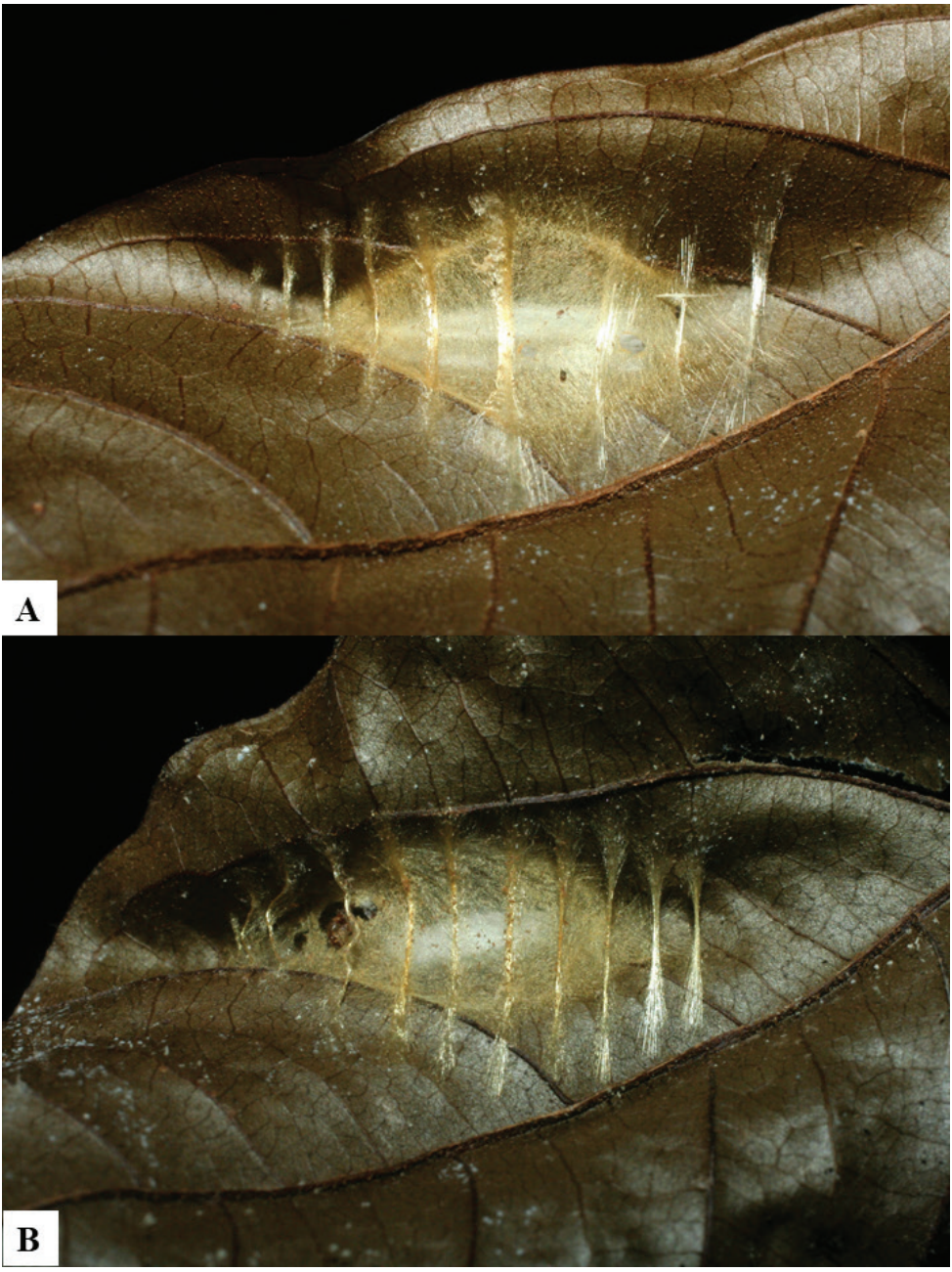

Figure 11.A, B Cocoons of *Dolichogenidea angelagonzalezae* sp. n.

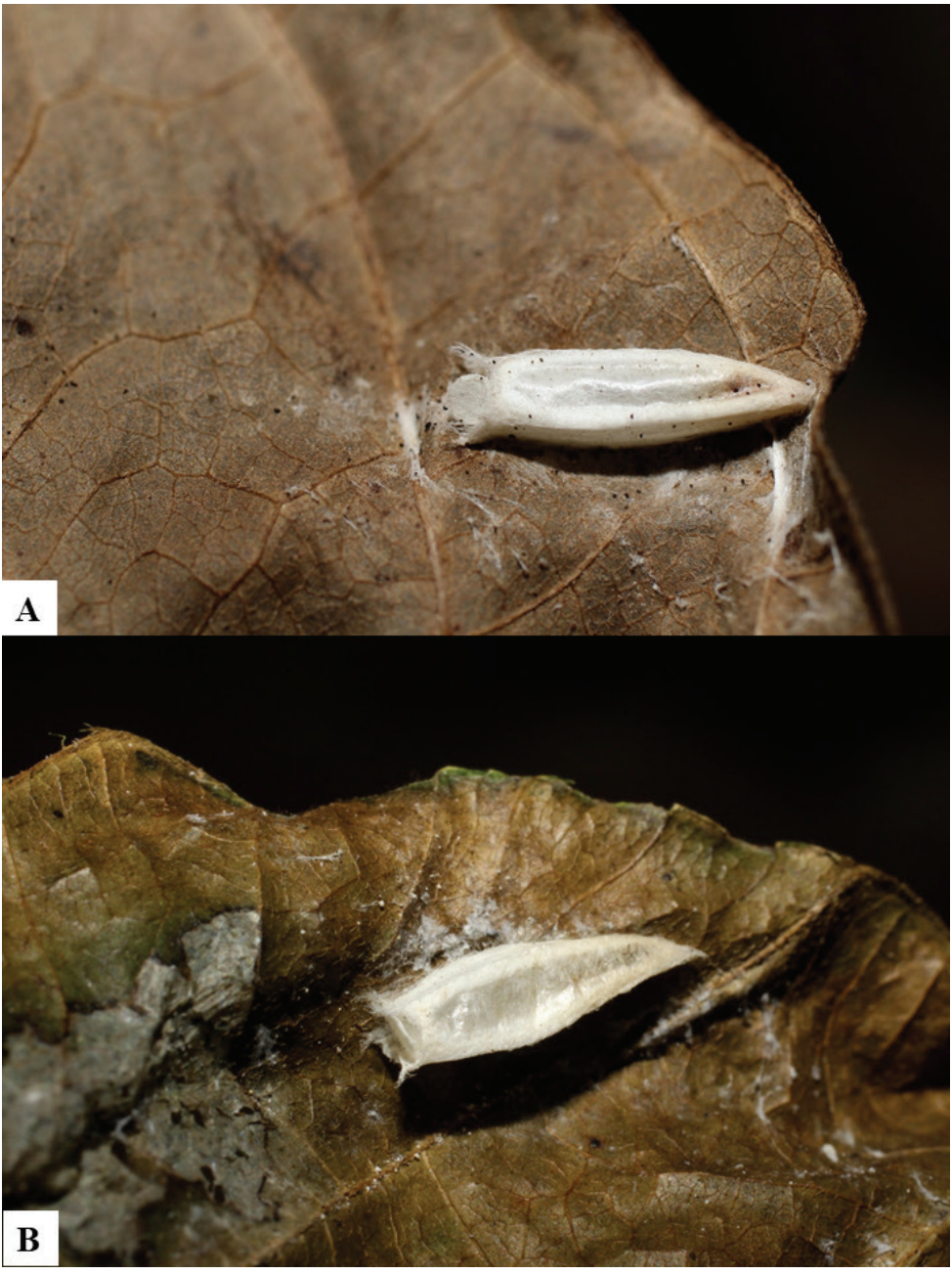

Figure 12. A, B Cocoons of *Dolichogenidea carlosmanuelrodriguezi* sp. n.

Figure 13.A Cocoons of *Dolichogenidea genuarnunezi* sp. n.

Figure 14. A, B Cocoons of *Dolichogenidea josealfredohernandezi* sp. n.

Figure 15. A, B Cocoons of *Dolichogenidea melaniamunozae* sp. n.

Figure 16. A, B Cocoons of *Dolichogenidea rogerblancoi* sp. n.

Figure 17. A, B Cocoons of *Dolichogenidea yeimycedenoae* sp. n.

0.76 (0.70–0.77). Pterostigma L: 0.70 (0.67–0.82). Pterostigma W: 0.22 (0.21–0.25). Fore wing vein R1 L: 0.88 (0.83–0.85). Fore wing vein r L: 0.28 (0.22–0.27). Fore wing vein 2RS L: 0.18 (0.17–0.21).

Biology. Reared from *Antaeotricha* Janzen126 (Depressariidae). This is the only species of *Dolichogenidea* known to parasitize that species of caterpillar in ACG, with one record out of three reared caterpillars of this species.

Distribution. Costa Rica, ACG, Sectores Pitilla & San Cristobal, 722–900 m. Rain forest ecosystem.

Molecular data. This species is represented in BOLD by 1 sequences belonging to BIN BOLD:ABY3724.

Etymology. *Dolichogenidea yeimycedenoi* is dedicated to Yeimy Cedeño Solis of Moravia & Ostional, Costa Rica, in recognition of her dedication to understanding and explaining the BioAlfa project to render Costa Rica bioliterate, to COP14 of the Convention for Biological Diversity in October 2018.

Comments. The holotype is a teneral specimen, and thus its coloration (as shown in Fig. 8, which contains only images of the holotype) is not the typical coloration found in the species (body mostly black to dark brown body). However, we still selected that specimen to be the holotype because the other available specimens are missing several legs and/or antennae, and also are mostly covered by dirt. The specimen we selected as the holotype, although having a much lighter coloration than the rest, is the best preserved from the series, is not missing any body part, and thus is the best choice to characterize the species (except for the body coloration, which anyways has no diagnostic value as all described species in the *Dolichogenidea carlosmanuelrodriguezi* group have the same black coloration).

Acknowledgments

We emphatically and gratefully acknowledge the support of the ACG parataxonomist team (Janzen & Hallwachs 2011) in finding and rearing these caterpillars, their parasites, and their hyperparasites, and Area de Conservación Guanacaste (ACG) for preserving the forests in which they live, and the Guanacaste Dry Forest Conservation Fund, the Wege Foundation, the International Conservation Fund of Canada, the JRS Biodiversity Foundation, Jessie Hill, Steve Stroud, Permian Global, and the University of Pennsylvania for funding portions of the research. This study was also supported by NSF DEB 0515699 to DHJ and by a Natural Sciences & Engineering Research Council of Canada (NSERC) Discovery Grants to MAS. Laboratory analyses of these sequences were funded by the Government of Canada through Genome Canada and the Ontario Genomics Institute (2008–0GI–ICI–03), and by BOLD/iBOL of the Centre for Biodiversity Genomics & University of Guelph. All authors are very thankful to the editor, reviewers, and copy editor (Kees van Achterberg, Erin Fagan-Jeffries, Nathalie Yonow, and an anonymous reviewer) for their very valuable suggestions that helped improving the manuscript.

References

Arias-Penna D, Whitfield J, Janzen D (2013) Three new species in the genus *Wilkinsonellus* (Braconidae, Microgastrinae) from the Neotropics, and the first host record for the genus. ZooKeys 302: 79–95. https://doi.org/10.3897/zookeys.302.4962

Fagan-Jeffries EP, Cooper SJB, Austin AD (2018) Three new species of Dolichogenidea Viereck (Hymenoptera, Braconidae, Microgastrinae) from Australia with exceptionally long ovipositors. Journal of Hymenoptera Research 64: 177–190. https://doi.org/10.3897/jhr.64.25219

Fernández-Triana J (2010) Eight new species and an annotated checklist of Microgastrinae (Hymenoptera: Braconidae) from Canada & Alaska. ZooKeys 63: 1–53. https://doi.org/10.3897/zookeys.63.565

Fernández-Triana J, Cardinal S, Whitfield J, Smith M, Janzen D (2013) A review of the New World species of the parasitoid wasp *Iconella* (Hymenoptera, Braconidae, Microgastrinae). ZooKeys 321: 65–87. https://doi.org/10.3897/zookeys.321.5160

Fernández-Triana J, Whitfield J, Rodriguez J, Smith M, Janzen D, Hajibabaei M, Burns J, Solis A, Brown J, Cardinal S, Goulet H, Hebert P (2014a) Review of *Apanteles sensu stricto* (Hymenoptera, Braconidae, Microgastrinae) from Area de Conservación Guanacaste, northwestern Costa Rica, with keys to all described species from Mesoamerica. ZooKeys 383: 1–565. https://doi.org/10.3897/zookeys.383.6418

Fernández-Triana J, Janzen D, Hallwachs W, Whitfield J, Smith M, Kula R (2014b) Revision of the genus *Pseudapanteles* (Hymenoptera, Braconidae, Microgastrinae), with emphasis on the species in Area de Conservación Guanacaste, northwestern Costa Rica. ZooKeys 446: 1–82. https://doi.org/10.3897/zookeys.446.8195

Fernández-Triana JL, Whitfield JB, Smith MA, Kula RR, Hallwachs W, Janzen DH (2015) Revision of the genera *Microplitis* & *Snellenius* (Hymenoptera, Braconidae, Microgastrinae) from Area de Conservacion Guanacaste, Costa Rica, with a key to all species previously described from Mesoamerica. Deutsche Entomologische Zeitschrift 62(2): 137–201. https://doi.org/10.3897/dez.62.5276

Fernández-Triana J, Boudreault C, Dapkey T, Smith MA, Rodriguez J, Hallwachs W, Janzen DH (2016) Revision of the genus *Promicrogaster* (Hymenoptera, Braconidae, Microgastrinae) from Area de Conservación Guanacaste, Costa Rica, with a key to all species previously described from Mesoamerica. Journal of Hymenoptera Research 50: 25–79. https://doi.org/10.3897/JHR.50.8220

Fleming AJ, Wood DM, Smith MA, Hallwachs W, Janzen DH (2018) Revision of the Mesoamerican species of *Calolydella* Townsend (Diptera: Tachinidae) and descriptions of twenty-three new species reared from caterpillars in Area de Conservación Guanacaste, northwestern Costa Rica. Biodiversity Data Journal 5, https://doi.org/10.3897/BDJ.6.e11223

Hansson C, Smith MA, Janzen DH, Hallwachs W (2015). Integrative taxonomy of New World *Euplectrus* Westwood (Hymenoptera, Eulophidae), with focus on 55 new species from Area de Conservacion Guanacaste, northwestern Costa Rica. ZooKeys 485: 1–236. https://doi.org/10.3897/zookeys.458.9124

Janzen DH, Hallwachs W (2011) Joining inventory by parataxonomists with DNA barcoding of a large complex tropical conserved wildland in northwestern Costa Rica. PLoS ONE 6(8): e18123. https://doi.org/10.1371/journal.pone.0018123

Janzen DH, Hallwachs W (2016) DNA barcoding the Lepidoptera inventory of a large complex tropical conserved wildland, Area de Conservacion Guanacaste, northwestern Costa Rica. Genome 59: 641–660 https://doi.org/10.1139/gen-2016-0005

Janzen DH, Burns JM, Cong Q, Hallwachs W, Dapkey T, Manjunath R, Hajibabaei M, Hebert PDN, Grishin NV (2017) Nuclear genomes distinguish cryptic species suggested by their DNA barcodes and ecology. Proceedings of the National Academy of Sciences 114(31): 8313–8318. https://doi.org/10.1073/pnas.1621504114

Kumar S, Stecher G, Li M, Knyaz C, Tamura K (2018) MEGA X: Molecular Evolutionary Genetics Analysis across Computing Platforms. Molecular biology and evolution 35(6): 1547–1549. https://doi.org/10.1093/molbev/msy096

Mason WRM (1981) The polyphyletic nature of *Apanteles* Foerster (Hymenoptera: Braconidae): A phylogeny and reclassification of Microgastrinae. Memoirs of the Entomological Society of Canada, Ottawa, Canada, 147 pp.

Sharkey M, Stoelb S, Tucker E, Janzen D, Dapkey T, Smith M (2011) *Lytopylus* Förster (Hymenoptera, Braconidae, Agathidinae) species from Costa Rica, with an emphasis on specimens reared from caterpillars in Area de Conservación Guanacaste. ZooKeys 130: 379–419. https://doi.org/10.3897/zookeys.130.1569

Sharkey MJ, Meierotto S, Chapman E, Janzen DH, Hallwachs W, Dapkey T, Solis MA (2018) *Alabagrus* Enderlein (Hymenoptera, Braconidae, Agathidinae) species of Costa Rica, with an emphasis on specimens reared from caterpillars in Area de Conservación Guanacaste. Contributions in Science of the Natural History Museum of Los Angeles 526: 31–180.

Smith MA, Rodriguez JJ, Whitfield JB, Deans AR, Janzen DH, Hallwachs W, Hebert PDN (2008) Extreme diversity of tropical parasitoid wasps exposed by iterative integration of natural history, DNA barcoding, morphology, and collections. Proceedings of the National Academy of Sciences 105 (34): 12359–12364. https://doi.org/10.1073/pnas.0805319105

Smith MA, Fernández-Triana JL, Eveleigh E, Gómez J, Guclu C, Hallwachs W, Hebert PDN, Hrcek J, Huber JT, Janzen DH, Mason PG, Miller SE, Quicke DLJ, Rodriguez JJ, Rougerie R, Shaw MR, Varkonyi G, Ward D, Whitfield JB, Zaldívar-Riverón A (2013) DNA barcoding and the taxonomy of Microgastrinae wasps (Hymenoptera, Braconidae): impacts after 8 years and nearly 20 000 sequences. Molecular Ecology Resources 13: 168–176. https://doi.org/10.1111/1755-0998.12038

Valerio AA, Whitfield JB, Janzen DH (2009) Review of world *Parapanteles* Ashmead (Hymenoptera: Braconidae: Microgastrinae), with description of fourteen new Neotropical species and the first description of the final instar larvae. Zootaxa 2084(1): 1–49.

Viereck HL (1911) Descriptions of six new genera and thirty-one new species of Ichneumon flies. Proceedings of the United States National Museum 40(1812): 173–196. https://doi.org/10.5479/si.00963801.1812.173

Whitfield JB (1997) Subfamily Microgastrinae. In: Wharton RA, Marsh PM, Sharkey MJ (Eds) Manual of the New World genera of the family Braconidae (Hymenoptera). Special Publication No. 1, International Society of Hymenopterists, Washington, DC, 333–364.

Whitfield J, Fernández-Triana J, Janzen D, Smith M, Cardinal S (2012) *Mariapanteles* (Hymenoptera, Braconidae), a new genus of Neotropical microgastrine parasitoid wasp discovered through biodiversity inventory. ZooKeys 208: 61–80. https://doi.org/10.3897/zookeys.208.3326

ZooKeys 835: 125–137 (2019)
doi: 10.3897/zookeys.835.32562
http://zookeys.pensoft.net

RESEARCH ARTICLE

A peer-reviewed open-access journal
ZooKeys
Launched to accelerate biodiversity research

Prognathodes geminus, a new species of butterflyfish (Teleostei, Chaetodontidae) from Palau

Joshua M. Copus[1], Richard L. Pyle[2], Brian D. Greene[3], John E. Randall[2]

1 *Hawai'i Institute of Marine Biology, 46-007 Lilipuna Road, Kāne'ohe, Hawai'i 96744, USA* **2** *Bernice Pauahi Bishop Museum, 1525 Bernice Street, Honolulu, Hawai'i 96817, USA* **3** *Association for Marine Exploration, 47-224 Kamehameha Highway, Kāne'ohe, Hawai'i 96744, USA*

Corresponding author: *Joshua M. Copus* (joshua.copus@gmail.com)

Academic editor: *D. Morgan* | Received 20 December 2018 | Accepted 5 March 2019 | Published 4 April 2019

http://zoobank.org/D71A7FBA-8539-47E2-9DF1-E0D8BFDA5005

Citation: Copus JM, Pyle RL, Greene BD, Randall JE (2019) *Prognathodes geminus*, a new species of butterflyfish (Teleostei, Chaetodontidae) from Palau. ZooKeys 835: 125–137. https://doi.org/10.3897/zookeys.835.32562

Abstract

A new species of the butterflyfish genus *Prognathodes* (Chaetodontidae) is described from two specimens collected at a depth of 116 m off Ngemelis Island, Palau. *Prognathodes geminus* **sp. n.** is similar to *P. basabei* Pyle & Kosaki, 2016 from the Hawaiian archipelago, and *P. guezei* (Maugé & Bauchot, 1976) from the western Indian Ocean, but differs from these species in the number of soft dorsal-fin rays, size of head, body width, and body depth. There are also subtle differences in life color, and substantial differences in the mtDNA cytochrome oxidase I sequence (d ≈ 0.08). Although genetic comparisons with *P. guezei* are unavailable, it is expected that the genetic divergence between *P. guezei* and *P. geminus* will be even greater than that between *P. geminus* and *P. basabei*. It is named for the strikingly similar color pattern it shares with *P. basabei*.

Keywords

Closed-circuit rebreather, Mesophotic Coral Ecosystem, Micronesia, systematic ichthyology

Introduction

The butterflyfish genus *Prognathodes* Gill, 1862 (type species *Chelmo pelta* Günther, 1860 = *Chaetodon aculeatus* Poey, 1860) currently includes twelve valid species: seven from the Atlantic [*P. aculeatus* (Poey, 1860), *P. aya* (Jordan, 1886), *P. brasiliensis* Burgess, 2001, *P. dichrous* (Günther, 1869), *P. guyanensis* (Durand, 1960), *P. marcellae* (Poll, 1950), and *P. obliquus* (Lubbock & Edwards, 1980)], two from the tropical eastern Pacific [*P. falcifer* (Hubbs & Rechnitzer, 1958), *P. carlhubbsi* Nalbant, 1995], one from the Hawaiian Islands [*P. basabei* Pyle & Kosaki, 2016], one from the central Indian Ocean and western Pacific [*P. guyotensis* (Yamamoto & Tameka, 1982)], and one from the western Indian Ocean [*P. guezei* (Maugé & Bauchot, 1976)], most of which are associated with deep coral-reef environments known as Mesophotic Coral Reef ecosystems (MCEs; 30–150 m; Hinderstein et al. 2010).

Several individuals of a butterflyfish with dark bars resembling both *P. guezei* from the Western Indian Ocean and a species from the Hawaiian Islands that was later described as *P. basabei* were recorded on video at depths in excess of 110 m during a series of submersible dives in Palau conducted by Patrick L Colin and Lori Bell Colin in 2001. In April 2007, while conducting a series of deep exploratory dives off Ngemelis Island, Palau (Republic of Belau) in the Caroline Islands, authors Pyle and Greene collected two specimens of this unidentified *Prognathodes* at a depth of 116 m. The fish were encountered among a patch of limestone rubble at the base of a prominent limestone outcropping.

Based on an examination of a combination of morphological and genetic characters of the Palauan specimens, in comparison to six specimens of *P. basabei* and two specimens of *P. guezei* (the two species that most closely resemble the Palauan specimens), we herein describe the new species as *Prognathodes geminus*.

Materials and methods

Two unknown fish of the genus *Prognathodes* were collected with hand nets during deep dives using mixed-gas, closed-circuit rebreathers off of Ngemelis Island (7.13791N, 134.22181E), at a depth of 116 m. In order to capture the live coloration, the specimens were brought to the surface alive, euthanized, and immediately photographed. A tissue sample was taken from each specimen prior to being placed in formalin. Methods of counts and measurements follow Pyle and Kosaki (2016).

Head length, depth of body, width of body, snout length, predorsal length, preanal length, length of dorsal-fin and anal-fin bases, orbit diameter, interorbital width, caudal peduncle depth, and lengths of fin spines and rays are expressed as percent of standard length (as SL). Counts and measurements for the paratype, if different from the holotype, are presented in parentheses after the value for the holotype.

The holotype has been deposited in the fish collection at the Bernice Pauahi Bishop Museum, Honolulu (**BPBM**), and the paratype has been deposited at the US National Museum of Natural History, Washington, DC (**USNM**).

Total genomic DNA was extracted using the 'HotSHOT' protocol (Meeker et al. 2007). A 533-base pair fragment of the mtDNA cytochrome c oxidase 1 (CO1) region was amplified using primers from Baldwin et al. (2009). Polymerase chain reaction (PCR) was performed in a 15 µl reaction containing 7.5 µl BioMix Red (Biolone Inc, Springfield, NJ, USA), 0.2 µM of each primer, 5–50 ng template DNA, and nanopure water (Thermo Scientific Barnstead, Dubuque, IA, USA) to volume. PCR cycling parameters were as follows: initial 95 °C denaturation for 10 min followed by 35 cycles of 94 °C for 30 sec, 55 °C for 30 sec, and 72 °C for 30 sec, followed by a final extension of 72 °C for 10 min. PCR products were visualized using a 1.5% agarose gel with GelStar (Cambrex Bio Science Rockland, Inc., Rockland, MA, USA) and then cleaned by incubating with 0.75 units of Exonuclease and 0.5 units of Shrimp Akaline Phosphate (ExoSAP; USB, Cleveland, OH, USA) per 7.5 µl of PCR product for 30 min. at 37 °C followed by 85 °C for 15 min. Sequencing was conducted in the forward and reverse direction using a genetic analyzer (ABI 3730XL, Applied Biosystems, Foster City, California) at the ASGPB Genomics Sequencing Facility at the University of Hawai'i at Mānoa. The sequences were aligned, edited and trimmed to a common length using Geneious Pro v.6.1.6 DNA analysis software (Biomatters. http://www.geneious.com/). CO1 haplotypes were deposited in GenBank and the Barcode of Life Database (BOLD).

Taxonomy

***Prognathodes geminus* sp. n.**
http://zoobank.org/BEAB3B7F-B4B1-44F7-8181-2FF950CA466A
Figures 1–3

Type Locality. Caroline Islands; Palau; Ngemelis Island, northwest side, "Blue Holes" (7.13791N, 134.22181E), 116 m.

Holotype. BPBM 40857, GenBank MG895424, Barcode of Life PROGE001-17, 73.1 mm SL, Caroline Islands; Palau; Ngemelis Island, northwest side, "Blue Holes", 7.13791N, 134.22181E; 27 April 2007; around limestone rock outcrop with limestone rubble; 116 m; hand nets; RL Pyle.

Paratype. USNM 440390, GenBank MG895423, Barcode of Life PROGE002-17, 1:70.0 mm SL, same location, habitat, collecting method, and date as holotype, BD Greene.

Diagnosis. A species of *Prognathodes* (sensu Smith et al. 2003) distinguished by the following combination of characters: dorsal-fin soft rays 17–19; anal-fin soft rays 15; head 2.48–2.49 in SL; body depth 1.71–1.76 in SL; pelvic-fin spine length 4.18–4.46 in SL; body color white with three broad dark brown bands, the first intersecting the eye.

Description. Dorsal fin XIII,17 (19), last soft ray branched to base; anal fin III,15, last soft ray branched to base; pectoral-fin rays 15; pelvic-fin rays I,5; principal

branched caudal rays 15; pored lateral-line scales 26 (27); scale rows above lateral line to origin of dorsal fin 11 (10); scale rows below lateral line to origin of anal fin 21 (20); gill rakers on upper limb 5 (6), on lower limb 10; vertebrae 24.

Body deep, depth 1.71 (1.76) in SL, and compressed, width 4.36 (3.2) in depth; head length 2.49 (2.48) in SL; snout produced, its length 2.37 (2.52) in head; orbit diameter 3.30 (3.53) in head; interorbital slightly convex, least bony width 4.59 (4.78) in head; least depth of caudal peduncle 4.59 (4.78) in head.

Mouth small, upper jaw 2.37 (2.52) in head, slightly diagonal, the gape forming an angle of about 20° to the horizontal, upper jaw slightly protruding; teeth in jaws densely setiform, longest 7.8 in orbit diameter; nostrils anterior to eye horizontally in line with center of iris, the anterior in a short membranous tube with a well-developed posterior flap, the posterior slightly larger, ovate, with a low fleshy rim. Lower edge of lacrimal smooth; margin of preopercle finely serrate; margins of other opercular bones smooth.

Lateral line forming a broad arc, ending below the base of third to fifth soft dorsal rays and within the second black band of the body. Scales ctenoid, moderately large on body except for chest and near origins of dorsal and anal fins, where small; head fully scaled except anterior portions of both jaws and around nostrils, scales on the head small; scales on fleshy sheath surrounding base of dorsal and anal fins moderately large anteriorly and proximally, reducing in size posteriorly and distally; scales on caudal peduncle and covering base of caudal fin small.

Origin of dorsal fin slightly anterior to upper end of gill opening, its base 1.5 (1.51) in SL; first dorsal-fin spine shortest, its length 4.03 in head; second dorsal-fin spine 1.85 (1.88),in head; fourth dorsal-fin spine longest, its length 1.18 (1.26) in head; third dorsal-fin spine nearly as long as fourth, its length 1.23(1.28) in head; fifth dorsal-fin spine shorter, its length 1.28 (1.29) in head; dorsal-fin spines progressively shorter posteriorly, the last 1.96 (1.89) in head; membranes between anterior dorsal-fin spines deeply incised, progressively less so posteriorly; first dorsal-fin soft ray the longest, approximately same length as last dorsal-fin spine, 1.87 (broken in paratype) in head, dorsal-fin soft rays progressively shorter posteriorly; first anal-fin spine shortest, its length 2.67 (2.56) in head; second anal-fin spine longest, its length 1.33 (1.38) in head; third anal-fin spine 1.44 (1.53) in head; first anal-fin soft ray longest, its length 1.40 (damaged in paratype) in head, anal-fin soft rays progressively shorter posteriorly; caudal fin damaged; pectoral fins damaged; pelvic spine 1.68 (1.8) in head; first soft ray of pelvic fin broken in both specimens.

Color in life as in Figures 1 and 2. Body white with three dark brown bands, the first beginning narrowly at origin of dorsal fin, curving slightly as it passes, mostly one-half eye diameter in width, to eye; second band originating at tips of third to fifth dorsal spines and basal half of fifth spine, crossing body ventrally, progressively narrower below lateral line to end on mid-abdomen one-half eye diameter in width; third dark brown band originating from outer third of eighth dorsal spine and tip of first two soft rays of fin, passing obliquely, equal in width, to lateral line, then narrowing to half that width at mid-base of soft portion of anal fin, and crossing

Figure 1. Holotype of *Prognathodes geminus* (BPBM 40857), collected at a depth of 116 m at Palau. Photograph by RL Pyle.

Figure 2. Paratype of *Prognathodes geminus* (USNM 440390), collected at a depth of 116 m at Palau. Photograph by RL Pyle.

fin to end on outer half of third anal spine; a yellowish brown bar, one-half eye diameter in average width (narrowing gradually to mid-peduncle depth), across caudal peduncle and base of caudal fin; remainder of caudal fin whitish; a yellowish brown band of pupil width passing obliquely from eye, narrowing on its anterior half, to end at tip of snout; eye silvery white with an oblique dark brown band in alignment with nape band across eye, the dorsal part half-pupil width, and the ventral part one-half that; opercular membrane bright yellow; margin of soft portion of anal fin dark yellowish brown, about pupil width on last rays and membranes, progressively narrower to first rays; a similar terminal margin on dorsal fin; pectoral fins translucent with a semicircular light gray bar at base, preceded on upper half by a bright yellow bar. about half-pupil diameter in width, in alignment with yellow margin of operculum; spine and first ray of pelvic fins white, the white continuing progressively shorter on remaining rays that are dark orange-yellow, the membranes translucent dark yellowish.

Color in alcohol similar to life color, except body a uniform dull yellow, bands dark brown, and orange areas pale brown.

Morphometric data for selected characters of type specimens are provided in Table 1.

Distribution. *Prognathodes geminus* is positively known only from Palau. However, individuals of what appear to be this species were collected by aquarium-fish collector Tim Bennett in the Coral Sea at a depth of 140 m (Fenton Walsh, pers. comm.), and video taken from a depth of about 120 m in New Caledonia (and reviewed by co-author Pyle) show what appears to be a similar fish. A similar species was recently described from the Hawaiian Islands (*P. basabei*), but numerous deep dives by the authors and others in regions between Palau and the Hawaiian Islands have not yielded any observations of this species, nor any other members of the genus *Prognathodes*.

Habitat. Type specimens and other individuals observed from submersible by Patrick L Colin (pers. comm.) in Palau were seen in association with limestone outcroppings on steep slopes at depths of 110–150 m. The type specimens were collected in an area with broken limestone rubble (Figure 3).

Etymology. We name this species *geminus*, Latin adjective for "twin", in reference to its similarity in color to *P. basabei* from the Hawaiian Islands.

Morphological comparisons

Prognathodes geminus appears to be most similar in color and morphology to *P. basabei* collected at similar depths in the Hawaiian Archipelago. These two species differ from each other in number of dorsal-fin soft rays (17–19 for *geminus*, compared to 21–22 for *basabei*) and anal-fin soft rays (15 compared to 16–17). *P. geminus* has a larger head (2.48–2.49 in SL, compared to 2.63–2.80 in SL), its body more elongate, the depth 1.71–1.76 in SL, compared to 1.58–1.69 for *P. basabei*, more slender, the width 7.46–7.95 in SL compared to 6.40–7.04, and a shorter pelvic-fin

Table 1. Morphometric and meristic data for selected characters of type specimens of *Prognathodes geminus*. Values of morphometric data (other than SL) are represented as % of SL.

Morphometrics	Holotype BPBM 40857	Paratype USNM 440390
Standard length (SL) in mm	73.1	70.1
Body depth	58	57
Body width	13	13
Head length	40	40
Snout length	16	17
Orbit diameter	12.2	11.4
Interorbital Width	9.0	8.0
Predorsal length	46	42
Preanal length	72	71
Base of dorsal fin	67	66
Base of anal fin	30	30
Caudal Peduncle Depth	8.8	8.4
Pelvic Spine	23.9	22.4
Pelvic Fin	–	–
First Dorsal Spine length	10	10
Second Dorsal Spine length	22	21
Third Dorsal Spine length	33	31
Fourth Dorsal Spine length	34	32
Fifth Dorsal Spine length	31	31
Last Dorsal Spine length	21	21
Longest Dorsal Ray length	21	–
First Anal Spine length	15	16
Second Anal Spine length	30	29
Third Anal Spine length	28	26
Longest anal ray length	29	–
Caudal fin length	–	–
Pectoral fin length	–	–
Meristics		
Dorsal Spines	XIII	XIII
Dorsal rays	17	19
Anal Spines	3	3
Anal Rays	15	15
Pectoral Rays	15	15
Caudal Rays	22	22
Pored lateral line scales	26	27
Dorsal scale rows	11	10
Ventral scale rows	21	20
Gill rakers	5+10	6+10

spine (4.18–4.46 in SL, compared to 3.63–4.07 in SL)[1] than the Palau species. The two species also differ in certain aspects of life color. The posterior edge of the first black band of *P. geminus* (Figures 1–3) ends at the origin of the first dorsal spine while it includes the first dorsal spine in *P. basabei* (Figure 4). The anterior edge of

1 Pyle and Kosaki (2016) incorrectly stated that the pelvic-fin spine of *P. basabei* was "shorter" than that of this species, although they correctly presented the corresponding proportional measurements.

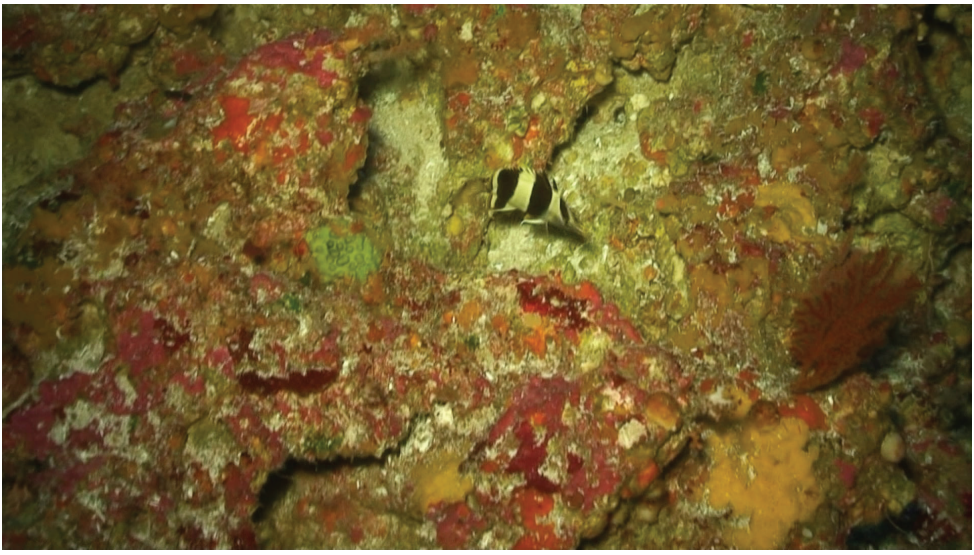

Figure 3. Holotype of *Prognathodes geminus* in its natural habitat at a depth of 116 m off Ngemelis, Palau. Photograph by JL Earle.

Figure 4. Holotype of *Prognathodes basabei* (BPBM 41290), collected at a depth of 61 m off Pearl and Hermes Atoll, northwestern Hawaiian islands. Photograph by RL Pyle.

Figure 5. *Prognathodes guezei* at a depth of 117 m off Sodwana Bay, South Africa. Photograph by RL Pyle.

the second black band of *P. geminus* originates at the third dorsal-fin spine, whereas this band originates on the fourth dorsal-fin spine in *P. basabei*. Moreover, both of the dark bands on *P. geminus* are proportionally broader dorsally, tapering more substantially ventrally than in *P. basabei*. Also, the pale areas between dark bands are white in *P. geminus*, but pale yellow in *P. basabei*, and the orangish coloration on the pelvic fins and posterior margin of the soft dorsal and anal fins of *P. geminus* are much darker (brownish) than in *P. basabei*.

Prognathodes geminus is also similar in color and morphology to *P. guezei* (Figure 5) from the western Indian Ocean. It differs from that species morphologically in number of dorsal-fin soft rays (17–19 for *geminus*, compared to 20 for *guezei*), body depth (1.71–1.76 in SL, compared to 1.87–1.95 in SL), and body width (7.46–7.95 in SL, compared to 7.16–7.27). There are also several differences in life color between the two species. In particular, *P. guezei* has more pronounced and discrete yellow bars on the body between the black bands, compared with more white in *P. geminus*. The two black bands on the body of *P. guezei* taper even more substantially than they do in the *P. geminus*. Also, the orangish coloration on the pelvic fins and posterior margin of the soft dorsal and anal fins of *P. guezei* are much paler and more yellowish than in *P. geminus*.

Genetic comparisons

A comparison of mtDNA COI sequences obtained from the holotype and paratype of *P. geminus* and from the holotype and two paratypes of *P. basabei* reveal 8% uncorrected sequence divergence, consistent with species-level divergences in other fish taxa (Johns and Avise 1998, Bowen et al. 2001, Bellwood et al. 2004, Fessler and Westneat 2007, Randall and Rocha 2009, Reece et al. 2010, Rocha 2004, Rocha et al. 2008). By contrast, the two specimens of *P. geminus* did not differ from each other genetically at COI, and the tree specimens of *P. basabei* differ only by 0.02%. While no tissue samples or DNA sequences have been reported for *P. guezei*, we expect that given the geographic distributions of *P. guezei* in the western Indian Ocean, and *P. geminus* and *P. basabei* in the Pacific Ocean, a much greater genetic divergence between *P. guezei* and the other two species likely exists.

Discussion

Mixed-gas closed-circuit rebreather diving technology has revolutionized the exploration of the deeper depths of coral reef environments across the globe (Pyle 1996, 2000). *Prognathodes geminus* is just one of many new fish species being discovered on MCEs and many more species are yet to be discovered and described. One of the more interesting aspects of this new species is the contrast between the strikingly similar color pattern it shares with *P. basabei*, against the substantial genetic differences. While genetic comparisons with *P. guezei* are not possible without appropriate tissue samples from that species, we expect that the genetic divergence between that species and *P. geminus* to be even greater than that between *P. geminus* and *P. basabei*. The disparity between the degree of difference in color relative to the genetic difference is striking in comparison to many species of butterflyfishes, which tend to have more substantial color differences relative to genetic differences (Hemingson et al. 2018).

Prognathodes geminus is the thirteenth member of the genus. Given the proclivity for species of this genus to inhabit relatively poorly explored MCEs, as well as the stark genetic differences between *P. basabei* and its closest known relative, it would not be unusual for other species of this genus to be discovered elsewhere throughout the tropical Indo-Pacific region. Indeed, video captured using a remotely operated vehicle at Rapa Nui (Easter Islands) reveals what appears to be another as-yet un-named species of banded *Prognathodes* inhabiting MCEs (Easton et al. 2017).

Acknowledgements

We are especially grateful to Fenton Walsh for providing us with images and information concerning populations of a similar species in the Coral Sea, to Patrick Colin for providing video footage of this species taken from a submersible in Palau, and to

John L Earle for providing the images of the holotype in its natural habitat. The type specimens were collected during an expedition funded by the British Broadcasting Corporation for the production of the documentary, *Pacific Abyss*. This work is Contribution No. 10655 of the University of Hawai'i School of Ocean and Earth Science and Technology and 1752 of the Hawai'i Institute of Marine Biology. This work was funded in part by the NSF OCE-15-58852.

References

Baldwin C, Mounts J, Smith D, Weigt L (2009) Genetic identification and color descriptions of early life-history stages of Belizean *Phaeoptyx* and *Astrapogon* (Teleostei: Apogonidae) with comments on identification of adult *Phaeoptyx*. Zootaxa 2008: 1–22.

Bellwood DR, van Herwerden L, Konow N (2004) Evolution and biogeography of marine angelfishes (Pisces: Pomacanthidae). Molecular Phylogenetics and Evolution 33: 140–155. https://doi.org/10.1016/j.ympev.2004.04.015

Bowen BW, Bass AL, Rocha LA, Grant WS, Robertson DR (2001) Phylogeography of the trumpetfish (*Aulostomus* spp.): ring species complex on a global scale. Evolution 55: 1029–1039. https://doi.org/10.1554/0014-3820(2001)055[1029:POTTAR]2.0.CO;2

Burgess WE (2001) *Prognathodes brasiliensis*, a new species of butterflyfish. Tropical Fish Hobbyist 49(6): 56–58, 60, 62–63.

Durand J (1960) Chaetodontidae (Poissons Téléostéens Percoidei) récoltés au large de la Guyane. Description d'une espèce nouvelle. Bulletin du Muséum national d'Histoire naturelle (Série 2) 32(3): 209–213.

Easton EE, Sellanes J, Gaymer CF, Morales N, Gorny M, Berkenpas E (2017) Diversity of deep-sea fishes of the Easter Island Ecoregion. Deep Sea Research Part II: Topical Studies in Oceanography 137: 78–88. https://doi.org/10.1016/j.dsr2.2016.12.006

Fessler JL, Westneat MW (2007) Molecular phylogenetics of the butterflyfishes (Chaetodontidae): Taxonomy and biogeography of a global coral reef fish family. Molecular Phylogenetics and Evolution 45: 50–68. https://doi.org/10.1016/j.ympev.2007.05.018

Gill TN (1862) Remarks on the relations of the genera and other groups of Cuban fishes. Proceedings of the Academy of Natural Sciences of Philadelphia 14: 235–242.

Günther A (1860) Catalogue of the fishes in the British Museum – Catalogue of the acanthopterygian fishes in the collection of the British Museum. Squamipinnes, Cirrhitidae, Triglidae, Trachinidae, Sciaenidae, Polynemidae, Sphyraenidae, Trichiuridae, Scombridae, Carangidae, Xiphiidae (Vol. 2). British Museum, London, 548 pp.

Günther A (1869) Report of a second collection of fishes made at St. Helena by JC Melliss, Esq. Proceedings of the Zoological Society of London 1869 (pt 2) (art. 4) (for 8 Apr. 1869): 238–239. [pl. 16]

Hemingson CR, Cowman PF, Hodge JR, Bellwood DR (2018) Colour pattern divergence in reef fish species is rapid and driven by both range overlap and symmetry. Ecology letters 22(1): 190–199. https://doi.org/10.1111/ele.13180

Hinderstein LM, Marr JCA, Martinez FA, Dowgiallo MJ, Puglise KA, Pyle RL, Zawada DG, Appeldoorn R (2010) Mesophotic coral ecosystems: characterization, ecology, and management. Coral Reefs 29: 247–251. https://doi.org/10.1007/s00338-010-0614-5

Hubbs CL, Rechnitzer AB (1958) A new fish, *Chaetodon falcifer*, from Guadalupe Island, Baja California, with notes on related species. Proceedings of the California Academy of Sciences (Series 4) 29: 273–313. [3 pls]

Johns GC, Avise JC (1998) A comparative summary of genetic distances in the vertebrates from the mitochondrial cytochrome *b* gene. Molecular Biology and Evolution 15: 1481–1490. https://doi.org/10.1093/oxfordjournals.molbev.a025875

Jordan DS (1886) Notes on some fishes collected at Pensacola by Mr. Silas Stearns, with descriptions of one new species (*Chaetodon aya*). Proceedings of the United States National Museum 9(565): 225–229. https://doi.org/10.5479/si.00963801.9-565.225

Lubbock R, Edwards AJ (1980) A new butterflyfish (Teleostei: Chaetodontidae) of the genus *Chaetodon* from Saint Paul's Rocks. Revue française d'Aquariologie Herpétologie 7(1): 13–16.

Maugé LA, Bauchot, R (1976) Une espèce nouvelle de Chétodon de l'océan Indien occidental: *Chaetodon guezei* (Pisces : Chaetodontidae). Bulletin du Muséum national d'Histoire naturelle (3)355: 89–101.

Meeker N, Hutchinson S, Ho L, Trede N (2007) Method for isolation of PCR-ready genomic DNA from zebrafish tissues. BioTechniques 43(5): 610–614. https://doi.org/10.2144/000112619

Nalbant G (1995) The genus *Prognathodes* (Pisces: Chaetodontidae) in eastern Pacific Ocean (Baja California – Galapagos) with discussion on the phylogeny of the group. Travaux du Muséum d'Histoire Naturelle 'Grigore Antipa' 35: 497–526.

Poey F (1860) Memorias sobra la historia natural de la Isla de Cuba, acompañadas de sumarios Latinos y extractos en Francés, Tomo 2. La Habana 2: 97–336.

Poll M (1950) Description de deux poissons percomorphes nouveaux des eaux côtières Aafricaines de l'Atlantique Sud (1948-1949). Bulletin de l'Institut Royal des Sciences Naturelles de Belgique 26(49): 1–14.

Pyle RL (1996) Exploring deep coral reefs: How much coral reef biodiversity are we missing? Global Biodiversity 6: 3–7.

Pyle RL (2000) Assessing undiscovered fish biodiversity on deep coral reefs using advanced self-contained diving technology. Marine Technology Society Journal 34: 82–91. https://doi.org/10.4031/MTSJ.34.4.11

Pyle RL, Kosaki RK (2016). *Prognathodes basabei*, a new species of butterflyfish (Perciformes, Chaetodontidae) from the Hawaiian Archipelago. ZooKeys 614: 137–152. https://doi.org/10.3897/zookeys.614.10200

Randall JE, Rocha LA (2009) *Chaetodontoplus poliourus*, A new angelfish (Perciformes: Pomacanthidae) from the tropical western Atlantic. The Raffles Bulletin of Zoology 57(2): 511–520. http://lkcnhm.nus.edu.sg/nus/pdf/PUBLICATION/Raffles%20Bulletin%20of%20Zoology/Past%20Volumes/RBZ%2057(2)/57rbz511-520.pdf

Reece JS, Bowen BW, Smith DG, Larson AF (2010) Molecular phylogenetics of moray eels (Muraenidae) demonstrates multiple origins of a shell-crushing jaw (*Gymnomuraena*, *Echidna*)

and multiple colonizations of the Atlantic Ocean. Molecular Phylogenetics and Evolution 57: 829–835. https://doi.org/10.1016/j.ympev.2010.07.013

Rocha LA (2004) Mitochondrial DNA and color pattern variation in three western Atlantic *Halichoeres* (Labridae), with the revalidation of two species. Copeia 4: 770–782. https://doi.org/10.1643/CG-04-106

Rocha LA, Lindeman KC, Rocha CR, Lessios HA (2008) Historical biogeography and speciation in the reef fish genus *Haemulon* (Teleostei: Haemulidae). Molecular Phylogenetics and Evolution 48: 91–928. https://doi.org/10.1016/j.ympev.2008.05.024

Smith WL, Webb JL, Blum SD (2003) The evolution of the laterophysic connection with a revised phylogeny and taxonomy of butterflyfishes (Teleostei: Chaetodontidae). Cladistics 19(2003): 287–306. https://doi.org/10.1111/j.1096-0031.2003.tb00374.x

Yamamoto E, Tameka S (1982) In: Okamura O, Amaoka K, Mitani F (Eds) Fishes of the Kyushu-Palau Ridge and Tosa Bay. The intensive research of unexploited fishery resources on continental slopes. Japan Fisheries Resource Conservation Association, Tokyo, 249 pp. [pl. 171]

ZooKeys 835: 139–152 (2019)
doi: 10.3897/zookeys.835.32697
http://zookeys.pensoft.net

RESEARCH ARTICLE

A peer-reviewed open-access journal
ZooKeys
Launched to accelerate biodiversity research

A taxonomic note on the helicoid land snail genus *Traumatophora* (Eupulmonata, Camaenidae)

Min Wu[1]

1 *School of Life Sciences, Nanjing University, Xianlindadao 163, Qixia, Nanjing 210023, China*

Corresponding author: *Min Wu* (minwu1969@aliyun.com)

Academic editor: *M. Haase* | Received 27 December 2018 | Accepted 7 March 2019 | Published 5 April 2019

http://zoobank.org/F1A0E68D-DB99-4162-B720-45D31465CA00

Citation: Wu M (2019) A taxonomic note on the helicoid land snail genus *Traumatophora* (Eupulmonata, Camaenidae). ZooKeys 835: 139–152. https://doi.org/10.3897/zookeys.835.32697

Abstract

Traumatophora triscalpta (Martens, 1875) is reported for the first time from the Tianmushan Mountains, Zhejiang Province, and its morpho-anatomy is described based on this new material. The genus *Traumatophora* is redefined on the basis of both shell and genital anatomy of its type species. The presence of the dart apparatus suggests this genus belongs to the subfamily Bradybaeninae rather than to the Camaeninae. This genus is distinguished from all other Chinese bradybaenine genera by the combination of the following key morphological characteristics: embryonic shell smooth, palatal teeth present, dart sac tiny with rounded proximal accessory sac that opens into a dart sac chamber, mucous glands well developed, entering an accessory sac through a papilla, epiphallic papilla absent, flagellum present. A comparison is also presented of Chinese bradybaenine genera with known terminal genitalia.

摘 要 本文首次从浙江省天目山报道了三痕刨螺 *Traumatophora triscalpta* (Martens, 1875)。基于贝壳和生殖系统解剖，对刨螺属*Traumatophora*进行了修订。恋矢器官在刨螺属中出现，表明刨螺属归属于巴蜗牛亚科而非坚螺亚科。刨螺属以其鉴别特征“胚螺层光滑。壳口腭具齿。矢囊极小。具极发达的开口于矢囊腔的球状基副矢囊 (proximal accessory sac)。粘液腺亦极发达；通过粘液腺乳突进入副矢囊。成荚器乳突阙如。具鞭状体”，可很好地区别于其他所有巴蜗牛亚科中生殖系统端部解剖结构已知的属。本文亦对已知生殖系统端部解剖结构的中国巴蜗牛亚科各类群进行了比较。

Keywords

Bradybaeninae, Camaeninae, China, distribution, *Traumatophora*, Zhejiang

Introduction

Camaenidae Pilsbry, 1895 (Bouchet et al. 2017) is a helicoid land snail family mainly distributed in Asia, Australia and some Pacific islands (Solem 1992, Schileyko 2003). In China, members of the Camaeninae (i.e., taxa lacking stimulatory organs; Wade et al. 2006, 2007; Hirano et al. 2014) are distributed south of the Qingling Mountains on the mainland, and on Taiwan and Hainan Island. They are grouped into eleven genera, namely *Camaena* Albers, 1850, *Amphidromus* Albers, 1850, *Ganesella* Blanford, 1863, *Satsuma* A. Adams, 1868, *Stegodera* Martens, 1876, *Traumatophora* Ancey, 1887, *Trichelix* Ancey, 1887, *Moellendorffia* Ancey, 1887, *Trichochloritis* Pilsbry, 1891, *Camaenella* Pilsbry, 1893 and *Moellendorffiella* Pilsbry, 1905 (Pilsbry 1890, 1894; Yen 1939; Chang 1989; Schileyko 2003; Wu et al. 2008; Du et al. 2013). Among them, only the genera *Camaena*, *Camaenella*, *Moellendorffia*, *Trichelix* and *Satsuma* have been defined by genital features (Chang 1989, Solem 1992, Azuma 1995, Schileyko 2003, Wu et al. 2008). In comparison to the genera in the Bradybaeninae which have a dart apparatus as a rule, the dart apparatus-absent camaenine genera of China share the following characteristics: dart sac absent; both an epiphallic papilla and flagellum present; and penial retractor muscle inserting on epiphallus.

In this paper, the genus *Traumatophora*, previously assigned to the Camaenidae (= Camaeninae sensu Bouchet et al. 2017), is reported from Zhejiang for the first time. Based on shell morphology, the genus *Traumatophora* is thought by some authors to be near the genus *Stegodera* (Ancey 1887, Schmacker and Boettger 1894). The genital anatomy, newly revealed in this work, suggests that this genus rather belongs to the subfamily Bradybaeninae.

Materials and methods

A living specimen was relaxed by drowning in water before being transferred to 70% ethanol for fixation, which was replaced with ethanol of the same concentration after three days. The shell and genitalia were measured with digital vernier callipers (genitalia from photo) to the nearest 0.1 mm. Whorl number was recorded as described by Kerney and Cameron (1979), with 0.125 whorl accuracy. Soft parts were measured after the specimens were sufficiently fixed in 70% ethanol. Directions used in descriptions: proximal = towards the genital atrium; distal = away from the genital atrium.

Abbreviations: AS – accessory sac; At – atrium; BC – bursa copulatrix; BCD – bursa copulatrix duct; DS – dart sac; DVM – membranous sac surrounding terminal genitalia; Ep – epiphallus; Fl – flagellum; FO – free oviduct; HBUMM – mollusc collection of the Museum of Hebei University, Baoding, China; MG – mucous glands/number of mucous gland duct; MGP – papilla distally leading to mucous glands on inner wall of accessory sac; P – penis; PAS – proximal accessory sac, a blind sac on proximal dart sac and opening into dart sac chamber or not; PLs – poly-layered structure in dart sac and/or accessory sac, produced by wavy and spongy connective tissue; PR – penial retractor muscle; PS – penis sheath; Va – vagina; VD – vas deferens; ZMB/Moll – Museum für Naturkunde, Berlin-Malakologie.

Systematics

Helicoidea Rafinesque, 1815
Camaenidae Pilsbry, 1895
Bradybaeninae Pilsbry, 1898

Traumatophora Ancey, 1887

Traumatophora Ancey, 1887: 54; Pilsbry 1890: 6; Pilsbry 1894: 145–146, subgenus of *Plectopylis* Benson, 1860; Schmacker and Boettger 1894: 173, subgenus of *Stegodera* Martens, 1876; Yen 1939: 125; Schileyko 2003: 1512–1513.

Type species. *Helix triscalpta* Martens, 1875; original designation.

Diagnosis. Embryonic shell smooth. Palatal teeth present. Dart sac tiny. A ball-shaped proximal accessory sac with opening leading to dart sac chamber. Mucous glands numerous; developed; entering accessory sac by a papilla. Epiphallic papilla absent. Flagellum present.

Description. Shell depressed; solid; with approximately five moderately convex whorls. Last whorl descending behind aperture. Embryonic whorls smooth. Aperture oblique; with three palatal lamellar teeth. Outer surface of body whorl with longitudinal depressions corresponding to teeth. Aperture margins reflexed. Umbilicus moderately broad (Schileyko 2003, slightly altered).

Membranous sac surrounding terminal genitalia absent. Penis sheath absent. Epiphallic papilla wanting. Penial caecum absent. Flagellum present. Dart sac tiny. Accessory sac developed; large; with transversal sphincter muscles. Mucous glands numerous; extremely developed; entering accessory sac by a papilla. A ball-shaped proximal accessory sac with opening leading to dart sac chamber. Poly-layered structure in dart apparatus absent (this study).

Distribution. S China (extant range: Jiangxi, Hubei, Fujian and Zhejiang; Pleistocene: Jiangsu).

Remarks. The genus *Traumatophora* is transferred herein to the subfamily Bradybaeninae based on the presence of a dart apparatus that is structurally similar to that of other genera in this subfamily. Features typical of the genus include presence of a penis sheath, flagellum, accessory and proximal accessory sac, mucous gland papilla and the absence of an epiphallic papilla, penial caecum, poly-layered structure, and a membranous sac surrounding the terminal genitalia; on this basis the genus *Traumatophora* is well distinguished from all the other anatomically known Chinese bradybaenine genera [Table 1; note: at transition of the penis-epiphallus in *Acusta* (Wu 2004: fig. 18E), *Laeocathaica* (Wu 2004: fig. B), *Eueuhadra* (Wu 2004: figs 7B, 7E) and *Aegistohadra* (Wu 2004: fig. 6C), the structures once called an "epiphallic papilla" are too invisibly tiny (especially compared with those in *Pfeifferia* Gray, 1853, *Pliocathaica* Andreae, 1900, etc.) to a true epiphallic papilla. Anatomy information of *Armandiella* Ancey, 1883 comes from *A. sarelii* (Martens, 1867) (HBUMM01113 specimen-3, collection information lost)]. However, until now detailed information on the anatomy of the

Table 1. Comparison of characteristics of terminal genitalia among Chinese bradybaenine genera (Chang 1990; Wu 2001a, 2001b; Wu and Guo 2003; Schileyko 2004; Wu 2004; Wu and Guo 2006; Wu and Prozorova 2006; Wu and Asami 2017; Páll-Gergely et al. 2018; * this study). AS–accessory sac; DVM–membranous sac surrounding terminal genitalia; EpP–epiphallus papilla; Fl–flagellum; MG–number of mucous gland ducts; MGP–papilla distally leading to mucous glands on inner wall of accessory sac; PAS–proximal accessory sac, a blind sac on proximal dart sac and opening into dart sac chamber or not; PC--penial caecum; PLs--poly-layered structure in dart sac and/or accessory sac, produced by wavy and spongy connective tissue; PS–penis sheath.

	PS	EpP	PC	Fl	PLs	DVM	AS	PAS	MG	MGP
Acusta Martens, 1860	●	○	○	○	○	○	●	○	2	●
Aegista Albers, 1850	●	●	○	●	●	○	●	○	2	○
Aegistohadra Wu, 2004	○	○	●	●	○	○	●	?	2	○
Armandiella Ancey, 1883*	●	○	○	○	○	●	●	○	2	○
Bradybaena Beck, 1837	●	○	○	○	●	●	○	○	2	○
Cathaica Möllendorff, 1884	●	○	○	○	●	○	●	○	>2	○
Coccoglypta Pilsbry, 1895	○	?	○	○	?	○	●	○	2	?
Dolicheulota Pilsbry, 1901	●	●	○	●	?	○	●	○	>2	?
Eueuhadra Wu, 2004	○	○	●	●	○	○	●	○	>2	○
Euhadra Pilsbry, 1890	●	●	○	●	○	□	●	○	>2	□
Karaftohelix Pilsbry, 1927	●	○	○	○	○	●	●	○	>2	○
Laeocathaica Möllendorff, 1899	●	○	○	○	○	○	●	□	>2	○
Landouria Godwin-Austen, 1918	○	●	○	●	N/A	N/A	N/A	N/A	N/A	N/A
Mastigeulota Pilsbry, 1895	●	○	●	○	●	○	●	○	>2	○
Mesasiata Schileyko, 1978	●	○	○	○	○	○	●	○	>2	○
Metodontia Möllendorff, 1886	●	○	○	○	●	○	○	○	2	○
Nesiohelix Kuroda & Emura, 1943	○	○	□	●	○	○	●	○	>2	●
Pancala Kuroda & Habe, 1949	○	?	○	●	N/A	N/A	N/A	N/A	N/A	N/A
Plectotropis Martens, 1860	●	●	○	●	●	○	●	○	2	○
Pliocathaica Andreae, 1900	●	●	○	○	○	○	●	○	>2	○
Ponsadenia Schileyko, 1978	●	○	○	○	○	○	●	○	1	○
Pseudaspasita Möllendorff, 1901	●	?	○	●	●	○	●	○	2	○
Pseudiberus Ancey, 1887	●	○	○	○	○	○	○	●	>2	○
Pseudobuliminus Gredler, 1886	●	○	○	○	○	●	○	○	2	○
Stilpnodiscus Möllendorff, 1899	●	○	○	○	○	○	●	□	≥2	○
Traumatophora Ancey, 1887*	●	○	○	●	○	○	●	●	>2	●
Trichobradybaena Wu, 2003	●	○	●	○	○	●	●	○	2	○
Trichocathaica Gude, 1919	●	○	○	○	?	●	●	○	>2	?
Yakuchloritis Habe, 1955	○	?	○	●	N/A	N/A	N/A	N/A	N/A	N/A

● –present, ○ –absent, □ –present or not, ? –unknown, N/A –not applicable

terminal genitalia of the following genera Chinese endemic genera still remains unknown: *Campylocathaica* Andreae, 1900 and *Xerocathaica* Andreae, 1900.

Traumatophora triscalpta **(Martens, 1875)**

Figs 1–6

Helix triscalpta Martens, 1875a: 2; Martens 1875b: 185–186; Heude 1882: 35–36, pl. 15, figs 7, 7a, 7b; Gredler 1884: 137; Möllendorff 1884: 388.

Helix (*Traumatophora*) *triscalpta* Pilsbry 1890: 6, 8, pl. 1, figs 1–8.
Stegodera (*Traumatophora*) *triscalpta* Schmacker and Boettger 1894: 173.
Traumatophora triscalpta Yen 1939: 126, pl. 13, fig. 7; Yen 1942: 271–272; Yen 1943: 297; Schileyko 2003: 1512, fig. 1949.

Material examined. *Helix triscalpta* von Martens, 1875, syntypes, ZMB/Moll-109875; Poyang-Yu (Lake Poyang), Kiangsi Province, China; 3 dried shells (major diameter of three shells: 31.0 mm, 30.5 mm, 26.3 mm. Measurement made by Christine Zorn); leg. von Martens. Tianmushan, Zhejiang Province, China; 1 fully matured empty shell (HBUMM06875 specimen-1) and 1 full matured animal (HBUMM06875 specimen-2, body whorl was partially removed to take out whole soft parts), May, 2016; coll. Zhou, Dakang (Beijing Botanical Garden). A piece of foot of HBUMM06875 specimen-2 was cut off and preserved in 99.7% alcohol at –20 °C.

Description. Shell (Figs 2, 3). Clearly depressed; thick and solid; dextral. Whorls convex. Suture impressed. Umbilicus approximately one fifth of shell major diameter. Bottom-umbilicus transition changed gently. Columella oblique. Columellar lip only slightly covering umbilicus. Protoconch smooth. On teleconch spiral furrows absent. Aperture strongly oblique; not sinuate at peristome. Body whorl descending abruptly

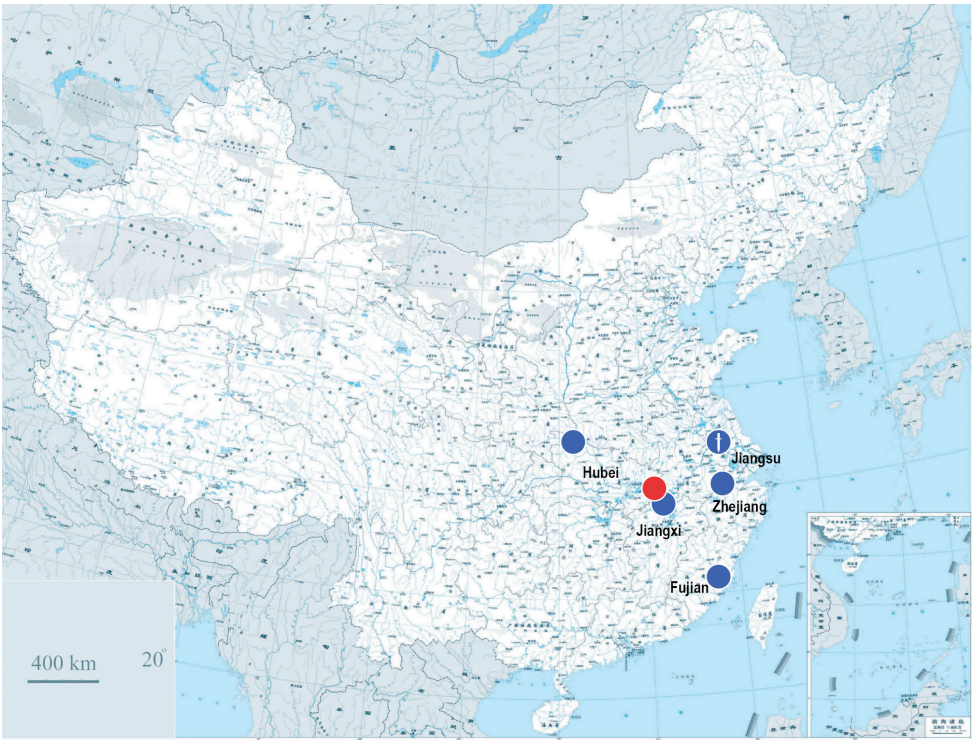

Figure 1. Known occurrence records of *Traumatophora* spp. Blue dots: *Traumatophora triscalpta* (Martens, 1875), fossil locality with sword mark; red dot: *T. fraterminor* (Gredler, 1884).

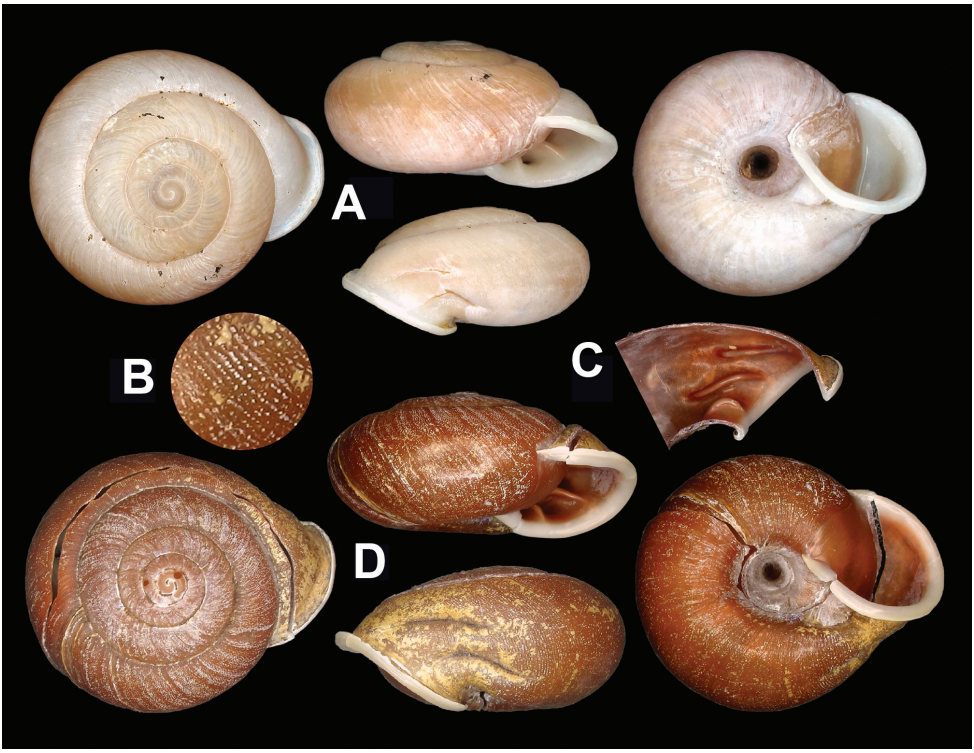

Figure 2. *Traumatophora triscalpta* (Martens, 1875). **A** HBUMM08236-specimen 1, shell **B** magnified shell surface, magnified showing growth lines breaking into granules **C** palatal part of body whorl, showing lamellar teeth **D** shell **B–D** HBUMM06875 specimen-2.

in front. Shell surface without ribs. Growth lines fine and broken into granules which are distributed evenly on whorls except on protoconch (Fig. 2B); not accompanied by irregular thickenings. Shell not perforated. Adult shell not hairy or scaly. Adult body whorl rounded at periphery; with bottom convex. Ring-like thickening within aperture absent. Aperture with three baso-palatal lamellar teeth (Figs 2C, 3A–C). Palatal tooth near columella shortest, approximately half length of other two teeth. Outer surface of body whorl with longitudinal depressions corresponding to teeth (Figs 2A, D, 3A–C). Peristome thin; white; narrowly and uniformly reflexed. Callus indistinct. Shell dull to somewhat glossy; uniformly in reddish brown; bandless. Measurements (HBUMM06875, n = 2): shell height 17.8–18.2 mm, shell breadth 35.4–37.2 mm, aperture height 10.4–11.0 mm, aperture width 16.6–17.5 mm, embryonic shell whorls 1.250–1.500, whorls 5.000–5.125, shell height/ breadth ratio 0.20–0.22.

General anatomy. Eversible head wart between ommatophore insertions absent. Tentacles and dorsum leaden-black. Sole and the remaining lower lateral side creamy white. Jaw arcuate; with 12 more or less projecting ribs (Fig. 4C).

Genitalia (Figs 4–6). A sheet of membrane (in Fig. 4A, the remnant membrane after dissection is arrowed), growing on oviducts and tightly connected with vas deferens, wrapping dart apparatus completely. Penis sheath very short; only restrictedly present near

Figure 3. *Helix triscalpta* von Martens, 1875 **A–C** syntypes, ZMB/Moll-109875; China, Province Kiangsi: Poyang-Yu (Lake Poyang); 3 dried shells; leg.: von Martens. The largest shell has a major diameter 31.0 mm.

insertion on dart sac. Penis very short; moderately thick; externally simple. Penial retractor muscle inserting on penis-epiphallus transition. Epiphallus as thick as the most swollen part of penis; approximately two times longer than penis. Flagellum approximately three times longer than penis; tapering. Epiphallic papilla absent. Penis internally with four pilasters. Penial pilasters uniformly-spaced; thickest at two thirds of their entire length distally (Fig. 5B). Dart sac tiny (Fig. 5D). Dart in dart sac not observed (maybe lost or regenerating) in HBUMM06875 specimen-2. Accessory sac developed; large in size; interiorly with pilasters; transversally with developed sphincter muscles (Figs 5E, 6A, B). Mucous glands nine; extending distally to more than half of bursa copulatrix duct (longest in the subfamily

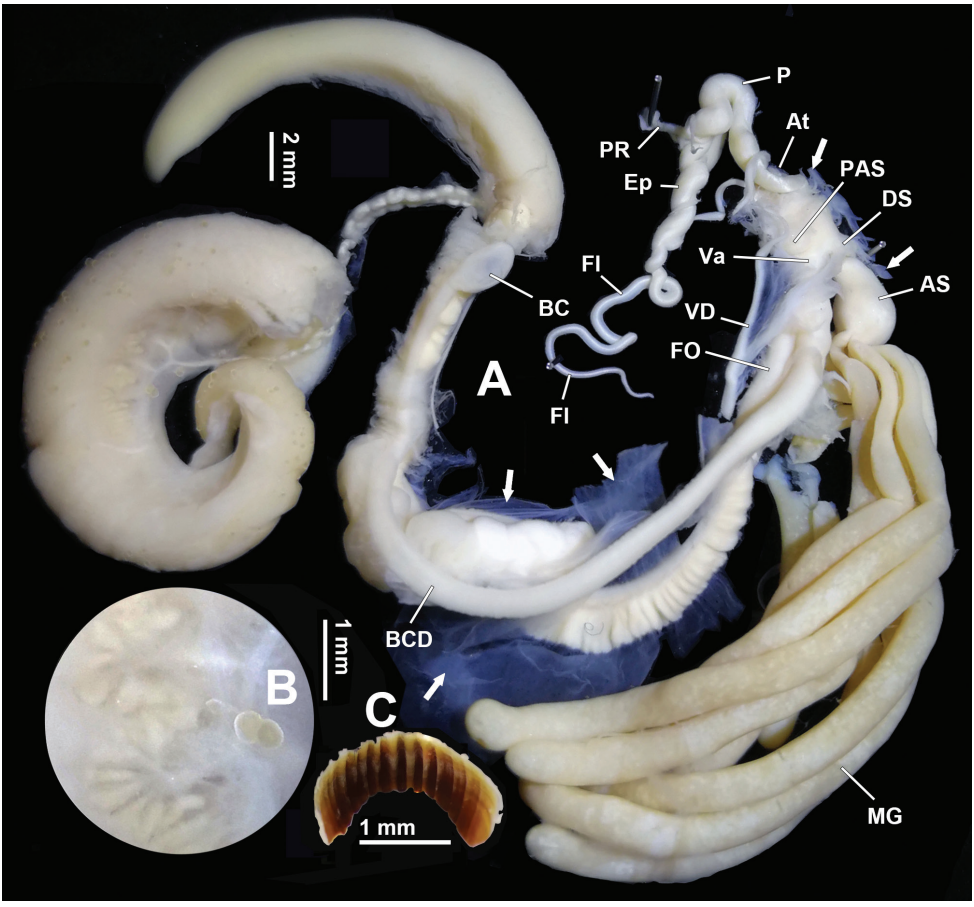

Figure 4. *Traumatophora triscalpta* (Martens, 1875). HBUMM06875 specimen-2. **A, B** genitalia **A** general view, the remnant membrane after dissection is arrowed **B** magnified hermaphroditic gland **C** jaw. AS–accessory sac; At–atrium; BC–bursa copulatrix; BCD–bursa copulatrix duct; DS–dart sac; Ep–epiphallus; Fl–flagellum; FO–free oviduct; MG–mucous glands; P–penis; PAS–proximal accessory sac, a blind sac on proximal dart sac opening into dart sac chamber or not; PR–penial retractor muscle; Va–vagina; VD–vas deferens.

Bradybaeninae); each thicker than penis; in volume larger than rest of genitalia (Fig. 4A); connected to each other by nerve fibres (Fig. 5C). Each mucous gland duct entering accessory sac through a separate pore; through papilla or not (Figs 5E, 6A, B). Vagina approximately as long as accessory sac; entering dart sac chamber. A ball-shaped proximal accessory sac (Figs 4A, 5A, D, E, 6A), about 1.5 mm in diameter, with opening leading to dart sac chamber near entrance of vagina. Gonad glands palm-shaped; with short peduncles (Fig. 4B). Measurement in HBUMM06875 specimen-2: DS–2.1 mm long; AS–4.1 mm long; MG–30.9 mm (average of 5 mucous glands); P–6.9 mm; Ep–10.3 mm; Fl–19.1; VD–22.0 mm; PR–3.2 mm; Va–3.2 mm; FO–4.9 mm; BC plus BCD–37.5 mm.

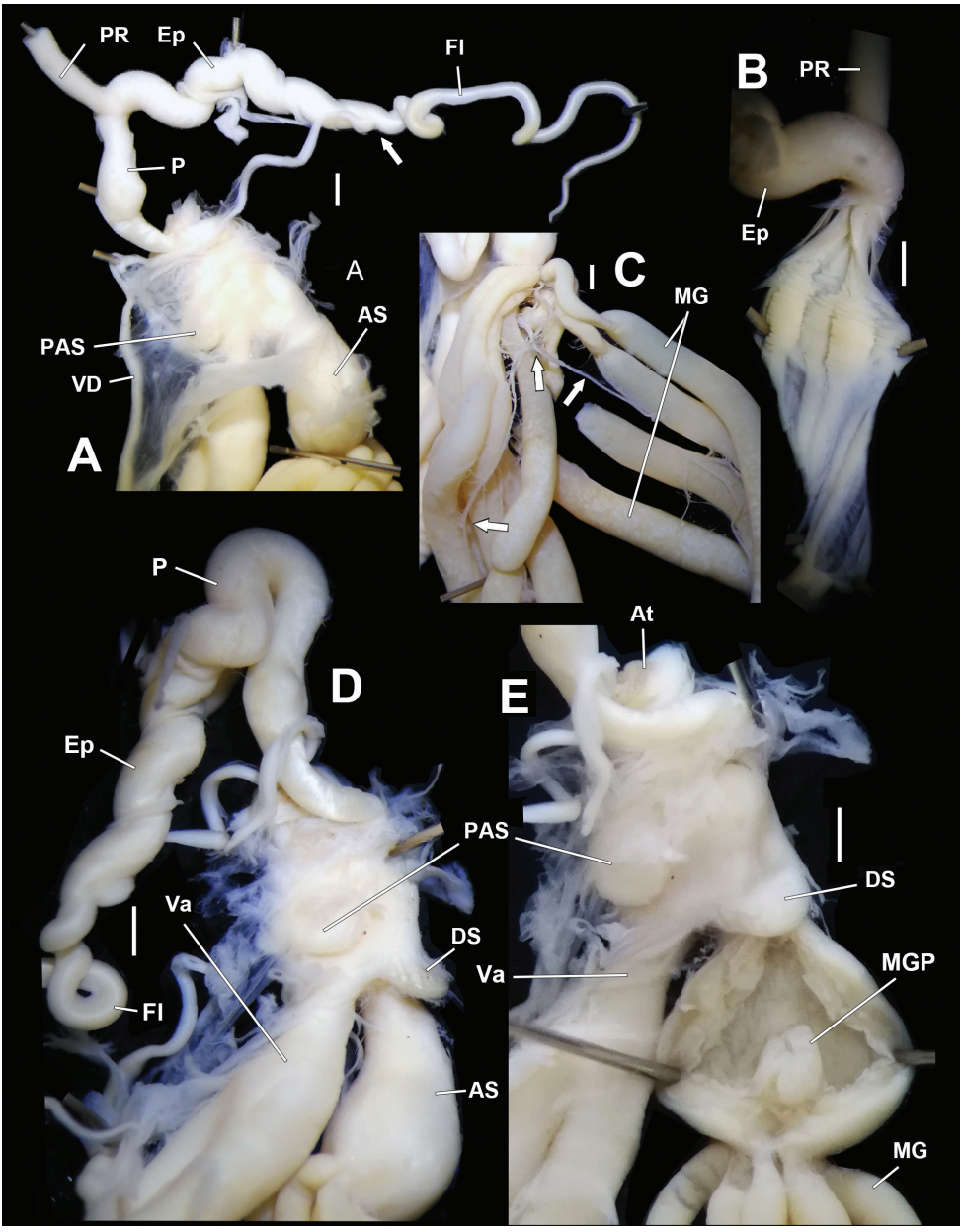

Figure 5. *Traumatophora triscalpta* (Martens, 1875). Genitalia, HBUMM06875 specimen-2. **A** male part, vas deferens insertion arrowed **B** exposed penis **C** mucous glands, showing nerve fibres (arrowed) connecting mucous gland ducts **D** dart apparatus, peculiarly showing the dart sac and the ball-shaped caecum **E** exposed accessory sac, showing mucous gland entering papilla Scale bars: 1 mm. AS–accessory sac; At–atrium; DS–dart sac; Ep–epiphallus; Fl–flagellum; MG–mucous glands; MGP– papilla distally leading to mucous glands on inner wall of accessory sac; P–penis; PAS–proximal accessory sac, a blind sac on proximal dart sac opening into dart sac chamber or not; PR–penial retractor muscle; Va–vagina; VD–vas deferens.

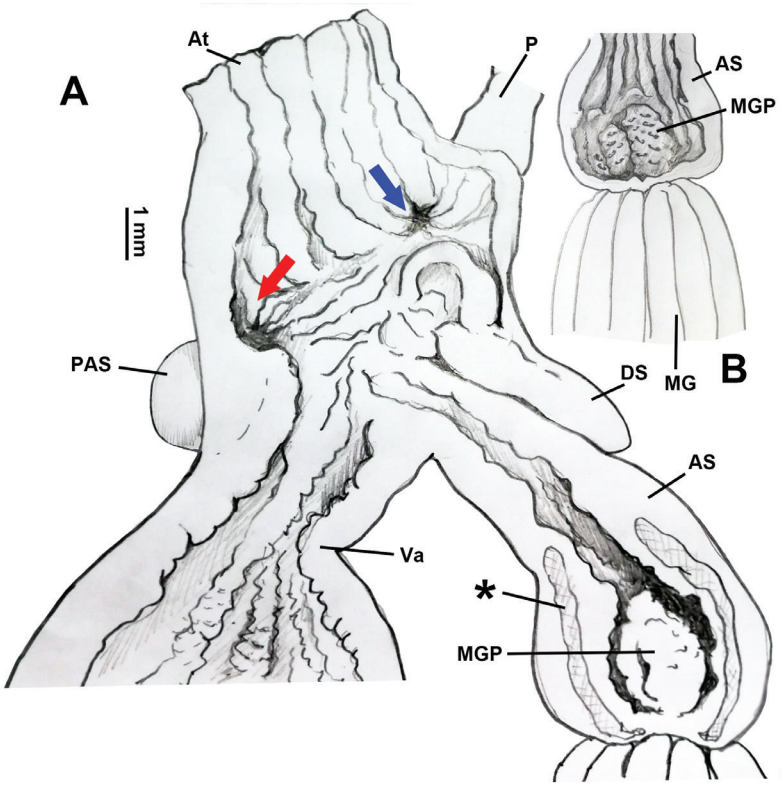

Figure 6. *Traumatophora triscalpta* (Martens, 1875). Terminal genitalia, HBUMM06875 specimen-2. **A** exposed terminal genitalia. Blue arrow, indicating penis entrance; red arrow, indicating PAS opening leading to dart sac chamber **B** exposed accessory. AS–accessory sac; At–atrium; DS–dart sac; MG–mucous glands; MGP–papilla distally leading to mucous glands on inner wall of accessory sac; P–penis; PAS–proximal accessory sac, a blind sac on proximal dart sac opening into dart sac chamber or not; Va–vagina; *–sphincter muscles.

Distribution. Extant distribution: Jiangxi (type locality: around Boyanghu; Lushan), Hubei (Ou-tang =Wudangshan Mts., Tong-san in Sei-zo), Fujian (Foochow= Fuzhou. Yen 1942), Zhejiang (Tianmushan Mts. This study). Pleistocene: Jiangsu (Chenkiang: Chiao-shan =Zhengjiang: Jiaoshan) (Fig. 1).

Ecology. Perhaps this species is among the rarest bradybaenine species in China, although the extant distribution range is large and covers Jiangxi, Hubei, Fujian and Zhejiang. *Traumatophora triscalpta* was known from higher altitudes of 1200–1500 m (Pilsbry 1890).

Taxonomic remarks. In this study, the *Traumatophora* specimens from Zhejiang are identified as *T. triscalpta* based on the original description and comparison of the type material (Fig. 3). I follow Yen (1943) in treating *T. triscalpta* and *T. fraterminor* (originally described as *Helix triscalpta fraterminor* Gredler, 1884: 137. *T. triscalpta fraterminor* Yen 1939: 126, pl. 13, fig. 8; Zilch 1974. *T. fraterminor* Yen 1943: 297) as two distinct species, although the only known difference between them is that the latter species is "smaller in diameter and higher in altitude, obtusely angulated at periph-

ery" (Pilsbry 1890). However, considering the frequency of convergence events in the evolution of shell morphology in the helicoids, it is reasonable to treat these two taxa that show detectable differences in shell morphology as two species. *Traumatophora fraterminor* is distributed between Hwang-tchou (today's Huangshi, Hubei Province) and Kiou-Kiang (today's Jiujiang, Jiangxi Province) (Pilsbry, 1890) (Fig. 1). Report of a Pleistocene fossil from Zhenjiang, Jiangsu as *T. fraterminor* (sensu Yen 1943) is somewhat doubtful because the relevant specimen was a juvenile shell.

Discussion

The anatomy of the terminal genitalia, especially the dart apparatus, varies greatly in the subfamily Bradybaeninae (Table 1) and is of considerable systematic significance. Most functions of these characteristic structures remain unclear, however,the function of some of these structures can be speculated to relate to the products of the dart apparatus, i.e., the love dart secreted in the dart chamber and the mucus secreted by the mucous glands, the function of which might be closely related to the reproductive success of the dart user as in the helicid snail *Cornu aspersum* (Lodi & Koene, 2016). *Traumatophora*, however, show an examples of the dart apparatus consisting of a tiny dart (proportionally the smallest in the Bradybaeninae) and disproportionately large mucous glands (proportionally the largest in the Bradybaeninae). Therefore, the genus *Traumatophora* provides a counter-example of the correlated evolution between stylophore and mucous glands (Koene and Schulenburg 2005: fig. 4A).

Traumatophora triscalpta has a rounded proximal accessory sac with an opening directly leading to the dart sac chamber. A similar structure is also present in some *Stilpnodiscus* species (*S. moellendorffi* Wu, 2001: Wu 2001a, figs 4A, B, E, F; *S. entochilus* Möllendorff, 1899: Wu 2001a, figs 2A, B) and in the *Pseudiberus* spp. distributed in Shandong and Hebei (unpublished) (Table 1). The function of such sac-like structure is unknown, although it is predicted to be related to the storage of mucus secreted by the mucous glands. What is also fascinating is that in *Traumatophora* the occurrence of both the sphincter muscles in the accessory sac (Fig. 6A) and the developed nerve fibres connecting the mucous gland ducts (Fig. 5C, arrowed) suggests that during dart-shooting in mating, there might be an instant ejection of mucus by the animal.

Acknowledgements

Thanks to Mr Dakang Zhou for specimen collection in the field. I am indebted to Ms Christine Zorn and Dr Thomas von Rintelen (Museum für Naturkunde, Berlin) for preparing photographs of the museum material of the syntype. Thanks go to The Biodiversity Heritage Library (www.biodiversitylibrary.org) for the access of precious literatures. I thank two reviewers Dr Frank Köhler and Dr Barna Páll-Gergely for helpful comments.

This study was supported by the National Natural Science Foundation of China (NSFC 31872196).

References

Ancey CF (1887) Description of new genera or subgenera of Helicidae. The Conchologists' Exchange 1: 53–54.

Azuma M (1995) Colored Illustrations of the Land Snails of Japan. Hoikusha: Osaka. Xvi + 343 pp. [80 pls.]

Bouchet P, Rocroi J-P, Hausdorf B, Kaim A, Kano Y, Nützel A, Parkhaev P, Schrödl M, Strong EE (2017) Revised classification, nomenclator and typification of gastropod and monoplacophoran families. Malacologia 61(1–2): 1–526. https://doi.org/10.4002/040.061.0201

Chang K (1989) Anatomy of *Coniglobus nux paiwanus* (Kuroda) and *Coniglobus pekanensis* (Rolle) from south Taiwan (Pulmonata: Camaenidae). Bulletin of Malacology, ROC 14: 1–8.

Chang KM (1990) Systematics on *Trichochloritis hungerfordianus* from Taiwan. Bulletin of Malacology, ROC 15: 35–41.

Du L, Xu Q, Wu M (2013) The monsoon forest refuge of the only Chinese *Amphidromus*. Tentacle 21: 43–44.

Gredler PV (1884) Zur Conchylien-Fauna von China. V. Stück. Jahrbücher der Deutschen Malakozoologischen Gesellschaft 11: 129–161.

Heude PM (1882) Notes sur les mollusques terrestres de la vallée du Fleuve Bleu. Mémoires concernant l'histoire naturelle de l'Empire chinois 1: 1–84.

Hirano T, Kameda Y, Kimura K, Chiba S (2014) Substantial incongruence among the morphology, taxonomy, and molecular phylogeny of the land snails *Aegista*, *Landouria*, *Trishoplita*, and *Pseudobuliminus* (Pulmonata: Bradybaenidae) occurring in East Asia. Molecular Phylogenetics and Evolution 70: 171–181. https://doi.org/10.1016/j.ympev.2013.09.020

Kerney MP, Cameron RAD (1979) A Field Guide to the Land Snails of Britain and North-West Europe. Collins, London. 288 pp. [24 pls.]

Koene JM, Schulenburg H (2005) Shooting darts: co-evolution and counter-adaptation in hermaphroditic snails. BMC Evolutionary Biology 2005(5): 25. https://doi.org/10.1186/1471-2148-5-25

Lodi M, Koene JM (2016) The love-darts of land snails: integrating physiology, morphology and behaviour. Journal of Molluscan Studies (2015): 1–10. https://doi.org/10.1093/mollus/eyv046

Martens E (1875a) Ostasiatische Land- und Süsswasserconchzlien. Sitzungs-Berichte der Gesellschaft Naturforschender Freunde, Berlin 1875: 2.

Martens E (1875b) Binnen-Mollusken aus dem mittlern China. Malakozoologische Blätter 22: 185–188.

Möllendorff OF (1884) Materialien zur Fauna von China. Jahrbücher der Deutschen Malakozoologischen Gesellschaft 11: 307–390. [pls. 7–9]

Páll-Gergely B, Hunyadi A, Asami T (2018) Enantiomorphs and taxonomy of three conchological species in flat-shelled snails *Trichocathaica* (Pulmonata, Camaenidae). Zookeys 810: 19–44. https://doi.org/10.3897/zookeys.810.29824

Pilsbry HA (1890) In: Tryon GW, Pilsbry HA (Eds) Manual of Conchology. (2)6, 5–324. [pls. 1, 39–69]

Pilsbry HA (1894) In: Tryon GW, Pilsbry HA (Eds) Manual of Conchology. (2)9, 1–366. [pls. 1–71]

Schileyko AA (2003) Treatise on recent terrestrial pulmonate molluscs. Part 11. Trigonochlamydidae, Papillodermidae, Vitrinidae, Limacidae, Bielziidae, Agriolimacidae, Boettgerillidae, Camaenidae. Ruthenica Supplement (2): 1467–1626.

Schileyko AA (2004) Treatise on recent terrestrial pulmonate molluscs. Part 12. Bradybaenidae, Xanthonychidae, Epiphragmophoridae, Helminthoglyptidae, Elonidae, Sphincterochilidae, Cochlicellidae. Ruthenica Supplement (2): 1627–1763.

Schmacker B, Boettger O (1894) Description of some Chinese land-shells. Proceedings of the Malacological Society 1: 169–174. https://doi.org/10.1093/oxfordjournals.mollus.a064109

Solem A (1992) Camaenid land snails from southern and eastern South Australia, excluding Kangaroo Island. Part 1. Systematics, distribution and variation. Records of the South Australian Museum, Monograph series 2: 338 pp. [72 pls.]

Wade CM, Mordan PB, Naggs F (2006) Evolutionary relationships among the Pulmonate land snails and slugs (Pulmonata, Stylommatophora). Biological Journal of the Linnean Society 87: 593–610. https://doi.org/10.1111/j.1095-8312.2006.00596.x

Wade CM, Hudelot C, Davison A, Naggs F, Mordan PB (2007) Molecular phylogeny of the helicoid land snails (Pulmonata: Stylommatophora: Helicoidea), with special emphasis on the Camaenidae. Journal of Molluscan Studies 73: 411–415. https://doi.org/10.1093/mollus/eym030

Wu M (2001a) Contribution to the knowledge of Chinese endemic genus *Stilpnodiscus* (Gastropoda: Pulmonata: Bradybaenidae), with descriptions of two new species. Folia Malacologica 9(2): 83–91. https://doi.org/10.12657/folmal.009.011

Wu M (2001b) One new species of Chinese endemic snails of *Trichocathaica* (Gastropoda: Stylommatophora: Bradybaenidae). Acta Zootaxonomica Sinica 26(3): 292–296.

Wu M (2004) Preliminary phylogenetic study of Bradybaenidae (Gastropoda: Stylommatophora: Helicoidea). Malacologia 46(1): 79–125.

Wu M, Asami T (2017) Taxonomical notes on Chinese camaenids with description of three species (Gastropoda: Pulmonata). Molluscan Research.

Wu M, Guo J (2003) Contribution to the knowledge of Chinese terrestrial malacofauna (Helicoidea): description of a new bradybaenid genus with three species. The Veliger 46(3): 239–251.

Wu M, Guo J (2006) Revision of Chinese Species of *Ponsadenia* (Gastropoda: Helicoidea, Bradybaenidae). Zootaxa 1316: 57–68.

Wu M, Prozorova LA (2006) The landsnail genus *Metodontia* Moellendorff (Pulmonata: Stylommatophora: Bradybaenidae) of China. Journal of Conchology 39(2): 159–173.

Wu M, Qi G (2006) A taxonomic note on *Pseudiberus* Ancey, 1887 (Gastropoda: Pulmonata: Bradybaenidae). Folia Malacologica 14(1): 25–30. https://doi.org/10.12657/folmal.014.003

Wu S, Hwang C, Lin Y (2008) Systematic revision of the arboreal snail *Satsuma albida* species complex (Mollusca: Camaenidae) with descriptions of 14 new species from Taiwan. Zoological Journal of the Linnean Society 154, 437–493. https://doi.org/10.1111/j.1096-3642.2008.00415.x

Yen TC (1939) Die chinesischen Land- und Süßwasser-Gastropoden des Natur-Museums Senckenberg. Abhandlungen der Senckenbergischen Naturforschenden Gesellschaft 444: 1–234. [16 pls.]

Yen TC (1942) A Review of Chinese Gastropods in the British Museum. Proceedings of the Malacological Society of London 24: 170–288. [pls. 11–28]

Yen TC (1943) Review and summary of Tertiary and Quaternary non-marine mollusks of China. Proceedings of the Academy of Natural Sciences of Philadelphia 95: 267–346.

Zilch A (1974) Vinzenz Gredler und die Erforschung der Weichtiere Chinas durch Franziskaner aus Tirol. Archiv für Molluskenkunde 104(4/6): 171–228.